# EARLY EVENTS FOLLOWING MURINE GAMMAHERPESVIRUS (MHV-68) INFECTION

Suganya Selvarajah

Doctorate in Philosophy

Department of Veterinary Pathology
University of Edinburgh


July 2001

# DECLARATION

I hereby declare that this thesis entitled 'Early events following murine gammaherpesvirus (MHV-68) infection' is not substantially the same as any that I have submitted for a degree, diploma or any other qualification at any other university. This thesis is the result of my work and does not include any work that is the outcome of a collaboration, except where duly acknowledged in the text.

# ACKNOWLEDGEMENTS

I would like to thank Professor Anthony Nash and Dr Bernadette Dutia for their excellent supervision. A special thanks to Professor Nash for offering me this great opportunity to do a Ph.D. in his laboratory. Both he and Dr Dutia always found the time to guide me through this project and have helped immensely in keeping my enthusiasm for science and a career in science alive.

I would like to acknowledge the scholarships, the Darwin Trust of Edinburgh and the Overseas Research Scholarship.

Thanks to Dr James Stewart, Dr Douglas Roy, my colleagues and all the technical staff within the Department of Veterinary Pathology for their assistance. Special thanks to Dr Kevin Robertson and Dr Bahram Ebrahimi for being supportive, always ready with a word of encouragement and a helping hand.

Away from work and most important of all, thanks to my parents, Selvarajah and Sathiyanayaki Selvarajah, for their courage in allowing me to travel to the UK for my studies. My parents, brother and sister have shown great faith in my ability and have showered me with their love and prayers. Finally thanks to Anup Pradhan whose love, support and understanding made my days brighter and life less lonely.

# ABSTRACT

Murine gammaherpesvirus (MHV-68) was isolated from a bank vole. It has pathobiological and genetic similarities to other gammaherpesviruses including Herpesvirus saimiri, Epstein-Barr virus (EBV) and Kaposi's sarcoma-associated herpesvirus (KSHV). It infects laboratory mice and forms plaques on cell monolayers in tissue culture. The pathogenesis and immunology have been widely studied in the mouse system and it has been identified as a useful "small animal model".

Mice were infected with $4x10^5$ PFU MHV-68 intranasally. The virus infects alveolar epithelial cells and causes interstitial pneumonia. In the lungs the virus undergoes lytic replication which is cleared by day 10. Subsequently the virus is found latent in B cells that have been found to be important in the establishment of latency and in the transmission of virus from the lungs to the spleen. The spleen and the lymph nodes at this stage exhibit splenomegaly and lymphadenopathy respectively. In B cell deficient (μMT) mice, latently infected cells are not detected in the spleen and splenomegaly is not observed.

In this study, the early events following MHV-68 infection *in vivo* were examined. The work focused on the mediastinal lymph node (MLN) that drains the lungs. Events occurring in the MLNs from the wild type C57BL/6 mice were compared to those of the μMT mice. The results demonstrated the absence of lymphadenopathy in μMT mice and indicated that lymphadenopathy in wild type C57BL/6 mice was brought about especially by the accumulation of B cells. Depletion of CD4+ T cells in wild type C57BL/6 mice demonstrated that the absence of CD4+ T cells only partially affected the accumulation of B cells and enlargement of the MLN. The μMT mouse showed the presence of latent virus in the MLN even in the absence of B cells. However by day 10 these cells were below levels of detection and there was no evidence of systemic transfer of virus.

In order to characterise the cells latently infected with virus in the MLNs of μMT mice, a recombinant MHV-68 virus expressing green fluorescent protein (GFP), LHΔgfp, was used. LHΔgfp has a deletion in the left-hand end and it was therefore characterised *in vivo* before further studies were initiated. In the MLN and spleen LHΔgfp did not show peak latent virus levels as seen with wild type MHV-68, but eventually it was able to establish the same level of latency in these tissues. Therefore LHΔgfp was shown to behave similarly to wild type MHV-68 *in vivo*. The use of LHΔgfp helped identify infected cells in the MLNs of μMT mice. Dendritic cells expressing CD11c and macrophages expressing F4/80 were found latently infected in the MLN. LHΔgfp was characterised in the IFN α/β receptor knockout system and shown to act like the wild type virus in this immunodeficient host by causing amplification of disease pathogenesis. This system also helped confirm that in the presence of B cells CD11c and F4/80 positive cells were infected very early during infection in the MLN.

In conclusion it can be said that the mediastinal lymphadenopathy is a critical event in the pathogenesis of MHV-68 infection in which B cells played an important regulatory role. Secondly, the use of recombinant virus expressing marker proteins is a useful tool for *in vivo* study of a natural gammaherpesvirus infection.

# TABLE OF CONTENTS

**DECLARATION** ..... II
**ACKNOWLEDGEMENTS** ..... III
**ABSTRACT** ..... IV
**TABLE OF CONTENTS** ..... VI
**LIST OF FIGURES** ..... XI
**LIST OF TABLES** ..... XIV
**ABBREVIATIONS** ..... XV

**CHAPTER ONE** ..... 1
**INTRODUCTION** ..... 1
**1.1 Herpesviruses: a general introduction** ..... 1
**1.2 Gammaherpesviruses** ..... 3
**1.3 Epstein-Barr virus** ..... 3
1.3.1 Lytic Infection ..... 4
1.3.2 EBV Latency ..... 6
**1.4 Kaposi's sarcoma-associated herpesvirus** ..... 8
1.4.1 Viral genes of KSHV ..... 8
1.4.2 Cell cycle regulation by KSHV ..... 10
1.4.3 Apoptosis regulation by KSHV ..... 11
1.4.4 Cytokine and Chemokine regulation by KSHV ..... 12
**1.5 Murine gammaherpesvirus-68** ..... 15
1.5.1 MHV-68 genome ..... 16
1.5.2 Infection, pathogenesis and susceptible cell types ..... 18
**1.6 Immune response to viruses** ..... 19
1.6.1 Cells ..... 19
1.6.1.1 Natural killer cells ..... 20
1.6.1.2 Macrophages ..... 21
1.6.1.3 Complement and collectins ..... 22
1.6.1.4 Dendritic cells ..... 23
1.6.1.5 T cells ..... 24
1.6.1.6 B cells ..... 25
1.6.2 Chemokines ..... 27

1.6.3 Cytokines ..... 28
**1.7 Immune response to EBV** ..... 29
1.7.1 Antibody response ..... 29
1.7.2 CTL response ..... 31
**1.8 Immune response to MHV-68** ..... 33
1.8.1 Innate immune response ..... 33
1.8.2 Humoral response ..... 33
1.8.3 T cell response ..... 35
1.8.3.1 CD4+ T helper cells ..... 35
1.8.3.2 CD8+ CTL ..... 36
**1.9 Evasion of immune responses by herpesviruses** ..... 37
1.9.1 Modulation of antigen presentation ..... 37
1.9.2 Modulation of cell death by apoptosis ..... 42
1.9.3 Modulation of cytokine and chemokine response ..... 43
1.9.4 Modulation of humoral immunity ..... 45
**1.10 Aim of the Project** ..... 46

**CHAPTER TWO** ..... 47
**MATERIALS AND METHODS** ..... 47
**2.1 Materials** ..... 47
2.1.1 Chemicals ..... 47
2.1.2 Tissue culture media ..... 47
2.1.3 Virus ..... 47
2.1.4 Mice ..... 48
2.1.5 Cell lines ..... 48
2.1.6 Biobond Coating ..... 48
**2.2 Methods** ..... 49
2.2.1 Preparation of virus working stock ..... 49
2.2.2 Cocultivation assay for infective centres in the lymph nodes and spleen ..... 49
2.2.3 Assay for infective virus ..... 50
2.2.4 Biotinylation of antibody ..... 50
2.2.5 Flow cytometric analysis of cells (FACS-fluorescent activated cell sorting) ..... 50
2.2.6 Imprints ..... 51
2.2.7 *In vivo* depletion of T cells ..... 51
2.2.8 Cytospins ..... 51

2.2.9 MHV-68 immunostaining of paraffin-embedded tissues ..... 52
2.2.10 Magnetic activated cell sorting (MACS) ..... 53
2.2.11 Interferon-γ CTL assay ..... 54
2.2.12 Staining cytospun cells ..... 55
2.2.13 Confocal microscopy ..... 55
2.2.14 Ammonium chloride lysis ..... 55
2.2.15 Electron microscopy ..... 56
2.2.16 Handling of DNA, RNA and molecular biological techniques ..... 56
2.2.17 DNA agarose gel electrophoresis ..... 56
2.2.18 RNA Extraction ..... 56
2.2.19 Preparation of cDNA from total RNA ..... 57
2.2.20 Polymerase chain reaction (PCR) ..... 57

**CHAPTER THREE** ..... 58
**ROLE OF B CELLS IN THE DRAINING LYMPH NODE DURING THE EARLY STAGES OF INFECTION** ..... 58
**3.1 Introduction** ..... 58
**3.2 Mediastinal lymphadenopathy and B cells** ..... 59
3.2.1 Mediastinal lymphadenopathy in the presence and absence of B cells ..... 59
3.2.2 Changes in cell populations during the process of lymph node enlargement ..... 60
3.2.3 FACS analysis for B cell surface markers ..... 61
**3.3 CD4+ T cell signalling and B cells in the MLN** ..... 62
3.3.1 Requirement for CD4+ T cell signalling in lymph node enlargement ..... 62
3.3.2 B cell numbers in the MLN following CD4+ T cell depletion ..... 63
3.3.3 Presence of latently infected cells in the MLN following CD4+ T cell depletion ..... 64
**3.4 Latently infected cells in the absence of B cells, in the MLN** ..... 65
3.4.1 Latently infected cells in the MLN of μMT mice ..... 65
3.4.2 Immunostaining for cells expressing virus encoded lytic proteins ..... 66
3.4.3 Detection of virus particles using electron microscopy ..... 66
3.4.4 Reverse transcription-polymerase chain reaction (RT-PCR) for viral transcripts on whole tissues ..... 67
**3.5 CD8+ CTL and B cells in the MLN** ..... 68
3.5.1 MHV-68 specific CTL response, in the absence of B cells ..... 68

**CHAPTER FOUR** ..... 69
**APPLICATION OF A GREEN FLUORESCENT PROTEIN (GFP) EXPRESSING GAMMAHERPESVIRUS** ..... 69
**4.1 Introduction** ..... 69
**4.2 Characterisation of LHΔgfp** ..... 71
4.2.1 Infective virus in the lungs of C57BL/6 mice infected with LHΔgfp as compared to wild type MHV-68 ..... 71
4.2.2 Latently infected cells in the mediastinal lymph node ..... 71
4.2.3 Extent of lymphadenopathy ..... 72
4.2.4 Latently infected cells in the spleen ..... 73
**4.3 LHΔgfp as a tool to study the trafficking of virus *in vivo*** ..... 73
4.3.1 GFP positive cells in the lungs and mediastinal lymph node imprints ..... 73
4.3.2 CD11c expressing cells enriched from μMT mice MLN ..... 74
4.3.3 CD11c enriched cells expressing GFP stained with F4/80 ..... 75
4.3.4 The advantages of using the IFN-α/β $R^{-/-}$ mouse system which displays an exaggerated MHV-68 disease pathogenesis ..... 76
4.3.5 CD11c enriched cells expressing GFP confirmed with surface staining ..... 77
**4.4 Pathogenesis of LHΔgfp in IFN-α/β $R^{-/-}$ mice versus WT129 mice** ..... 78
4.4.1 Infective virus in the lungs ..... 78
4.4.2 Lymphadenopathy ..... 79
4.4.3 Latently infected cells in the mediastinal lymph node and spleen ..... 79
4.4.4 Cryosections of the MLN and spleens of IFN-α/β $R^{-/-}$ mice to identify cells expressing GFP ..... 80
**4.5 FACS analysis for various cell populations and the pattern of GFP expression in the MLN of IFN-α/β $R^{-/-}$ and WT129 mice** ..... 81
4.5.1 CD11c staining for dendritic cells ..... 81
4.5.2 F4/80 staining for macrophages ..... 82
4.5.3 CD19 staining for B cells ..... 83
4.5.4 Staining for CD4+ T cells ..... 83
4.5.5 Staining for CD8+ T cells ..... 84
**4.6 The FACS percentages of cells expressing GFP in the spleens of IFN-α/β $R^{-/-}$ mice and WT129 mice** ..... 85

**CHAPTER FIVE** ..... 87
**DISCUSSION** ..... 87

**5.1 MLN is a critical site in MHV-68 pathogenesis where the B cells play an important role** ..... 88
5.1.1 Requirement for B cells in lymphadenopathy ..... 88
5.1.2 B cell expansion is only partly dependent on CD4+ T cell signalling ..... 89
5.1.3 B cells are required for long-term latency and viral dissemination from the MLN ..... 90
5.1.4 Latently infected B cells are required for the presence of an active MHV-68 specific CTL response in the MLN ..... 91
**5.2 Cells other than B cells are infected in the MLN** ..... 92
5.2.1 Dendritic cells and macrophages, target cells for MHV-68 infection in the MLN ..... 92
5.2.2 Dendritic cells in trafficking virus ..... 94
5.2.3 Dendritic cells and macrophages as reservoirs of virus ..... 95
**5.3 Pathogenesis and use of recombinant LHΔgfp** ..... 95
5.3.1 Effects on disease pathogenesis of LHΔgfp as a result of the deleted genes ..... 95
5.3.2 LHΔgfp, a useful marker virus ..... 96
**5.4 Pathogenesis of LHΔgfp in IFN-α/β $R^{-/-}$ and WT129 mice** ..... 97
5.4.1 Disease pathogenesis in the lung, MLN and spleen ..... 97
5.4.2 Reduced lymphadenopathy in IFN-α/β $R^{-/-}$ mice ..... 98
**5.5 Future work** ..... 99
**5.6 Summary** ..... 100

**BIBLIOGRAPHY** ..... 101

# LIST OF FIGURES


| Figure | Title | Pages |
|---|---|---|
| 1.1 | The organisation of MHV-68 genome as compared to EBV and KSHV | 15-16 |
| 1.2 | MHV-68 infection in mice deficient in lymphocyte subsets and cell surface molecules | 35-36 |
| 1.3 | MHV-68 infection in mice deficient in lymphocyte subsets and cell surface molecules | 35-36 |
| 3.1 | Lymphadenopathy of the mediastinal lymph node in wild type C57BL/6 and B cell deficient (μMT) mice | 59-60 |
| 3.2a | Phenotype of cells in the enlarged lymph nodes of C57BL/6 mice | 60-61 |
| 3.2b | Phenotype of cells in the enlarged lymph nodes of C57BL/6 mice | 60-61 |
| 3.3a | Expression of B cell markers in the enlarged lymph nodes of C57BL/6 mice | 61-62 |
| 3.3b | Expression of B cell markers in the enlarged lymph nodes of C57BL/6 mice | 61-62 |
| 3.4 | FACS analysis for CD4+ T cells in the MLN | 63-64 |
| 3.5 | Cellularity of the mediastinal lymph node in C57BL/6 mice depleted of CD4+ T cells | 63-64 |
| 3.6 | B cell numbers in the mediastinal lymph node of C57BL/6 mice depleted of CD4+ T cells | 63-64 |
| 3.7 | Infective centres in the mediastinal lymph node of C57BL/6 mice depleted of CD4+ T cells | 64-65 |
| 3.8 | Infective centres in the spleens of C57BL/6 mice depleted of CD4+ T cells | 64-65 |
| 3.9 | Infective centres in the mediastinal lymph node and cervical lymph node (CLN) in C57BL/6 and μMT mice | 65-66 |
| 3.10 | Lung and MLN tissues from IFN α/β R-/- mice immunostained for MHV-68 lytic viral proteins | 66-67 |
| 3.11 | Transmission electron microscopy to detect virus particles in MLN cells from μMT mice infected with MHV-68 | 66-67 |
| 3.12 | RT-PCR for viral transcripts on whole MLNs from μMT and C57BL/6 mice | 67-68 |

| | | |
|---|---|---|
| 3.13 | MHV-68 specific CTL response in the MLN of μMT and C57BL/6 mice | 68-69 |
| 4.1 | Infective virus in the lungs of C57BL/6 mice infected with either LHΔgfp or MHV-68 | 71-72 |
| 4.2 | Infective centres in the mediastinal lymph node of C57BL/6 mice infected with either LHΔgfp or MHV-68 | 72-73 |
| 4.3 | Lymphadenopathy of the mediastinal lymph node of C57BL/6 mice infected with either LHΔgfp or MHV-68 | 72-73 |
| 4.4 | Infective centres in the spleens of C57BL/6 mice infected with either LHΔgfp or MHV-68 | 73-74 |
| 4.5 | GFP positive cells in the lungs and mediastinal lymph node imprints of μMT mouse infected with LHΔgfp | 74-75 |
| 4.6 | FACS analysis dot plots representing scatter data and staining of CD11c cells obtained from MACS enrichment of μMT mouse MLN | 75-76 |
| 4.7 | GFP expressing cells stained with F4/80 antibody | 75-76 |
| 4.8 | FACS analysis dot plots representing scatter data and staining of CD11c cells obtained from MACS enrichment of IFN $\alpha/\beta$ $R^{-/-}$ mouse MLN | 77-78 |
| 4.9 | Fluorescence images of cells enriched for CD11c using MACS | 77-78 |
| 4.10 | CD11c enriched cells from IFN $\alpha/\beta$ $R^{-/-}$ mice MLN expressing GFP and stained for surface markers | 77-78 |
| 4.11 | Infective virus in the lungs of IFN $\alpha/\beta$ $R^{-/-}$ and WT129 mice infected with LHΔgfp | 78-79 |
| 4.12 | Lymphadenopathy of the mediastinal lymph node of IFN $\alpha/\beta$ $R^{-/-}$ and WT129 mice infected with LHΔgfp | 79-80 |
| 4.13 | Infective centres in the mediastinal lymph node of IFN $\alpha/\beta$ $R^{-/-}$ and WT129 mice infected with LHΔgfp | 79-80 |
| 4.14 | Infective centres in the spleens of IFN $\alpha/\beta$ $R^{-/-}$ and WT129 mice infected with LHΔgfp | 79-80 |
| 4.15 | Cryosections of tissues from IFN $\alpha/\beta$ $R^{-/-}$ mice to identify cells expressing GFP | 80-81 |
| 4.16 | The FACS percentages of different cell types and the percentage expressing GFP in the mediastinal lymph node of IFN $\alpha/\beta$ $R^{-/-}$ and WT129 mice infected with LHΔgfp | 81-82 |

4.17 The total numbers of cells expressing GFP in the mediastinal lymph node of IFN $\alpha/\beta$ $R^{-/-}$ and WT129 mice infected with LHΔgfp 85-86

4.18 The FACS percentages of different cell types and the percentage expressing GFP in the spleen of IFN $\alpha/\beta$ $R^{-/-}$ and WT129 mice infected with LHΔgfp 85-86

# LIST OF TABLES


| Table | Title | Pages |
|---|---|---|
| 1.1 | Characteristics of the gammaherpesviruses | 3-4 |
| 2.1 | Antibodies used in FACS analysis | 48-49 |
| 2.2 | PCR Primer sequence | 57-58 |

# ABBREVIATIONS

| | |
|---|---|
| ADCC | Antibody dependent cell-mediated cytotoxicity |
| AFC | Antibody forming cells |
| APC | Antigen presenting cells |
| BCBL | Body cavity-based lymphomas |
| BFA | Brefeldin-A |
| BH | Bcl homology |
| BHK | Baby hamster kidney cell line |
| BHV-4 | Bovine herpesvirus-4 |
| cDNA | Complementary deoxyribonucleic acid |
| CDK | Cyclin dependent kinases |
| CLN | Cervical lymph node |
| CMV | Cytomegalovirus |
| CTL | Cytotoxic T lymphocytes |
| DC | Dendritic cells |
| $dH_2O$ | Distilled water |
| DNA | Deoxyribonucleic acid |
| EA | Early antigen |
| EBNA | Epstein-Barr virus nuclear antigen |
| EBV | Epstein-Barr virus |
| EHV-2 | Equine herpesvirus-2 |
| ER | Endoplasmic reticulum |
| FACS | Fluorescent activated cell sorter |
| Fc | Fragment crystallisable |
| Fc$\gamma$R | Fragment crystallisable–$\gamma$ receptor |
| FITC | Fluorescein isothiocyanate |
| GAR | Glycine-alanine repeat |
| GC | Germinal centres |
| GFP | Green fluorescent protein |
| GMEM | Glasgow's modified Eagle's medium |
| GPCR | G-protein coupled-receptor |

| | |
|---|---|
| HCMV | Human cytomegalovirus |
| HHV 6 | Human herpesviruses-6 |
| HHV 7 | Human herpesviruses-7 |
| HHV-8 | Human herpesvirus-8 |
| HIRF | Cellular interferon regulatory factor |
| HIV | Human immunodeficiency virus |
| HSV | Herpes simplex virus |
| HVS | Herpesvirus saimiri |
| IAV | Influenza A virus |
| IE | Immediate-early |
| IFN $\alpha/\beta$ $R^{-/-}$ | Interferon $\alpha/\beta$ receptor gene knockout mice |
| IFN | Interferon |
| Ig | Immunoglobulin |
| IL | Interleukin |
| IL-8R | IL-8 receptor |
| IM | Infectious mononucleosis |
| IRF | Interferon regulatory factor |
| INOS | Inducible nitric oxide synthase |
| KS | Kaposi's sarcoma |
| KSHV | Kaposi's sarcoma-associated herpesvirus |
| LANA | Latency-associated nuclear antigen |
| LC | Langerhans cell |
| LCL | Lymphoblastoid cell lines |
| LCMV | Lymphocytic choriomeningitis virus |
| LHΔgfp | Recombinant MHV-68 virus |
| LUR | Long unique coding region |
| MA | Membrane antigen |
| MACS | Magnetic activated cell sorting |
| MCMV | Murine cytomegalovirus |
| MHC | Major histocompatability complex |
| MHV-68 | Murine gammaherpevirus-68 |
| MIP | Macrophage-inflammatory proteins |

| | |
|---|---|
| MLN | Mediastinal lymph node |
| mRNA | Messenger ribonucleic acid |
| NBCS | New born calf serum |
| NK | Natural killer cells |
| PE | Phycoerythrin |
| ORF | Open reading frames |
| PBS | Phosphate buffered saline |
| PECs | Peritoneal exudate cells |
| PEL | Primary effusion lymphomas |
| PFU | Plaque forming unit |
| PKR | Protein kinase R |
| POD | Peroxidase |
| Pp | Phosphoprotein |
| R | Receptor |
| Rb | Retinoblastoma protein |
| RNA | Ribonucleic acid |
| RT-PCR | Reverse transcription-polymerase chain reaction |
| SCID | Severe combined immuno-deficient mice |
| sIg | Surface immunoglobulin |
| SP-A | Surfactant protein-A |
| SWB | Staining wash buffer |
| TAP | Transporter associated with antigen processing |
| TBS | Tris buffered saline |
| TLN | Thoracic lymph node |
| Th | T helper |
| TNF-$\alpha$ | Tumour necrosis factor |
| TPA | Tetra decanoylphorbol acetate |
| TPB | Tryptose phosphate broth |
| TRITC | Tetramethyl rhodamine isothiocyanate |
| tRNA | Transfer ribonucleic acid |
| VCA | Virus capsid antigen |
| v-cyclin | Viral cyclin |

| | |
|---|---|
| vFLIP | Viral FLICE inhibitory protein |
| vIRF | Interferon regulatory factor homologues |
| VSV | Vesicular stomatitis virus |
| WT129 | Wild type 129/Sv/Ev mice |
| μMT | B cell deficient mice |

# CHAPTER ONE

# INTRODUCTION

## 1.1 Herpesviruses: a general introduction

The Herpesviruses are large double stranded DNA viruses, classification of which was previously based on the architecture of the virion. A typical herpesvirion consists of a core containing linear double stranded DNA, an icosadeltahedral capsid, a proteinaceous tegument and an envelope with lipid membrane carrying external glycoproteins (Schrag *et al.*, 1989). The family Herpesviridae comprises over 100 viruses that infect a wide range of vertebrates (Roizman *et al.*, 1992). These viruses are ubiquitous but are usually host specific and infection is restricted to a single species. Herpesviruses vary in their biology, but one common feature is their ability, following primary infection, to establish life-long latent infections.

On the criteria of host range, duration of reproductive cycle, cytopathology and characteristics of latent infection herpesviruses have been divided into three sub-families: the Alpha-, Beta-, and Gamma Herpesvirinae (Roizman *et al.*, 1992). More recently classification has been reviewed and it now takes into consideration gene content and sequence similarities.

Alphaherpesvirinae have a variable host range in cell culture, have a short growth cycle, spread rapidly with efficient destruction of infected cells and are neurotropic in that they can establish latent infection primarily in sensory ganglia. Examples are Herpes simplex type 1 & 2 (HSV-1 and HSV-2) and Varicella zoster virus which infect humans. This subfamily comprises the Simplexvirus and Varicellovirus genera.

Betaherpesvirinae have a narrow host range, long reproductive cycle in cell culture with slow virus spread. Infected cells become enlarged. Virus may become latent in secretory glands and lymphoreticular cells. Examples are Cytomegalovirus (CMV)

and human herpesviruses 6 & 7 (HHV 6 and HHV 7) which infect humans. This subfamily comprises of Cytomegalovirus and Muromegalovirus genera.

Gammaherpesvirinae are associated with lymphoproliferative diseases in their natural hosts, and infect lymphoblastoid cells *in vitro*. These viruses are specific for B and T lymphocytes, in which they are found latent. Examples are Epstein-Barr virus (EBV) and Kaposi's sarcoma-associated herpesvirus (KSHV) which infect humans. This subfamily includes two genera: the lymphocryptovirus (γ1) and rhadinovirus (γ2). EBV is the prototype lymphocryptovirus (Kieff, 1996). Herpesvirus saimiri (HVS) is the prototype for the rhadinovirus genus. KSHV has also been classified as a rhadinovirus.

All herpesviruses specify enzymes and other factors involved in nucleic acid synthesis metabolism, as well as a variable number of enzymes in DNA metabolism. Herpesviruses specify at least one protease and a variable number of protein kinases. DNA synthesis is initiated from one or more origins of DNA replication and genome head-to-tail concatamers appear to be generated by a rolling circle mechanism. The synthesis of viral DNA and assembly of capsids occur in the nucleus. Envelopment of the capsid as it transits through the nuclear membrane is obligatory. Production of infectious progeny virus is invariably accompanied by the irreversible destruction of infected cells. The herpesviruses examined are able to remain latent in their natural hosts. In cells harbouring latent virus, the viral genome takes the form of closed circular molecules, where only a small subset of viral genes are expressed (Roizman *et al.*, 1992).

Herpesviruses persist within their hosts primarily in a state of latency, with only occasional interruptions in the form of lytic infections. Latency is defined as the inability to recover infectious particles from disrupted cells that harbour the virus. This condition should be distinguished from a persistent infection in which a low level of viral replication and infectious particles are recoverable from disrupted cells. Once thought to be completely dormant, latent herpesvirus genomes are now

recognised to be transcriptionally active. As many as 10 viral transcripts in EBV and as few as one in Herpes simplex virus have been identified during latency.

Lytic genes can be divided into immediate early (IE) or α genes which are transcribed prior to viral protein synthesis, early or β genes which are transcribed in the absence of viral DNA synthesis, and late or γ genes which represent the structural proteins, and are expressed only after viral DNA synthesis (Honess and Roizman, 1974).

## 1.2 Gammaherpesviruses

The Gammaherpesvirus subfamily includes viruses that can establish latent infection in lymphocytes as well as cause cell proliferation. This subfamily has also been associated with the ability to cause malignancies in a related foreign host, although under specific conditions natural hosts develop malignancies too e.g. EBV and KSHV in humans. Table 1.1 lists the characteristics of gammaherpesviruses and the lymphomas caused in their respective natural host or a related foreign host. The human gammaherpesviruses EBV and KSHV are dealt with in the following sections with emphasis on the genes encoded by these viruses.

## 1.3 Epstein-Barr virus

Epstein-Barr virus, a human gammaherpesvirus with a marked tropism for B lymphocytes, is carried by a vast majority of individuals as a life-long asymptomatic infection. However in some cases it acts as the causative agent of infectious mononucleosis (IM). EBV is also strongly linked to at least three lymphoid malignancies: endemic Burkitt's lymphoma, the immunoblastic B cell lymphomas seen in immunocompromised patients, and a subset of cases of Hodgkin's disease, as well as to the epithelial tumour, nasopharyngeal carcinoma (Rickinson and Kieff, 1996, Epstein and Crawford, 1998). This is believed to be due to the potent growth-transforming ability of the virus, which maps to a specific subset of genes, namely the latency genes. Allelic polymorphism in some of the latency genes defines two

| Virus common name | Designation | Host | Disease association in normal host | Disease association in other species | References |
|---|---|---|---|---|---|
| Epstein-Barr Virus (EBV) | Human Herpesvirus 4 | Human | Infectious mononucleosis<br>Burkitt's lymphoma<br>Nasopharyngeal carcinoma<br>Hodgkin's lymphoma | Lymphoproliferative disease in cotton-top tamarins | Epstein & Crawford 1998, Kieff, 1996, Rickinson & Kieff, 1996 |
| Kaposi's sarcoma associated herpesvirus (KSHV) | Human herpesvirus 8 | Human | Kaposi's sarcoma<br>Multicentric Castleman's disease | | Chang *et al.*, 1994, Moore *et al.*, 1996 Boshoff & Chang, 2001 |
| Herpesvirus papio (HVP) | Cercopithecine herpesvirus 12 | Baboon | | | Heller & Kieff, 1981 |
| African green monkey EBV-like virus | Cercopithecine herpesvirus 14 | African green monkey | | | Blakely *et al.*, 1973 |
| African green monkey gamma-2 herpesvirus (ChRV 1 & 2) | Chlorocebus rhadinovirus 1<br>Chlorocebus rhadinovirus 2 | African green monkey<br>African green monkey | | | Greensill *et al.*, 2000<br>Greensill *et al.*, 2000 |
| Rhesus rhadinovirus (RRV) | | Rhesus monkey *Macaca mulatta* | | | Desrosiers *et al.*, 1997 |
| Retroperitoneal fibromatosis herpesvirus (RFHVMm) | | Rhesus monkey *Macaca mulatta* | Retroperitoneal fibromatosis | | Rose *et al.*, 1997 Bosch *et al.*, 1999 |
| Retroperitoneal fibromatosis herpesvirus (RFHVMn) | | Rhesus monkey *Macaca nemestrina* | Retroperitoneal fibromatosis | | Rose *et al.*, 1997 |

**Table 1.1.** Characteristics of the gammaherpesviruses. (Continued).

| Virus common name | Designation | Host | Disease association in normal host | Disease association in other species | References |
|---|---|---|---|---|---|
| Rhesus EBV-like herpesvirus | Cercopithecine herpesvirus 15 | Rhesus monkey *Macaca mulatta* | Malignant lymphoma | Malignant lymphomas in rabbits | Rangan *et al.*, 1986 |
| EBV-related herpesvirus of *Macaca arctoides* | | Rhesus monkey *Macaca arctoides* | Lymphoma | | Wutzler *et al.*, 1995 |
| Chimpanzee KSHV-like virus | Pan rhadinovirus 1a | African green monkey | | | Lacoste *et al.*, 2000 |
| | Pan rhadinovirus 1b | African green monkey | | | Lacoste *et al.*, 2000 |
| Gorilla KSHV-like virus | Gorilla rhadinovirus 1 | Gorilla | | | Lacoste *et al.*, 2000 |
| Herpesvirus pan | Pongine herpesvirus 1 | Chimpanzee | | | Heller *et al* 1982 |
| Herpesvirus pong | Pongine herpesvirus 2 | Orangutan | | | Rasheed *et al.*, 1977 |
| Herpesvirus gorilla | Pongine herpesvirus 3 | Gorilla | | | Neubauer *et al.*, 1979 |
| Herpesvirus ateles | Ateline herpesvirus 2 | Spider monkey | | | Deinhardt *et al.*, 1973 |
| Herpesvirus saimiri | Saimiriine herpesvirus1 | Squirrel monkey | | Fatal T lymphoproliferations in other New World monkeys (e.g. marmosets and Owl monkeys) | Simonds *et a*l., 1975 |
| Movar herpesvirus | Bovine herpesvirus 4 | Cows | | | Bublot *et al.*, 1990 |
| Sheep-associated malignant catarrhal fever of cattle herpesvirus | Ovine herpesvirus 2 | Sheep | | Malignant catarrhal fever in cattle | Bridgen & Reid, 1991 |

**Table 1.1**. Characteristics of the gammaherpesviruses (Continued)

| Virus common name | Designation | Host | Disease association in normal host | Disease association in foreign host | References |
|---|---|---|---|---|---|
| Wilderbeest herpesvirus | Alcelaphine herpesvirus 1 | Wildebeest | | Malignant catarrhal fever of European cattle | Bridgen *et al.*, 1989, |
| Goat-associated malignant catarrhal fever | Caprine herpesvirus 2 | Domestic goat | Malignant catarrhal fever | | Li *et al.*, 2001a<br>Chmielewicz *et al.*, 2001 |
| Porcine lymphotropic herpesvirus 1 (PLHV-1) | | Domestic and feral pigs | | | Ulrich *et al.*, 1999<br>Ehlers *et al.*, 1999 |
| Porcine lymphotropic herpesvirus 2 (PLHV-2) | | Domestic and feral pigs | | | Ulrich *et al.*, 1999<br>Ehlers *et al.*, 1999 |
| Hartebeest herpesvirus | Alcelaphine herpesvirus 2 | Hartebeest | | | Reid & Rowe , 1973 |
| Guinea-pig herpesvirus 1 | Caviid herpesvirus 1 | Guinea-pig | | | Bhatt *et al.*, 1971 |
| Equine herpesvirus 2 | Equid herpesvirus 2 | Horse | | | Telford *et al*, 1993 |
| Equine herpesvirus 5 | Equid herpesvirus 5 | Horse | | | Telford *et al*, 1993 |
| Gammaherpesvirus of seals | Phocid herpesvirus 2 | Seal | | | Harder *et al.*, 1996 |
| Herpesvirus sylvilagus | Leproid herpesvirus 1 | Cottontail rabbit | Lymphoproliferative disease and lymphomas | | Hinze, 1971 |
| Woodchuck herpesvirus | Marmoid herpesvirus1 | Woodchuck | | | Schechter *et al.*, 1988 |
| Murine γ-herpesvirus 68 | Murid herpesvirus 4 | Voles and mice | Lymphomas | | Blaskovic *et al.*, 1980 |
| MHV-Brest | Murid herpesvirus 7 | Shrew *Crocidura russula* | | | Chastel *et al.*, 1994 |

**Table 1.1**. Characteristics of the gammaherpesviruses. Adapted from Stewart *et al.*, 1999.

broad types of EBV isolates, type 1 and type 2, which show subtle differences in transforming function. Spread of EBV occurs by close contact. Primary infection classically occurs sub-clinically during childhood. Subsequently individuals become life-long virus carriers. Primary infection results in IM in around 50% of cases. IM is a benign lymphoproliferative disease, which has been extensively studied as a model for primary EBV infection and establishment of latency (Rickinson and Kieff, 1996). EBV enters the body through the mouth and replicates in the oropharynx, producing infectious virus into the oral cavity (Faulkner *et al.*, 2000). The cellular site of this replication is unclear, it is assumed that either some squamous epithelial cells in the oropharynx become infected or that intraepithelial B-cells in this region are infected directly (Anagnostopoulos *et al.*, 1995). Studies on X-linked agammaglobulinemia (lack of mature B cells) individuals showed no evidence of EBV infection indicating that in the absence of B cells the environment is non-permissive for EBV latency (Faulkner *et al.*, 1999).

### 1.3.1 Lytic Infection

There is no effective *in vitro* culture system which mimics EBV lytic cycle phase, and hence different methods and partially permissive cells lines have been developed over time to overcome this problem. Genes expressed during the EBV lytic cycle have been characterised in EBV infected lymphoblastoid cell lines (LCL) induced by various agents, e.g. tetra decanoylphorbol acetate (TPA) (zur Hausen *et al.*, 1978). A few cell lines can be consistently induced to permit lytic virus replication in 10% of the cells. One cell line, Akata, can be induced to higher levels of lytic infection by cross-linking surface immunoglobulin (sIg) and is currently the best source of large quantities of EBV (Takada and Ono, 1989). As with other herpesviruses, transcription follows a certain pattern, each set of genes being activated by the previous set.

Induction of lytic infection in Akata cells by sIg cross-linking and incubation of the cells in the presence of moderately high concentrations of inhibitors of protein synthesis (cyclohexamide) results in expression of the BZLF1 (Z) and BRLF1 (R) mRNA, indicating that these are immediate early gene products (Takada and Ono, 1989). The products of these two genes are transactivators of early genes and are

derived from three mRNA species, one of which encodes both R and Z sequences (Kieff, 1996). Z is a DNA binding protein that shows homology to the DNA binding domain AP1 (Sinclair *et al.*, 1991). The Z and R promoters (Zp, Rp) contain AP1 sites and so Z transactivates its own activity as well as that of R gene. Z facilitates the transition from latent to lytic infection. Subsequently R protein too has been shown to have the capacity to disrupt viral latency both in epithelial cells and in B cells (Zalani *et al.*, 1996, Rogoczy *et al.*, 1998). Z appears to associate with p53, which could lead to the inhibition of apoptosis during EBV DNA replication (Zhang *et al.*, 1994). As p53 plays an important role in cell cycle regulation, Z is also thought to be able to arrest cell cycle progression and facilitate viral DNA replication. R interacts with another cell cycle regulator retinoblastoma (Rb) protein and it is thought to function in a similar fashion (Zacny *et al.*, 1998). Z and R transactivate early genes such as BMRF1 (Biggin *et al.*, 1987), BHRF1 (Hardwick *et al.*, 1988) and BRLF1 (Sinclair *et al.*, 1991).

Early genes are differentiated from late genes by their synthesis in the presence of inhibitors of viral DNA synthesis (Baer *et al.*, 1984, Biggin *et al.*, 1987). The genes expressed include BMLF1, BMRF1, BHRF1 and BORF2 as well as others involved in viral DNA replication (Hardwick *et al.*, 1988). Some of the components involved in lytic viral DNA replication include BALF5, which encodes the core DNA binding protein; BALF2, the single strand DNA binding protein; BMRF1, the processivity factor; BSLF1 and BBLF4, the primase and helicase complex; BBLF2/3, a spliced primase-helicase complex component and BKRF3, the uracil DNA glycosylase (Baer *et al.*, 1984, Kieff, 1996).

The viral capsid proteins have not been analysed in detail due to lack of a fully lytic system *in vitro*. The major capsid protein p160 is encoded by BALF4 open reading frame (ORF). Seven EBV encoded glycoproteins have been identified, three of which become components of the viral envelope (Kieff, 1996). Two, gp350/220 and gp85 have been studied in detail because they induce production of neutralising antibodies and are potential vaccine candidates (Thorley-Lawson and Geilinger, 1980). Gp350/220 is coded by the BLLF1. Alternate splicing of mRNA creates the

two forms of the protein. Gp350/220 mediates virus attachment to the B cell surface by binding to the EBV receptor CR2 (also called CD21) (Nemerow *et al.*, 1987). Thus both naturally occurring and experimentally induced antibodies to gp350/220 prevent infection by blocking attachment.

### 1.3.2 EBV Latency

There are at least three latency types defined in EBV, as latency I, II and III, based upon the differential expression of latent genes. *In vitro* EBV infection of human B lymphocytes leads to the establishment of latently infected transformed LCL. The latency in LCL is called latency type III. The lymphocytes are immortal and can cause tumours when injected into severe combined immuno-deficient mice (SCID) mice (Rowe *et al.*, 1991). In LCL the viral genome is seen in a circular episomal form. A limited number of EBV genes are expressed in latently infected LCL cells, these include genes encoding the six nuclear antigens, EBNA1, 2, 3A, 3B, 3C and leader protein (LP) and the three membrane associated proteins LMP1, LMP2A and LMP2B. In addition LCL show abundant expression of small RNA's, EBER1 and EBER2. It is thought that six latent proteins (EBNA1, 2, 3A and 3C, LMP1 and EBNA-LP) are required for B-cell transformation (Hammerschmidt and Sugden, 1989, Cohen *et al.*, 1989, Kaye *et al.*, 1993). The LMP2 proteins are thought to function in the maintenance of EBV latency, possibly through blocking a switch into lytic cycle after signalling through the B cell antigen receptor complex (Miller *et al.*, 1995). LCL generated by EBV infection of B cells at different stages of differentiation all display the same cell surface phenotype and characteristic growth in cell aggregates. EBV immortalised LCL express B cell activation antigens CD23, CD30, CD39 and CD70 and the cellular adhesion molecules LFA1 (CD11a/18), ICAM1 (CD54) and LFA3 (CD58) (Wang *et al.*, 1990, Rowe *et al.*, 1991). Kempkes *et al* (1995) demonstrated that expression of EBNA2 in B cells resulted in up-regulation of the same cellular proteins as did polyclonal activation of primary B cells.

In contrast to the above pattern of virus latent gene expression that characterises LCL, a second type of non-productive EBV infection, designated 'latency I' has been

identified in Burkitt's lymphoma biopsy cells/cell lines. These cells typically express EBNA1, EBER and BamH1A transcripts, whereas the remaining EBNAs (EBNA2, EBNA3A, 3B, 3C & LP) and three membrane proteins (LMP1, 2A & 2B) seen in 'latency III' are not detectable (Rowe *et al.*, 1987). However, during early passage EBV positive BL cells (latency I) are not stable and move towards a latency III pattern of gene expression. An alternate pattern of transcription, 'latency II', is seen in Reid-Sternberg cells in EBV positive Hodgkin's disease and the malignant epithelial cells of nasopharyngeal carcinoma. Here EBNA1 is expressed along with LMP1 and 2. Several studies have addressed a potential role of DNA methylation in the control of viral gene expression and virus latency (Robertson and Ambinder, 1997).

EBV latency patterns *in vivo* in asymptomatic carriers provide us with clearer ideas about the mechanisms the virus uses to establish life-long latency in humans. EBV latency in the peripheral blood was found mainly restricted to the resting memory B cells (Miyashita *et al.*, 1995, Babcock *et al.*, 1998). These cells, unlike EBV immortalised B cells *in vitro*, do not express CD23 and are in a $G_o$ state in cell cycle (Miyashita *et al.*, 1995, 1997). Infected cells were also found to down-regulate the co-stimulatory molecule B7. This could prevent effective recognition by cytotoxic T cells and help escape immune surveillance. EBV positive resting memory B cells obtained from the peripheral blood expressed only LMP2A gene (Miyashita *et al.*, 1997). The LMP2A expression *in vivo* in B cells has been proposed as the true "latency-program". Subsequent studies were able to show that memory B cells from the tonsillar tissues of healthy carriers express EBNA1 from the Qp promoter as well as LMP1 and LMP2 (Babcock *et al.*, 2000a). This was the first demonstration *in vivo* in normal B cells unlike in EBV-associated tumour cells where this pattern of gene expression was shown to be present. On the other hand naïve B cells isolated from the tonsils were found to express EBNA2, LMP1and LMP2 (Babcock *et al.*, 2000b). However, as all these different EBV gene expression patterns *in vivo* are unravelled, it is becoming clearer that EBV uses the normal B cell differentiation biology to gain access to long-lived memory B cells.

## 1.4 Kaposi's sarcoma-associated herpesvirus

Kaposi's sarcoma (KS) is the most frequent neoplastic complication seen in patients infected with human immunodeficiency virus (HIV) and is especially prevalent in male homosexual AIDS patients. In 1994, Yuan Chang, Patrick Moore and colleagues at the Columbia University identified DNA sequences belonging to a new infectious agent in AIDS-related KS patients. They used a PCR based technique called representational difference analysis (RDA) in which short restriction fragments from KS lesion tissues were compared to unaffected tissues from the same patient. The sequences obtained showed close similarity to HVS and EBV sequences however there were distinct tegument and capsid gene sequences indicating it was a novel DNA sequence (Chang *et al.*, 1994). These sequences were also identified in non-Hodgkin's lymphomas in HIV-positive patients, especially in body cavity-based lymphomas (BCBL). Cell lines established from these were termed BC-1 and BC-2 (Cesarman *et al.*, 1995). Primary sequence characterisation showed that the DNA in the nucleus was in an episomal form, a characteristic feature of herpesviruses. Phylogenetic analyses showed that this was a gamma-2-herpesvirus of the Rhadinovirus genus, the first member identified in humans (Moore *et al.*, 1996b). They called it Kaposi's Sarcoma-Associated Herpesvirus (KSHV). Being the eighth human herpesvirus, it is also designated human herpesvirus 8 (HHV-8). Further evidence of KSHV as the infectious agent was seen when BCBL derived cell lines treated with TPA produced herpesvirus like particles (Renne *et al.*, 1996). The genome was fully sequenced and mapped using cosmid and phage genomic libraries from BC-1 cell line (Russo *et al.*, 1996). In addition to body cavity-based large cell lymphomas, KSHV has also been found in HIV-seropositive patients with multicentric Castleman's disease (MCD). Like EBV, KSHV has been detected in latently infected B lymphocytes, endothelial cells and pluripotent mesenchymal precursors (Boshoff, 1998).

### 1.4.1 Viral genes of KSHV

The KSHV genome sequenced from the primary effusion lymphomas (PEL) cell lines (BC-1), consists of 140.5 kb long unique coding region (LUR) flanked by

approximately 800 bp terminal repeat sequences with high G/C content (Russo *et al.*, 1996). In the KSHV LUR, 81 open reading frames (ORF) have been identified, including 66 with sequence similarity to HVS ORFs. Like other gammaherpesviruses KSHV has blocks of conserved genes that are required for the replication and assembly of virus progeny. They include major structural proteins, DNA synthetic enzymes, glycoproteins, assembly protein, dihydrofolate reductase and thymidylate synthase (Moore *et al.*, 1996b, Russo *et al.*, 1996). The non-conserved gene blocks of KSHV are genes that are found in other rhadinoviruses, and also some that are unique to KSHV designated K1-K15 (Russo *et al.*, 1996, Nicholas *et al.*, 1997a, Dittmer *et al.*, 1998). An extraordinary number of recognisable genes pirated from eukaryotic cellular DNA are encoded by KSHV. KSHV encodes several homologues of cellular proteins which are also up-regulated by EBV latent proteins, suggesting that both viruses might employ the same cellular signalling pathways to survive in their host (Moore *et al.*, 1996a). So far, there are at least 14 reading frames of KSHV that are homologous to known cellular genes. Although for most of these captured genes it is not very likely that they are essential for virus replication in cell culture, they may have important functions in the natural habitat of the virus. Virus encoded cyclin, interleukin (IL)-6, and IL-8 receptor enhance cell proliferation and may thus expand the pool of infected cells. The three macrophage-inflammatory proteins (MIP-I, II and III) might help in attracting susceptible cells. Apoptosis is a typical response of the host to infection by a virus. KSHV carries two genes ORF16 (viral bcl-2 or vbcl-2) and ORFK13 (viral FLICE inhibitory protein or vFLIP) both of which can prolong the life span of infected cells through the inhibition of apoptosis by different mechanisms. These pirated genes with functions similar to cellular genes will be discussed in more detail in the following sections.

The team from Columbia University has classified KSHV gene transcription into three classes. Class I genes, such as those encoding viral cyclin (v-cyclin or ORF72), latency-associated nuclear antigen (LANA; ORF73) and vFLIP (ORFK13), are constitutively transcribed in latently infected PEL cells and are unaffected by TPA induction. Class II genes are transcribed without TPA stimulation of cells, but are induced to higher transcription levels by TPA treatment (includes the vIL-6, vIRF

and vMIP-II). Class III genes are primarily structural and replication genes that are transcribed only following TPA treatment and are thus mainly responsible for lytic virion production (Sarid *et al.*, 1998).

The class I genes ORF72 and ORF73 were reported as a cluster of latently expressed genes in KSHV (Dittmer *et al.*, 1998). These transcripts are found in BCBL-1 cells prior to TPA induction. They were also expressed in >70% of KS spindle cells in primary KS tumours which confirmed that these transcripts are indeed latent RNA and suggested a role for their product in viral persistence and in KSHV associated proliferation. Two major latent transcripts encoding v-cyclin were mapped using 5'RACE (5' rapid amplification of cDNA ends). They are LT1 and LT2 and both transcripts are spliced. They have the same start site, and encode ORFK13 (vFLIP) and ORF72 (v-cyclin). The latency-associated nuclear antigen (LANA; ORF 73) is encoded by LT1 but is spliced from LT2. It is proposed that by encoding these essential genes as a cluster, KSHV could control the expression of these genes depending on different cell cycle signals and latency patterns during the course of infection (Sarid *et al.*, 1999).

### 1.4.2 Cell cycle regulation by KSHV

Work on tumour viruses has shown that they tend to exploit the cell cycle checkpoints that are normally controlled by regulatory molecules such as D-type cyclins, pRb (retinoblastoma) and p53. KSHV ORF 72 codes a cellular homologue of the D-type cyclin, v-cyclin (Chang *et al.*, 1996). The function of cyclins within a cell is to bind to cyclin dependent kinases (cdk) and this complex is able to phosphorylate cell cycle checkpoint proteins allowing the cell to move from G1 phase into S phase. KSHV v-cyclin was found to have kinase activity and the ability to phosphorylate retinoblastoma protein (Rb) *in vitro*. When v-cyclin was co-expressed with Rb in SAOS-2 osteosarcoma cells, it was able to reverse the cell cycle block caused by Rb (Chang *et al.*, 1996). KSHV v-cyclin complexed with Cdk6 was shown to phosphorylate not only Rb but also histone H1. This was distinctly different from the activity of cellular cyclin D-cdk6 kinase (Godden-Kent *et al.*, 1997). Viral cyclin was found expressed in primary KS biopsies and in PEL

(Chang *et al.*, 1996, Cesarman *et al.*, 1996). In normal cells, proteins such as cdk inhibitors would regulate cyclin/cdk complex activity. The v-cyclin was shown to form active complexes with cdk6 and this complex is resistant to inhibition by cdk inhibitor proteins such as p16, p21 and p27 (Godden-Kent *et al.*, 1997, Swanton *et al.*, 1997). They also showed that the osteosarcoma cell line U2-OS when transiently transfected with cdk inhibitors (p16, p21 or p27), underwent a G1 arrest but on co-transfection with v-cyclin the cells overcame the inhibition. It was later shown that v-cyclin/cdk6 complex phosphorylates $p27^{kip}$ and destabilises this inhibitor. They were also able to isolate $p27^{kip}$ phosphorylating cdk6 complex from cells lines derived from PEL and KS lesions (Ellis *et al.*, 1999).

Viral cyclin/cdk6 complex was shown to induce apoptosis in U2OS and COS-7 cells and this was not prevented by cellular bcl-2 (Ojala *et al.*, 2000). On the other hand vbcl-2 was able to prevent apoptosis induced by v-cyclin/cdk6 complex to a large extent. It was shown that v-cyclin and cellular cdk6 complex can phosphorylate bcl-2 and inactivate the anti-apoptotic function and induce apoptosis in cells expressing large quantities of both v-cyclin and cdk6. This could be a mechanism the virus uses to negatively regulate the v-cyclin/cdk6 induced proliferation.

### 1.4.3 Apoptosis regulation by KSHV

KSHV ORF16 encodes a viral bcl-2 molecule that is homologous to other gammaherpesvirus bcl-2 genes such as EBV BHRF1 and HVS ORF16. Bcl-2 family members can block cell death caused by growth factor deprivation, γ-irradiation and cytotoxic drugs. In a cell, the bcl-2 molecule is an inhibitor of apoptotic death but some other members in this family such as bax and bak are promoters of apoptosis. These proteins are expressed in normal cells and interact with each other maintaining a critical balance. However, when the cell is subjected to stress this balance is disrupted and the cell will either undergo apoptosis or survive depending on the levels of these different proteins (Meinl *et al.*, 1998).

KSHV vbcl-2 has conserved domains similar to human bcl-2, BH (Bcl homology) 1 and BH-2 domains are well conserved while BH-3 is poorly conserved. These

domains in cellular bcl-2 are normally involved in the formation of homodimers or heterodimers (Cheng *et al.*, 1997). KSHV vbcl-2 is found in low levels in BCBL cell lines but on stimulation with TPA higher levels are induced and therefore categorised under class II genes (Sarid *et al.*, 1998). Over expression of vbcl-2 inhibits Sindbis Virus-I induced apoptosis in cells. Co-immunoprecipitaion and yeast two-hybrid analysis have shown that vbcl-2 neither homodimerizes nor heterodimerizes with cellular bcl-2, bcl-$x_L$, bax or bak (Cheng *et al.*, 1997). It has been speculated that by not binding to proapototic molecules such as bax and bak within infected cells vbcl-2 escapes from negative regulation by these molecules.

KSHV ORFK13 encodes viral FLICE inhibitory protein (vFLIP) which is involved in inhibiting Fas induced apoptosis (Thome *et al.*, 1997), the first evidence of such a specialised molecule. Thome *et al* (1997) were also able to find similar sequences to vFLIP encoded by HVS, EHV-2, BHV-4 and a human mollusci poxvirus (*Molluscum contagiosum* virus, MCV). FLIP protein was subsequently detected in uninfected cellular cytoplasm as well. Cytotoxic T cells expressing FasL (Fas-Ligand) can trigger apoptosis in virus infected cells through Fas/FasL interactions. The KSHV-FLIP expressing B cell lymphoma cells when injected into mice developed tumours that were resistant to apoptosis triggered by T cells, indicating vFLIP to be a tumourigenic factor (Djerbi *et al.*, 1999).

### 1.4.4 Cytokine and Chemokine regulation by KSHV

KSHV gene ORFK2 codes for a vIL-6 that is 25% identical to human IL-6 and is a secreted cytokine which maintains proliferation of IL-6 dependent cells lines (Moore *et al.*, 1996a; Nicholas *et al.*, 1997a). The specific function is unknown but it is speculated that the KSHV cytokine would behave in a similar fashion to cellular IL-6 that is induced by EBV (Tanner *et al.*, 1996). Cellular IL-6 has been demonstrated to be a paracrine or autocrine growth factor (Tosato *et al.*, 1990) for EBV-immortalised B cells, resulting in increased immunoglobulin (Ig) production and B cell immortalization. It has also been shown that if IL-6 is expressed at high levels in EBV immortalised cells, it will promote tumour formation by impairing the activity of natural killer (NK) cells. Studies on vIL-6 using ELISA and co-

immunoprecipitation assays have shown that vIL-6 can bind directly to receptor subunits gp130 and IL-6R. Viral IL-6 can also induce gp130 and IL-6R complex formation (Li *et al.*, 2001b). However the vIL-6 is different from the cellular IL-6 in that it can signal through the gp130 subunit alone while the cellular IL-6 needs both gp130 and IL-6R complex for effective signalling. KSHV vIL-6 has been classified as a class II gene which is seen in BC-1 cells, but can be induced to higher levels on TPA treatment (Moore *et al.*, 1996a). Comparative studies on the expression of vIL-6 in KS and multicentric Castleman's disease (MCD) have shown that vIL-6 can be found co-localised mainly in the nucleus of lymphoid cells in MCD tissues and also at very low frequencies in the spindle cells of KS. It is believed that vIL-6 can be expressed in latently infected cells even in the absence of replicative cycle (Brousset *et al.*, 2001). There is evidence of vIL-6 in the sera of both classical KS patients as well as KS positive HIV+ patients. Higher levels of serum IL-6 were detected in HIV+ patients even in the absence of malignancies such as KS, PEL or MCD. It is believed this is due to increased replicating virus in an immune deficient environment (Aoki *et al.*, 2001).

KSHV gene ORFK4, K4.1 and K6 code for proteins that have homology to the chemokine macrophage inflammatory protein (MIP) family of proteins and are named the vMIP-II, vMIP-III and vMIP-I respectively (Moore *et al.*, 1996a; Russo *et al.*, 1996; Nicholas *et al.*, 1997b). ORFK4 and ORFK6 code for CC chemokines. They are expressed at low levels in BCBL cells and can be induced with TPA treatment. HIV requires attachment to chemokine receptors along with CD4 for cellular entry and therefore CC and CXC chemokines can block chemokine coreceptors and prevent virus entry. Synthetic peptides derived from vMIP-II (Klendal *et al.*, 1997, Boshoff *et al.*, 1997) and vMIP-I sequences (Boshoff *et al.*, 1997) showed the KSHV chemokines to have significant HIV inhibitory activity. Viral MIP-II acts as an antagonist by binding to members of the G-protein coupled-receptor (GPCR) CCR3, CCR5 and CXCR4 families (Klendal *et al.*, 1997). KSHV vMIP-II also acts as an agonist and signals through CCR3 leading to eosinophil chemotaxis (Boshoff *et al.*, 1997). KSHV vMIP-II has amino acid sequence homology of 37-43% to other cellular CCR3 agonists such as Eotaxin-1, RANTES

and MCP-3, but it exhibits distinct topology that is unique to vMIP-II particularly in the presumed receptor binding site (Moore *et al.*, 1996a, Fernandez *et al.*, 2000). Although these genes were originally pirated from cellular genes they have evolved over time to help the virus and give it a growth advantage over the host. For example, vMIP-I and vMIP-II induce new blood vessel formation or angiogenesis in the chick chorioallantoic membrane. This angiogenic activity may play an important role in KSHV derived tumours (Boshoff *et al.*, 1997).

KSHV ORFK9 encodes a protein homologous to interferon regulatory factor (vIRF-1) (Russo *et al.*, 1996). Viral IRF is expressed in moderate amounts similar to IL-6 in BC-1 cell lines even before treatment with TPA (Sarid *et al.*, 1998). ORFK9 expression inhibits interferon (IFN)-$\alpha$ and IFN-$\gamma$ signalling although no direct binding of vIRF-1 to the DNA binding domains of IFN genes has been detected (Zimring *et al.*, 1998). KSHV vIRF-1 when cotransfected with cellular IRF was found to inhibit the transcription activation of cellular IRF. These *in vitro* assays suggest an important role for vIRF in immune evasion and immune regulation *in vivo*. KSHV genome analysis has shown that it can encode four proteins of IRF family. Other than vIRF-1, two more IRF molecules vIRF-2 and vIRF-3, have been cloned and characterised. Viral IRF-3 was found to down-regulate the synthesis of interferon by inhibiting the activity of cellular IRF-3 and IRF-7 (Lubyova and Pitha, 2000). Detailed characterisation of vIRF-2 has shown that it is a nuclear protein that is constitutively expressed in PEL cell lines. Moreover, vIRF-2 is a class I protein that is expressed along with LANA and vCYC during latency. vIRF-2 interacts with protein kinase (PKR) and inhibits the kinase activity of this protein on activation by double stranded RNA (Burysek and Pitha, 2001). PKR down-regulates protein synthesis by blocking eukaryotic translation initiation factor 2$\alpha$ (eIF-2$\alpha$). Therefore vIRF-2 inhibits interferon mediated surveillance by inhibiting PKR but it is not known whether vIRF-1 and vIRF-2 act in a similar manner or are involved in the inhibition of other pathways.

KSHV ORF74 encodes a viral G-protein coupled-receptor (vGPCR) (Cesarman *et al.*, 1996). The sequence is similar to the human IL-8 receptor (IL-8R) which is the

receptor for CXC chemokines. NIH3T3 cells expressing vGPCR exhibited foci of transformed cells. These cells cause tumours when transferred into nude mice (Bais *et al.*, 1998) indicating that vGPCR alone can lead to transformation of cells. The vGPCR was able to induce constitutive stimulation of down-stream signalling cascades involving JNK/SAPK and p38MAPK kinases. Signalling through this receptor induces vascular endothelial growth factor (VEGF) that can induce angiogenic phenotype in human umbical vein endothelial cells (HUVECs) (Bais *et al.*, 1998). Studies on *Xenopus* oocytes and mammalian cells have shown that constitutively signalling through vGPCR results in depletion of calcium pools within the cell which leads to heterologous desensitisation of responses mediated by other GPCR receptors (Lupu-Meiri *et al.*, 2001). KSHV vGPCR induced constitutive stimulation may be a phenomenon used by the virus for protection from extracellular regulatory factors and survive within cells.

## 1.5 Murine gammaherpesvirus-68

Murine gammaherpesvirus-68 (MHV-68) was originally isolated from *Clethrionomys glarolus* (bank vole) in Slovakia (Blaskovic *et al.*, 1980). Preliminary analysis of the viral genome revealed homology to gammaherpesviruses (Efstathiou *et al.*, 1990a). The infection pattern in mice was similar to that seen in infectious mononucleosis with EBV infection in humans. The observation that MHV-68 establishes infection in B cells that are harboured mainly in the spleen indicated its biological similarity to EBV and other members of the B cell lymphotropic gammaherpesvirus subgroup (Sunil-Chandra *et al.*, 1992b). The genome organisation of MHV-68 as compared to EBV and KSHV is represented in Figure 1.1.

A common feature of gammaherpesvirus infection is the development of lymphoproliferative disorders, such as lymphomas that are seen in humans infected with EBV and KSHV. MHV-68 has been linked to lymphoma induction in mice. 18-24 months after infection 10% of the infected mice developed lymphoproliferative disease, and 50% of these had high-grade lymphomas (Sunil-Chandra *et al.*, 1994). This provides an amenable animal model to study the natural infection and latency of

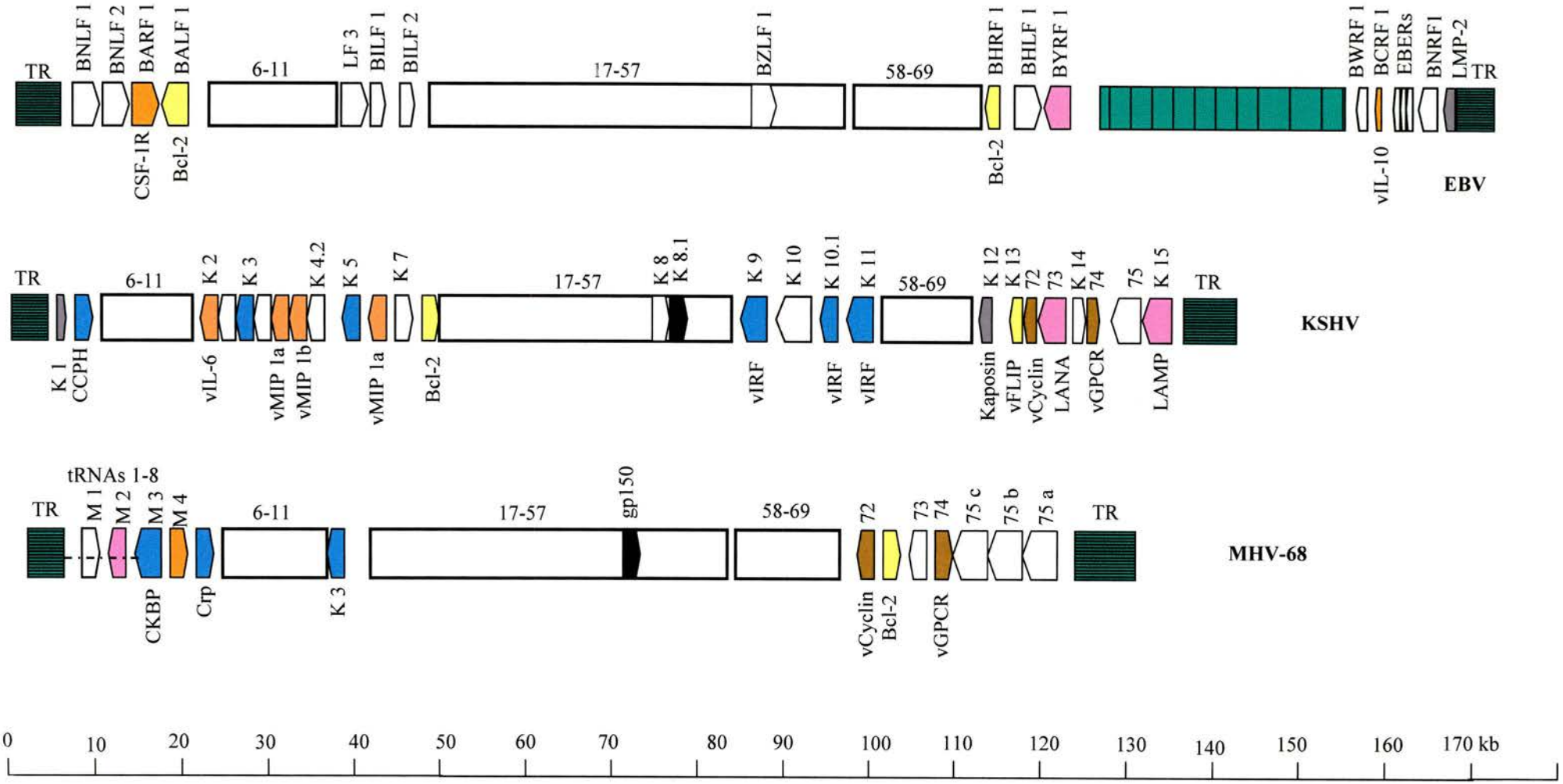


Figure 1.1 The organisation of MHV-68 genome as compared to EBV and KSHV. The open boxes show HV core gene blocks. These are genes involved in DNA replication and virus structure. γ-HV specific genes are indicated above and below the genome structures. Functions of genes are colour coded as: Cytokine, chemokine proteins and receptors ( ), latency associated protein ( ), viral oncogenes ( ), modulators of host immune response ( ), modulators of cell cycle and signal transduction ( ), and regulators of apoptosis ( ).
Diagram adapted from Nash *et al.*, 2001.

gammaherpesviruses. The model is also considered an ideal system for studying the interaction between gammaherpesviruses and the CD4+ and CD8+ T-cell responses in the host system (Doherty *et al.*, 2001). MHV-68 pathogenesis in knockout models offers a good experimental system for assessing the mechanisms underlying compromised immune surveillance and for screening possible chemotherapy-, cytokine-, or cell based protocols to limit gammaherpesvirus associated diseases.

### 1.5.1 MHV-68 genome

The MHV-68 genome has been sequenced (Virgin *et al.*, 1997, Nash *et al.*, 2001). It consists of 118kb unique double-stranded DNA, flanked on either side by terminal repeat region made up of variable number of 1.2kb repeat unit (Efstathiou *et al.*, 1990b). In addition to the terminal repeats the genome contains two internal repeats, a 40bp repeat and a 100bp repeat. There are 80 predicted ORF. Of these ORFs there are blocks of genes that are similar among other gammaherpesviruses including HVS, EBV and KSHV. There is a gene block unique to MHV-68 (M1- M4) located at the left-hand end of the genome interspersed with tRNA like sequences (vtRNA).

The role of the putative vtRNAs is unknown and it is believed that they do not function as tRNAs since five out of eight sequences lack clear anticodons. These vtRNA sequences are expressed both in lytic and latent MHV-68 infected cells. This has proved to be a very useful tool in the detection of virus infected cells using RNA *in situ* hybridisation techniques (Bowden *et al.*, 1997).

In the last couple of years, some of the unique M genes in the MHV-68 genome have been characterised *in vitro*. The M1 gene sequence shows some limited homology to poxvirus serpins, although M1 lacks the active site (Bowden *et al.*, 1997). The M1 gene is found to be most homologous to M3 gene of MHV-68. The characterisation of a mutant MHV-68 lacking four tRNA sequences and the M1 gene showed that these genes were dispensable for lytic replication *in vitro.* Mice infected with this virus showed that these genes did not affect the establishment of latency *in vivo* (Simas *et al.*, 1998). More recently with the help of a M1 gene knockout virus this result was confirmed (Clambey *et al.*, 2000). The mice were infected

intraperitoneally and they carried peritoneal exudate cells (PECs) that harboured latent virus that reactivated with greater efficiency than in the case of wild type MHV-68 infection. It was not established whether the M1 gene and/or a closely linked gene or genes brought this about.

The M2 gene has been identified as a latency-associated gene although with unknown function (Husain *et al.*, 1999). Husain *et al* showed that M2 epitope specific CD8+ T cells could be isolated from infected mice and that a CTL line specific to this epitope can kill S11 cells (MHV-68, latently infected B cell tumour cell line). The M3 gene is found expressed during both lytic and latent stages of the virus infection. It was found to be an abundantly secreted protein (van Berkel *et al.*, 1999). It was subsequently shown to have the capacity to bind to most classes of chemokines, CC-, CXC, C- and CX3C (van Berkel *et al.*, 2000 and Parry *et al.*, 2000). M4 is also characterised as a secreted protein (Wan, unpublished data) and appears early during lytic cycle. Knockout viruses lacking M2, M3 and M4 are being constructed in different laboratories to identify their role in pathogenesis and in immune evasion strategies *in vivo*.

MHV-68 genome encodes homologues of cellular genes such as complement regulatory protein, D-type cyclin, bcl-2 and IL-8 receptor. MHV-68 ORF4 has significant homology to multiple complement regulatory proteins. There are four regions within ORF4, which bear homology to complement regulatory proteins, particularly murine decay accelerating factor (DAF) and human membrane cofactor protein (MCP). Both DAF and MCP regulate C3 convertase. This suggests a potential role for ORF4 of MHV-68 in regulating C3 convertase, possibly by inhibiting C3 mediated lysis or chemotactic effects of C3a (Virgin *et al.*, 1997). ORF72 of MHV-68 encodes a D-type cyclin. This gene is found expressed during lytic cycle. The generation of MHV-68 v-cyclin transgenic mice expressing v-cyclin under control of the lck promoter which is expressed early in T cell development was used to examine the role of this gene on primary T cells (van Dyk *et al.*, 1999). The T cells showed increased proliferation indicating that MHV-68 v-cyclin promotes cell cycle progression and the transgenic mice developed high grade lymphoblastic

lymphomas indicating that this gene was also oncogenic. ORFM11 has a weak homology to bcl-2 family members and encodes a protein with 24% identity to EBV BHRF1 gene product. The latter has been shown to inhibit apoptosis in several systems (Henderson *et al.*, 1993). Similarly, the KSHV bcl-2 homologue inhibits apoptosis (Cheng *et al.*, 1997). The MHV-68 bcl-2 is expressed during lytic as well as latent infection *in vivo*. Cells expressing vbcl-2 have shown that the expression of this gene can inhibit apoptosis induced by tumour necrosis factor (TNF)-α and Fas/FasL pathways (Wang *et al.*, 1999, Roy *et al.*, 2000). MHV-68 ORF74 is homologous to genes encoding G-protein coupled receptors (GPCRs) in particular to IL-8 receptor. The MHV-68 GPCR is found expressed *in vivo* during lytic and latent infection (Wakeling *et al.*, 2001). *In vitro* expression of the MHV-68 GPCR leads to transformation and therefore it is thought to be an oncogenic gene.

### 1.5.2 Infection, pathogenesis and susceptible cell types

To mimic the likely natural route of infection, mice were infected with 4 x $10^5$ plaque forming units (PFU) MHV-68 intranasally. The virus infects alveolar epithelial cells and causes interstitial pneumonia of the lungs leading to an infiltration of mononuclear cells. The virus at this stage is predominantly lytic. The lytic infection in the lungs is cleared by day 10 post-infection (Sunil-Chandra *et al.*, 1992a). The virus is found latent in alveolar epithelial cells and when uninfected B cells are adoptively transferred into a previously infected μMT (B cell deficient) mouse, the latent virus in the lungs was shown to be capable of infecting these cells which could then be detected in the spleen (Stewart *et al.*, 1998). This indicated that the lungs could be an active reservoir for infecting new cells during the lifetime of a host.

The clearance of the lytic infection from the lungs, mainly mediated by CD8+ T cells, is followed by latent infection of cells in the lymphoid tissue in particular the spleen (Ehtisham *et al.*, 1993, Sunil-Chandra *et al.*, 1992a). The cells predominantly containing latent virus are the B cells and peak levels of those are seen two weeks post-infection. The spleens at this stage exhibit splenomegaly and the lymph nodes

that drain the lungs such as the mediastinal lymph node (MLN) and some neighbouring lymph nodes harbour latently infected cells and exhibit lymphadenopathy (Sunil-Chandra *et al.*, 1992a, Sarawar *et al.*, 1996). The number of latently infected cells decreased by four weeks post-infection but a constant low level was maintained for the lifetime of the host. Latently infected cells were also found in low frequency in the bone marrow (Cardin *et al.*, 1996).

Mice infected intraperitoneally with MHV-68 showed for the first time that macrophages expressing F4/80 marker among the peritoneal exudate cells (PECs) carried latent virus (Weck *et al.*, 1999b). This was later seen with mice infected intranasally (Weck *et al.*, 1999a). Dendritic cells expressing the CD11c marker have also been reported to harbour latent virus (Flano *et al.*, 2000). However the data are restricted to spleens removed from mice on day 14 post-infection. The dendritic cell population sorted from the spleen on day 14 exhibited a higher frequency of latently infected cells than B cells or macrophages. However experiments showed that these latently infected dendritic cells could not activate T cell hybridomas specific to MHV-68 *in vitro* whereas the latently infected B cells could activate T cells (Flano *et al.*, 2000). All three known professional APC can be infected by MHV-68, which may provide information on how the virus escapes immune surveillance mechanisms.

## 1.6 Immune response to viruses

### 1.6.1 Cells

The defence mechanism in higher order vertebrates is comprised of innate and adaptive immune responses. Innate immune response is the initial response to a foreign antigen and is non-specifically aimed towards molecular structures or "patterns". These patterns are recognised by the pattern recognition receptors (PRRs) on the surface of cells that mediate these responses against "pathogen associated molecular patterns" (PAMPs). On the other hand adaptive immune response is specific to a particular foreign antigen and exhibits long lasting recognition or memory (Medzhitov and Janeway, 1998).

The cellular mediators of the innate immune response are mainly macrophages and natural killer (NK) cells and these responses localise to the specific region that is affected. This is followed by specialised cells involved in adaptive immune response such as the T and B lymphocytes. These cells undergo clonal selection on recognition of antigens on the surface of APC such as the dendritic cells and macrophages. These events occur in specialised regions of the immune system called the lymphoid organs.

#### 1.6.1.1 Natural killer cells

Natural killer (NK) cells are large lymphoid cells with prominent intracellular granules. NK cells form a small fraction of the peripheral blood lymphoid cells. They are mainly involved in early defence against pathogens and play a prominent role especially against herpesviruses. *In vitro* NK cell activity is enhanced by exposing them to interferon (IFN)-α, β and IL-12 (Biron, 1998). Infection is controlled by the production of IFN-γ and TNF-α. The specific ligands that NK cells recognise are not known, hence it is proposed that NK cells differentiate between normal host cells and infected cells by the recognition of "altered-self". They possess two types of surface receptors. One type is the calcium-binding C-type lectins that can trigger killing on recognition of an altered cell. The second type is the one that can inhibit activation and prevent killing of host cells. These are multigene family of C-type lectins called Ly49 in mice and KIR (killer inhibitory receptors) in humans. These receptors are specific for major histocompatabilty complex (MHC) class I alleles and therefore selectively kill target cells bearing low levels of MHC class I or altered MHC (Brutkiewicz and Welsh, 1995, Karre and Welsh, 1997). They also recognise changes in cell surface glycoproteins induced by viruses.

NK cell deficient individuals show sensitivity to severe dissemination of HSV, EBV and HCMV. A severe herpesvirus infection has been observed in an adolescent human deficient in NK cells. Elevated NK cell activity is also observed during murine cytomegalovirus (MCMV) and lymphocytic choriomeningitis virus (LCMV) infections and these infections in mice have helped study some of the *in vivo* NK cell responses (Welsh *et al.*, 1991, Salazar-Mather *et al*, 1996). MCMV infected livers

produce high levels of MIP-1α that induces NK cell recruitment and focal inflammation in the tissue. These elevated numbers of NK cells recruited into the region were shown to be important in controlling the infection (Salazar-Mather *et al.*, 1998). Systemic IFN-α/β that is produced following most viral infections has been shown to induce NK cell trafficking from bone marrow to secondary sites such as spleen (Salazar-Mather *et al.*, 1996). NK cell mediated immune responses can be mediated by production of cytokines such as IFN-γ and TNF-α, that can activate macrophages. IFN-α/β and interferon inducers have been found to be potent at stimulating NK cell mediated cytotoxicity (Gidlund *et al*, 1978). Cytotoxic attack by NK cells is similar to cytotoxic T lymphocytes (CTL) and is mediated through perforin/granzyme.

NK cells can also play a role during humoral immunity by recognising antibody coated target cells. The surface receptor CD16 recognises the Fc (fragment crystallisable) region of IgG1 and IgG3 antibodies and mediates what is called antibody dependent cell-mediated cytotoxicity (ADCC) (Nash and Usherwood, 1998).

### 1.6.1.2 Macrophages

Macrophages are derived from circulating monocytes as they leave the circulation and move into tissues. They are found in large numbers in the gastrointestinal tract, lung, liver (Kuppfer cells) and spleen. Macrophages can engulf opsonised particles coated with antibodies or complement and pathogens directly. Pathogens crossing the epithelial barrier encounter phagocytes that can engulf and destroy them directly, or secrete cytokines that can lead to non-adaptive responses from other cells. Macrophages can also act as professional antigen-presenting cells by processing antigens along with co-stimulatory molecules triggering an adaptive immune response (Nash and Usherwood, 1998). CD4+ T cells involved in the adaptive immune response can recruit macrophages e.g. HSV (Nash and Cambouropoulos, 1993). This leads to macrophage activation and involves two signals, IFN-γ and the second provided by a variety of other means for example CD40 ligand. These

activated macrophages can produce proteins involved in anti-viral activity such as IFN-α/β, TNF-α and arginase.

T and B cell independent macrophage activation seems to play a critical role in the innate immune response to herpesviruses such as MCMV infection in SCID mice. Macrophage activation and recruitment is induced by IFN-γ and TNF-α and depletion of these cytokines gave rise to increased virus titres in peripheral organs (Heise and Virgin, 1995). Macrophages produce an enzyme called inducible nitric oxide synthase (iNOS) which synthesises nitric oxide (NO) and is involved in the inhibiting replication of certain viruses for example, vaccinia virus (Harris *et al*, 1995).

### 1.6.1.3 Complement and collectins

Collectins are soluble proteins found in serum, lung and nasal secretions and they can act as a first line of defence against infectious agents. They include mannose-binding protein (MBP), conglutinin and lung surfactant proteins A and D. *In vitro* and *in vivo* experiments with Influenza A virus infection strongly support an important role for surfactant collectins in the initial containment of this virus in the airway. This is thought to be brought about by direct inhibition of viral infectivity, agglutination of viral particles and/or the promotion of viral uptake by phagocytic cells (Eggleton and Reid, 1999, Crouch *et al.*, 2000). Surfactant protein-A (SP-A) has been shown to promote the uptake of HSV by alveolar macrophages. Work on SP-A deficient mice showed increased susceptibility to respiratory syncytial virus.

Complement proteins can directly target viruses or virus infected cells and they can also function in association with antibodies (Lambris *et al.*, 1999) Activation of complement leads to generation of highly potent proinflammatory mediators C3a and C5a. These are peptide fragments cleaved from C3 and C5 that are commonly called anaphylatoxins. Both C3a and C5a can bind to specific G-protein coupled receptors on the surface of phagocytic cells and cause their migration and activation. They can also attract neutrophils and eosinophils (Song *et al.*, 2000). The fact that several

herpesviruses and poxviruses carry homologues of complement regulatory proteins, suggests that complement is important in defence against these viruses.

### 1.6.1.4 Dendritic cells

Dendritic cells (DC) are the most specialised among the professional antigen-presenting cells. They are found traversing most non-lymphoid tissues especially the mucosal tissues and skin. The Langerhans cells in the skin and the pulmonary dendritic cells in the lungs are in an immature state and have the capacity to sample the environment through a process called macropinocytosis. Immature dendritic cells can also capture antigens and microbes by phagocytosis and also by receptor mediated antigen uptake. Once these processes are initiated these dendritic cells migrate into lymph nodes and undergo differentiation. The maturing cells stop phagocytosis and start processing antigens for presentation on MHC class II molecules on the surface of cells along with other co-stimulatory molecules (Steinman, 1991, Banchereau and Steinman, 1998). The mature dendritic cells can stimulate quiescent, naïve and memory B and T lymphocytes. They are unique in that they are the only cells that can stimulate naïve T cells. Mature DCs produce large amounts of IL-12 that can enhance innate immunity through NK cells and also adaptive immunity through B and T cells (Lane and Brocker, 1999). It has also been shown that dendritic cells can also present exogenous antigens on MHC class I by their ability to engulf apoptotic cells and present them for CD8+ T cell activation (Albert *et al.*, 1998).

In the secondary lymphoid organs of mice, three major subpopulations of DCs have been described: CD8α+ lymphoid DCs, CD8α– myeloid DCs and Langerhans cell (LC) derived DCs. LC-derived DCs in the lymph node have the phenotype CD11c + CD11b+ DEC205+ CD8+/-. Both the lymphoid and myeloid subsets express high levels of CD11c and MHC class II and significant levels of CD86 and CD40, but differ in the expression of several other markers (Steinman, 1991, Pulendran *et al.*, 2001). Plasmocytoid cells from the human blood expressing CD4+ and MHC class I have been identified as precursors of type 2 dendritic cells (pDC2s). These cells constitutively express type 1 interferon and have been shown to be the major

interferon producing cells (IPCs) in the blood (Siegal *et al.*, 1999). They are believed to play an important role in fighting viruses by migrating to virus infected cells and tissues.

### 1.6.1.5 T cells

T cells form a major subset of effector cells of the adaptive immune response. They are derived from bone marrow stem cells but undergo selection and differentiation in the thymus. Mature T cells are then seen in the T cell areas of the lymphoid tissues as well as in circulation. There are two main types of T cells: CD4+ T-helper cells and the CD8+ cytotoxic T lymphocytes (CTL). Both these subsets recognise antigens presented on MHC molecules on the cell surface. They require a 'second signal' from a co-stimulatory molecule to become activated.

The CD4+ T helper cells recognise antigens loaded on MHC class II molecules on the cell surface of specialised APC such as dendritic cells, macrophages or B cells (Jenkins *et al.*, 2001). In this case free pathogen or target cells infected with the pathogen are phagocytosed by APC, processed in the cytoplasmic compartment into peptides of 20 amino acids or longer, and loaded on to MHC class II molecules and transported to the surface (Miller and Sedmak, 1999). T helper cells recognise this with the help of their T cell receptor (TCR) complex. A viable second signal from molecules such as B7, CD40, OX40 or 41BB is mandatory for the successful activation of the cell (Whitmire and Ahmed, 2000). These T cells in turn can stimulate the humoral response by signalling B cells through CD40/CD40L and/or activate macrophages by the production of cytokines such as IFN-$\gamma$ and TNF-$\alpha$. T helper cells have been classified into two main subsets depending on their response. Th1 type response is dominated by the production of IFN-$\gamma$ and associated with cell-mediated immunity and Th2 type response is characterised by the production of IL-4 and IL-5 and is associated with humoral immunity. In the case of viral infections this distinction of T helper cell subsets is not as well defined as in other microbial or parasitic infections.

CD8+ T cells recognise antigens loaded on MHC class I molecules on the surface of host cells infected with a pathogen. In this case the foreign proteins synthesised in the cytoplasm are broken down into peptides of 8-10 amino acids and transported to the surface on MHC class I molecules (Ehrlich, 1997). The activation of CD8+ T cells can be CD4+ T cell dependent in which case the APC bound through the CD40L/CD40 on CD4+ T cell acts as a bridge and activates the CD8+ T cell. However, in many viral infections a CD8+ T cell response can be brought about in the absence of CD4+ T cells. This has led to the conclusion that CD8+ T cells use different co-stimulatory signals from those of the CD4 + T cells (Whitmire and Ahmed, 2000). CD8+ T cells, also called cytotoxic T lymphocytes (CTL), destroy infected cells with the help of perforins/granzymes or Fas/FasL signalling (Trapani *et al.*, 1999). They can also control microbial infection through the production of TNF-$\alpha$ and IFN-$\gamma$ (Slifka and Whitton, 2000).

Following a viral infection both CD4+ T cells and CD8+ T cells undergo an activation/expansion phase in which the naïve cells proliferate and differentiate into effector cells. This is dealt with in detail in the section on immune response to MHV-68. This initial phase is followed by a death phase in which cells undergo apoptosis and cells with the highest overall antigen affinity survive giving rise to a memory pool. The memory cell repertoire comes into action during a subsequent infection (Freitas and Rocha, 1999).

#### 1.6.1.6 B cells

B cells are the major players in the humoral immunity against pathogens. The mature B cells in the periphery can be subdivided broadly into two groups depending on surface phenotype. These are CD5+ B cells and CD5- B cells which are referred to as B-1 versus B-2 B cells, respectively. The B1 cells mainly develop at the foetal stage in the liver while the B2 cells develop in the bone marrow in the adult (Hardy and Hayakawa, 2001). The CD5+ B cells produce natural antibodies mainly of the IgM class. The natural antibodies produced by these cells were shown to play an important role during Vesicular stomatitis virus (VSV) and LCMV infections, by preventing the dissemination of virus to peripheral organs such as the kidney and

brain while trapping the antigens in secondary lymphoid organs (Ochsenbein *et al.*, 1999). The B-2 B cells are the major subset of B cells found in adults and they undergo their initial development in the bone marrow (BM) and the rest in the periphery. Unlike T cells that leave the thymus only as mature T cells, the B cells leave the BM as transitional B cells. At this stage the B cells have undergone germ-line rearrangements coding for the heavy chain and the light chains of the immunoglobulin receptor and express surface $IgM^{high}/IgD^{low}$. The next stage of development depends on antigen recognition that drives somatic mutations followed by class switching and antibody production (Benschop and Cambier, 1999). The second level of maturation takes place mainly in the T cell rich regions of the spleen and secondary lymphoid tissues called the germinal centres (GC). Germinal centres are highly specialised microenvironments where the B cells undergo massive proliferation and selection. The B cells selected in the GC express antigen specific B cell receptors (BCR) and re-enter the GC cycle or leave the GC cycle and enter the memory compartment. The cells that leave the GC are of two kinds, antibody secreting plasma cells or the non-secreting memory cells (McHeyzer-Williams and Ahmed, 1999). The antibody secreting plasma cells are long lived and can secrete antibody long after the antigen is cleared and are seen to migrate and localise in the bone marrow. The non-secreting memory cells on the other hand undergo GC cycle on secondary exposure to the antigen and it is many fold higher than the primary antibody produced.

Viral infections trigger the humoral arm of the adaptive immune system and the antibodies produced are able to clear the infection on their own, for example in VSV infection. In other cases they act in combination with virus specific CTL. It is seen that during primary VSV infection the B cell activation and maturation can also be brought about in the absence of T cells (Szomolanyi-Tsuda and Welsh, 1998). It is believed under these conditions B cells are stimulated by repetitive antigen sequences present on the virus surface and control infection by secreting IgM neutralising antibodies. Influenza virus needs T cell help for the activation and maturation of B cells and this is brought about by the CD40L-CD40 interactions (Bachmann and Zinkernagel, 1997). Antibodies are able to restrict viral infections by

binding to them and blocking entry into host cells through their cellular receptors. A second way of blocking is by changing the conformation of the coat proteins of the virus (Bachmann and Kopf, 1999).

### 1.6.2 Chemokines

Chemokines are a superfamily of small 8-10kDa proteins. They are pro-inflammatory and are involved in leukocyte trafficking. They play a crucial role in immune reactions and in viral infections (Mantovani, 1999). Chemokines can also affect angiogenesis and proliferation of haematopoietic precursors. Four main subsets have been identified depending on the arrangement of cysteine residues and designated CXC, CC, C and CX3C. They function as signalling molecules by interacting with different G-protein coupled receptors on the surface of leukocytes. Some of the chemokine receptors identified so far are CCR1, CXCR1 and CX3CR1. The chemokines and chemokine receptors exhibit redundancy where a single chemokine can bind to different receptors and vice versa (Mantovani, 1999). The CXC chemokines are active on polymorphonulear neutrophils (PMNs), T and B cells. The CC chemokines do not act on PMNs but act on a wide range of other cells such as monocytes, eosinophils, T cells, dendritic cells and NK cells. The main function of chemokines is chemotaxis of leukocytes. Monocytes respond to the widest array of chemokines, for example, macrophage inflammatory proteins (MIP), monocyte-chemotactic protein (MCP), RANTES, fractalkine and others.

In the past couple of years the mechanisms by which chemokines recruit lymphocytes from the blood into tissues by arresting them through an integrin-dependent adhesion mechanism have been identified (Campbell *et al.*, 1998). Chemokine based mechanisms involving tissue homing of leukocytes too have rendered very useful insights into the function of chemokines (Campbell and Butcher, 2000). Studies on viral pathogenesis have also been instrumental in furthering our knowledge of chemokines and their importance in normal immune responses.

### 1.6.3 Cytokines

Cytokines are secreted proteins that serve a critical role as regulators of immune and inflammatory responses. IFN-α and IFN-β also called the type I interferons are potent cytokines involved in anti-viral defence (Biron, 1998, Bogdan, 2000). They are produced by most cells and are encoded by one IFN-β and several IFN-α genes. Only a single IFN-α/β receptor has been identified so far. Increased levels of IFN-α/β are seen during viral infection for example LCMV and MCMV. They play a major role in the innate response to viruses and were initially identified as molecules that restrict viral replication. One of the ways this cytokine family is stimulated is by the presence of double stranded RNA (dsRNA). This activates RNAseL via 2'-5' oligoadenylate synthetase and dsRNA dependent protein kinase R (PKR) to degrade RNA and inhibit translation initiation respectively, thereby restricting the protein synthesis in the host cell. A second route for some viruses is production of virus-activated factor (VAF), containing interferon regulatory factors such as IRF-3 and IRF-7. They bind to the IFN-β promoter and lead to transcription activation (Biron, 1999). IFN-α/β produced following MCMV and LCMV infections have been shown to be involved in bone marrow derived NK cell trafficking into the splenic sub-compartments and the production of IFN-γ during immune response to these viruses (Salazar- Mather *et al*, 1996). IFN-α/β can also modulate the adaptive immune response. IFN-α/β produced during viral infections has been shown to help CTL response, by mediating the survival of pre-existing memory cells and in augmenting primary immune response by acting as an adjuvant (Tough *et al*, 1996).

The other cytokines involved in direct anti-viral responses are TNF-α, IL-1, IL-6, IL-12 and IL-18 (Biron, 1998). TNF-α, IL-1, IL-12 and IL-6 pro-inflammatory cytokines overlap in function with IFN-α/β although IL-12 is seen in some viral disease as negatively regulated by IFN-α/β. Murine models of HSV infection have been useful in demonstrating the anti-viral effects of cytokines such as IL-12 and IL-18 (Carr *et al.*, 1997, Fujioka *et al.*, 1999).

## 1.7 Immune response to EBV

Host immune responses are of great importance in limiting the primary infection and in controlling the life-long virus carrier state. Primary and persistent phases of infection are associated with the appearance of different combinations of antibodies specific to lytic and latent antigens (Rickinson and Kieff, 1996). Of these, antibodies to the envelope glycoprotein gp350 are of importance due to their capacity to neutralise viral infectivity (Thorley-Lawson and Geilinger, 1980), and to mediate antibody dependent cellular cytotoxicity against cells in the late phase of virus replication. The frequency with which EBV-positive lymphoproliferative disease and clinically apparent virus replication lesions are seen in T cell immunocompromised patients strongly suggests an important role for the cell mediated immune response in the context of EBV. There are a few other non-specific immune mechanisms that have been identified that can delay or prevent virus-induced transformation of B cells *in vitro* such as cytokines from T or NK like cells (Rickinson and Kieff, 1996). The most effective mechanism that leads to regression of B cell transformation is mediated by virus-specific cytotoxic T lymphocytes as seen from *in vitro* cultures.

### 1.7.1 Antibody response

The immune response to primary EBV infection in humans has been mainly worked out from IM patients. The antibody response to this virus is usually measured using an immunofluorescence assay. It measures antibody response to the following:

| ANTIGEN | VIRAL PROTEINS | INFECTIVE PHASE |
|---|---|---|
| EB nuclear antigen (EBNA) | EBNA 1, 2, 3A, 3B, 3C & LP | Expressed within latently infected cells |
| Early antigen (EA) | BZLF1(I.E), BALF2, BHRF1, BMRF1 & BSMLF1 | Expressed within cells early in lytic cycle |
| Virus capsid antigen (VCA) | Virus encoded nucleocapsid & envelope proteins(gp110,gp350) | Expressed within cells late in lytic cycle |
| Membrane antigen (MA) | Gp 350 | Expressed on the surface of cells late in lytic cycle |

At the onset of clinical symptoms most IM patients secrete IgM antibodies to VCA and rising IgG titres to both VCA and EA (Henle *et al.*, 1987). A transient IgA response to these antigens is also detected (Sixbey and Yao, 1992). IgM anti-VCA disappears over the next couple of months whereas IgG anti-VCA titres rise to a peak and then fall slightly in the next couple of months and reach a stable steady state. IgG anti-EA levels fall faster than anti-VCA IgG levels and are almost undetectable or at very low levels. Neutralising antibodies against MA antigen gp350 (Thorley-Lawson and Geilinger, 1980) are at low titres during IM but slowly rise and reach a stable level. The anti-EBNA antibodies against latent proteins in acute IM patients are mainly IgG against EBNA-2 protein whereas the response to EBNA-1 is seen mostly during convalescence (Henle *et al.*, 1987). In addition to EBV specific antibodies there are increased levels of total serum IgM, IgG and IgA which are thought to be caused by the polyclonal activation of B cells that EBV infection initiates. There is also a transient appearance of heterophile antibodies with the capacity to agglutinate sheep and horse erythrocytes, which are used as a diagnostic test for classic EBV-associated IM.

There is a strong antibody response to lytic cycle antigens in IM patients but the importance of these antibodies in the overall control of primary infection is uncertain (Rickinson and Kieff, 1996). The polymeric IgA anti-gp350 is thought to facilitate the transfer of virus through epithelial compartments (Sixbey and Yao, 1992). The IgG response to gp350 may help in antibody-dependent cellular cytotoxicity (Thorley-Lawson and Geilinger, 1980) but this IgG is not found during acute IM.

Antibodies to VCA, gp350 and EBNA-1 are seen in healthy virus carriers. However it is doubtful that any of the antibodies raised against lytic cycle antigens play a role in control of persistent infection. The virus is mainly found latent and is almost unrecognisable to the immune system. It is only when some of these cells reactivate and undergo lytic cycle that antibody-dependent cellular cytotoxicity (ADCC) may have a role to play (Rickinson and Kieff, 1996).

### 1.7.2 CTL response

Svedmyr and Jondal (1975) were the first to show the presence of effector cells specific to EBV from the peripheral blood of patients with IM. Analysis *ex vivo* indicated that these cells could mainly be T cells specific for EBV genome carrying B cells. However the role of cell mediated immunity in limiting primary EBV infection had come into focus (Rickinson and Moss, 1997).

Acute IM is characterised by lymphocytosis involving CD4+ and CD8+ T cells. It was thought that CD8+ T cells underwent polyclonal expansion and that superantigen or non-specific activation drove this expansion. Experiments using antibodies against TCR variable beta chain-specific monoclonal antibodies in combination with polymerase chain reaction (PCR) to their Vβ transcripts demonstrated the presence of a large monoclonal or oligoclonal rather than polyclonal population of CD8+ T cells, which was driven by antigen specific activation (Callan *et al.*, 1996). The results showed that few dominant clones of CD8+ T cells expanded and indicated that they might be the ones playing an important role during initial infection. These clones were also seen to disappear as the patients recovered from IM.

The CD8+ CTL in IM patients are mainly targeted towards the latent antigens EBNA 3A, 3B and 3C (Steven *et al.*, 1996). However CTL responses to multiple lytic antigens also can be detected against immediate early proteins BZLF1 and BRLF1 and to three out of six early proteins BMLF1, BMRF1 and BALF2 (Steven *et al.*, 1997). The use of advanced techniques such as tetrameric major histocompatibility complex-peptide complexes to directly visualise antigen-specific clusters of CD8+ T cells has helped identify massive expansions of activated, antigen-specific T cells in IM patients (Callan *et al.*, 1998). One patient showed as high as 44% CD8+ T cells in the peripheral blood specific for a single epitope. The antigen specific cells had activated/memory phenotype CD45RO, HLA-DR, CD38 positive and low levels of CD45RA and CD62 leukocyte (CD62L). After recovery from IM, the frequency fell but could still be detected 3 years after infection.

The persistent viral infection is primarily controlled by CD8+ CTL (Rickinson and Moss, 1997). The CTL show specificity to all viral encoded latent proteins except EBNA1 (Murray *et al.*, 1992; Levitskaya *et al.*, 1995). *In vitro* reactivation studies using autologous LCL showed the bulk of the effector population to be CD8+ CTL (Wallace *et al.*, 1982). Assays to determine the antigenic specificity showed a marked skewing of responses towards the EBNA 3A, 3B, 3C subset of antigens (Murray *et al.*, 1992). Subdominant responses recognising other latent proteins have been detected, the most frequent target being LMP2, less frequently EBNA2, EBNA-LP or LMP1 and very rarely EBNA1 (Khanna *et al.*, 1992).

There appears to be a hierarchy of immunodominance among the EBV latent antigens. Another striking finding is the extreme rarity of CD8+ CTL responses to EBNA1. There is evidence that an internal glycine-alanine repeat (GAr) domain protects the EBNA1 protein from the HLA class I pathway of antigen presentation (Levitskaya *et al.*, 1995). Inserting a known CTL epitope into the EBNA1 primary sequence renders it not presentable to CD8+ CTL unless the GAr domain is deleted in the chimeric protein; conversely, insertion of the GAr domain into the EBNA3B sequence greatly induces its capacity to be presented. Significantly, all natural EBV isolates do show conservation of this GAr domain even though this domain is not required in its principal function, namely maintenance of the episomal viral genome in latently infected cells. This may reflect the importance to the virus of rendering nonimmunogenic the one viral protein whose expression is likely to be essential for virus persistence. A second unusual feature of antigen processing in the EBV system involves the subdominant antigen LMP2. Experiments in a transporter associated with antigen processing (TAP) negative LCL background showed that while EBNA 3A, 3B or 3C proteins are not presented for CTL recognition, some CTL epitopes within LMP2 are still presented (Khanna *et al.*, 1996). This is an example of TAP-independent processing of an endogenously expressed viral protein.

## 1.8 Immune response to MHV-68

### 1.8.1 Innate immune response

Much of our insight into the immune response to MHV-68 comes from work done on gene knockout mice. The importance of IFN-α/β in restricting MHV-68 infection came from work on IFN-α/β $R^{-/-}$ mice (Dutia *et al.*, 1999a). These mice suffered from severe lung infection followed by ten times increase in latently infected cells in the spleen. The majority of mice succumbed to the infection and died. If mice were infected with a lower virus titre of 4 x $10^3$ instead of 4 x $10^5$, 50% mice still died within two weeks of infection. A similar effect was seen in IRF-1 deficient mice, an important activator of IFN-α/β response. The published data representing the effect of MHV-68 infection in IFN-α/β $R^{-/-}$ mice is depicted in Figure 1.2. The results indicate that in the absence of IFN-α/β response the viral replication leads to increased virus load in the lungs and spleen.

Macrophages in the peritoneum and spleen harbour latent MHV-68 (Weck *et al.*, 1999b, Flano *et al.*, 2000). However there is no direct evidence of the role of macrophages during innate immune response. The importance of macrophages and nitric oxide is based on a study on inducible nitric oxide synthase (iNOS) gene knockout mice in which all the mice died following MHV-68 infection (Kulkarni *et al.*, 1997). There is also a contradictory result where MHV-68 infected iNOS knockout mice fully recovered from MHV-68 infection, but this may be due to the genetic background of the mice (Dutia *et al.*, 1999a). The cytokine profile following MHV-68 infection shows that high levels of IL-6 and IFN-γ are produced in the mediastinal lymph node and cervical lymph node (Sarawar *et al.*, 1996). The high levels of IFN-γ seen by day 10 post-infection are thought to be produced by macrophages and NK cells activated during the early phase of MHV-68 infection.

### 1.8.2 Humoral response

MHV-68 specific antibodies were detected on days 12 and 28 post-infection in normal C57BL/6 mice, CD8+ T cell deficient mice and in IFN-γ deficient mice

(Kulkarni *et al.*, 1997). The neutralising antibodies to MHV-68 were low during the first two weeks following infection and then increased over the subsequent 50-70 days post-infection (Stevenson and Doherty, 1998). It has also been shown that following MHV-68 infection total serum IgG levels increase and remain high (Stevenson and Doherty, 1998). This is different from the increased IgM levels that are seen in the case of EBV infected IM patients. In the case of MHV-68 it was shown that infection of B cells *in vitro* causes non-antigen specific activation of B cells in the absence of CD4+ T cell stimulation and is marked by increased cell size, increased CD69 activation marker and the production of IgM antibodies. However *in vivo* CD4+ T cells are required for the production of anti-MHV-68 specific IgG and neutralising antibodies (Stevenson and Doherty, 1999).

Experiments with μMT mice have shown that the initial clearance of the virus from the lung following MHV-68 infection does not require antibodies (Figure 1.2) (Usherwood *et al.*, 1996b, Kulkarni *et al.*, 1997). However subsequent experiments that dealt with the control of MHV-68 infection in the long-term showed antibodies to be important. Wild type C57BL/6 and μMT mice 54 days post-infection with MHV-68 were subjected to depletion of CD8+ and CD4+ T cells. The C57BL/6 mice exhibited only a minimal reactivation of virus in the lung while the μMT mice showed very high titres of infective virus equivalent to levels found during acute infection (Stewart *et al.*, 1998). This demonstrated that antibodies do play an important role in preventing reactivation of MHV-68 over time in infected hosts.

A recent study of the MHV-68 specific antibody response showed that this response was similar to that caused by other viruses such as Sendai virus and Influenza virus, with a general predominance of IgG2a and IgG2b isotypes (Sangster *et al.*, 2000). Antibody forming cells (AFC) specific to MHV-68 were detected in the MLN and cervical lymph node (CLN) although delayed and of a smaller magnitude compared to other respiratory viral infections like Influenza A virus. Non-specific AFC were also detected in the lymph nodes and spleen and this was due to the non-specific stimulation of B cells that were also undergoing germinal centre processes and producing increased IgG2a and IgG2b antibodies. Substantial numbers of these non-

specific AFCs were found over long-term and fascinatingly found localised in the bone marrow. It is thought that these AFCs were involved in the increased levels of IgG that was seen in the serum following MHV-68 infection (Sangster *et al.*, 2000).

### 1.8.3 T cell response

#### 1.8.3.1 CD4+ T helper cells

Depletion of CD4+ T cells in BALB/c mice prior to infection with MHV-68 led to only a slight delay in the clearance of lung infection compared to normal control mice (Ehtisham *et al.*, 1993). The main difference was observed during the initial establishment of latency where the CD4+ T cell depleted mice failed to exhibit peak levels of latently infected cells compared to the control mice (Usherwood *et al.*, 1996a). However over the long-term the CD4+ T cell depleted mice had the same number of latently infected cells as the control mice. The characteristic lymphoproliferation leading to splenomegaly was not observed in the depleted mice (Ehtisham *et al.*, 1993 and Usherwood *et al.*, 1996a). Similarly, no splenomegaly was observed in MHC class II deficient mice infected with MHV-68 (Figure 1.3) (Cardin *et al.*, 1996). On day 22 positive infective virus could be detected in the lungs of the MHC class II deficient mice. Virus titres rose and the majority of mice died due to a wasting disorder by day 120-133. Subsequently it was shown that the CD8+ T cell response was intact in the MHC class II deficient mice and this was not the reason for the reactivation of the virus in the lungs (Stevenson *et al.*, 1998). Hence, CD4+ T cells were shown to be important in long-term control of MHV-68 infection.

CD4+ T cells can mediate protection by secreting IFN-γ therefore experiments looking at the effect of IFN-γ gene knockout and IFN-γ $R^{-/-}$ have been carried out. The infection patterns on IFN-γ gene knockout mice from a BALB/c background have shown no significant difference in infection patterns following MHV-68 infection (Sarawar *et al.*, 1997). The experiments with IFN-γ $R^{-/-}$ have shown similar results where clearance of infection from the lungs was not affected although it was seen that the spleen exhibited fibrosis and the destruction of splenic architecture

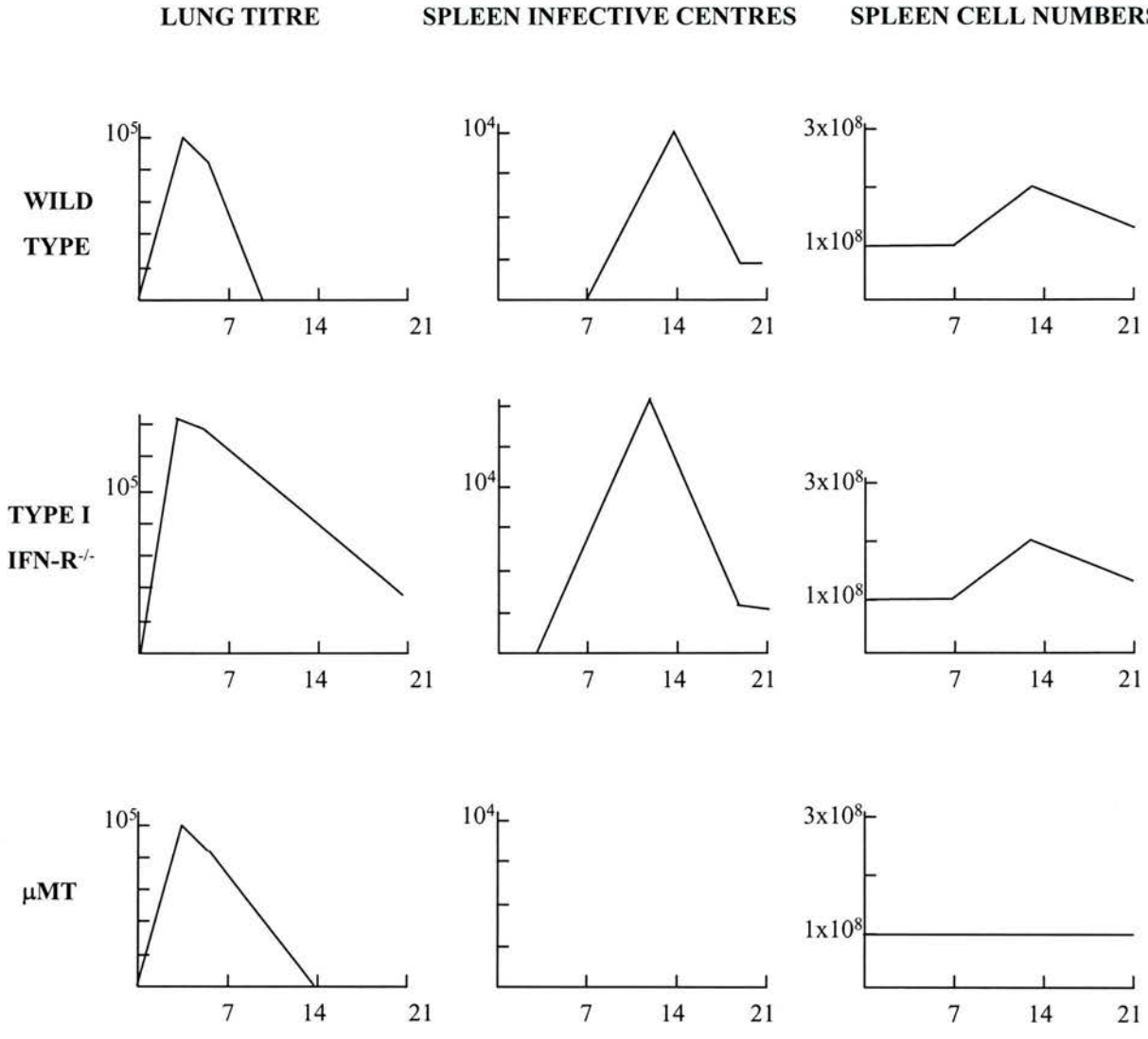


Figure 1.2 MHV-68 infection in mice deficient in lymphocyte subsets and cell surface molecules In each case three graphs are shown representing data: the far left hand side graph for infectious virus in the lungs as measured by plaque assays, the middle graph for latent virus in the spleen as measured by infective centre assay and the far right hand side graph for total spleen cell number. Data from Ehtisham *et al.*, 1993, Dutia *et al.*, 1999 and Usherwood *et al.*, 1996a. Diagram adapted from Stewart *et al.*, 1999.

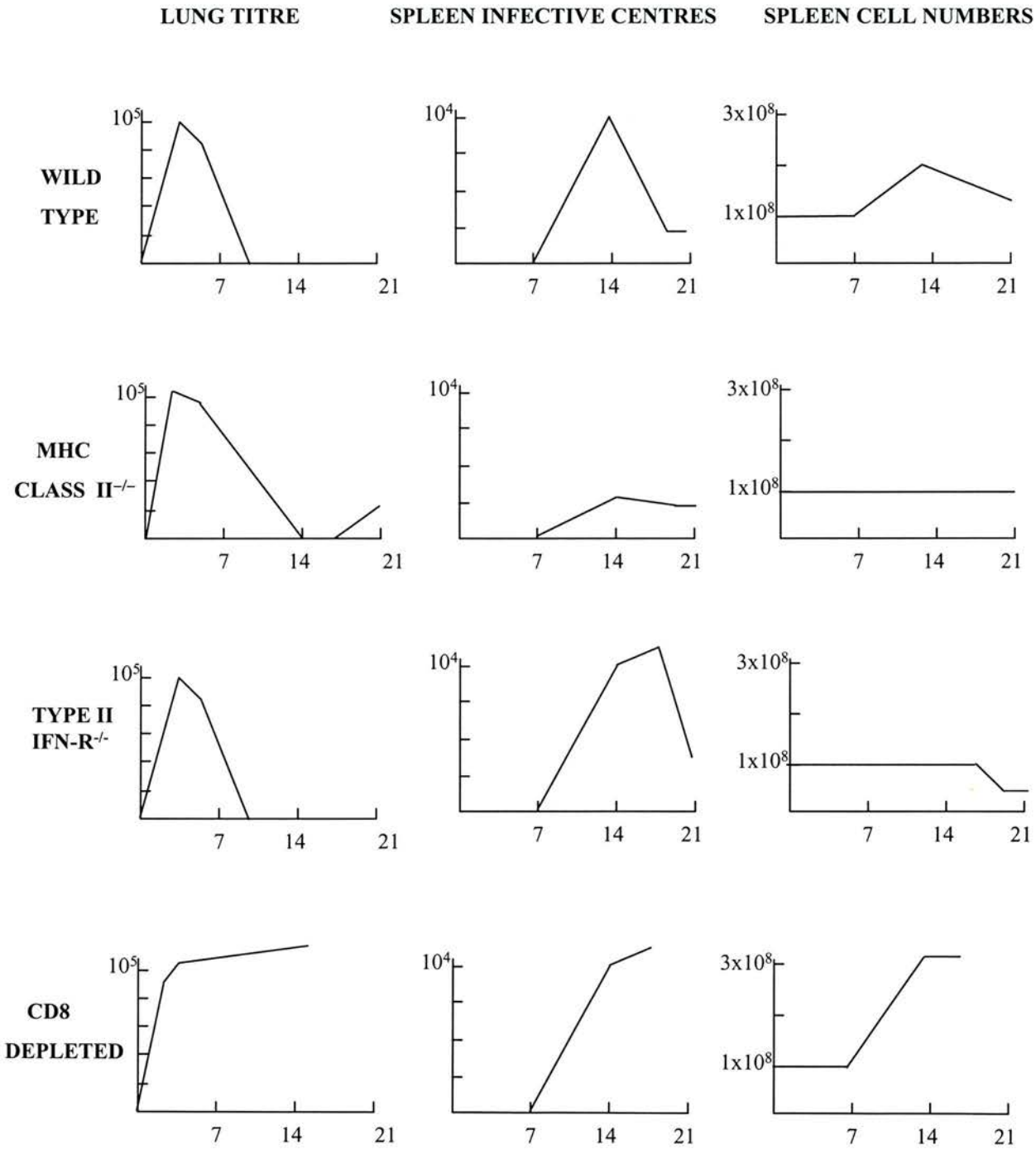


Figure 1.3 MHV-68 infection in mice deficient in lymphocyte subsets and cell surface molecules In each case three graphs are shown representing data: the far left hand side graph for infectious virus in the lungs as measured by plaque assays, the middle graph for latent virus in the spleen as measured by infective centre assay and the far right hand side graph for total spleen cell number. Data from Ehtisham *et al.*, 1993, Cardin *et al.*, 1996, Dutia *et al.*, 1997 and Ebrahimi *et al.*, 2001. Diagram adapted from Stewart *et al.*, 1999.

(Dutia *et al.*, 1997). The number of latently infected cells was 10-100 fold higher on days 14 to 17 but reached normal levels by day 21 post-infection. This was paralleled by the fall in the total number of lymphocytes in the spleen and splenic atrophy. This trend is depicted in Figure 1.3. The experiments in environments devoid of normal IFN-γ signalling did not indicate any direct role played by IFN-γ in mediating immune clearance.

In order to show that CD4+ T cells are important for controlling MHV-68 infection irrespective of their help to B cells or to CD8+ T cells subset, μMT mice depleted of CD8+ T cells were infected with MHV-68 (Christensen *et al.*, 1999). It was seen that CD4+ T cells alone could control the levels of virus in the lungs. It was further shown that this effect was mainly mediated by IFN-γ secreted by CD4+ T cells. The flow cytometric (FACS) analysis for activation markers ($CD62L^{low}$) expressed by CD4+ T cells showed a high prevalence of activated T cells in the spleens from day 15 to 25 following infection with MHV-68 (Christensen and Doherty, 1999).

MHV-68 infected S11 cells when injected subcutaneously into nude mice gave rise to tumours. This tumour growth regressed on adoptive transfer of restimulated splenocytes depleted of CD8+ T cells and failed when CD4+ T cells or both CD4+ and CD8+ T cells were depleted. These results too showed that CD4+ T cells are important effector cells during MHV-68 infection (Robertson *et al.*, 2001).

#### 1.8.3.2 CD8+ CTL

The initial experiments to determine the importance of CD8+ T cells in MHV-68 clearance were carried out in CD8+ T cell depleted BALB/c mice. These mice could not clear the infection and they died of increased virus infection (Figure 1.3)(Ehtisham *et al.*, 1993). However C57BL/6 mice depleted of CD8+ T cells did not succumb to the disease (Stevenson *et al.*, 1999c). The experiments using perforin knockout mice to determine whether the CTL mediated killing was brought about by perforin did not show any difference in clearance from wild type mice. The conclusion at this point was that CTL killing was brought about by other means such

as Fas/FasL stimulation or that the perforin knockout mice had some other compensatory pathways functioning (Usherwood *et al.*, 1997).

CTLs specific to different lytic MHV-68 viral genes have been identified (Stevenson *et al.*, 1999b). The most highly immunodominant of the peptides named p56 and p79 are encoded by ORF6 and ORF61, respectively. These are peptides obtained from lytic gene transcripts. The ELISPOT method of identifying MHV-68 specific CTL was substantiated with the help of techniques like IFN-γ CTL assay and MHC-tetramer methods. Peak CTL response is seen around 20-25 days post-infection in the spleen where 5% CD8+ T cells were found to be specific for viral peptides p56 and p79. This percentage fell to 1% in the next 80 to 150 days post-infection (Stevenson *et al.*, 1998).

Work on MHC class II deficient mice that lack CD4+ T helper cells has shown that CTL responses can develop in the absence of CD4+ T cell help (Stevenson *et al.*, 1998). These mice seem to have increased percentages of CTL on day 80-150 post-infection but they suffered from reactivating virus in the lung over long periods of time. Therefore, both CD8 and CD4 responses are required to control the long-term infection with MHV-68.

## 1.9 Evasion of immune responses by herpesviruses

The main strategy employed by herpesviruses to evade host defences is latency. However, these viruses have evolved a number of other methods to disrupt recognition of infected cells during primary and recurrent infection. The approaches can interfere with a diversity of innate and adaptive responses that includes interfering with IFN responses and down-regulating MHC class I expression, thwarting CTL recognition.

### 1.9.1 Modulation of antigen presentation

The viral clearance brought about by cytotoxic T lymphocytes (CTL) depends on effective processing and presentation of viral antigens by the MHC class I molecules.

The MHC class I molecule is composed of a heavy chain and a light chain (β-2 microglobulin). This unstable complex is attached to the endoplasmic reticulum (ER). Cytosolic proteins that are ubiquitinylated are broken down by the proteasome complex. Peptides entering the ER are transported to the MHC by the transporter associated with antigen processing (TAP). The TAP associated peptide is then loaded onto the MHC by tapasin. The stable final complex is formed when an 8-10 amino acids residue is loaded onto the peptide groove. The final complex leaves the ER and is transported to the cell surface through the secretory pathway involving the Golgi (Ehrlich, 1997). Virus immune evasion mechanisms studied so far are just the tip of the iceberg but already there are examples showing their ability to block every step in the assembly and trafficking of MHC class I molecule (Ehrlich, 1997, Ploegh, 1998, Miller and Sedmak, 1999, Tortorella *et al.*, 2000).

Herpes simplex virus (HSV) *in vitro* infection of human fibroblast renders cells resistant to CTL killing. Within 3 hours of infection, MHC class I molecules with no peptide loaded were found retained in the ER. This effect is due to HSV immediate-early (IE) protein ICP47 (York *et al.*, 1994). ICP47 is found in the cytoplasm and does not seem to be membrane associated. Using co-precipitation assays it was shown that ICP47 binds to the cytosolic region of TAP and prevents the translocation of peptides into the ER (Hill *et al.*, 1995, Fruh *et al.*, 1995). It has subsequently been demonstrated that ICP47 binds specifically to the peptide-binding site of TAP with very high affinity in a stable fashion (Tomazin *et al.*, 1996).

A number of proteins have also been identified in the betaherpesviruses human cytomegalovirus (HCMV) and MCMV that prevent MHC class I presentation by blocking at different stages of assembly and transport (Reddehase, 2000). HCMV encodes a phosphoprotein (pp65) that phosphorylates the principal IE1 protein and makes it resistant to cleavage (Gilbert *et al.*, 1996). HCMV US6 product inhibits peptide translocation by TAP (Ahn *et al.*, 1997). It functions slightly differently from ICP47. It is inserted into the ER membrane and the luminal part of US6 prevents peptide bound to TAP from being transported inside the ER. US6 itself is retained in the ER and is not translocated to the cytoplasm for presentation. HCMV US11 also is

an ER resident transmembrane glycoprotein that dislocates newly synthesised class I molecules from the ER to the cytosol where they undergo rapid degradation (Wiertz *et al.*, 1996). US3 product of HCMV goes one step further; it can prevent a final MHC complex with peptide from leaving the ER (Ahn *et al.*, 1996). US3 is an IE product while US11 and US6 are early/late products. Consistent with this expression pattern it is thought that US3 prevents peptide loaded MHC class I complex from leaving the ER immediately after infection (Ahn *et al.*, 1996). Taking into consideration all these different strategies it has been suggested that HCMV have different T cell escape strategies at different times during infection cycle in the host.

MCMV seems to have evolved strategies that differ from that of the HCMV. MCMV gene m152 encodes a transmembrane glycoprotein that is expressed during early infection. The expression of m152 leads to the accumulation of MHC class I complex loaded with peptide in the early Golgi compartments and prevents the complex from being transported along the Golgi (Ziegler *et al.*, 1997). MCMV m06 is also an early transmembrane glycoprotein. This protein forms a tight complex with β2-microglobulin associated MHC class I molecule. After passing the Golgi the complex enters the endocytic route and is transported to the lysosome where it is degraded (Reusch *et al.*, 1999).

All these HCMV and MCMV mechanisms reduce CTL killing but the reduced expression of MHC class I can make them susceptible to NK cell recognition. These viruses have evolved methods to evade this by expressing decoy MHC molecules on the surface of cells. HCMV codes for a decoy class I homologue UL18. When UL18 was expressed in cells lacking MHC class I, they were found to be resistant to NK cell killing (Reyburn *et al.*, 1997). MCMV m144 codes for a MHC class I homologue. Recombinant MCMV virus with a m144 gene mutation exhibited poor replication *in vivo* in mice compared to wild type virus but on depleting NK cells the replication was restored. This indicated that expression of m144, a class I homologue, partially rendered the virus infected cells resistant to NK cell lysis (Farrell *et al.*, 1997). MCMV coded gp34 is also thought to be involved in preventing NK cell recognition. It binds to MHC class I complex and prevents ER retention and

allows transport and expression on the cell surface (Kleijnen *et al.*, 1997). It is thought to act as a negative regulator for the rest of the proteins that prevent MHC class I expression on the surface and prevents MHC class I on the surface from falling too low.

Gammaherpesviruses too exhibit mechanisms like alpha- and betaherpesviruses aimed at down-regulating CTL recognition. EBV latency associated protein EBNA1 is resistant to proteolytic cleavage due to the presence of glycine-alanine repeats in the protein backbone (Levitskaya *et al*, 1995). The glycine-alanine repeat makes the ubiquitinylated EBNA1 unstable for proteolytic cleavage and therefore the CTL response to this protein requires exogenous processing (Blake *et al.*, 1997). EBV coded viral IL-10 (vIL-10) has been demonstrated to down-regulate cellular TAP1 protein expression. This in turn leads to reduced peptide translocation and expression of peptides on MHC class I molecules (Zeidler *et al.*, 1997). Two of KSHV unique genes ORFK3 and ORFK5 are found to be capable of down-regulating MHC class I expression. The mechanism is thought to be distinct from other herpesviruses as the K3 and K5 proteins are involved in targeting MHC class I peptide complex from the cell surface to the endocytic pathway for degradation (Coscoy and Ganem, 2000). This down-regulation of MHC class I complex would render the KSHV infected cells protection from CTL recognition but as in the case of HCMV and MCMV this could make the cells susceptible to NK cell recognition and killing. However, it has subsequently been shown that ORFK5 can prevent NK cell recognition as well. ORFK5 was shown to be able to manipulate surface molecules such as ICAM-1 and B7-2 that are the cellular ligands for NK cell-mediated cytotoxicity receptors (Ishido *et al.*, 2000). Human B cell line BJAB expressing KSHV K3 protein is susceptible to NK cell mediated killing due to MHC class I complex down-regulation, but when K5 is expressed in these cells, they become resistant. This was brought about by the down-regulation of ICAM-1 and B7-2. Preliminary *in vitro* characterisation of MHV-68 K3 gene has shown similar effect to KSHV K3 at down-regulating MHC class I presentation and inhibiting antigen presentation (Stevenson *et al.*, 2000). It would be interesting to see the effect of this gene *in vivo* and this might shed more light on the activity of the KSHV K3 in infected humans.

T helper cells or CD4+ T cells recognise antigens presented on MHC class II molecules. Macrophages, dendritic cells and B cells are the main subsets of cells expressing MHC class II on their surface. The antigens in this case are engulfed and broken down in the endocytic or lysosomal compartments. The MHC molecule is made up of α and β heterodimer and this is bound to an invariant chain (Ii). Signalling through the Ii chain helps this complex to move into the endocytic pathway. In this compartment proteases cleave the invariant chain into a fragment called the CLIP that is attached to the peptide groove. The CLIP is later exchanged for a peptide and the final complex transported to the cell surface (Miller and Sedmak, 1999, Tortorella *et al.*, 2000).

There are fewer examples where viruses disrupt MHC class II expression. HCMV US2 degrades class II DR-α and class II DM-α molecules (Tomazin *et al.*, 1999). It prevents MHC class II presentation and exhibits reduced or abolished antigen presentation to CD4+ T cells. It is thought that it almost would make HCMV infected macrophages invisible to CD4+ T cells during the process of reactivation. The EBV BZLF2 protein can bind to the cell surface as well as MHC class II. It affects the generation of CTL *in vitro* in mixed lymphocyte cultures (Spriggs *et al.*, 1996). There are examples where viruses indirectly down-regulate MHC class II expression, either by interfering with the endocytic pathway or by modulating cytokines like IFN-γ. For example, EBV secretes vIL-10 (BCRF1) which can suppress T cell activation by affecting IFN-γ production (Hsu *et al.*, 1990, Bejarano and Masucci, 1998). Human IL-10 has also been shown to inhibit MHC class II presentation and activation of CD4+ T cells. Work on human monocytes has shown that IL-10 specifically inhibits MHC class II complex exocytosis and recycling. Complexes seem to be accumulating in intracellular vesicles rather than being transported to the plasma membrane (Koppelman *et al*, 1997). It is thought that vIL-10 secreted by EBV could act in a similar fashion.

### 1.9.2 Modulation of cell death by apoptosis

Cells that have replicating virus undergo apoptosis or are detected by CTL or NK cells and signalled for cell death. Viruses have to produce progeny virus and prevent untimely death of the host cell therefore they have evolved various mechanisms that subvert apoptosis. Apoptosis induced by NK cells and CTL is brought about by TNF-α, granzymes, perforins or cell surface receptors like FasL. Work on gammaherpesviruses (KSHV, HVS, BHV-4 {Bovine herpesvirus-4} and EHV-2 {Equine herpesvirus-2}) has identified viral encoded proteins called v-FLIP that can disrupt the down-stream signalling through Fas by binding to FADD (Fas activated death domain) and caspase-8 through their death-effector domains (DED) (Thome *et al.*, 1997).

A cellular protein that protects cells from apoptosis is bcl-2 and many gammaherpesviruses (EBV, KSHV, MHV-68, HVS and BHV-4) encode viral homologues (vbcl-2). The presence of vbcl-2 protein is thought to inhibit cells from undergoing apoptosis. Recent work comparing the vbcl-2 molecule from five different gammaherpesviruses (EBV, KSHV, HVS, BHV-4 and MHV-68) has shed more light on the evolution of this molecule as a powerful death suppressor (Bellows *et al.*, 2000). Bcl-2, although anti-apoptotic, on cleavage by caspases is converted into a potent proapoptotic factor, it was therefore considered important to determine that this was the same with the viral homologues. All vbcl-2 (EBV, KSHV, HVS and BHV-4) except MHV-68 bcl-2 were resistant to cleavage by caspases (1, 3 and 8). In addition the cleaved product of MHV-68 bcl-2 lacked proapoptotic characteristic. When the C-terminal regions of the different gammaherpesvirus vbcl-2 were expressed in cells it was found that only KSHV C-terminal region was proapoptotic. However as the full-length vbcl-2 failed to undergo cleavage by caspases this region does not appear to be proapoptotic in infected cells (Bellows *et al.*, 2000). This work showed that although the vbcl-2 shared homology with cellular bcl-2, the gammaherpesviruses have been successful in retaining only specific properties that are advantageous for their survival within host cells. EBV BHRF1 (Henderson *et al.*, 1993), BALF1 (Marshall *et al.*, 1999) and LMP-1 (Rowe *et al.*, 1994) activate

cellular bcl-2 expression. This may be a strategy used by the virus to prevent early apoptotic death of an infected cell.

### 1.9.3 Modulation of cytokine and chemokine response

In the past decade a large amount of literature has amassed on the proteins encoded by DNA viruses, especially the herpesvirus and poxvirus groups that can modulate cytokine and chemokine responses. However, most of our knowledge about their immuno-modulatory functions comes from structural similarity to known host proteins or *in vitro* functional studies. For example, KSHV encode an array of cytokine and chemokine modulators but their function *in vivo* is not known as most of the evidence is from structural homology to cellular proteins and *in vitro* binding studies. The *in vivo* functions of these molecules during host response can only be determined with the help of animal models.

Almost all the cytokines described previously as important host responses to viruses such as IFN-α/β, TNF-α, IL-1β and IFN-γ can be subverted by different poxvirus molecules (Kotwal, 2000). Virus encoded proteins secreted outside the host cell are named "virokines" and a subset of them are called "viroreceptors". Viroreceptors are homologues of cell surface receptors that can bind to host mediators such as cytokines and chemokines. Vaccinia viruses secrete two such viroreceptors vTNFr and vIL-1βr that bind and sequester host TNF-α and IL-1β respectively. These molecules are seen to restrict host pro-inflammatory responses (Kotwal, 2000). Among herpesviruses there seem to be more examples of virokines that may subvert host responses by suppressing the pro-inflammatory cytokine secretion. For example EBV secreted vIL-10 can negatively regulate IL-12 and thereby affect IFN-γ production. KSHV secretes vIL-6 and HVS a homologue of IL-17 (Spriggs, 1999). The only soluble cytokine receptor identified in the herpesvirus family to date is colony-stimulating factor 1 receptor (CSF-1R) encoded by EBV BARF1 (Strockbine *et al.*, 1998). Recombinant BARF1 protein inhibits the ability of CSF-1 to induce proliferation of mouse bone marrow macrophages and secretion of IFN-α by human monocytes.

Chemokine mediated cell migration and inflammatory responses have come into focus and seem to be essential in the movement of cells towards infected regions and also in movement away from infected sites into lymph nodes carrying important information for priming the adaptive response to viruses and other pathogens. Therefore it is not surprising that the viruses have evolved mechanisms to block these responses. There are different strategies devised by viruses to subvert chemokine signalling (Price *et al.*, 1999, Tortorella *et al.*, 2000).

One strategy is to code for secretory chemokine binding molecules (vCkBs). These can bind and sequester chemokines from the vicinity of the infected cell or cells and thereby prevent chemokine binding to the extracellular matrix and chemotaxis of effector cells. MHV-68 ORF M3 codes for a novel chemokine binding protein that is a secreted molecule. *In vitro* characterisation of the MHV-68 M3 protein has shown that it is a broad spectrum chemokine binding protein that can bind to a wide range of chemokines, including CC, CXC, C and CX3C chemokines (Parry *et al.*, 2000, van Berkel *et al.*, 2000). There were some subsets of these chemokines that M3 did not bind, for example, some B cell specific CXC chemokines, indicating selective activity. MHV-68 M3 was found to block calcium signalling induced by RANTES, MIP-1A and MCP-1 (Parry *et al.*, 2000, van Berkel *et al.*, 2000).

Another strategy viruses use is to code for chemokine binding receptors (vCkBRs) (Lalani *et al.*, 2000). Cells infected with HCMV express a homologue of CCR5 receptor US28, which can bind to an array of chemokines including RANTES, MCP-1 and MIP-1$\alpha/\beta$ and prevent their binding to other cells. The binding of these molecules to US28 leads to their internalisation and degradation (Tortorella *et al.*, 2000, Fortunato *et al.*, 2000). A number of gammaherpeviruses including KSHV, HVS and MHV-68 express viral IL-8R. It is a G-coupled receptor (CXCR2) that binds to IL-8, CXC and CC. The HVS IL-8R is coded by ECRF3 gene and has been shown to act as a functional receptor that binds to IL-8, GRO/melanoma growth stimulatory activity (MGSA), and NAP-2 (Nicholas *et al.*, 1992, Ahuja and Murphy, 1993).

Viruses can also code for chemokine receptor binding proteins (CkRB). KSHV secretes a variety of chemokine antagonists, vMIP-I and vMIP-II. These antagonists bind to CCR and CXCR receptors and prevent cellular chemokine binding but also inhibit signalling down-stream (Klendal *et al.*, 1997, Boshoff *et al.*, 1997, Lalani *et al.*, 2000).

### 1.9.4 Modulation of humoral immunity

HSV-1 and HSV-2 encode for proteins that can subvert humoral immunity. The HSV genes US8 and US7 code for glycoprotein E (gE) and gI proteins can bind to monomeric as well as aggregates of IgG. They act as Fcγ receptors (FcγR). The binding of antibodies through their Fc region to the cell surface of infected cells can obstruct Fab recognition of antigenic peptides on the same surface. This has been shown as the reason for the ineffective antibody-dependent cellular cytotoxicity response in HSV infected cells (Dubin *et al.*, 1991). This could also explain the reason why so many of the herpesviruses (HCMV, MCMV, VZV) code for FcγR homologues.

A second target in the host humoral response is the complement cascade. The virus binding to IgG Fc region prevents the classical complement pathway, in which complement recognises antibody-coated cells and particles and destroys them. Viruses also target the alternate pathway by producing proteins that can inactivate either C3 or the C3 convertase (Lindahl *et al.*, 2000). Gammaherpesviruses such as HVS, KSHV and MHV-68 code for genes that are homologous to complement regulatory proteins. The HVS coded HVSCD59 has sequence homology to human terminal complement regulatory protein CD59 and is expressed mainly during the lytic cycle of the virus. Cells stably transfected with HVSCD59 are resistant to lysis by both human and rat serum (Rother *et al.*, 1994).

## 1.10 Aim of the Project

The overall aim of the work described in this thesis was to investigate the early events following MHV-68 infection *in vivo* in the draining lymph node mainly the mediastinal lymph node. It was hoped that any information obtained would help discern:

- The effect of MHV-68 infection on B cells in the mediastinal lymph node during the very onset of infection.

and

- Cell types other than B cells latently infected in the lymph node and involved in virus trafficking.

The approaches adopted were:

- To compare events in B cell deficient (μMT) host environment to that in wild type host.

- To characterise a recombinant MHV-68 virus (LHΔgfp) expressing green fluorescent protein (GFP) and use it as a marker to track infected cells.

- To use the Type I IFN $R^{-/-}$ host that displays amplified disease pathogenesis to characterise infected cell types.

# CHAPTER TWO

# MATERIALS AND METHODS

## 2.1 Materials

### 2.1.1 Chemicals

Unless otherwise stated all chemicals were of analytical grade where available and supplied by Merck-BDH Chemicals, Poole, Dorset, England, or Sigma-Aldrich Chemical Co, Poole, Dorset, England.

Life Technologies Ltd supplied plastic ware for tissue culture purposes.

### 2.1.2 Tissue culture media

Glasgow's modified Eagle's medium (GMEM) (Life Technologies Ltd) and RPMI 1640 (Life Technologies Ltd) were prepared in the department of Veterinary Pathology, University of Edinburgh.

### 2.1.3 Virus

Murine gammaherpesvirus-68 (MHV-68) was obtained from Prof. Blaskovic (Blaskovic *et al.*, 1980) and the clone g2.4 was isolated by Efstathiou *et al* 1990b.

LHΔgfp is a recombinant MHV-68 and was a gift from Dr. D. J. Roy and Dr. J. Stewart, Department of Veterinary Pathology, University of Edinburgh. It has an enhanced green fluorescent protein gene (EGFP) under a human cytomegalovirus (CMV) immediate early promoter (Vector pEGFP-C1, Clontech Laboratories, USA) inserted in to the left-hand end of MHV-68. It has a deletion of nucleotides 1-3223bp that comprises five tRNA coding sequences and most of the M1 gene of wild type MHV-68.

### 2.1.4 Mice

Wild type C57BL/6 mice were obtained from B and K Universal Ltd (Hull, UK) aged 3-4 weeks on arrival. μMT/μMT (Kitamura *et al.*, 1991) on a C57BL/6 background were also obtained from B and K Universal Ltd and bred in-house. These mice have a targeted lesion in the μ-immunoglobulin chain resulting in the failure to express IgM; consequently, B cells development is arrested at the pre-B-cell stage. These mice are referred to in this thesis as μMT mice.

IFN-α/β $R^{-/-}$ mice (Muller *et al.*, 1994) were obtained from B and K Universal Ltd and bred in-house.
Wild type 129/Sv/Ev matching the IFN-α/β $R^{-/-}$ background were also obtained from B and K Universal Ltd and bred in-house. These wild type mice are referred to in this thesis as WT129.

Male and female mice were infected at 4-7 weeks of age intranasally with 4 x $10^5$ PFU MHV-68 (40μl inoculum) under Halothane anaesthesia.

### 2.1.5 Cell lines

Baby hamster kidney cell line (BHK-21) (MacPherson and Stoker, 1962) were maintained in Glasgow's modified Eagle's medium supplemented with 10% tryptose phosphate broth (TPB) (Life Technologies, Paisley) and 10% new born calf serum (NBCS) (Harlan Sera-Lab), L-glutamine (2mM), penicillin (70μg/ml) and streptomycin (10μg/ml). Cell lines were maintained at 37°C in 5% $CO_2$ incubator.

### 2.1.6 Biobond Coating

Glass slides (BDH) were washed in 2% Decon detergent followed by distilled water. Slides were coated with 2% Biobond (British BioCell, International, Cardiff, UK) in acetone for 4 minutes, rinsed in distilled water and stored for subsequent use.

Table 2.1 Antibodies used in FACS analysis

| **Primary Antibodies** | **Source** | **Dilution** | **Cell Marker** | **Reference** |
|---|---|---|---|---|
| Goat-anti-mouse IgMμ-biotinylated | Serotec | 1:200 | B cells | Wykes *et al.*, 1998 |
| Rat-anti-mouse B220 | ATCC RA3-3A1/6.1 | neat | B cells | Coffman and Weissmann, 1981 |
| Rat-anti-mouse CD19 | PharMingen | 1:200 | B cells | Stevenson and Doherty, 1999 |
| Goat-anti-mouse IgG-FITC | Serotec | 1:25 | B cells | Wykes *et al.*, 1998 |
| Hamster-anti-mouse CD69 | Serotec | 1:50 | Activation marker for T and B cells | Stevenson and Doherty, 1999 |
| Rat-anti-mouse CD21 | PharMingen | 1:200 | B cells | Wang *et al.*, 1990 |
| Rat-anti-mouse CD23 | PharMingen | 1:400 | B cells | Wang *et al.*, 1990 |
| Mouse-anti-mouse MHC class-II-FITC | Serotec | neat | B cells, dendritic cells, macrophages | Wykes *et al.*, 1998 |
| Rat-anti-mouse CD8 | YTS169 hybridoma | neat | T cells | Cobbold *et al.*, 1984 |
| Rat-anti-mouse CD4 | YTS191 hybridoma | neat | T cells | Cobbold *et al.*, 1984 |
| Rat-anti-mouse CD4-FITC | Sigma | 1:50 | T cells | Sarawar *et al.*, 1996 |
| Rat-anti-mouse CD8-FITC | Sigma | 1:50 | T cells | Sarawar *et al.*, 1996 |
| Rat-anti-mouse CD25 | Serotec | 1:2500 | Activation marker for T cells | Moreau *et al.*, 1987 |
| Rat-anti-mouse F4/80 | Serotec | 1:200 | Macrophages | Leenen *et al.*, 1998 |
| Hamster-anti-mouse CD11c-biotinylated | PharMingen | 1:50 | Dendritic cells | Sevilla *et al.*, 2000 |
| Rat-anti-mouse DEC-205 (NLDC145) | Serotec | 1:50 | Interdigitating and Dendritic cells | Kraal *et al.*, 1986 |
| Mouse-anti-mouse NK1.1-biotinylated | Gift from Dr. Cobbold | 1:100 | NK cells | Salazar-Mather *et al.*, 1996 |

## 2.2 Methods

### 2.2.1 Preparation of virus working stock

BHK-21 cells were infected with MHV-68 at a multiplicity of infection (MOI) of 0.001. Suspensions were incubated at 37°C for 1 hour on a shaker. Infected cells were transferred to T175 tissue culture flasks containing 50ml of complete medium. 5-6 days post-infection the cells were removed along with supernatant using a cell scraper. The cells were centrifuged at 275g (Beckman TJ-6) for 20 minutes at 4°C. Cells were resuspended in phosphate buffered saline (PBS) {0.8% sodium chloride, 0.02% potassium chloride, 0.144% disodium hydrogen phosphate ($Na_2HPO_4$) and 0.24% potassium dihydrogen phosphate ($KH_2PO_4$) at pH 7.4}. Cells were then homogenised using a Dounce homogeniser (Wheaton, USA) 20-30 times, over ice and centrifuged at 750g for 20 minutes at 4°C. Supernatant, which contains the virus, was removed and kept carefully on ice. The pellet was resuspended in 1ml PBS and once again homogenised. The homogenate was centrifuged at 750g and the supernatant was pooled with the previous one, dispensed in 0.2ml volume aliquots and stored at -70°C.

### 2.2.2 Cocultivation assay for infective centres in the lymph nodes and spleen

Mice were killed by carbon dioxide ($CO_2$) inhalation. Cervical lymph node (CLN), mediastinal lymph node (MLN) and spleens were removed into 2ml RPMI 1640 supplemented with 10% foetal calf serum and kept individually on ice. A single cell suspension was obtained from each of these tissues by dissociation with the help of scalpel blades. In the case of spleen, erythrocytes (red blood cells) were lysed by water lysis (1ml sterile $dH_2O$ and 9ml PBS). The cells were resuspended in complete media. The cells were counted after diluting in trypan blue (0.1%) using a haemocytometer. The cells were cocultivated at different dilution along with $1x10^6$ BHK-21 cells in RPMI complete medium {RPMI 1640; 10% foetal calf serum; L-glutamine (2mM); β-mercaptoethanol (0.05mM); penicillin (70μg/ml) and streptomycin (10μg/ml)} in 60 mm tissue culture dishes at 37°C in 5% $CO_2$ incubator for 5 days. The monolayers were fixed in 10% formal saline (Surgipath-Europe Ltd) and stained with 0.1% toluidine blue (w/v in $dH_2O$), and the number of infective

centres were counted using a dissection microscope (Wild, Heerbrugg) (method as described by Sunil-Chandra, 1992a).

### 2.2.3 Assay for infective virus

Single cell suspensions were obtained from lymph nodes and spleen tissues as described in the previous method. In the case of lung tissues, they were stored in vials at -70°C soon after removal from mice. They were thawed and homogenised individually in 1ml ice cold media using glass homogenisers (Soham Scientific, UK). Cell homogenates were transferred to cryovials and refrozen at –70°C. The cells were freeze thawed twice. The cell debris was spun down and the supernatant was recovered. The supernatant was added at different dilutions to $1x10^6$ BHK-21 cells in Glasgow modified Eagle's medium and incubated for an hour at 37°C in a shaker before plating on to 60mm tissue culture dishes. The cells were then cultured for 4 days at 37°C in 5% $CO_2$. The monolayers were fixed in 10% formal saline and stained with 0.1% toluidine blue. The plaques on plate were counted using a dissection microscope.

### 2.2.4 Biotinylation of antibody

The stock antibody (immunoglobulin from PK136 line) was diluted to 1mg/ml in 0.1M bicarbonate buffer (pH8.5). 1ml of the antibody was dialysed against the bicarbonate buffer at 4°C, overnight. 200µl of biotin (10mg/ml) in DMSO (dimethyl sulfoxide) was added to the dialysed antibody in an eppendorf and mixed at 4°C for 5 hours. 500µl of 5% (w/v) sodium azide was added to the antibody solution and this was dialysed against PBS/0.05% azide, overnight. This was followed by another dialysis against PBS/20% glycerol overnight.

### 2.2.5 Flow cytometric analysis of cells (FACS-fluorescent activated cell sorting)

Cell suspensions from tissues were adjusted to $4 \times 10^6$ cells per ml in RPMI complete media and 100µl ($4 \times 10^5$ cells) was used for staining with each individual antibody. The primary antibodies were diluted in FACS buffer (PBS with 1% bovine serum

albumin and 0.1% sodium azide). The primary antibodies used in FACS are listed in Table 2.1 under section (2.1). 50µl of diluted antibody was added to the respective tubes and incubated for 15 minutes at room temperature. The cells were washed twice using 700µl of FACS buffer. Subsequently the cells were incubated with 50µl of secondary antibody fluorescent conjugate (PharMingen or Serotec) diluted appropriately, at room temperature in the dark for 15 minutes. The cells were washed and fixed in 1% formaldehyde in PBS. The cells were analysed by flow cytometry (Becton Dickinson 'FACStar' flow cytometer using the Cellquest software).

### 2.2.6 Imprints

Mice were killed by carbon dioxide inhalation. In the case of the mediastinal lymph node, the node was removed cut into two halves and the cells were squashed onto a Biobond coated slide each. The slides were allowed to air dry and then fixed in ice cold acetone for 2 minutes. In the case of the lung tissue small pieces of the tissue was cut using scalpel blades. The tissue was then dabbed on to a Biobond coated slide using forceps. It was then aid dried and fixed.

### 2.2.7 *In vivo* depletion of T cells

The CD4+ T cell subset was depleted using the rat monoclonal antibody YTS191.1 (Cobbold *et al.*, 1984). Mice were injected intravenously in the tail with 0.1ml of antibody at 10mg/ml stock solution, two days before and two days after MHV-68 or mock infections. Subsequently, mice were injected with the same dose intraperitonially 7 days after the original injection. (Method similar to Ehtisham *et al.*, 1993)

### 2.2.8 Cytospins

Cells were resuspended at $1x10^6$/ml in PBS and 100µl was centrifuged on to Biobond coated slide. The cytospin (Cytospin 2, Shandon) was performed for 5 minutes at 1000 rpm. The cytospins were air-dried, mounted using Citifluor (UKC, Canterbury, UK) and observed using a fluorescent microscope (Nikon, Diaphot 200).

### 2.2.9 MHV-68 immunostaining of paraffin-embedded tissues

Paraffin tissue sections cut on to Biobond coated slides had to be dewaxed and permeablised before the addition of antibodies. Slides were dewaxed by immersion in xylene for 15 minutes at room temperature. This was followed by a wash in absolute alcohol for 5 minutes and treatment with 0.3% hydrogen peroxide in methanol for 30 minutes at room temperature to block the endogenous peroxidase activity. Tissue sections were then hydrated through a series of alcohol (100%, 95%, 70%, 50% and 30%) for approximately 30 seconds each, washed twice in distilled water ($dH_2O$) for a minute and immersed in 1% Triton X-100 in $dH_2O$for 1.5 minutes followed by two washes (5 minute each) in $dH_2O$. Permeablisation of cells was improved further by carrying out a proteinase-K (10μg/ml in 20mM Tris and 2mM calcium chloride at pH7.0) digestion for 20 minutes in a 37°C water-bath. Immersing slides for 5 minutes in PBS containing glycine (2g/L) and EDTA (ethylene-diamino-tetra acetic acid) (5mM) inactivated proteinase-K.

Slides were immersed in PBS at all times to prevent drying of tissue sections. Slides at this stage were ready for antibody staining. The slides were laid out in a moist chamber and a blocking step using 2% normal goat serum was carried out overnight to prevent non-specific binding of antibodies. Prior to addition of primary antibody the blocking serum was decanted. 50μl of rabbit polyclonal MHV-68 antibody (diluted 1/500 in 2% normal goat serum) was added to each section and placed in the moist chamber and incubated at room temperature for 2 hours. The slides were washed three times (5 minutes each) in PBS to remove excess antibody. Goat anti-rabbit biotinylated IgG (diluted 1/500 in 2% normal goat serum) was added to each slide and incubated for 2 hours at room temperature. Slides were washed in PBS. Streptavidin conjugated to horseradish peroxidase (diluted 1/1000 in PBS) (Boehringer-Mannheim) was added to the sections and incubated for 1 hour at room temperature. Slides were washed three times in PBS (5 minutes each). 3, 3'-Diaminobenzidine tablets (Sigma), the substrate for peroxidase (POD), were dissolved in 5ml $dH_2O$ and added to sections. Colour change was monitored closely and reaction stopped within 5-10 minutes by immersing in PBS.

Slides were washed in water and lightly counter-stained with Harris's haematoxylin. The slides were dehydrated by passing through a series of alcohols (30%, 50%, 70%, 90% and 100%) and then dipped in xylene before mounting in Surgipath 'micromount'.

### 2.2.10 Magnetic activated cell sorting (MACS)

Mediastinal lymph nodes were pooled and dissociated into single cell suspension. The cells were counted and 5 x $10^7$ cells were resuspended in MACS buffer (PBS supplemented with 1% bovine serum albumin, 5μM EDTA and 0.1% sodium azide). To this 100μl of CD11c (hamster N418) microbeads (Miltenyi Biotec, UK) was added and incubated for 30 minutes at 10°C. Cells were washed with 20ml of buffer, centrifuged and resuspended in 500μl buffer.

CD11c positive cells were purified by positive selection on $RS^+$ magnetic columns. During cell staining the columns were placed in the magnetic field of the Vario-magnetic separator (Miltenyi Biotec) and 500μl of ice-cold buffer passed through to equilibrate. 500μl of CD11c bound sample was added to the column and negative cells allowed to flow through. Columns were washed twice with 500μl of ice cold buffer to remove unbound cells. The column was removed from the separator and using a syringe 500μl of buffer was back-flushed. The column was replaced in the magnetic field and buffer allowed to flow through. The column was removed from the separator, 1ml buffer was added and the positive cells were flushed from the column using the plunger supplied.

A second $RS^+$ column was placed in the magnetic separator and equilibrated with buffer. The positive cells from the first column were applied to this column in order to increase the purity of the CD11c+ cells. The column was washed with buffer. Then the column was removed from the magnet and positive cells flushed out using a plunger. The cells were counted and an aliquot taken for FACS analysis. Surface markers were stained in suspension before centrifugation on to slides in a cytospin.

### 2.2.11 Interferon-γ CTL assay

In this assay CD8+ T cells are quantitated for their ability to produce interferon-γ (IFN-γ) after a short *in vitro* stimulation (Murali-Krishna *et al.*, 1998). Secretion of IFN-γ is prevented by carrying out the stimulation in the presence of Brefeldin-A (BFA) a compound that inhibits transport of proteins in to the Golgi from the Endoplasmic reticulum (ER).

Mediastinal lymph nodes and spleens were removed from MHV-68 infected mice into RPMI complete medium. Splenocytes were teased out from each spleen separately while the mediastinal lymph nodes were pooled. Erythrocytes were lysed by ammonium chloride lysis (2.2.14). Cells were washed, counted and resuspended at a concentration of $10^7$ cells/ml. The samples were seeded in triplicates. Each of the wells in 96 well plate (round bottom) was seeded with 1 x $10^6$ cells in 200µl complete medium containing 10µg/ml BFA (Sigma) and 10U/ml interleukin-2 (Life Technologies Ltd). The positive control set of wells the cells were stimulated with 50ng/ml PMA (Phorbol myristic acid)(Sigma) and 50ng/ml Ionomycin (Sigma). MHV-68 specific CD8+ T cells were stimulated using MHC class I specific peptide epitopes from two early lytic transcripts ORF6 and ORF61. The ORF6 (H-2$D^b$-restricted) epitope is AGPHNDMEI that is referred to as p56 and the ORF61 (H-2$K^b$-restricted) epitope is TSINFVKI that is referred to as p79 (Stevenson *et al.*, 1998). They were used at a concentration of 1µM. Cells were incubated for 5 hours at 37°C in a 5% $CO_2$ incubator.

Cells were pelleted in the 96 well plate by centrifugation at 275g for 5 minutes at 4°C, washed once with staining wash buffer (SWB: 2% FCS and 0.1% sodium azide in PBS) containing 10µg/ml BFA. Fc receptors were blocked using anti-CD16/CD32 (PharMingen, diluted 1/100 in SWB and 10µg/ml BFA) for 10 minutes on ice. Cells were spun and 50µl of primary antibody (anti-mouse CD8-FITC, Sigma, diluted 1/60 in SWB and 10µg/ml BFA) was added to cells and incubated for 20 minutes on ice. Cells were washed twice with PBS containing 10µg/ml BFA. The cells were fixed using 100µl of PBS containing 10µg/ml BFA with 100µl of 2% formol saline and

incubated for 20 minutes at room temperature. Cells at this stage had to be permeablised in order to facilitate the entry of antibodies that can detect IFN-γ accumulated intracellularly. Permeablisation was carried out by incubation in 0.5% Saponin (Sigma) in SWB for 10 minutes at RT. The cells were then incubated with rat anti-mouse IFN-γ phycoerythrin conjugate (PharMingen, diluted 1/250 in permeablisation buffer) or an isotype control (PharMingen, diluted 1/85) for 30 minutes on ice. The cells were washed with PBS to remove unbound antibody and resuspended in 100µl SWB to be analysed by flow cytometry.

### 2.2.12 Staining cytospun cells

The cytospun slides were washed in PBS. Slides were treated for 1.5 minutes in 0.1% (v/v) TritonX-100 then washed 2x5 minutes in $dH_2O$. The cells were blocked with 5% (v/v) normal goat serum (NGS) for half an hour at room temperature. Excess NGS was removed and primary antibody (polyclonal anti-rabbit MHV-68) was added at a dilution of 1:500 in 2% NGS. Slides were incubated for 2 hours at room temperature then washed 3 x 5 minutes in PBS. Secondary antibody, goat anti-rabbit IgG-biotin (1/500 in 2% NGS) was added and slides were incubated for 1 hour. Slides were washed 3x5 minutes in PBS. Streptavidin-TRITC 1:300 or Streptavidin-FITC 1:500 was added and incubated for 1 hour. Slides were washed 3x5 minutes in PBS. The stained cytospins were air dried and mounted using Vecta-shield (Vector laboratory) and observed using a fluorescent microscope (Nikon, Diaphot 200)

### 2.2.13 Confocal microscopy

The Confocal microscope used for viewing stained cells was a Leica TCS-NT (Germany). It is a central facility in the Biomedical Sciences Section, University of Edinburgh.

### 2.2.14 Ammonium chloride lysis

Lysis buffer was made up of ammonium chloride (0.16M) and Tris-hydrochloric acid (0.17M) (pH6.5-7) at a ratio of 9:1 and warmed to 37°C. Cells to be lysed were

resuspended in 1ml complete media. To this, 3.5ml of the lysis buffer was added, left to stand for 30 seconds till the solution clarified indicating erythrocyte lysis had occurred. The cells were spun down and washed twice with complete media.

### 2.2.15 Electron microscopy

Cells to be analysed for the presence virus particles by transmission electron microscopy were centrifuged in to a tight pellet and fixed with 3% glutaraldehyde in 0.1M Sodium Cacodylate buffer. Staff at the Electron microscope unit (Royal Dick School of Veterinary Studies, University of Edinburgh) carried out the subsequent processing.

### 2.2.16 Handling of DNA, RNA and molecular biological techniques

Many of these methods used in handling of DNA or RNA were based on methods given in 'Molecular cloning'-'A laboratory manual' (Sambrook. *et al.*, 1989)

### 2.2.17 DNA agarose gel electrophoresis

Electrophoresis of DNA was carried out in 1% (w/v) agarose (Seakem agarose, Flowgen, UK). Horizontal gels were prepared in TAE buffer (0.04M Tris-acetate and 0.001M EDTA)(Sambrook. *et al.*, 1989) to which was added 1μg/ml ethidium bromide. The gels were electrophoresed at 80mA for 30 minutes to 2 hours in 1x TAE buffer. Samples were diluted in loading buffer (15%{w/v} Ficoll-400 and 0.1% {w/v} Orange-G dye). DNA size was estimated by comparison with a 1Kb DNA ladder (Life Technologies Ltd) was used. DNA was viewed over an ultraviolet transilluminator.

### 2.2.18 RNA Extraction

Tissue samples were snap frozen in liquid nitrogen as soon as possible after removal from the animal and kept frozen at -70°C till further use. Tissue samples were homogenised in 500μl of RNAzol B (Biogenesis, Poole, England). 50μl of

chloroform was added and samples were mixed well for 15 seconds, then kept on ice for 5 minutes. The aqueous and phenol phases were separated by centrifugation at 11600g for 15 minutes at 4°C. The aqueous phase was transferred to a fresh tube and an equal volume of isopropanol added to it. This was kept on ice for an hour and then centrifuged at 11600g for 15 minutes at 4°C. The pellet was washed once with 70% (v/v) ethanol and centrifuged at 5800g for 8 minutes at 4°C. The pellet was air dried for 15 minutes and resuspended in 10µl milliQ-$H_2O$ (Millipore).

### 2.2.19 Preparation of cDNA from total RNA

Prior to reverse transcription (RT) of total RNA, samples were treated with RNAse free DNAse to ensure removal of any DNA contaminating the total RNA. The reaction mixture contained 2.5mM di-thiothreitol (DTT), 1x reverse transcriptase buffer and 1U Amp grade DNAse enzyme (Life Technologies Ltd) in a total volume of 20µl. The reaction was carried out at 37°C for 30 minutes. The enzyme was inactivated at 80°C for 5 minutes. The above reaction mixture was increased in volume to 25µl and reverse transcription reaction was set up by adding 100pM random primers (Roche); 1mM dNTP (Roche); 200U reverse transcriptase (Superscript II, Life technologies). Reaction was carried out for a 1 hour at 45°C, then heat inactivated at 95°C for 5 minutes. cDNA (complementary-DNA) was stored at -20°C.

### 2.2.20 Polymerase chain reaction (PCR)

A 50µl polymerase chain reaction mixture was prepared with 200nM dNTP, 2mM $MgCl_2$ and 100 pM forward and reverse primers and 0.5U Taq DNA polymerase (Life technologies). 50µl of mineral oil was added on top and the tubes were left at 95°C for 5 minutes prior to the PCR cycles. A 35 cycle PCR was carried out: denaturing 95°C for 45 seconds, annealing 45°C for 1 minutes (or 55°C) extension 72°C for 2 minutes. This was followed by a final cycle at 72°C for 10 minutes. The primer sequences, the size of the fragment and the annealing temperatures are tabulated in the Table 2.2.

**Table 2.2 PCR Primer sequence**

| PCR PRIMERS | PRIMER SEQUENCES 5'-3' | ANNEALING TEMP | SIZE OF FRAGMENT |
|---|---|---|---|
| β-Actin (F) | TGTGATGGTGGGAATGGGTCA | 45°C | 514 bp |
| β-Actin (R) | TTTGATGTCACGCACGATTTC | | |
| ORF50 (F) | AAAAGTTCTGCATCCCAGACCC | 55°C | 293 bp |
| ORF50 (R) | AGGGCTAATGGGTGAAAATGGC | | |
| M3 (F) | TGGCACTCAAACTTGGTTGTGG | 55°C | 359 bp |
| M3 (R) | TAACAGGCAGATTGCCATTCCC | | |

# CHAPTER THREE

# ROLE OF B CELLS IN THE DRAINING LYMPH NODE DURING THE EARLY STAGES OF INFECTION

## 3.1 Introduction

The importance of the draining lymph node associated with the site of primary infection by viruses has been looked at in great detail over the past decade (Doherty *et al.*, 1997). It is the site where professional antigen-presenting cells (APC) such as the dendritic cells, macrophages and B cells migrate following foreign antigenic exposure. It is at this site that the antigen-presenting cells orchestrate the different arms of the immune system to control the infection and bring about the clearance and termination of virus infections. In the case of the Influenza A virus infection of mouse lungs, the mediastinal lymph node is the main site where the various arms of the immune system are triggered. The CD8+ T cells primed in the mediastinal lymph node effect the clearance and control of the virus (Hamilton-Easton and Eichelberger, 1995, Tripp *et al.*, 1995).

MHV-68 infection of the alveolar epithelial cells in the mouse lungs leads to changes in the mediastinal lymph node (MLN). Trafficking of virus to the MLN results in the establishment of latency and lymphadenopathy (Sarawar *et al.*, 1996). Lymphadenopathy is the result of a single or multiple events such as proliferation of cells following activation, recruitment of cells and/or retention of cells at the site (Gresser *et al.*, 1981). The lymph node is constituted of a variety of cell types that could be affected during the course of the infection depending upon the specific arm of the immune mechanism that is called into play. It was therefore considered important to find out whether MHV-68 caused any distinct changes in this environment during the progression of infection.

In EBV and MHV-68 infections B cells are considered the major subset of cells that carry latent virus during the initial course of infection. In the case of EBV the issue of whether B cells directly get infected at the mucosal site or whether there are any

intermediary cells involved such as epithelial cells or dendritic cells is unsolved (Anagnostopoulos *et al.*, 1995). In the case of MHV-68 the alveolar epithelial cells are the primary targets where the virus undergoes a productive infection. Lytic virus is cleared by day 10 and subsequently latently infected B cells are found in the spleen (Sunil-Chandra *et al.*, 1992b). The issue of whether virus is transmitted to B cells directly from infected epithelial cells in the lungs has not been solved even with MHV-68. There is evidence that B cells are important for establishment of latency in the spleen as seen from experiments with B cell deficient (μMT) mice (Usherwood *et al.*, 1996b).

The aim of the work described in this chapter was to analyse the early events of MHV-68 infection in the mediastinal lymph node including (a) the role of B cells in the development of early pathogenesis, (b) the involvement of cells other than B cells in trafficking of virus from the lungs and (c) the role of CD4+ T cells in lymphadenopathy.

## 3.2 Mediastinal lymphadenopathy and B cells

### 3.2.1 Mediastinal lymphadenopathy in the presence and absence of B cells

In order to investigate the importance of B cells in lymphadenopathy the MLN from mice deficient in B cells (μMT mice, Kitamura *et al.*, 1991) were compared with wild type C57BL/6 following MHV-68 infection. Uninfected MLN contain between 1-2 million lymphocytes. Therefore, it was necessary to pool lymph nodes from 4-6 mice for each time point under investigation in order to obtain adequate number of cells for the various assays.

C57BL/6 and μMT mice (4-5 weeks of age) were infected intranasally with $4 \times 10^5$ PFU MHV-68. MLN were pooled from 5 mice from each group taken on days 3, 7, 10 post-infection and dissociated to obtain single cells suspensions and counted. The results are represented in Figure 3.1.

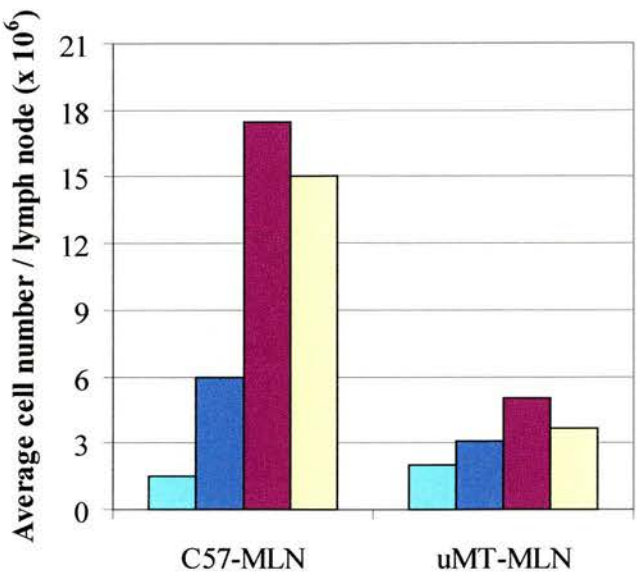


Figure 3.1 Lymphadenopathy of the mediastinal lymph node in wild type C57BL/6 and B cell deficient (μMT) mice C57BL/6 and μMT mice (4-5 weeks of age) were infected intranasally with 4 x $10^5$ PFU MHV-68. MLN cells were pooled from five mice in each group, counted and used for subsequent analysis as described in the following sections. The graph shows the average number of cells per MLN in uninfected MLN ( □ ) and on 3 ( ■ ), 7 ( ■ ) and 10 ( □ ) days post-infection. The fold difference is representative of three independent experiments.

C57BL/6 mice showed almost a 10-fold increase in cell numbers in the MLN on days 7 and 10 of MHV-68 infection. The μMT mice failed to show any dramatic changes in cell numbers as compared to the wild type mice.

The results demonstrate that B cells are involved in the increased cellularity of the MLN seen during early phases of MHV-68 infection.

### 3.2.2 Changes in cell populations during the process of lymph node enlargement

In order to investigate further the nature of the cells in the MLN of C57BL/6 mice we performed FACS analysis on the main cell subsets. MLN cells were stained with antibodies against surface markers for B cells (anti-mouse-IgMμ and anti-mouse-B220), T cells (anti-mouse-CD4 and anti-mouse-CD8), natural killer cells (anti-mouse-NK1.1), macrophages (anti-mouse-F4/80) and dendritic cells (anti-mouse-DEC205). Cells were also stained with antibodies against activation markers for B and T cell (anti-mouse-CD69) and T cell activation marker (anti-mouse-CD25).

The results are represented in Figures 3.2(a) and 3.2(b). A 4-5-fold increase in the total number of B cells in the MLN was detected on days 7 and 10 compared to day 3 post-infection. CD4+ and CD8+ T cells did not show similar increases, with CD4+ T cells showing less than a 2-fold increase. There were increased numbers of natural killer cells, macrophages and dendritic cells that may also contribute towards the enlargement of the MLN. However B cell numbers calculated by correlating FACS percentage to the total number of cells from MLN of C57BL/6 mice were far higher than any other cell subset in the enlarged MLN on days 7 and 10 post-infection.

It was concluded that B cells are the major contributors to lymphadenopathy seen in C57BL/6 mice and this is confirmed by the absence of lymph node enlargement in μMT mice that had no B cells.

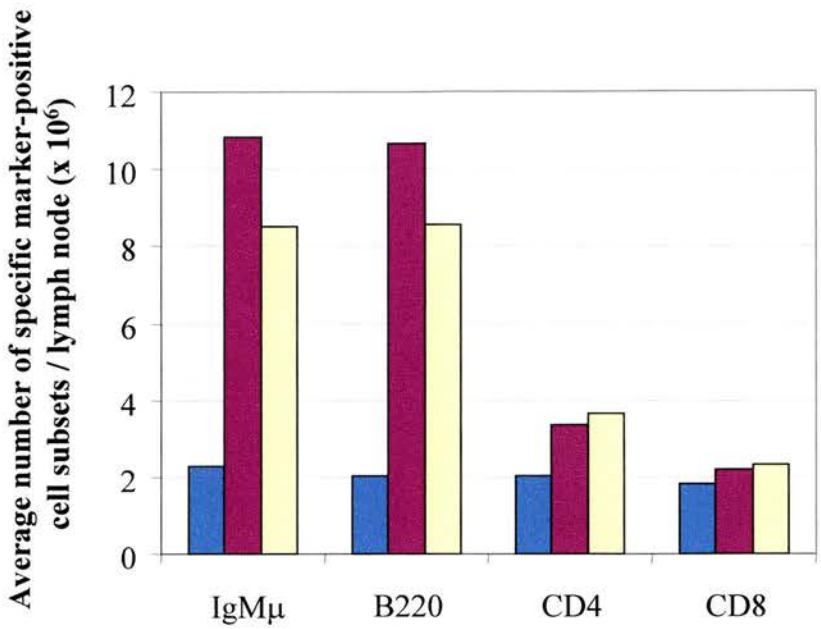


Figure 3.2a Phenotype of cells in the enlarged mediastinal lymph nodes of C57BL/6 mice C57BL/6 mice were infected intranasally with 4 x $10^5$ PFU MHV-68. On days 3 ( ■ ), 7 ( ■ ) and 10 ( □ ), mediastinal lymph nodes (MLN) were pooled from five mice. The MLNs were dissociated to obtain single cell suspensions counted and taken for flow cytometric analysis. The cells were stained with either biotinylated anti-mouse IgMμ monoclonal antibody, anti-mouse B220 monoclonal antibody, anti-mouse CD4 (YTS177) monoclonal antibody or anti-mouse CD8 (YTS105) monoclonal antibody. 10,000 cells were counted in each analysis. The average number of specific marker-positive cell subsets per MLN is presented above. The fold difference is representative of three independent experiments.

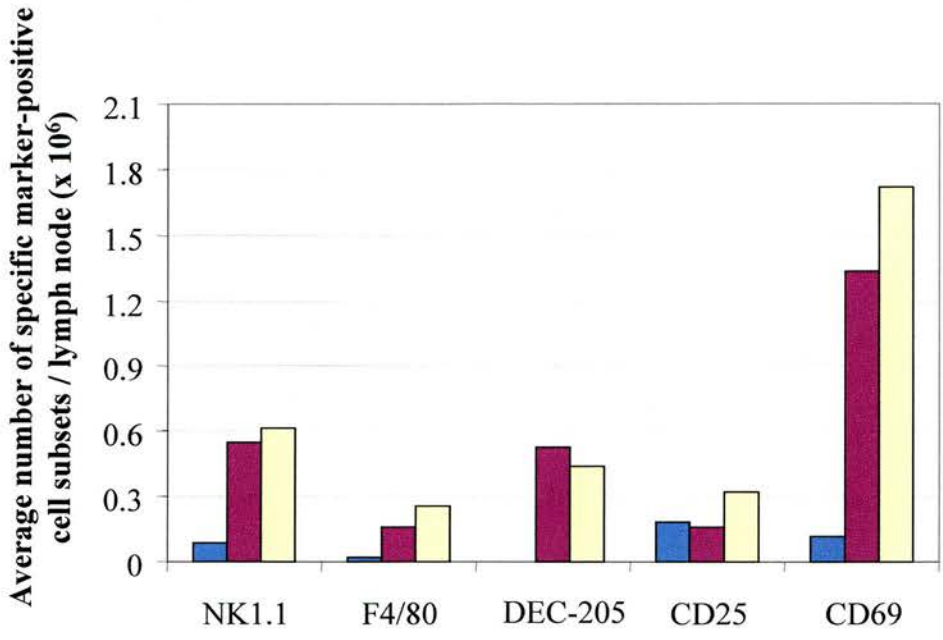


Figure 3.2b Phenotype of cells in the enlarged mediastinal lymph nodes of C57BL/6 mice C57BL/6 mice were infected intranasally with 4 x $10^5$ PFU MHV-68. On days 3 ( ■ ), 7 ( ■ ) and 10 ( □ ), mediastinal lymph nodes (MLN) were pooled from five mice. The MLNs were dissociated to obtain single cell suspensions, counted and taken for flow cytometric analysis. The cells were stained with either biotinylated anti-mouse NK1.1 monoclonal antibody, anti-mouse F4/80 monoclonal antibody, anti-mouse DEC-205 (NLDC145) monoclonal antibody, anti-mouse CD25 monoclonal antibody or anti-mouse CD69 monoclonal antibody. 10,000 cells were counted in each analysis. The average number of specific marker-positive cell subsets per MLN is presented above. The fold difference is representative of three independent experiments.

### 3.2.3 FACS analysis for B cell surface markers

Since B cells were the major subset undergoing proliferation in the MLN of infected mice the decision was made to look at B cells in more detail using different cell surface markers and some activation markers that undergo changes during germinal centre (GC) formation.

The B cell specific surface markers expressed uniformly in most mature B cells are CD19, B220 and IgMμ. B cells that undergo class switching in GCs lose IgM and start expressing IgG. They also express MHC class II but the marker is also seen on macrophages and dendritic cell populations. The activation marker CD69 is expressed on both activated B and T cells. CD21 and CD23 are expressed on mature B cells but they are lost as these cells differentiate into antibody producing cells (Clark and Lane, 1991). CD21 is of interest as EBV infects B cells via CD21 (Nemerow *et al.*, 1987) and leads to subsequent proliferation (Roberts *et al.*, 1996). CD23 is the low affinity receptor for IgE (Ravetch and Kinet, 1991) and is found on follicular dendritic cells (FDCs) and monocytes. Both CD21 and CD23 are activated during EBV infection (Wang *et al.*, 1990) and therefore were of interest in the case MHV-68 infected B cells.

The MLN were pooled from 5 mice, dissociated into single cells and stained for the markers discussed above and analysed by flow cytometry. The changes in B cell surface markers were observed daily over the first seven days of infection and then on days 10 and 12 in the MLN of C57BL/6 mice. The results are presented in Figure 3.3(a) and 3.3(b).

The Figure 3.3a shows that B cells detected with CD19, B220 and IgMμ had comparable patterns of staining over the days examined. The total cell number of B cells as seen from these surface marker showed a 10-15-fold rise on days 5 to 12 compared to number of B cells in uninfected control mice. In the same time course the CD4+ and CD8+ T cell numbers increased only by 4-5-fold. In the figure 3.3b, IgMμ versus CD69 staining showed that there was minimal B cell activation as detected by double staining and the increase in CD69 alone could be due to the

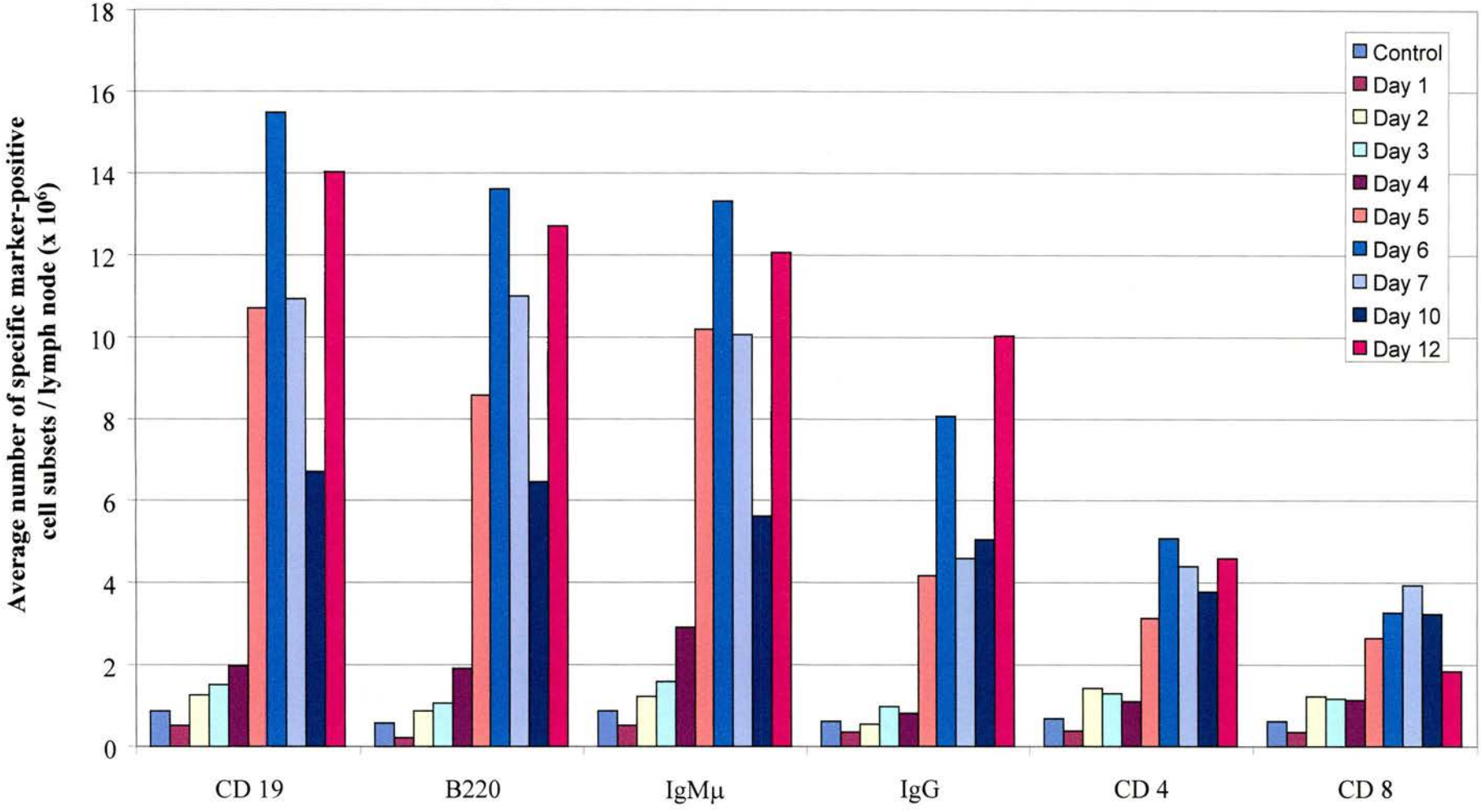


Figure 3.3a Expression of B cell markers in the enlarged lymph nodes of C57BL/6 mice

Figure 3.3a Expression of B cell markers in the enlarged lymph nodes of C57BL/6 mice C57BL/6 mice were infected intranasally with 4 x $10^5$ PFU MHV-68. On days 1-7, 10 and 12, MLN were removed and pooled from five mice. The colour coding for different days is shown in the panel within the graph. The MLNs were dissociated to obtain single cell suspensions counted and taken for flow cytometric analysis. The cells were stained with either anti-mouse CD19, anti-mouse B220 monoclonal antibody, biotinylated anti-mouse IgMμ monoclonal antibody, FITC conjugated anti-mouse IgG, anti-mouse CD4 (YTS177) monoclonal antibody or anti-mouse CD8 (YTS105) monoclonal antibody. 10,000 cells were counted in each analysis. The average number of specific marker-positive cell subset per MLN is presented.

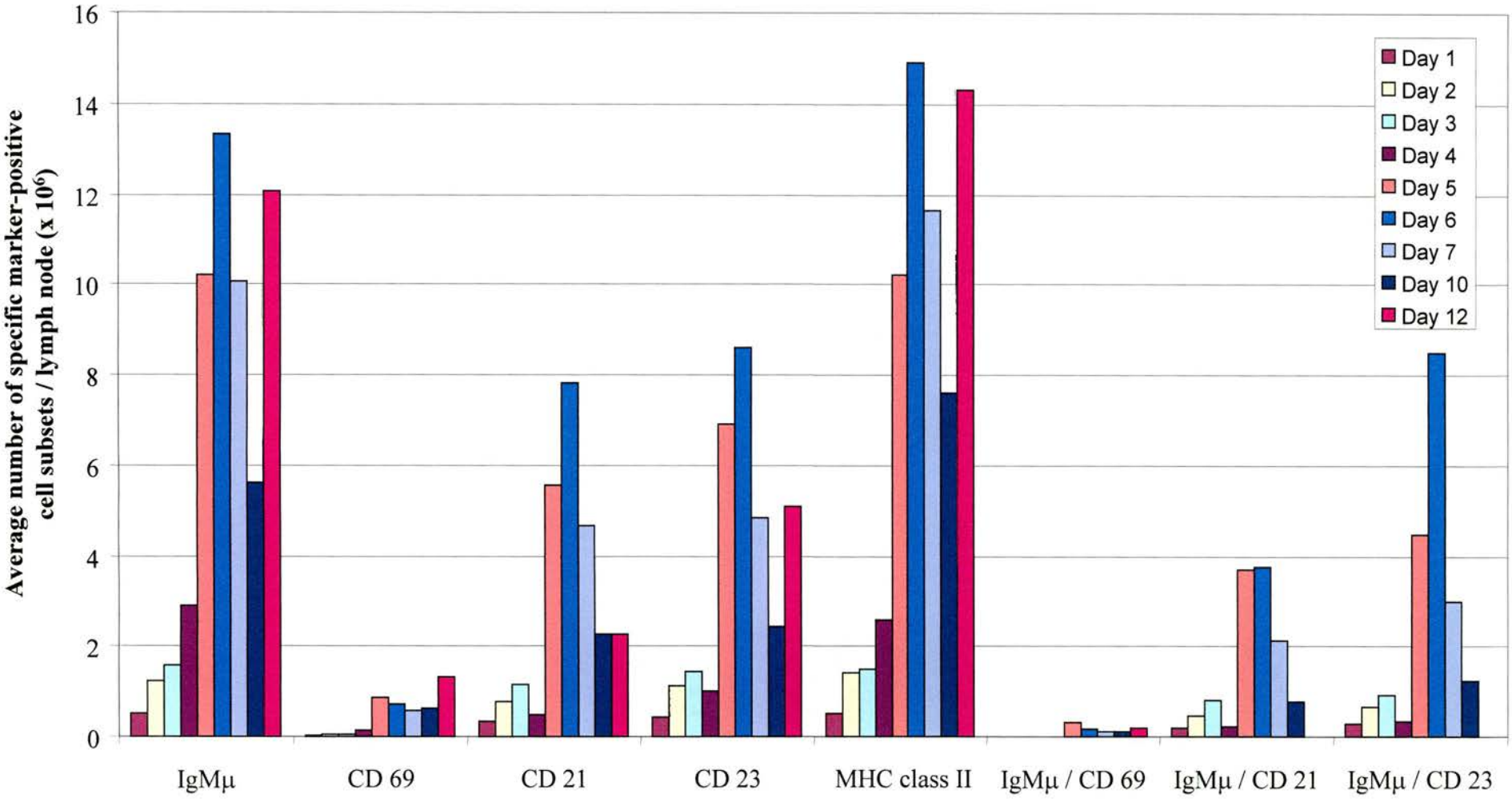


Figure 3.3b Expression of B cell markers in the enlarged lymph nodes of C57BL/6 mice

Figure 3.3b Expression of B cell markers in the enlarged lymph nodes of C57BL/6 mice C57BL/6 mice were infected intranasally with 4 x $10^5$ PFU MHV-68. On days 1-7, 10 and 12, MLN were removed and pooled from five mice. The colour coding for different days is shown in the panel within the graph. The MLNs were dissociated to obtain single cell suspensions counted and taken for flow cytometric analysis. The cells were stained with either biotinylated anti-mouse IgMμ monoclonal antibody, anti-mouse CD21 monoclonal antibody, anti-mouse CD23 monoclonal antibody, FITC conjugated anti-mouse CD69 monoclonal antibody or FITC conjugated anti-mouse MHC class II monoclonal antibody. The graph also shows cells double positive for IgMμ + CD69, CD21 or CD23. 10,000 cells were counted in each analysis. The average number of specific marker-positive cell subsets per MLN is presented.

expression of this marker on T cells. The IgMμ versus CD21 or CD23 levels increased by days 5 and 6 but had fallen by day 10 post-infection. This might be an indication of B cells moving in to the germinal centres for clonal selection at this stage.

The clear rise in B cell numbers detected using an array of surface markers substantiates the results seen in section 3.2.2. There is a sudden peak of B cells appearing on day 5, which remain elevated on day 12 post-infection. The cells double-stained for IgMμ/CD21 and IgMμ/CD23 increased on days 5 and 6, indicating that there were many mature B cells being recruited into this region on these days. The reasons for the massive increase in B cell numbers may be due to virus coded proteins in the environment leading to B cell accumulation or due to host cytokine or cellular signalling leading to proliferation.

## 3.3 CD4+ T cell signalling and B cells in the MLN

### 3.3.1 Requirement for CD4+ T cell signalling in lymph node enlargement

The increase in the number of B cells in the MLN seen during the initial course of MHV-68 infection could involve a major role for virus genes in promoting B cell proliferation and/or a role for CD4+ T cells in driving B cell proliferation.

In this section the role of CD4+ T cells was investigated by depleting these T cells from mice. The method used is described in section (2.2.7). There were two groups of mice, one set depleted of CD4+ T cells (Group 2) and another the control group of mice (Group 1). In order to deplete CD4+ T cells the group 2 mice were injected intravenously with 1mg of YTS191 rat-anti-mouse CD4 antibody in a 100μl volume. Two days later both group 1 and group 2 mice were infected intranasally with $4 \times 10^5$ PFU MHV-68. On the second day post-infection the group 2 mice were injected intravenously with 1mg of YTS191 antibody. Four mice each were sampled on days 3 and 7. On day 7 the remaining group 2 mice were injected intraperitoneally with 1mg of YTS191 antibody. The MLN from 4 mice were pooled for each group on

days 3, 7, 10 and 16 post-infection. We confirmed the depletion through FACS analysis, the results shown in Figure 3.4.

The MLN were pooled, dissociated and total number of cells per MLN was calculated for the CD4+ T cell depleted group and compared to the control group over the time course of infection. The results are represented in Figure 3.5.

The CD4+ T cell depleted mice showed an increase in the number of MLN cells over time particularly on day 10 post-infection there was a 5-fold increase. On the other hand the infected control group of mice showed a 10-fold increase in the number of cells on day 10 post-infection. Therefore there was only a 50% reduction in lymphadenopathy on depleting CD4+ T cells.

The results show that CD4+ T cell signalling is important for the development of lymphadenopathy to the extent seen in the control group but is not the only reason the MLN exhibited lymphadenopathy during MHV-68 infection.

### 3.3.2 B cell numbers in the MLN following CD4+ T cell depletion

In view of the reduction in lymphadenopathy in CD4+ T cell depleted mice the impact on B cell numbers was investigated. The MLN from 4 mice were pooled from CD4+ T cell depleted and control mice on days 3, 7, 10 and 16 post-infection. The MLN were dissociated to obtain single cell suspensions and cells taken for flow cytometric analysis (FACS). The cells were stained either with anti-mouse CD19 monoclonal antibody, biotinylated-anti-mouse IgMμ monoclonal antibody, FITC-conjugated anti-mouse IgG monoclonal antibody, FITC-conjugated anti-CD8 monoclonal antibody or FITC-conjugated anti-CD4 monoclonal antibody. The results are represented in Figure 3.6.

The control group of mice showed a 4-fold increase in the number of B cells on days 7 and 10 compared to day 3 post-infection, similar to what was seen in section 3.2.3. The CD19 expressing B cell numbers in the CD4+ T cell depleted group was much

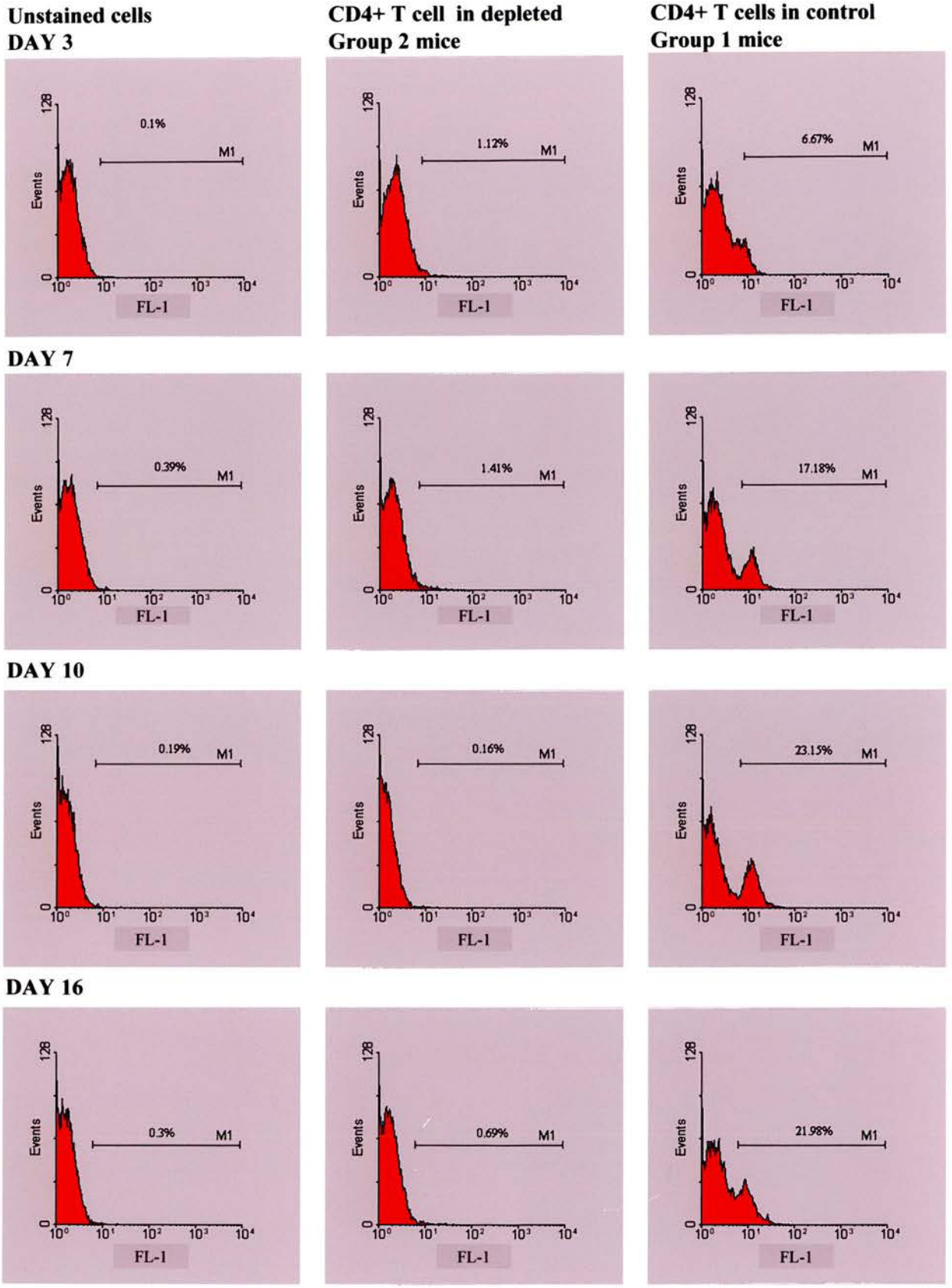


Figure 3.4 FACS analysis for CD4+ T cells in the MLN The graphs on the left-hand panel are unstained control cells, right-hand panel are cells stained with anti-mouse CD4+ T cells from the MLNs of control mice and the middle panel are cells from the MLNs of mice depleted of CD4+ T cells on days 3, 7, 10 and 16 post-infection. The FACS percentages of CD4+ T cell are represented above the bars marked M1.

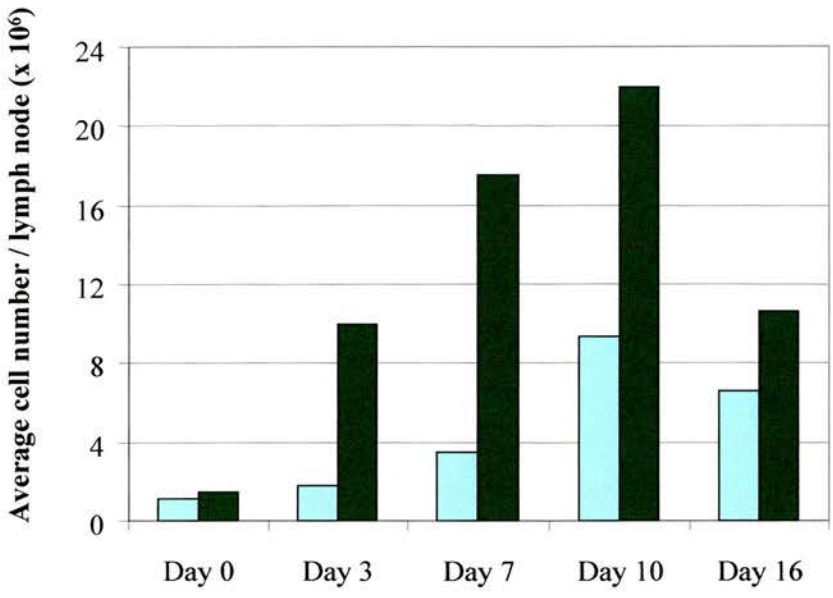


Figure 3.5 Cellularity of the mediastinal lymph node in C57BL/6 mice depleted of CD4+ T cells C57BL/6 mice were divided into two groups. Group 1 was the infected but non-depleted control group and Group 2 was the infected and depleted of CD4+ T cells. In order to deplete CD4+ T cells the group 2 mice were injected intravenously with 1mg of YTS191 rat-anti-mouse CD4 antibody in a 100µl volume. Two days later both Group 1 and Group 2 mice were infected intranasally with 4 x $10^5$ PFU MHV-68. On the second day post-infection the Group 2 mice were injected intravenously with 1mg of YTS191 antibody. Four mice each were sampled on days 3 and 7. On day 7 the remaining Group 2 mice were injected intraperitoneally with 1mg of antibody. The mediastinal lymph nodes from four mice were pooled for each group on days 0, 3, 7, 10 and 16 post-infection. The MLNs were dissociated to obtain single cell suspensions and cell number counted. The graph represents the average cell numbers per MLN obtained for the control Group 1 (■ ) and the CD4+ T cell depleted Group 2 ( □ ) mice. The fold difference is representative of three independent experiments.

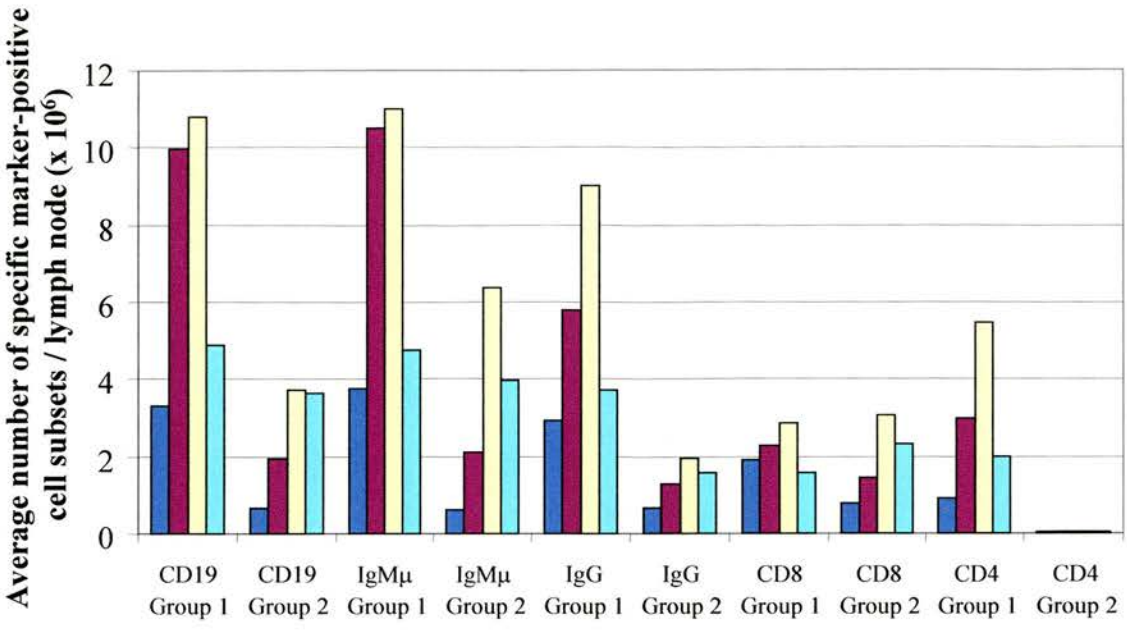


Figure 3.6 B cell numbers in the mediastinal lymph node of C57BL/6 mice depleted of CD4+ T cells C57BL/6 mice were divided in to two groups. Group 1 was the infected but non-depleted control group (control) and Group 2 was the infected and CD4+ T cell depleted group. (The depletion was carried out successfully as shown in figure 3.4). The mediastinal lymph nodes (MLN) from 4 mice were pooled for each group on days 3 ( ■ ), 7 ( ■ ), 10 ( □ ) and 16 ( □ ) post-infection. The MLNs were dissociated to obtain single cell suspensions and cells taken for flow cytometric analysis. The cells were stained with either anti-mouse CD19 monoclonal antibody, biotinylated-anti-mouse IgMμ monoclonal antibody, FITC-conjugated anti-mouse IgG monoclonal antibody, FITC-conjugated anti-CD8 monoclonal antibody or FITC-conjugated anti-CD4 monoclonal antibody. The graph shows the average number of specific marker-positive cell subset per MLN. The fold difference is representative of three independent experiments.

lower on day 3 compared to control group, but as the infection progressed a 5-fold increase was seen on days 10 and 16 post-infection. The IgG surface marker was used to detect class switching by B cells. The cells were also stained for CD4+ and CD8+ T cells.

The results in this section show that B cells proliferation is possible in the absence of CD4+ T cells and could result from the direct proliferation mediated effects of the virus.

### 3.3.3 Presence of latently infected cells in the MLN following CD4+ T cell depletion

Cells carrying latent virus are determined by infective centre assay as described in the methods section (2.2.2). Productive virus is ascertained using a simple freeze thawing method described in section (2.2.3) and those values are subtracted from the number of infective centres to obtain the final value of latently infected cells within tissues. Usherwood *et al* (1996a) showed that on depleting CD4+ T cells there was a comparative reduction in the number of latently infected cells in the spleen of BALB/c mice. They also observed the absence of splenomegaly on depleting CD4+ T cells.

The following experiments investigated the changes in the number of latently infected cells in the MLN and spleen on depleting CD4+ T cells in C57BL/6 mice. The results are presented in Figures 3.7 and 3.8.

The control group of C57BL/6 mice showed a typical increase in the number of latently infected cells in the MLN on days 10 and 16 post-infection. The CD4+ T cell depleted mice showed a slight increase in the number of latently infected cells on day 10 post-infection but the overall number of cells was comparatively reduced in the MLN. In the spleen, too, the number of latently infected cells was reduced in the CD4+ T cell depleted group compared to control groups of mice

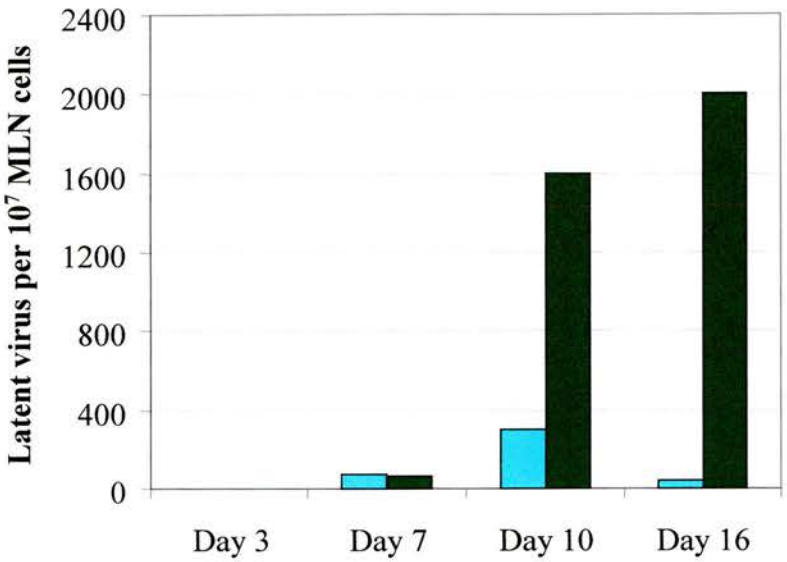


Figure 3.7 Latent virus in the mediastinal lymph node of C57BL/6 mice depleted of CD4+ T cells C57BL/6 mice were divided into two groups. Group 1 was the infected but non-depleted control group and Group 2 was the infected and CD4+ T cell depleted group. In order to deplete CD4+ T cells the group 2 mice were injected intravenously with 1mg of YTS191 rat-anti-mouse CD4 antibody in a 100µl volume. Two days later both Group 1 and Group 2 mice were infected intranasally with 4 x $10^5$ PFU MHV-68. On the second day post-infection the Group 2 mice were injected intravenously with 1mg of YTS191 antibody. Four mice each were sampled on days 3 and 7. On day 7 the remaining Group 2 mice were injected intraperitoneally with 1mg of antibody. The MLNs from four mice were pooled for each group on days 3, 7, 10 and 16 post-infection. The MLNs were dissociated to obtain single cell suspensions and cell numbers counted. The graph represents the number of infective centres (latent virus) per $10^7$ cells in the MLN of the control Group 1( ■ ) and the CD4+ T cell depleted Group 2 ( ■ ) mice. The fold difference is representative of three independent experiments.

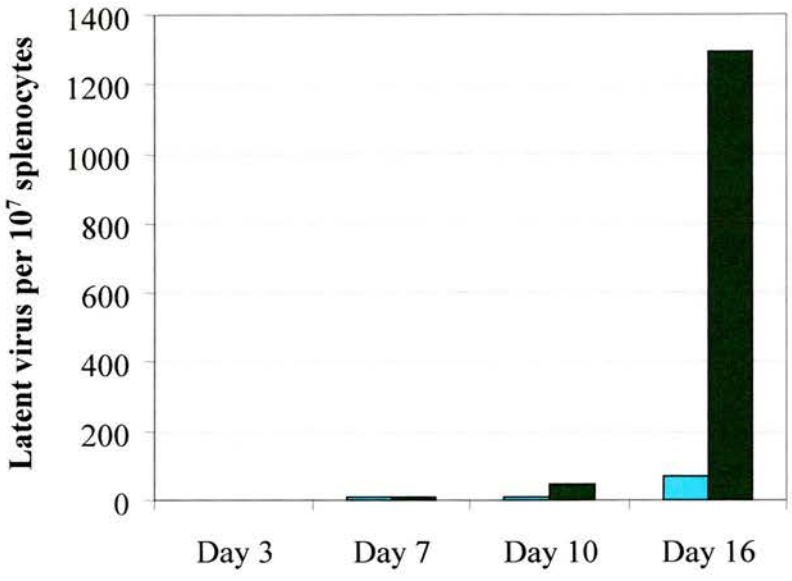


Figure 3.8 Latent virus in the spleens of C57BL/6 mice depleted of CD4+ T cells

C57BL/6 mice were divided in to two groups. Group 1 was the infected but non-depleted control group and Group 2 was the infected and CD4+ T cell depleted group. In order to deplete CD4+ T cells the group 2 mice were injected intravenously with 1mg of YTS191 rat-anti-mouse CD4 antibody in a 100µl volume. Two days later both Group 1 and Group 2 mice were infected intranasally with 4 x $10^5$ PFU MHV-68. On the second day post-infection the Group 2 mice were injected intravenously with 1mg of YTS191 antibody. Four mice each were sampled on days 3 and 7. On day 7 the remaining Group 2 mice were injected intraperitoneally with 1mg of antibody. The spleens were sampled on days 3, 7, 10 and 16 post-infection. The spleens were dissociated to obtain single cell suspensions and cell number counted. The graph represents the number of infective centres (latent virus) per $10^7$ splenocytes of the control Group 1 ( ■ ) and the CD4+ T cell depleted Group 2 ( □ ) mice.

The observations in the MLN show that the establishment of latency very early during the course of MHV-68 is dependent on the presence of CD4+ T cells just as was previously observed in the spleen. However, CD4+ T cells may be important mainly in driving the transient peak of latent infection and not in the long-term establishment of latency.

## 3.4 Latently infected cells in the absence of B cells, in the MLN

### 3.4.1 Latently infected cells in the MLN of μMT mice

The previous work on the B cell deficient (μMT) mice (Usherwood *et al*, 1996b) showed that these mice lacked detectable latently infected cells in the spleens following MHV-68 infection. This indicated the importance of B cells in establishing latency in the spleen.

In order to detect whether cells other than B cells were involved in trafficking virus into the MLN, the μMT mice were compared to the C57BL/6 mice on days 3, 7 and 10 post-infection. The MLN was the main target organ but the cervical lymph node (CLN) was also examined in order to detect the systemic transfer of virus during infection. The lymph nodes were pooled and latently infected cells were assayed using infective centre assay. The results are presented in Figure 3.9.

The μMT mice had a detectable level of latently infected cells in the MLN on days 3 and 7 post-infection similar to the C57BL/6 mice. On day 10 post-infection the C57BL/6 mice had a large increase in the number of latently infected cells and in contrast the μMT mice had none. The CLN of μMT mice showed no detectable levels of latently infected cells on any of the days investigated while the C57BL/6 mice had latently infected cells on days 7 and 10 post-infection.

The results of this experiment demonstrated that the virus could infect cells other than B cells very early during infection as observed in the μMT mouse MLN.

### 3.4.2 Immunostaining for cells expressing virus encoded lytic proteins

Cells with productive virus infection (infective virus) or cells reactivated from latency express virus encoded proteins that can be detected by immunostaining with antibodies generated against lytic MHV-68. Immunostaining assay was carried out to look for lytic virus positive cells in the MLN of μMT mice following MHV-68 infection.

The IFN-α/β $R^{-/-}$ mice exhibit higher number of cells infected with virus as compared to normal wild type mice as deduced from studies on disease pathogenesis of MHV-68 (Dutia *et al.*, 1999a). Therefore these tissues were used as positive controls. Lungs and MLN from infected μMT and IFN-α/β $R^{-/-}$ mice were fixed in 10% formaldehyde and subsequently paraffin embedded. The paraffin embedded tissues sections cut on to Biobond coated slides were used for immunostaining as described in the methods section (2.2.9). The tissue samples were dewaxed and stained using anti-MHV-68 antibodies.

The immunostained lung and MLN tissues sections of IFN-α/β $R^{-/-}$ mice is shown in Figure 3.10. There were no cells stained with MHV-68 antibodies detectable in the MLN tissue sections of μMT mice.

### 3.4.3 Detection of virus particles using electron microscopy

Virus capsids can be detected in cells containing productive virus. Herpesviruses being large viruses have 120-150nm capsids and can be visualised using a transmission electron microscope (TEM).

Cells from μMT mice MLN on day 7 post-infection were enriched for surface marker CD11c by MACS as described in the methods section (2.2.10) and the purified cells were fixed for transmission electron microscope (2.2.15). The images are shown in Figure 3.11.

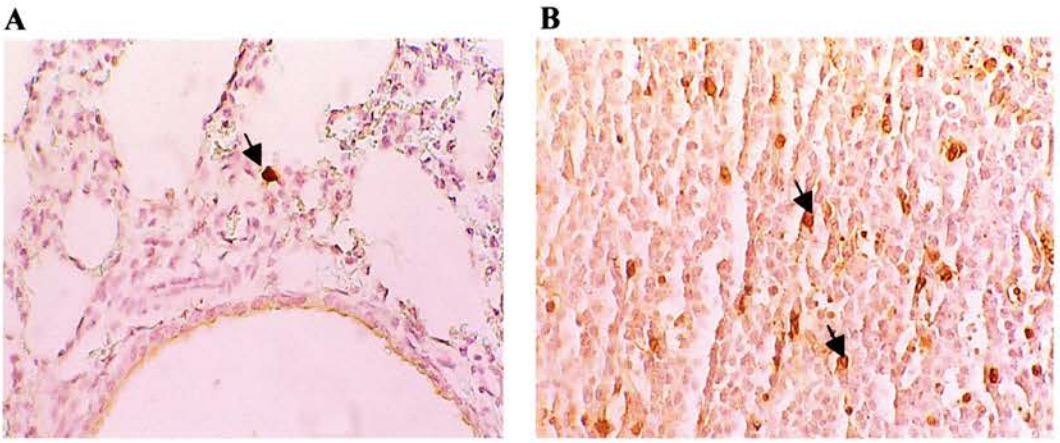


Figure 3.10 Lung and MLN tissues from IFN α/β R-/- mice immunostained for MHV-68 lytic viral proteins Paraffin embedded tissue sections from IFN-α/β $R^{-/-}$ mice infected with 4 x $10^5$ PFU MHV-68 on day 7 post-infection were dewaxed and immunostained for virus coded proteins as described in the methods section (2.2.9). The tissue sections were incubated with rabbit polyclonal MHV-68 antibody. The figure represents (A) lung tissue (magnification X200) and (B) MLN (magnification X200). The positively stained cells are those that are stained dark brown (indicated by arrows).

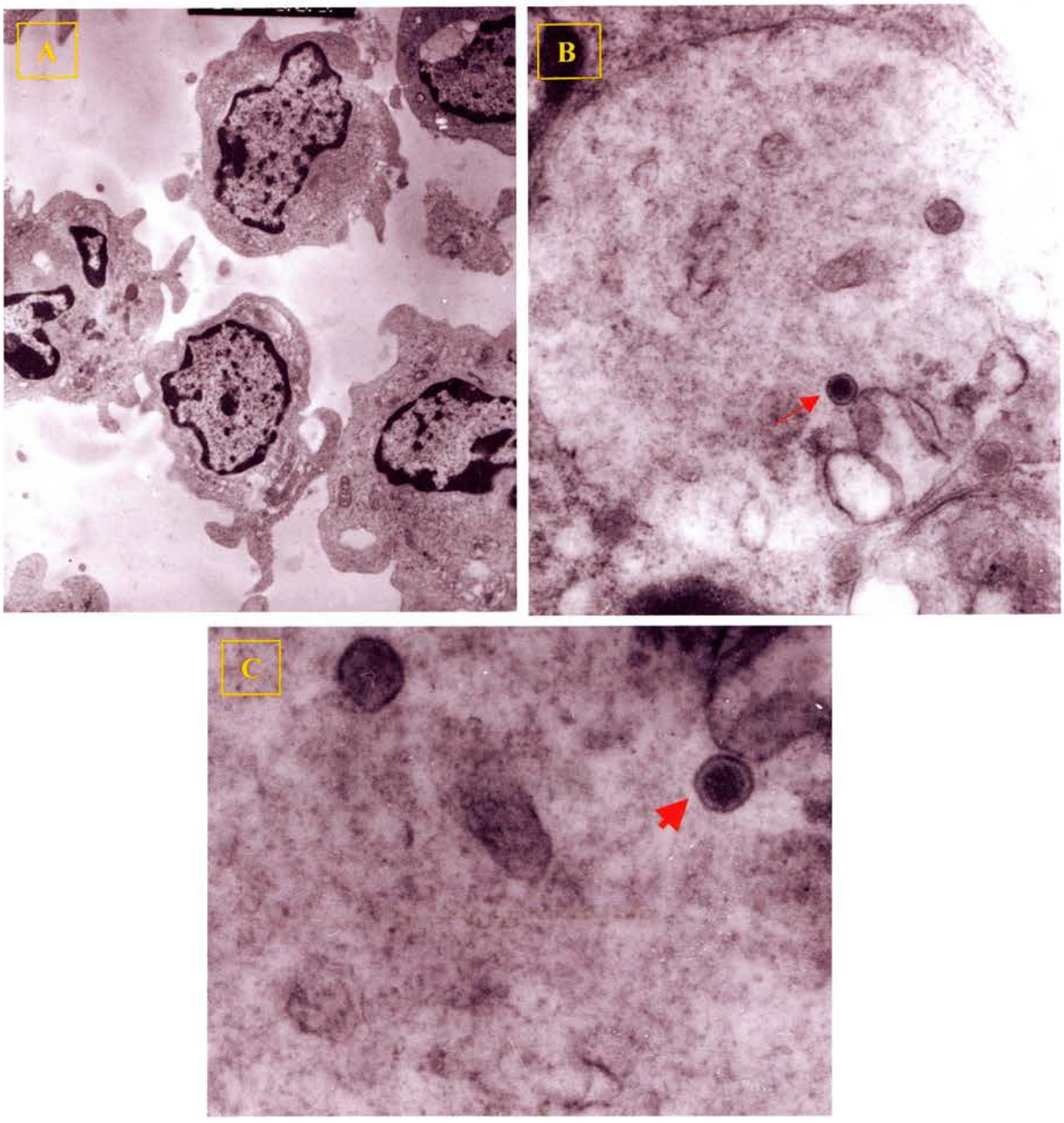


Figure 3.11 Transmission Electron Microscopy to detect virus particles in MLN cells from μMT mice infected with MHV-68 μMT mice were infected with 4 x $10^5$ PFU MHV-68 intranasally. On day 7 post-infection MLNs from 6 mice were pooled, dissociated into single cells and enriched for the CD11c surface marker using magnetic activated cell sorting (MACS) as described in the methods section (2.2.15). The enriched cells were subsequently processed for electron microscopic (EM) analysis. The Figure represents (A) the morphology of the CD11c enriched population (magnification: X5000), (B) vesicle within the cytoplasm of a cell, arrows showing virus particle (magnification: X35,000) and (C) the same virus particle under higher magnification: X60,000.

The μMT MLN had no cells with capsids that were detectable in the nucleus. There were a few cells that contained a single capsid in cytoplasmic vesicles. These could be virus particles that have been engulfed into the cell following virus attachment to the cell. Therefore, there were no cells detectable in the MLN with replicating virus as determined by the presence of virus capsids in the nucleus.

### 3.4.4 Reverse transcription-polymerase chain reaction (RT-PCR) for viral transcripts on whole tissues

Replicating virus express a large number of genes but during latency most of the structural gene expression is shutdown and genes involved in maintaining virus latency are turned on. In the case of MHV-68 clear differences between lytic and latent genes have not been established. However, an experiment was designed to look at ORF50 an immediate early transcript and M3 an early/latency associated transcript in the MLN of μMT mice.

To investigate the gene expression, RT-PCR was carried out on whole lymphoid tissue. MLN were taken from infected mice on days 3, 5, 7 and 10 post-infection and snap frozen in liquid nitrogen. RNA was extracted as described in the method section (2.2.18). 2μg of RNA for each sample was treated with DNAse and an aliquot removed prior to RT to be used as controls. Complementary-DNA (cDNA) was made as described in the methods section (2.2.19). The cDNA was used for PCR amplification of MHV-68 gene transcripts ORF50 and M3 and the cellular β-actin transcript (control) as described in the methods section (2.2.20). The results are presented in Figure 3.12. The samples removed prior to RT were used in a PCR with M3 primers to confirm that the DNAse step was successful.

The RT-PCR results show that both in the MLN of C57BL/6 and the μMT mice ORF50 and M3 positive transcripts were present on all days investigated.

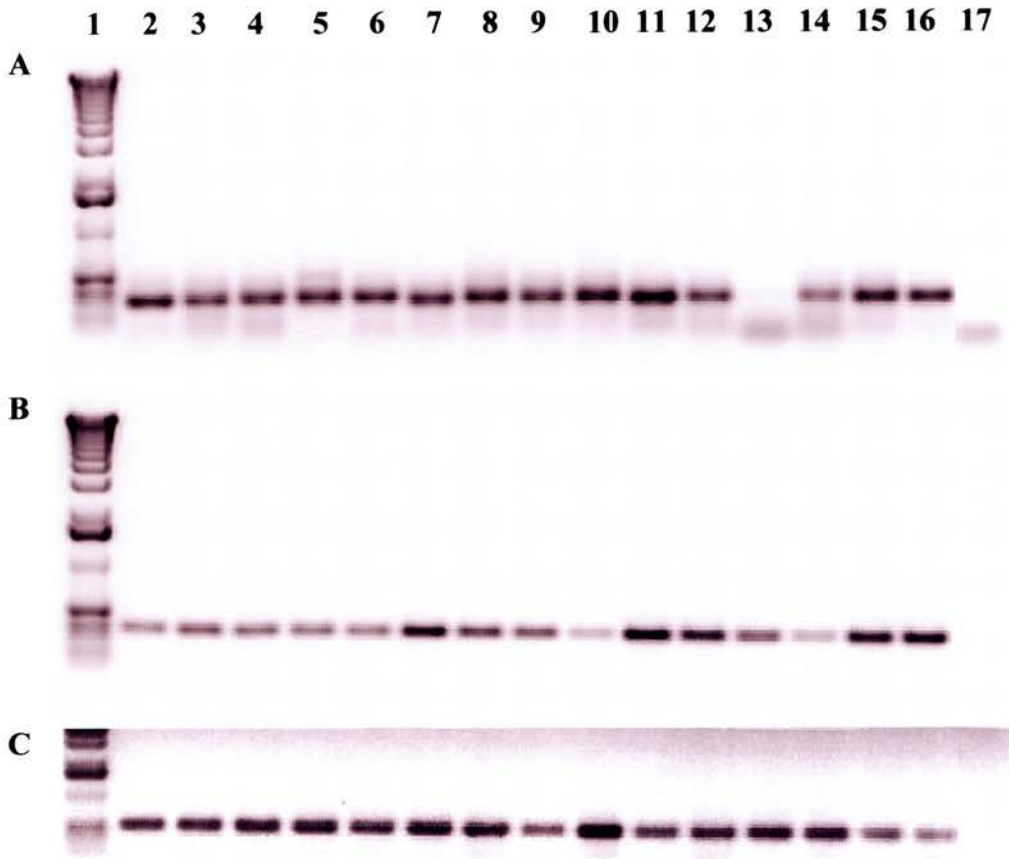


Figure 3.12 RT-PCR for viral transcripts on whole MLNs from μMT and C57BL/6 mice μMT mice and C57BL/6 mice were infected with $4x10^5$ PFU MHV-68 intranasally. MLNs from infected mice on days 3, 5, 7 and 10 post-infection were snap frozen in liquid nitrogen. cDNA was made from 2μg of RNA extracted from the individual MLNs as described in the methods sections (2.2.18 and 2.2.19). The cDNA was used for PCR amplification of MHV-68 gene transcripts as described in the methods section (2.2.20). The figure represents (A) samples amplified for MHV-68 ORF50, (B) samples amplified for MHV-68 M3 and (C) samples amplified for cellular β-actin transcript. In the figure the lane number (1) 1Kb Lambda Marker, (2 and 3) μMT mice MLNs on day 3 post-infection, (4) C57BL/6 mouse MLN on day 3, (5 and 6) μMT mice MLNs on day 5 post-infection, (7 and 8) C57BL/6 mice MLNs on day 5 post-infection, (9 and 10) μMT mice MLNs on day 7 post-infection, (11 and 12) C57BL/6 mice MLNs on day 7 post-infection, (13 and 14) μMT mice MLNs on day10 post-infection, (15 and 16) C57BL/6 mice MLNs on day 10 post-infection and (17) PCR negative control.

## 3.5 CD8+ CTL and B cells in the MLN

### 3.5.1 MHV-68 specific CTL response, in the absence of B cells

The experiments with CD8+ T cell depleted mice (Ehtisham *et al.*, 1993) and with β2-microglobulin deficient mice (Weck *et al.*, 1996) have shown the importance of CD8+ T cells in MHV-68 infection. The CD8+ T cells play a critical role in the clearance of lytic MHV-68 from the lungs and also in the prevention of latent virus reactivation from tissues (Stevenson *et al.*, 1998).

The presence of B cells infected with MHV-68 may play an important role in enhancing CTL activity in the MLN. In order to determine the importance of B cells we compared CTL activity in μMT and C57BL/6 mice. The IFN-γ CTL assay described in section (2.2.11) was used to measure the frequency of CTL specific for the immuno-dominant peptides obtained from ORF6 and ORF61 of MHV-68 (Stevenson *et al.*, 1998). The results are represented in Figure 3.13.

The μMT mice showed CTL activity as early as day 6 in the MLN, although the numbers fell by days 10 and 17 post-infection. The C57BL/6 mice showed 10-fold higher virus specific CTLs on days 10 and 17 post-infection compared to μMT mice.

The CTL activity on day 6 post-infection seen in the MLN of μMT mice could be due to (a) professional APCs presenting antigen from the lung and/or (b) cells in the MLN that might be infected.

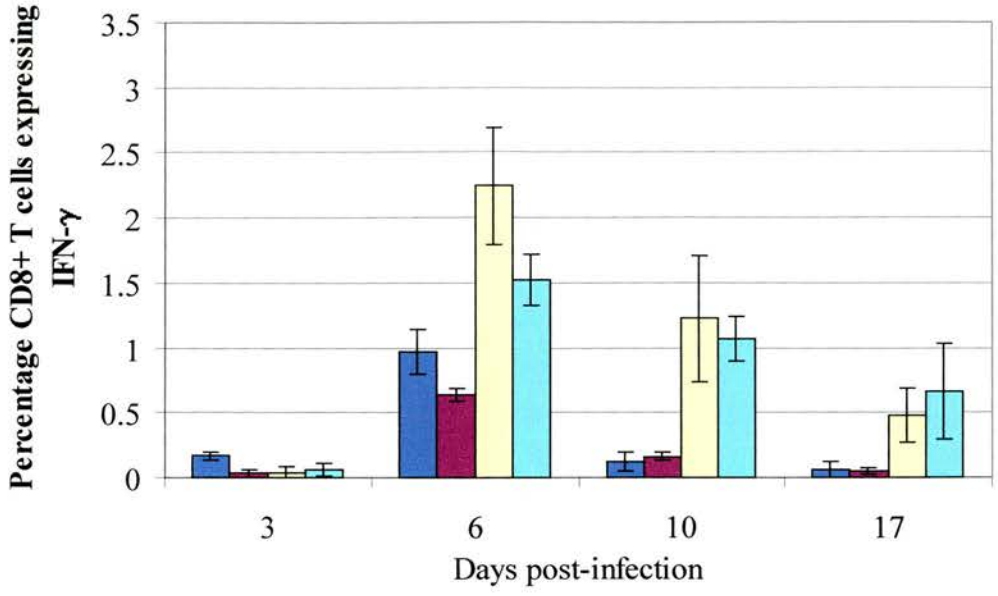


Figure 3.13 MHV-68 specific CTL response in the MLN of μMT and C57BL/6 mice The μMT mice and C57BL/6 mice were infected intranasally with 4 x $10^5$ PFU MHV-68. MLN from 6 mice in each group were pooled and made into single cell suspensions and 96 well plates were seeded with 1 x $10^6$ cells each. The IFN-γ CTL assay was carried out as described in the method section (2.2.11). Cells were stimulated using the MHV-68 specific peptides pep1 and pep2 coded by the ORF6 and ORF61 respectively. The cells were incubated for 5 hours and double-stained for CD8+ T cells and for IFN-γ in permeablised cells and analysed by flow cytometry. The graph represents the percentage of CD8+ T cells expressing IFN-γ in the MLNs of μMT mice for pep 1 ( ■ ), μMT mice for pep 2( ■ ), C57BL/6 mice for pep 1( □ ) and C57BL/6 mice for pep 2 ( □ ) on days 3, 6, 10 and 17 post-infection. The error bars represent the standard error of the mean.

# CHAPTER FOUR

# APPLICATION OF A GREEN FLUORESCENT PROTEIN (GFP) EXPRESSING GAMMAHERPESVIRUS

## 4.1 Introduction

The experiments described in Chapter 3 (section 3.4) demonstrated the presence of cells other than B cells infected with MHV-68 in the MLN of μMT mice early in infection. However, due to the fewer number of positive cells and the sensitivity of the assays, it was difficult to identify the type of cells that harboured virus. Therefore, the decision was made to use a recombinant MHV-68 virus expressing green fluorescent protein (GFP). The recombinant virus, LHΔgfp was a gift from Dr. D. Roy and Dr. J. Stewart (Veterinary Pathology, University of Edinburgh). The reason that led us to believe that this virus could be a useful tool was that *in vitro* cells infected by the virus expressed GFP. If the same occurred *in vivo* this would be a marker to help identify cells carrying virus.

In the case of human gammaherpesvirus infections such as EBV and KSHV the primary cell targets infected by the virus have remained controversial. In individuals infected with KSHV, different cell types have been shown to carry latent virus but the primary site of infection and cell type infected is not clearly understood. In EBV infection, B cells have been shown to be the major reservoirs of virus during latency but whether they are the first cells to be infected is under debate (Faulkner *et al.*, 2000). MHV-68 infection of mice is an amenable model and is an ideal system to study the cell types infected at the very early stage of infection and their role in trafficking virus to other tissues. Intranasal infection of mice has shown that epithelial cells and monocytes are infected in the lungs (Sunil-Chandra *et al.*, 1992a). It has also been shown that B cells are capable of transferring virus to the spleen. In experiments where MHV-68 infected μMT mice were injected with B cells from uninfected mice, the virus was subsequently detected in the spleen (Stewart *et al.*, 1998). The experiment showed that B cells could become infected directly from the

lungs, but the question as to whether during normal infection all the B cells were infected from the lungs or whether there were other cells acting as reservoirs in the MLN has not been addressed.

Dendritic cells are professional antigen-presenting cells (APC) and their role in immune surveillance is indisputable with their ability to capture and transfer antigens from foreign organisms to sites of immune activity. Lungs being an important tissue that remains in continuous contact with the environment, dendritic cells play a very critical role at this site. The immature dendritic cells present in the lungs on antigenic exposure start maturing and move into draining lymph nodes where they act as effective antigen-presenting cells. In recent years there has been evidence that a number of viruses infect dendritic cells and use them for their own advantage to traffic to tissues within the host and to manipulate immune activation. Studies with HIV indicated that dendritic cells from the mucosal sites could acquire the virus and migrate to the draining lymph node where the virus could subsequently infect CD4+ T cells (Knight and Patterson, 1997). This is a compelling mechanism that might also be exploited by other viruses. This chapter examines this mechanism with respect to MHV-68.

LHΔgfp has a GFP gene under the human cytomegalovirus (HCMV) immediate-early promoter inserted into the left-hand terminal end of the virus. This insertion has led to the deletion of five tRNA sequences and the M1 gene from the MHV-68 genome. Wild type MHV-68 has eight tRNA sequences that are expressed in infected cells both during lytic and latent phases of the virus infection but their function is unknown (Bowden *et al.*, 1997). The published work on the M1 gene indicates that the M1 gene deletion mutant has an increased ability to reactivate from latency (Clambey *et al.,* 2000). Therefore, this recombinant virus could behave differently from the wild type MHV-68. In order to determine any changes in pathogenesis or establishment of latency, studies on pathogenesis were carried out with LHΔgfp in comparison with wild type MHV-68 and the results are presented in the following section.

## 4.2 Characterisation of LHΔgfp

### 4.2.1 Infective virus in the lungs of C57BL/6 mice infected with LHΔgfp as compared to wild type MHV-68

The experiments described in this section were aimed to investigate the *in vivo* growth characteristics of the recombinant LHΔgfp virus as compared to the wild type MHV-68. The virus titres in the lungs and number of latently infected cells in the mediastinal lymph node and spleen were examined.

Intranasal administration of virus leads to the infection of alveolar epithelial cells. At this stage the virus undergoes lytic replication. C57BL/6 mice were infected with 4 x $10^5$ PFU of either LHΔgfp or MHV-68. C57BL/6 mice were used because the studies with LHΔgfp as a marker virus were to be carried out in the μMT mice of the same background. The lungs were removed, homogenised and the amount of replicating virus determined using the infective virus assay as described in the methods section (2.2.3). The results are represented in Figure 4.1.

The wild type virus (MHV-68) showed typical growth patterns in the lungs in agreement with previous studies (Usherwood *et al.*, 1996b), where the virus titres peaked around day 8 and were absent by day 10 post-infection. In the case of the recombinant virus (LHΔgfp) the titres peaked around day 4 and the levels fell by day 8 post-infection. However, there was no statistically significant (Student t-Test analysis) difference between the two groups.

### 4.2.2 Latently infected cells in the mediastinal lymph node

The results in Chapter 3 demonstrate the importance of the MLN during the progression of MHV-68 infection. The results showed that even as the lytic phase progresses in the lungs, MHV-68 latent in certain types of cells is transferred to other sites such as the MLN and eventually the spleen. It was therefore essential to determine the presence of latently infected cells in the MLN that may be present in mice infected with LHΔgfp. It was also thought that if a recombinant virus was

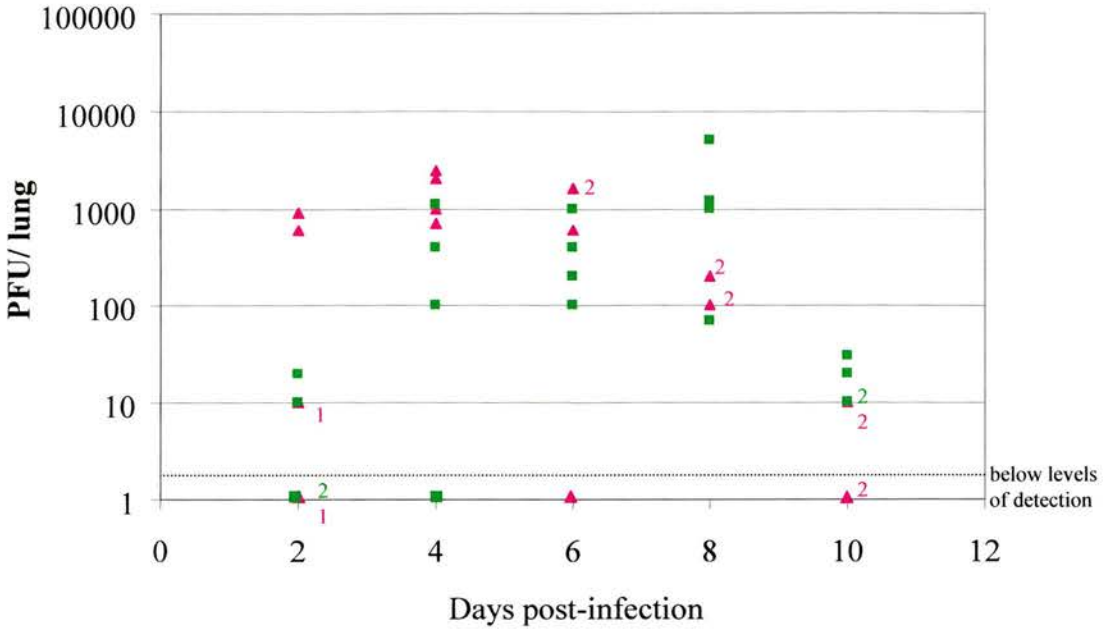


Figure 4.1 Infective virus in the lungs of C57BL/6 mice infected with either LHΔgfp or MHV-68 C57BL/6 mice were divided in to two groups. Group 1(■) mice were infected intranasally with 4 x $10^5$ PFU MHV-68. Group 2 (▲) mice were infected intranasally with 4 x $10^5$ PFU LHΔgfp. Lungs from four mice in each group was removed on days 2, 4, 6, 8 and 10 post-infection and frozen at -70°C. Subsequently, the lungs were homogenised and assayed for infective virus particles. The graph represents the number of infective virus as plaque forming units (PFU) per set of lungs, in logarithmic scale on the y-axis and days post-infection on the x-axis. The coloured number adjacent to the points on the graph show the number of overlapped points for the respective group. The graph is representative of two independent experiments.

extremely debilitated the host immune response would clear the virus from the lungs and there would be no systemic transfer of virus. The MLN would be the ideal site to look for any such changes during the early stages of infection.

MLN were removed at times post-infection, starting at day 6 and up to day 31. The MLN were pooled from four C57BL/6 mice for each virus, homogenised and the number of latently infected cells determined using the infective centre assay as described in the method section (2.2.2). The results are represented in Figure 4.2.

Latently infected cells were observed in the case of both LHΔgfp and wild type MHV-68. The wild type MHV-68 showed a distinct peak of latently infected cells on days 10 and 15 post-infection, but this peak failed to appear in the case of the recombinant LHΔgfp.

The results demonstrate that the recombinant virus is able to spread systemically and the infection progression is similar to the wild type virus as it appears in the MLN and it is also able to establish latency.

### 4.2.3 Extent of lymphadenopathy

Lymph node enlargement was a noticeable change during MHV-68 infection (Sarawar *et al.*, 1996). Therefore it was considered important to determine the total number of lymphocytes accumulating in the MLN during LHΔgfp infection. The results are represented in Figure 4.3.

It was observed that the extent of lymphadenopathy in the MLN of mice infected with LHΔgfp closely resembled the wild type MHV-68 infected mice. The reduced number of latently infected cells in the MLN of mice infected with LHΔgfp (as observed in the previous section) did not affect the accumulation of cells in the MLN.

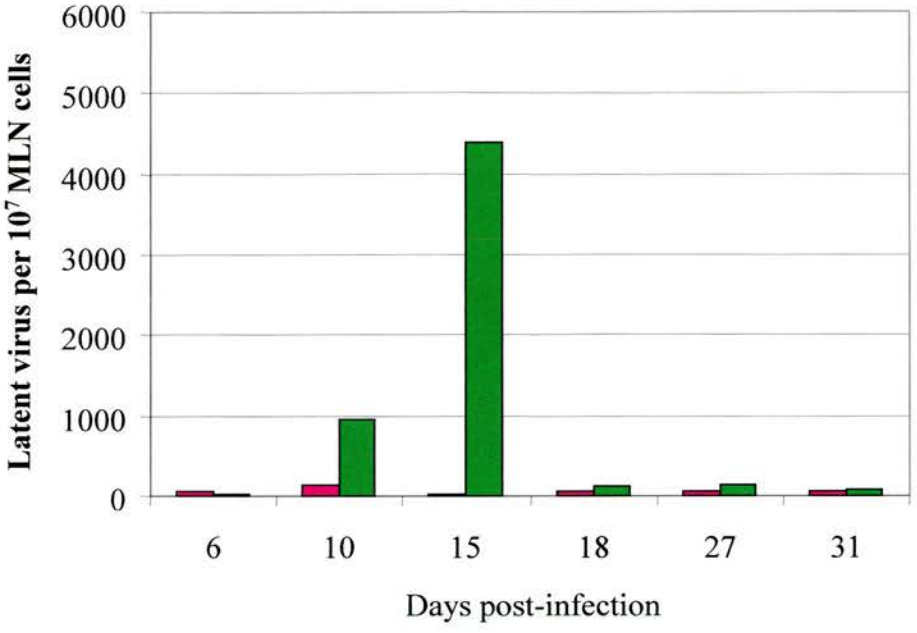


Figure 4.2 Latent virus in the mediastinal lymph node of C57BL/6 mice infected with either LHΔgfp or MHV-68 C57BL/6 mice were divided in to two groups. Group 1( ■ ) mice were infected intranasally with $4x10^5$ PFU MHV-68. Group 2 ( ■ ) mice were infected intranasally with $4 \times 10^5$ PFU LHΔgfp. MLNs were pooled from four mice in each group on days 6, 10, 15, 18, 27 and 31 post-infection. The MLNs were dissociated to obtain single cell suspensions and plated with BHK cells to assay for infective centres as described in methods section (2.2.2). The graph represents the latent virus per $10^7$ MLN cells on the y-axis against days post-infection on the x-axis. The graph is representative of two independent experiments.

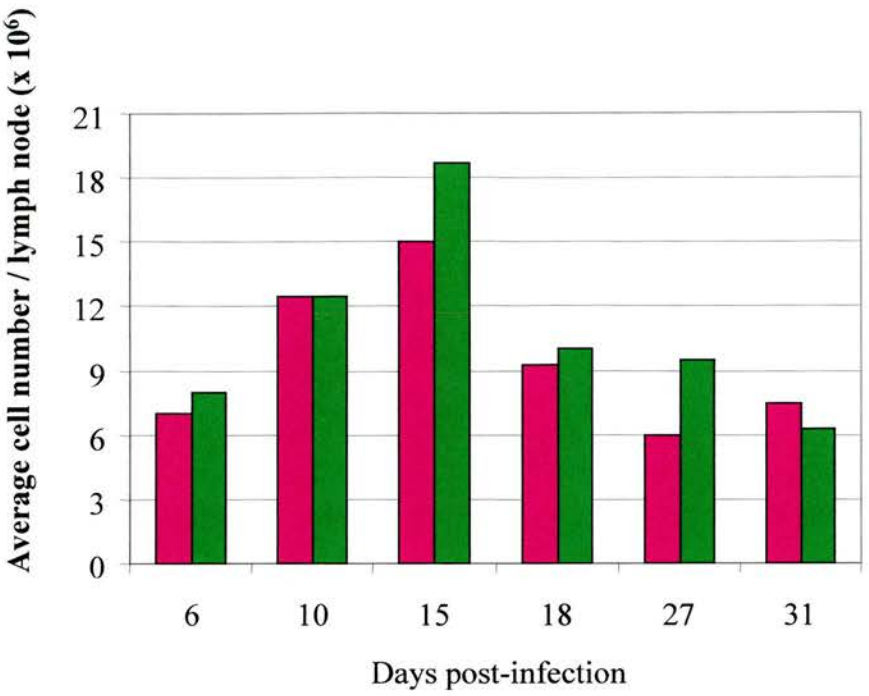


Figure 4.3 Lymphadenopathy of the mediastinal lymph node of C57BL/6 mice infected with either LHΔgfp or MHV-68 C57BL/6 mice were divided in to two groups. Group 1(■ ) mice were infected intranasally with $4x10^5$ PFU MHV-68. Group 2 ( ■ ) mice were infected intranasally with $4 \times 10^5$ PFU LHΔgfp. MLNs were pooled from four mice in each group on days 6, 10, 15, 18, 27 and 31 post-infection. The MLNs were dissociated to obtain single cell suspensions and counted. The graph represents the average number of MLN cells (x $10^6$) on the y-axis against days post-infection on the x-axis. The graph is representative of two independent experiments.

### 4.2.4 Latently infected cells in the spleen

The experiment was aimed at measuring the levels of latently infected cells in the spleens of mice infected with either LHΔgfp or wild type MHV-68. The spleens from infected mice were removed at different day points of infection and the number of latently infected cells measured using infective centre assay as described in the methods section (2.2.2). The results are represented in Figure 4.4.

Latently infected cells were detected as early as day 7 post-infection and there were similar numbers of latently infected cells in the case of both LHΔgfp and wild type MHV-68 on day 10 post-infection. However, on day 15 the peak levels of latently infected cells in wild type MHV-68 were not seen with LHΔgfp, by day 28 and 31 both viruses showed the same levels of latency.

These results demonstrate a significant difference on day 15 post-infection in the spleens of wild type MHV-68 and LHΔgfp infected mice ($p = 0.0001$, analysed using Student's t-Test). However, LHΔgfp was capable of establishing an overall latency pattern similar to wild type MHV-68. Therefore, LHΔgfp could be used as a marker virus to seek answers to questions regarding virus trafficking and the cell types involved.

## 4.3 LHΔgfp as a tool to study the trafficking of virus *in vivo*

### 4.3.1 GFP positive cells in the lungs and mediastinal lymph node imprints

The results from MHV-68 infected μMT mice (presented in section 3.4) demonstrated that cells other than B cells could be detected with latent virus during the early stages of infection.

To investigate whether LHΔgfp behaved similarly to wild type MHV-68 in the MLN of μMT mice, μMT mice were infected intranasally with $4 \times 10^5$ PFU LHΔgfp. The lungs and the MLN were removed and tissue imprints were made as described in the method section (2.2.6). The imprints were viewed under fluorescence microscope

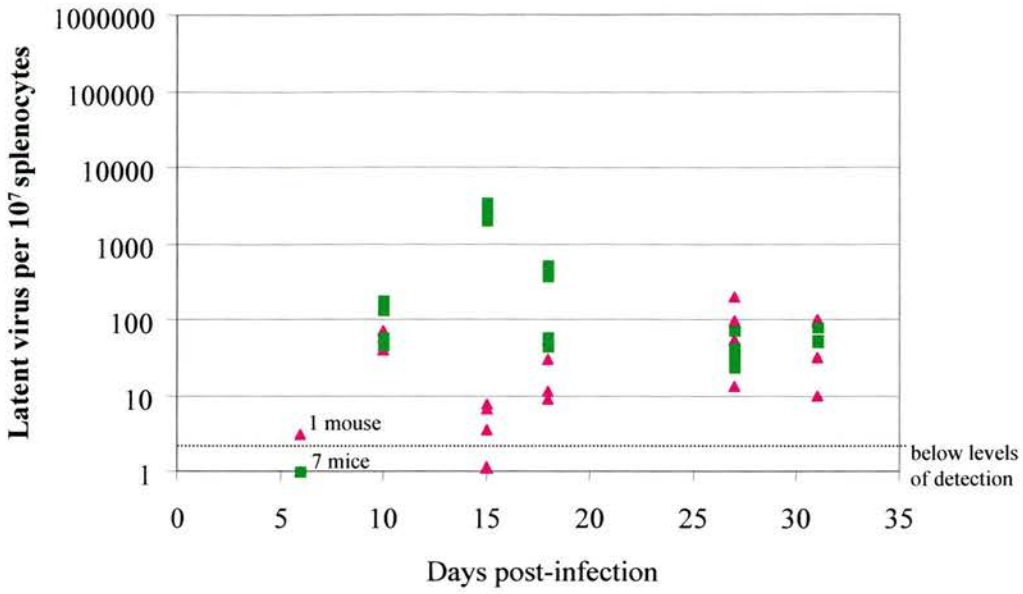


Figure 4.4 Latent virus in the spleens of C57BL/6 mice infected with either LHΔgfp or MHV-68 C57BL/6 mice were divided in to two groups. Group 1( ■ ) mice were infected intranasally with 4 x $10^5$ PFU MHV-68. Group 2 ( ▲ ) mice were infected intranasally with 4 x $10^5$ PFU LHΔgfp. Spleens were removed from four mice in each group on days 6, 10, 15, 18, 27 and 31 post-infection. The spleens were sheared to obtain single cell suspensions and plated with BHK cells to assay for infectious centres as described in methods section (2.2.2). The graph represents the latent virus per $10^7$ splenocytes in logarithmic scale on the y-axis against days post-infection on the x-axis. The graph is representative of two independent experiments.

to look for GFP expressing cells at various days of infection. The fluorescence micrographs obtained on day 5 post-infection in the lung and MLN imprints of μMT mice are represented in Figure 4.5.

Cells expressing GFP were identified in lung tissue and, at lower levels in the MLN on day 5 post-infection. Therefore, using LHΔgfp it was possible to detect the rare cells infected by the virus. This was the first demonstration that this recombinant virus could express GFP "*in vivo*", aiding in tracking infected cells.

### 4.3.2 CD11c expressing cells enriched from μMT mice MLN

There is evidence that gammaherpesviruses are capable of infecting monocytes. During KSHV infection there are instances where monocytes isolated from patients suffering from Kaposi's sarcoma lesions have been found to be infected with the virus (Blasig *et al.*, 1997). In the case of MHV-68 there is evidence from immunostained lung tissues that large monocytic cells were infected with MHV-68 (Sunil-Chandra *et al.*, 1992a). There is also evidence that macrophages in the peritoneal fluid become latently infected following MHV-68 infection (Weck *et al.*, 1999b).

The CD11c surface marker is present on most subtypes of dendritic cells although it is also seen in small amounts on macrophages and B cells; it is the best broad-spectrum marker for murine dendritic cells (Steinman, 1991). The decision was made to examine the dendritic cell population that drains into the MLN from the lungs as a candidate cell type that might be susceptible to infection very early during MHV-68 infection.

Magnetic beads coated with hamster anti-mouse CD11c (N418) antibodies were purchased from Miltenyi Biotech. The assay was carried out as described in the methods section (2.2.10). μMT mice were infected with $4 \times 10^5$ PFU LHΔgfp. MLN from 7 mice were pooled to obtain single cell suspensions. The cells were incubated with CD11c coated magnetic beads, washed and then passed through the MACS

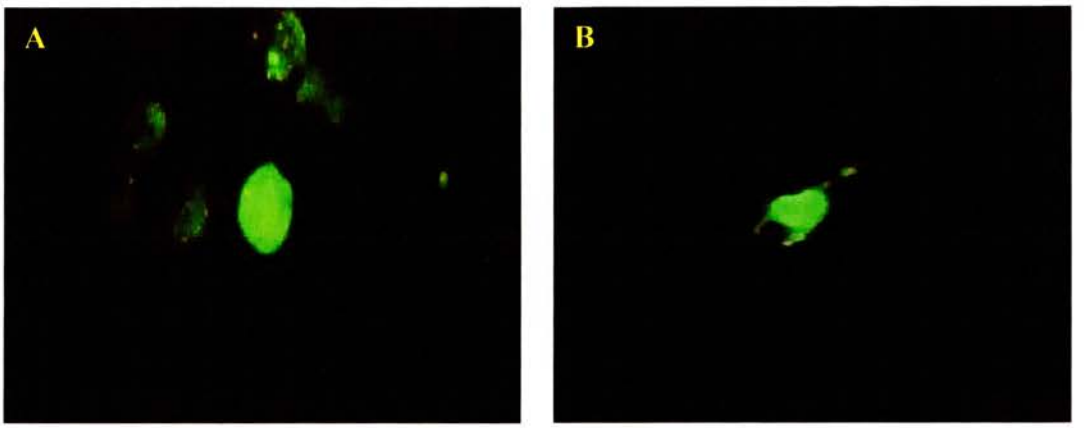


Figure 4.5 GFP positive cells in the lungs and mediastinal lymph node imprints of μMT mouse infected with LHΔgfp μMT mice were infected intranasally with 4 x $10^5$ PFU LHΔgfp. On day 5 post-infection the lungs and MLN were sampled from mice and dabbed on to Biobond coated slides as described in the methods section (2.2.6). The slides were fixed with ice cold acetone, air dried and viewed under a fluorescence microscope. The panel marked (**A**) in the figure represents lung imprints, panel (**B**) represents imprints of cells from the MLN, showing GFP expressing cells (magnification: X320).

columns. The cells recovered from the columns were subjected to FACS analyses, to ascertain that the enriched cells were large morphologically and expressed CD11c on staining with anti-hamster IgG conjugated to PE. The cells were also analysed for intracellular GFP expression. The results are represented in the Figure 4.6.

The FACS analysed dot plot in Figure 4.6 (3.a) shows the scatter data of cells that were positively enriched for CD11c+ cells, which were slightly larger cells compared to the total cell population {Figure 4.6 (1.a)} or the unbound cells (flow through) {Figure 4.6 (2.a)}. The FACS staining in Figure 4.6 (3.b) shows the FACS staining for CD11c+ cells on the y-axis, where 55% of the cells expressed this marker. The FACS staining on the x-axis shows the cells expressing GFP. Of the 55% CD11c positive cells around 3% of the cells were also positive for GFP

The results obtained from the FACS analyses demonstrated that there were cells positive for CD11c that were also expressing GFP and they can be obtained from the MLN of μMT mice infected with LHΔgfp on day 5 post-infection.

### 4.3.3 CD11c enriched cells expressing GFP stained with F4/80

The FACS analysis of the MACS enriched cells showed that 55% were CD11c expressing cells and the rest were CD11c- cells. Therefore it was deemed necessary to stain these cells with other surface markers to ascertain that there were no other cell types expressing GFP in the μMT mouse MLN. The published data (Weck *et al.*, 1999b) on F4/80 positive macrophages carrying latent virus in the peritoneal exudate cells (PECs) of normal mice prompted the use of this surface marker.

The cells were selected by MACS for CD11c and the enriched population was resuspended in a small amount of FACS buffer and stained with monoclonal antibody against F4/80, as described in the methods section (2.2.5). Subsequently the cells were cytospun on to Biobond coated slides and viewed using a Leitz Confocal microscope. The results are presented in Figure 4.7.

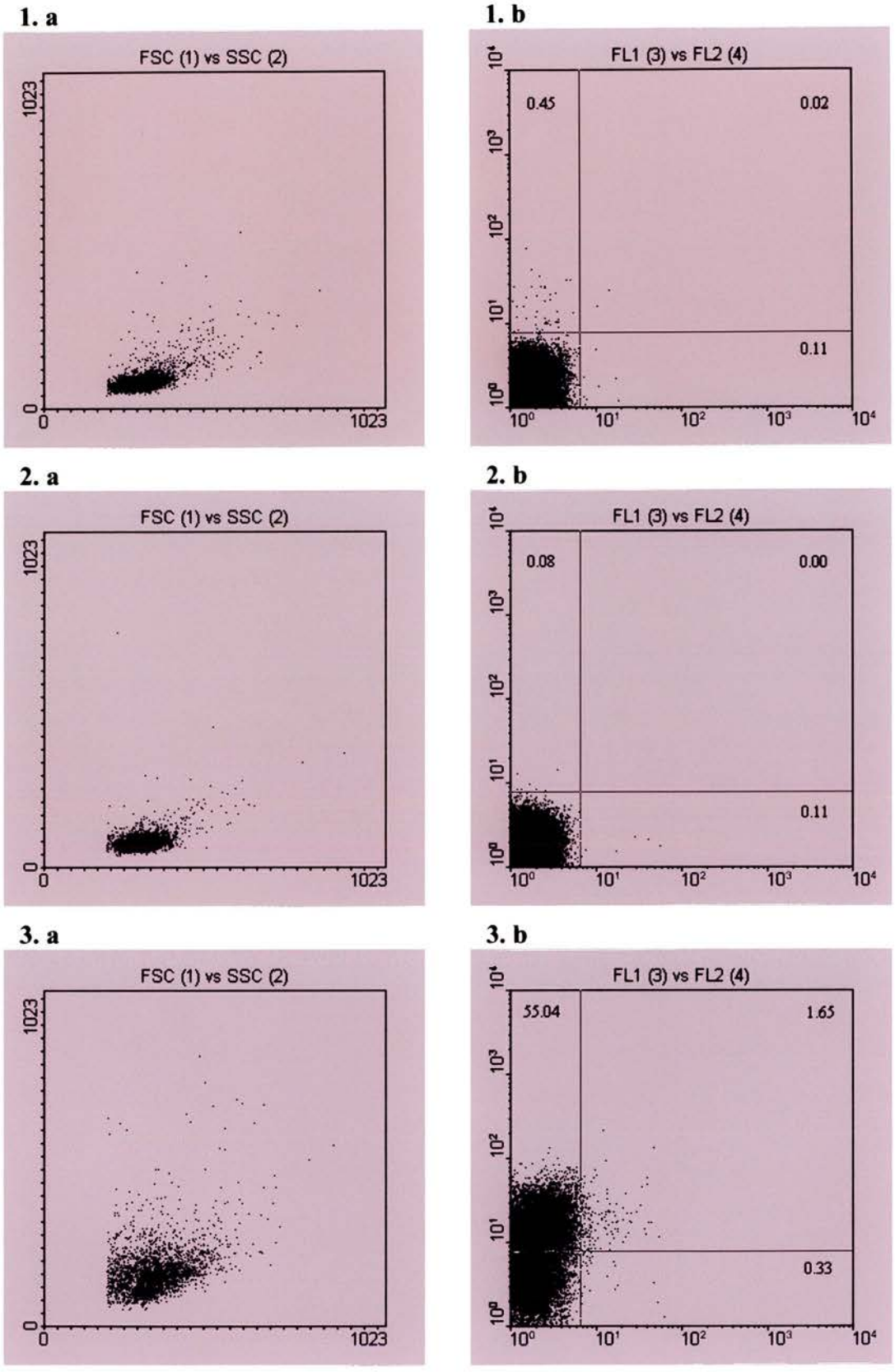


Figure 4.6 FACS analysis dot plots representing scatter data and staining of CD11c cells, obtained from MACS enrichment of μMT mouse MLN

Figure 4.6 FACS analysis dot plots representing scatter data and staining of CD11c cells, obtained from MACS enrichment of μMT mouse MLN μMT mice were infected intranasally with 4 x $10^5$ PFU LHΔgfp. On day 5 post-infection the MLN were pooled from seven mice and dissociated to obtain single cell suspensions. The cells were counted, resuspended in MACS buffer and incubated with hamster anti-mouse CD11c antibody (clone N418) coated magnetic beads (Miltenyi Biotech) as described in the method section (2.2.10). A small aliquot of cells was removed for FACS analysis of the total cell population. The rest of the cells were passed through the MACs columns. The unbound cells (flow through) were also collected for analysis. The bound cells were removed from the column and passed through a second column to decrease the amount of contaminating cell population. All the aliquots of cells were stained with anti-hamster IgG conjugated to PE. In the figure panels 1.a, 2.a and 3.a represent the forward scatter (x-axis) and side scatter (y-axis) of the total cells prior to passing through the column, the unbound cells and the MACS enriched cells respectively. The panels 1.b, 2.b and 3.b represents the staining profile with anti-hamster IgG-PE (y-axis) and the intracellular GFP expression (x-axis) of the total cells prior to passing through the column, the unbound cells and the MACS enriched cells respectively.

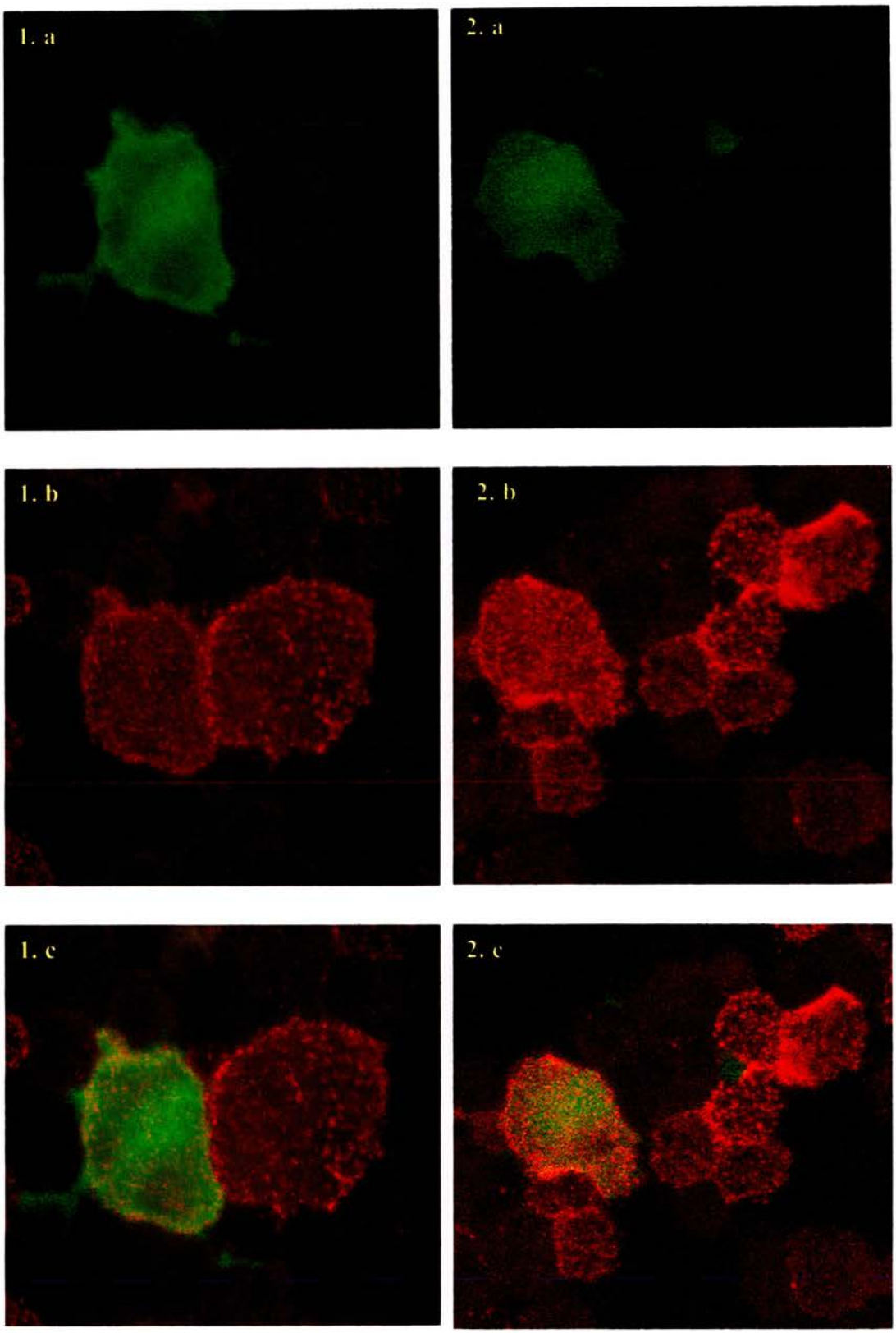


Figure 4.7 GFP expressing cells stained with F4/80 antibody

Figure 4.7 GFP expressing cells stained with F4/80 antibody μMT mice were infected intranasally with 4 x $10^5$ PFU LHΔgfp. On day 5 infection mediastinal lymph nodes (MLN) from seven mice were pooled and dissociated to obtain single cell suspensions. The cells were firstly MACS enriched for CD11c as discussed in the section 4.3.2. The enriched cells were resuspended and stained with anti-mouse F4/80 monoclonal antibody followed by anti-rat IgG conjugated to TRITC. The cells were cytospun on to Biobond coated slides and viewed under a confocal microscope. The figure represents confocal images of these cells (magnification: X600). In the figure the panels 1a, 1b and 1c are images from the same field; 1a, shows intracellular GFP (green) expression; 1b, shows TRITC staining (red) of cells expressing F4/80; 1c, shows the overlap of 1a and 1b where a cell expressing GFP is also positive for F4/80 staining. The panels 2a, 2b and 2c is another field. It is ordered similar to panels 1a to 1c.

The fluorescence images for cellular expression of GFP confirm that the cells examined contained diffused GFP within cells and not GFP in vacuoles from engulfed virus infected cells. The results show GFP expressing cells stained with F4/80 surface marker. This could mean that macrophages expressing F4/80 too were cells that carried latent virus during the early course of infection and can be found localised in the MLN.

### 4.3.4 The advantages of using the IFN-α/β $R^{-/-}$ mouse system which displays an exaggerated MHV-68 disease pathogenesis

The work with the μMT mouse system provided very important evidence as to the cell types that may be involved in trafficking virus into the MLN at very early stages of infection. However, the work with this system was restricted because of the small number of cells infected. In order to amplify the number of cells infected at early times in the MLN an alternative mouse model was investigated-the IFN-α/β $R^{-/-}$ mouse system. This system was of interest, as it would not only make it possible to increase the number of infected cells but also indicate what happens in the absence of interferon signalling in the MLN of MHV-68 infected mice.

Previous work (Dutia *et al.*, 1999a) on IFN-α/β $R^{-/-}$ mice infected with MHV-68 shows that this system is extremely susceptible to the virus and it exhibits disseminated infection in which more than 80% of mice succumb to the disease even with the normal dose of 4 x $10^5$ PFU MHV-68. The data also showed that there is a 100-fold increase in the number of latently infected cells in the spleens as compared to the wild type counterpart, WT129 mice. The number of latently infected cells in the spleens is controlled over time in the spleen. These results demonstrate the importance of IFN-α/β in clearance of lytic lung infection and in keeping the number of latently infected cells under check during early MHV-68 infection.

To investigate the level of infection in CD11c+ cells obtained from IFN-α/β $R^{-/-}$ mice at early times post-infection IFN-α/β $R^{-/-}$ mice were infected intranasally with 4 x $10^5$ PFU LHΔgfp and MLN were pooled from 6 mice on day 5 infection and

dissociated into single cell suspensions. The cells were incubated with CD11c magnetic beads and MACS separation carried out. They were analysed using FACS, as shown in Figure 4.8. The Figure 4.9 represents cells enriched for CD11c+ from MLN on day 4 post-infection showing intracellular GFP expression.

The results demonstrated that the MACS method enriched CD11c cells by 50% from MLN of IFN $\alpha/\beta$ $R^{-/-}$ mice. Of those cells, 10% also expressed GFP. This result confirms that, even in the presence of B cells, CD11c+ cells can be infected during the early stages of infection in the MLN. In the IFN-$\alpha/\beta$ $R^{-/-}$ mice there were three times more CD11c+ cells expressing GFP as compared to the μMT mice. The fluorescence micrographs of the cells show a uniform expression of GFP in the cytoplasm, confirming that the GFP is from within these cells and not from vacuoles carrying engulfed cells.

### 4.3.5 CD11c enriched cells expressing GFP confirmed with surface staining

The MACS enriched CD11c cells were stained and analysed under high power using a Leitz Confocal microscope. The enriched cells were analysed for FACS using anti-hamster IgG conjugated to PE that bound primary CD11c antibody (clone N418). Although the wavelength of PE staining was not ideal for the fluorescence microscope the results for GFP expressing cells and images are presented in Figure 4.10 (1.a and 1.b).

The enriched cells were also stained with another anti-CD11c (clone HL-3) antibody conjugated to biotin (PharMingen). The cells were washed and subsequently stained with streptavidin conjugated to TRITC. The confocal micrograph images are represented in Figure 4.10 (2.a and 2.b). The Figure 4.10 (3.a and 3.b) shows the enriched cells that were stained with anti-mouse DEC-205 (NLDC145) followed by anti-rat IgG conjugated to TRITC.

The staining of GFP positive cells with anti-CD11c by two methods confirmed that virus was infecting the CD11c+ population. Some of the GFP expressing cells were

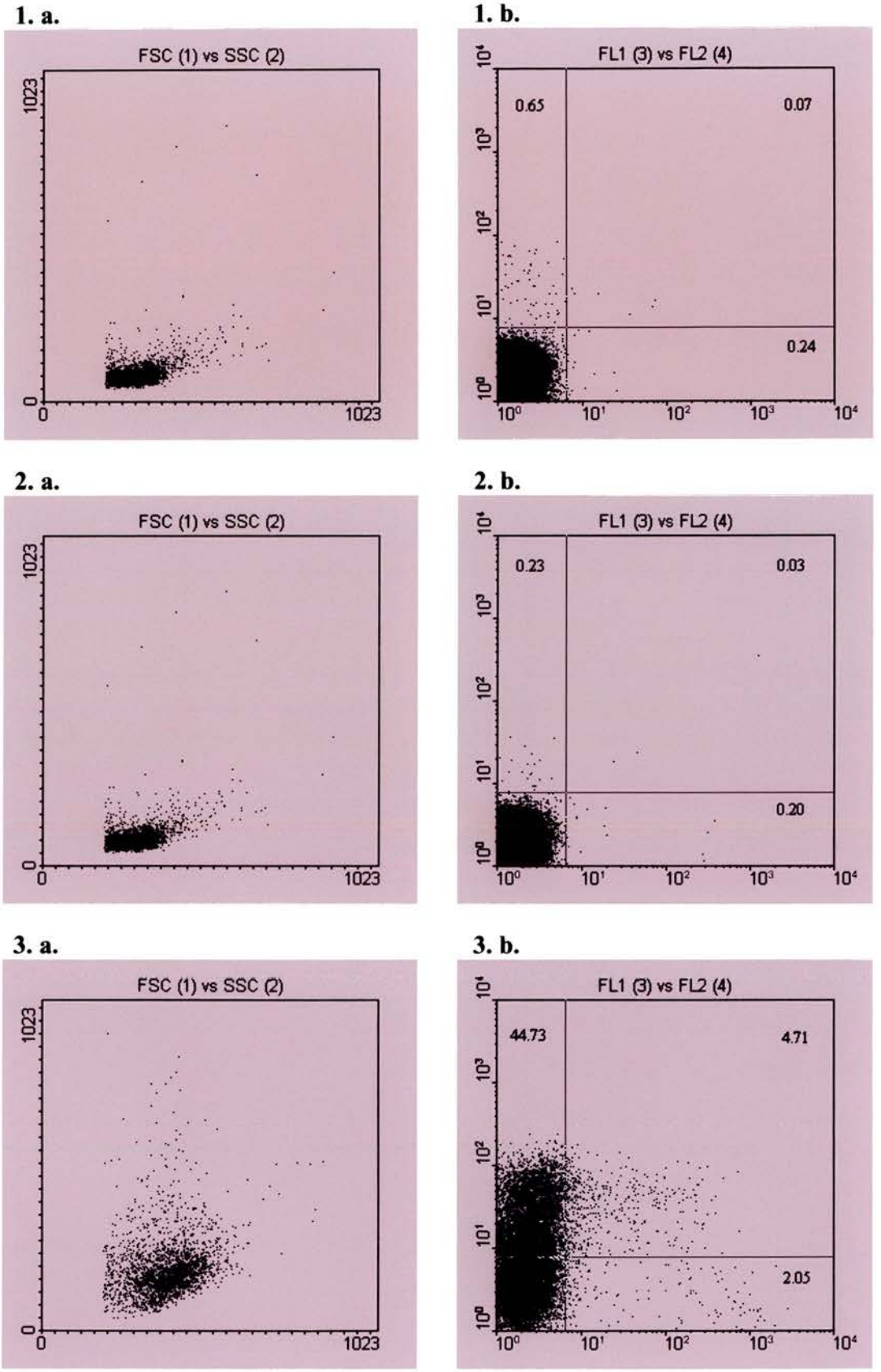


Figure 4.8 FACS analysis dot plots representing scatter data and staining of CD11c cells, obtained from MACS enrichment of IFN-α/β R-/- mouse MLN

Figure 4.8 FACS analysis dot plots representing scatter data and staining of CD11c cells, obtained from MACS enrichment of IFN-α/β R-/- mouse MLN IFN-α/β $R^{-/-}$ mice mice were infected intranasally with 4 x $10^5$ PFU LHΔgfp. On day 5 post-infection the MLN were pooled from seven mice and dissociated to obtain single cell suspensions. The cells were counted, resuspended in MACS buffer and incubated with hamster anti-mouse CD11c antibody (clone N418) coated magnetic beads (Miltenyi Biotech) as described in the method section (2.2.10). A small aliquot of cells was removed for FACS analysis of the total cell population. The rest of the cells were passed through the MACs columns. The unbound cells (flow through) were collected for analysis too. The bound cells were removed from the column and passed through a second column to decrease the amount of contaminating cell population. All the aliquots of cells were stained with anti-hamster IgG conjugated to PE. In the figure panels 1.a, 2.a and 3.a represent the forward scatter (x-axis) and side scatter (y-axis) of the total cells prior to passing through the column, the unbound cells and the MACS enriched cells respectively. The panels 1.b, 2.b and 3.b represents the staining profile with anti-hamster IgG-PE (y-axis) and the intracellular GFP expression (x-axis) of the total cells prior to passing through the column, the unbound cells and the MACS enriched cells respectively.

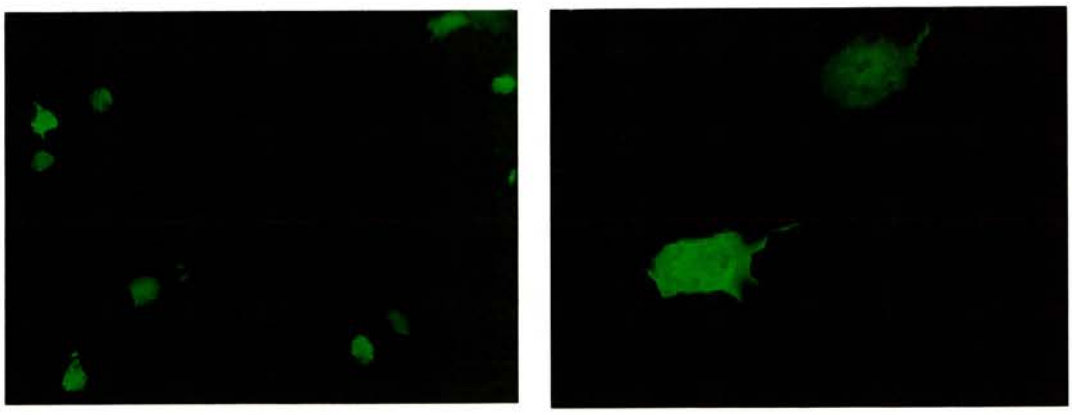

Figure 4.9 Fluorescence images of cells enriched for CD11c using MACS

IFN-α/β $R^{-/-}$ mice were infected intranasally with 4 x $10^5$ PFU LHΔgfp. Mediastinal lymph nodes from seven mice were pooled on day 4 post-infection. The cells were enriched for CD11c cells using MACS as discussed in the methods section (2.2.10). The enriched cells were cytospun on to Biobond coated slides and viewed under a fluorescence microscope. The figure represents the intracellular expression of green fluorescent protein (GFP) in a few of the cells. The panel on the right-hand side is a higher magnification (X320) of cells seen on the left-hand side panel (X200).

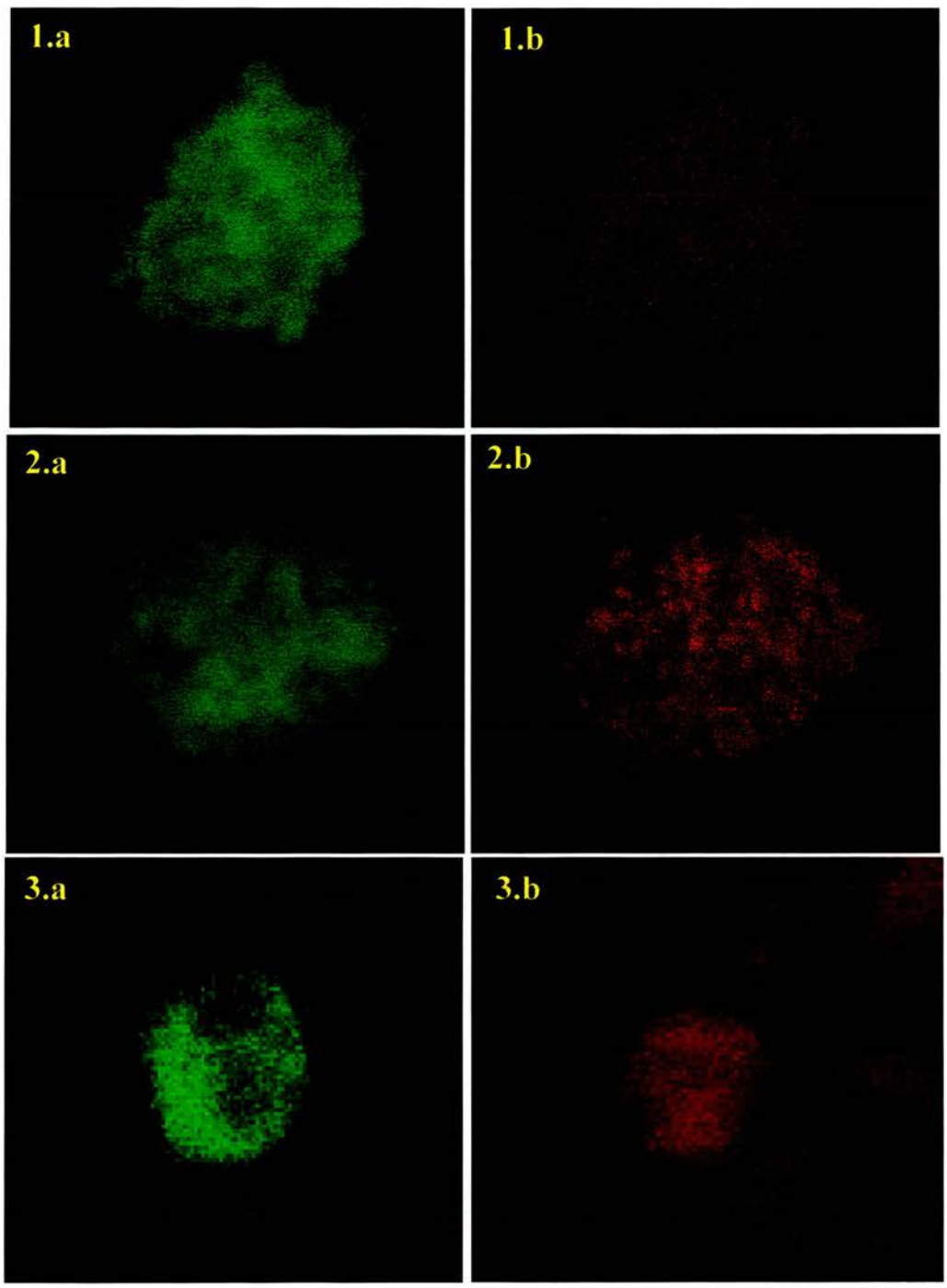


Figure 4.10 CD11c enriched cells from IFN-α/β R-/- mice MLN, expressing GFP and stained for surface markers

Figure 4.10 CD11c enriched cells from IFN-α/β R-/- mice MLN, expressing GFP and stained for surface markers IFN-α/β $R^{-/-}$ mice were infected intranasally with 4 x $10^5$ PFU LHΔgfp. The mediastinal lymph nodes were pooled from 7 mice, dissociated to obtain single cell suspensions and cells were used for MACS enrichment as described in the methods section (2.2.10). The cells were enriched using magnetic beads (Miltenyi Biotech) coated with hamster anti-mouse CD11c monoclonal antibody (clone N418). All the panels in the figure represent cells that were obtained after CD11c enrichment and viewed under a Confocal microscope. The panels 1.a and 1.b in the figure represent cells that were stained with anti-hamster IgG conjugated to PE. These cells were used for FACS analysis and the data is represented in figure 4.8. The panel 1.a shows the intracellular GFP expression in a cell and panel 1.b shows the same cell stained with anti-hamster PE antibody. The panels 2.a and 2.b represent cells that were stained with CD11c-biotin (clone HL-3) and streptavidin-TRITC. The panel 2.a shows GFP expression in a cell and panel 2.b shows the same cell stained with CD11c-biotin plus streptavidin-TRITC. The panels 3.a and 3.b represent cells that were stained with anti-mouse DEC-205 (NLDC145). 3.a shows GFP expression in a cell and 3.b shows the same cell stained with anti-mouse DEC-205 followed by anti-rat IgG conjugated to TRITC. Magnification: X600.

also stained with DEC-205 a dendritic cell specific surface marker. This data gave further confirmation of the presence of CD11c+ cells infected with LHΔgfp in the MLN during the early stages of infection.

## 4.4 Pathogenesis of LHΔgfp in IFN-α/β $R^{-/-}$ mice versus WT129 mice

### 4.4.1 Infective virus in the lungs

Pathogenesis of LHΔgfp was examined in IFN-α/β $R^{-/-}$ and WT129 mice over a time course of infection to verify that the recombinant virus exhibited amplified disease pathogenesis similar to wild type MHV-68. The experiment would also provide us with answers as to whether the CD11c+ cells infected by the virus persisted over the full duration of infection.

IFN-α/β $R^{-/-}$ and WT129 mice were infected with 4 x $10^5$ PFU LHΔgfp. The lung tissue was removed from three mice in each group on days 3, 5, 7 and 10 post-infection and frozen at -70°C. Subsequently the lungs were homogenised and assayed for infective virus as described in the methods section (2.2.3). The results are represented in Figure 4.11.

The results demonstrated that as early as day 3 post-infection the IFN-α/β $R^{-/-}$ mice had 20-30 times more infective virus in the lung tissue compared to the WT129 mice. By day 10 post-infection the virus levels were declining in the WT129 mice lungs while the lung tissues in the IFN-α/β $R^{-/-}$ system showed more than a 100 fold higher infective virus levels. IFN-α/β and IFN-α/β receptor induced signalling are clearly important in controlling the virus load in the lungs. This data is similar to the previously published data with wild type MHV-68 (Dutia *et al.*, 1999). Therefore the recombinant LHΔgfp virus has similar characteristics to the wild type virus in the lungs of IFN-α/β $R^{-/-}$ mice.

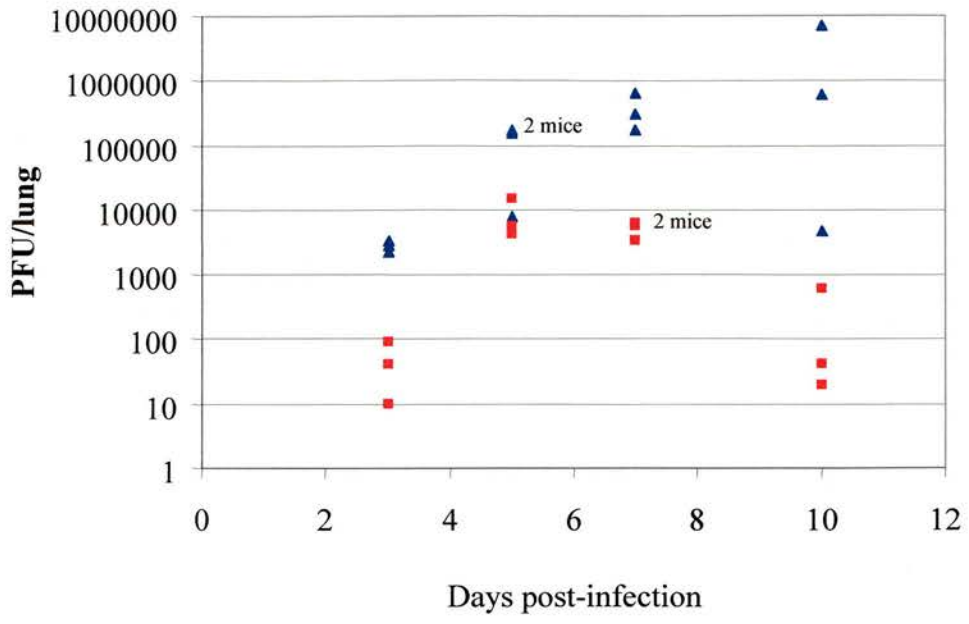


Figure 4.11 Infective virus in the lungs of IFN-α/β R-/- and WT129 mice infected with LHΔgfp IFN-α/β R-/- and WT129 mice were infected intranasally with 4 x $10^5$ PFU LHΔgfp. Lungs from three mice in each group were removed on days 3, 5, 7 and 10 and frozen at -70°C. Subsequently, the lungs were homogenised and assayed for infective virus particles as described in the methods section (2.2.3). The graph represents the number of infective virus as plaque forming units (PFU) per set of lungs, in the IFN-α/β $R^{-/-}$ (▲) and in WT129 mice (■), in logarithmic scale on the y-axis and days post-infection on the x-axis.

### 4.4.2 Lymphadenopathy

The MLN of C57BL/6 mice infected with LHΔgfp showed lymphadenopathy similar to that observed with the wild type MHV-68 infected mice (section 4.2.3). In order to look for similar changes the total number of cells in the MLN of IFN-α/β $R^{-/-}$ mice and WT129 mice infected with LHΔgfp were analysed. The results are represented in Figure 4.12.

WT129 mice exhibited enlargement of the MLN similar to C57BL/6 mice, but the IFN-α/β $R^{-/-}$ mice showed a different pattern. There was a fall in the number of lymphocytes on day 7 post-infection and a subsequent increase but not to the levels observed with wild type mice.

The results show that different events take place in the MLN of IFN-α/β $R^{-/-}$ environment compared to the wild type mice infected with LHΔgfp. However the effect on the MLN of IFN-α/β $R^{-/-}$ mice infected with wild type MHV-68 virus has not been examined so far and it would be interesting to see whether similar differences can be detected. These events in the MLN may not be solely virus-driven as the IFN-α/β secretion has been linked to lymphadenopathy (Gresser *et al.*, 1981). Therefore IFN-α/β receptor-dependent signalling may be a key inducer of lymphadenopathy in MHV-68 infection.

### 4.4.3 Latently infected cells in the mediastinal lymph node and spleen

The latently infected cells in the MLN and spleens of the infected animals were analysed using the infective centre assay as described in the methods section (2.2.2). The results are represented in Figure 4.13 and 4.14.

The latently infected cells in the MLN of IFN-α/β $R^{-/-}$ mice on day 3 post-infection were 10-fold higher than the levels in WT129 mice. By day 7 post-infection that had increased dramatically to 50-fold. However by days 10 and 14 post-infection the levels of latently infected cells in the MLN of IFN-α/β $R^{-/-}$ mice had fallen to the levels comparable with the WT129 mice.

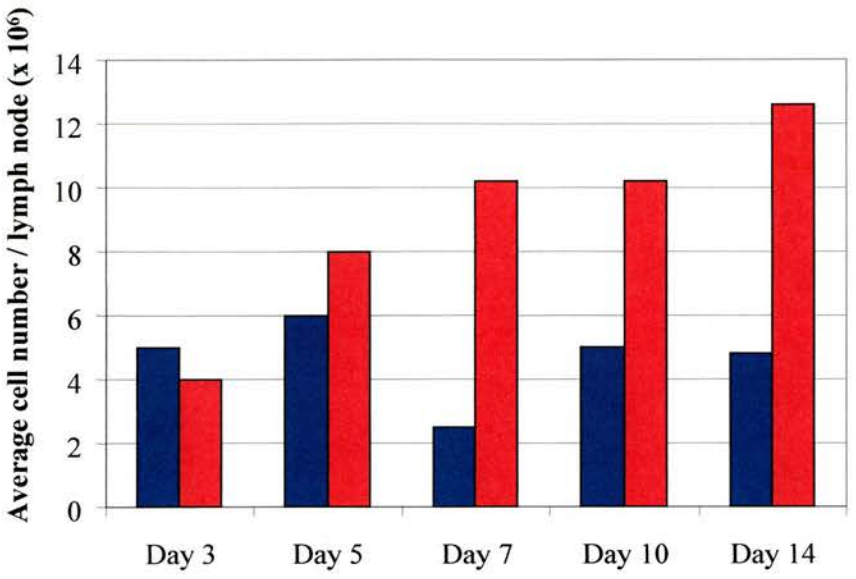


Figure 4.12 Lymphadenopathy of the mediastinal lymph node of IFN-α/β R-/- and WT129 mice infected with LHΔgfp IFN-α/β $R^{-/-}$ and WT129 mice were infected intranasally with 4 x $10^5$ PFU LHΔgfp. MLNs were pooled from six mice in each group on days 3, 5, 7, 10 and 14 post-infection. The MLNs were dissociated to obtain single cell suspensions and total cell numbers per MLN was counted. The graph shows the number of MLN cells in the IFN-α/β $R^{-/-}$ mice ( ■ ) and WT129 mice ( ■ ), on the y-axis against days post-infection on the x-axis.

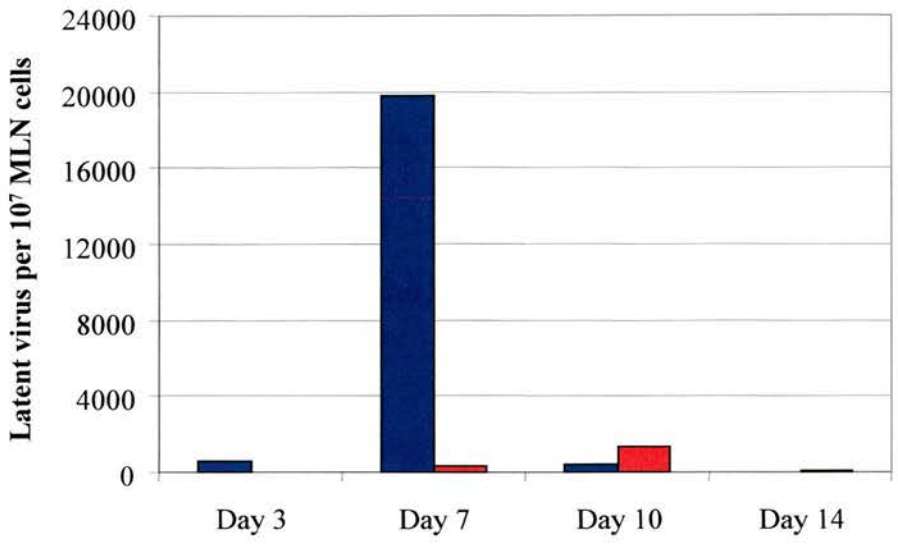


Figure 4.13 Latent virus in the mediastinal lymph node of IFN-α/β R-/- and WT129 mice infected with LHΔgfp IFN-α/β $R^{-/-}$ and WT129 mice were infected intranasally with 4 x $10^5$ PFU LHΔgfp. MLNs were pooled from six mice in each group on days 3, 7, 10 and 14 post-infection. The MLNs were dissociated to obtain single cell suspensions and plated with BHK cells to assay for latently infected cells using infective centre assay as described in methods section (2.2.2). The graph represents the latent virus per $10^7$ MLN cells in IFN- α/β $R^{-/-}$ ( ■ ) and WT129 mice (■ ) on the y-axis against days post-infection on the x-axis.

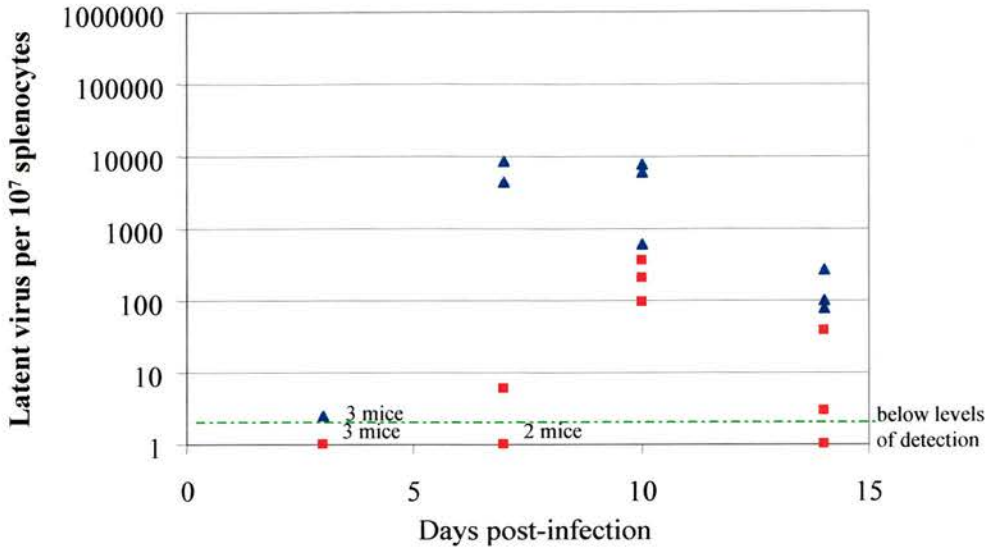


Figure 4.14 Latent virus in the spleens of IFN-α/β R-/- and WT129 mice infected with LHΔgfp IFN-α/β $R^{-/-}$ and WT129 mice were infected intranasally with 4 x $10^5$ PFU LHΔgfp. Spleens were removed from three mice in each group on days 3, 7, 10 and 14 post-infection. The spleens were dissociated to obtain single cell suspensions and plated with BHK cells to assay for latently infected cells using infective centre assay as described in methods section (2.2.2). The graph represents the latent virus per $10^7$ splenocytes in spleens of the IFN-α/β $R^{-/-}$ ( ▲ ) and WT129 mice ( ■) on the y-axis against days post-infection on the x-axis.

The spleens of IFN-α/β $R^{-/-}$ mice infected with LHΔgfp directly reflect the events in the MLN. By day 7 post-infection there was a 100-fold increase in the number of latently infected cells as compared to the WT129 mice. These numbers were reduced by day 10 and 14 post-infection.

### 4.4.4 Cryosections of the MLN and spleens of IFN-α/β $R^{-/-}$ mice to identify cells expressing GFP

The advantage of using LHΔgfp is emphasised mainly by the ability to express GFP in infected cells *in vivo* as shown previously. It could help trace the localisation of infected cells within tissues and even help understand trafficking of virus. Figure 4.15 (A and B) shows a tissue sections from the MLN of IFN-α/β $R^{-/-}$ mice taken on day 5 post-infection. Cells expressing GFP were seen mainly located near the margin of the lymph node rather than the central regions. Single cells expressing GFP could also be detected from the tissue section in Figure 4.15 (C). However, in the tissues from WT129 mice the frequency of cells expressing GFP was low and hence it was difficult to find GFP positive tissue sections.

The infective centre patterns in the spleen of the IFN-α/β $R^{-/-}$ mice infected with LHΔgfp on day 7 post-infection showed a very striking difference to the rest of the days of infection and also to that of the wild type mice. Therefore, it was considered important to check whether this was also reflected by the intracellular expression of GFP in these tissues.

On day 8 post-infection spleen tissue was removed from IFN-α/β $R^{-/-}$ and frozen for cryo-sectioning using isopentane/dry ice. Subsequently sections of the frozen tissue were viewed under a fluorescence microscope. The images are presented in Figure 4.15 (D).

The images show that on day 8 post-infection the tissues had large patches of GFP expressing cells in these tissues. This may correlate with the large amount of latently

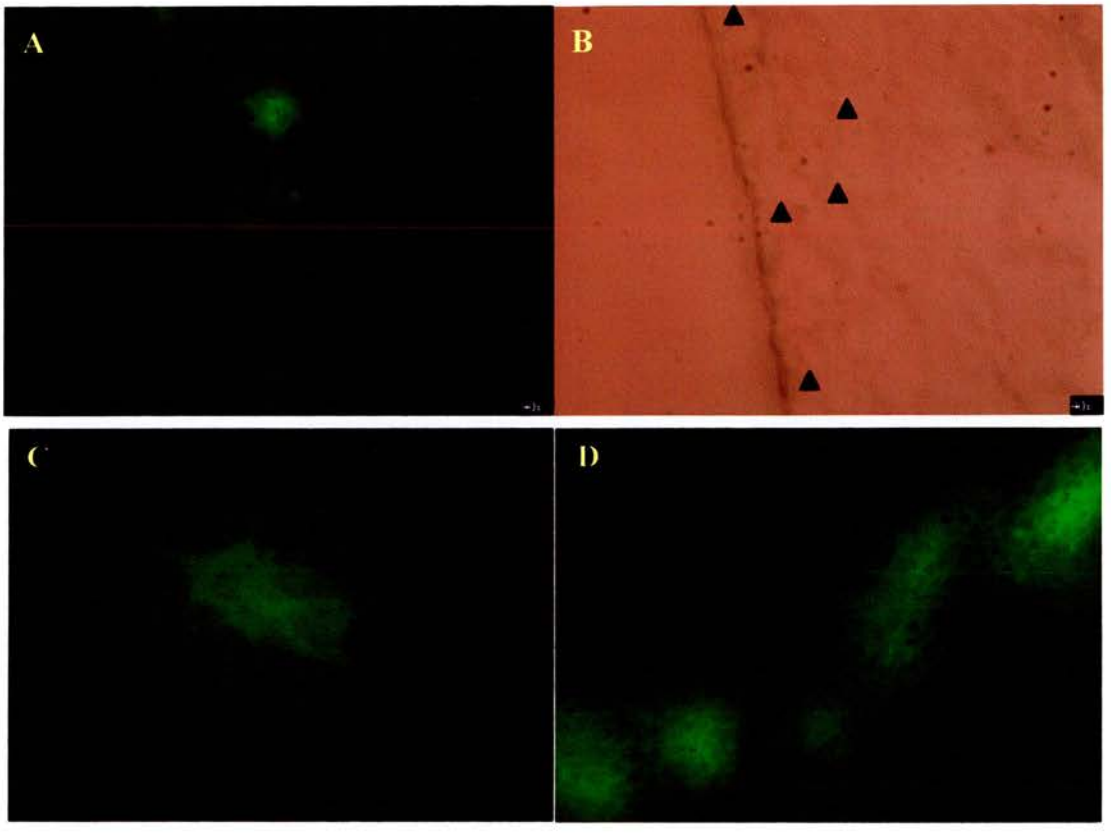


Figure 4.15 Cryosections of tissues from IFN-α/β R-/- mice to identify cells expressing GFP IFN-α/β $R^{-/-}$ mice were infected intranasally with 4 x $10^5$ PFU LHΔgfp. On day 5 post-infection the MLN from these mice were removed and frozen for cryo-sectioning. The figures shows (A) the images from a fluorescence microscope of the MLN (magnification: X320), (B) the same field as (A) under normal light showing the margin of the MLN and triangles indicate the localisation of GFP positive cells, (C) a morphologically large single cell (magnification: X800) from the MLN on day 5 post-infection. Figure (D) is a tissue section from the spleen of IFN-α/β $R^{-/-}$ mice on day 8 post-infection (magnification: X200).

infected cells detected on day 7 post-infection in these tissues as seen with infective centre assays examined in the previous section (4.4.3).

## 4.5 FACS analysis for various cell populations and the pattern of GFP expression in the MLN of IFN-α/β $R^{-/-}$ and WT129 mice

Sections 4.3.2 and 4.3.4 demonstrated that by FACS analysis it is possible to detect CD11c+/GFP expressing cells that may be infected with the LHΔgfp virus. In order to determine the *in vivo* infection kinetics of different cell subsets over the first two weeks of infection, lymphocytes from the MLN of IFN-α/β $R^{-/-}$ and WT129 mice were analysed in a similar fashion at different time intervals.

IFN-α/β $R^{-/-}$ and WT129 mice were infected intranasally with 4 x $10^5$ PFU of LHΔgfp. MLN were pooled from 6 mice in each group on days 5, 7, 10 and 14 post-infection. The MLN were dissociated to obtain single cell suspensions, counted and used for FACS analysis. The cells were stained with antibodies against specific surface markers to identify the cell subset. Positive cells were stained with PE conjugated antibodies and analysed by FACS. The intracellular GFP expression was analysed on the FL-1 axis. The results are presented in Figure 4.16. The graphs show the FACS percentage of specific cell subsets found in the MLN over the course of infection and also the FACS percentage of the respective cell type that was expressing GFP.

### 4.5.1 CD11c staining for dendritic cells

The graph 4.16 (1.a and 1.b) shows the FACS percentages of MLN cells stained with hamster-anti-mouse CD11c (clone HL-3) biotin conjugate, followed by streptavidin-PE. The CD11c surface staining was used as a marker to identify dendritic cell population. The graph 4.16 (1.a) shows the percentage of CD11c+ cells in the MLN of IFN-α/β $R^{-/-}$ mice. On days 5 and 7 post-infection 3-5% of MLN cells were CD11c+, the levels were reduced by (1%) by days 10 and 14 post-infection. Of these

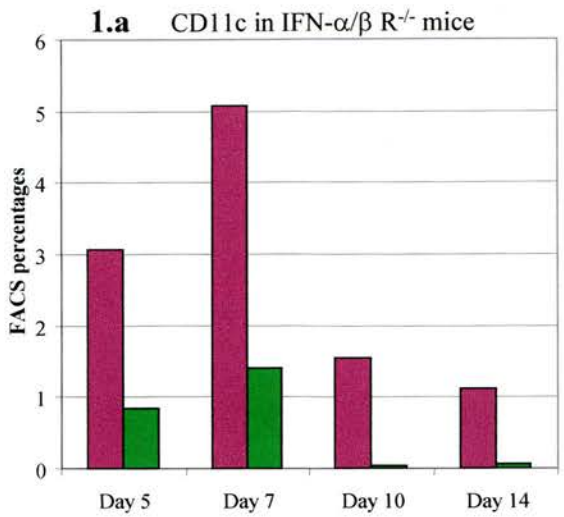


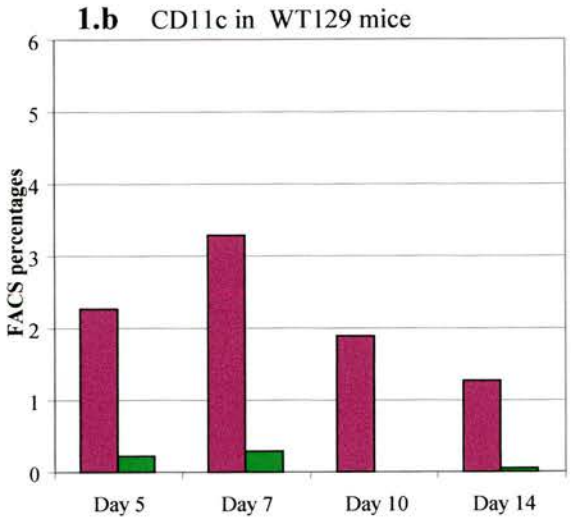


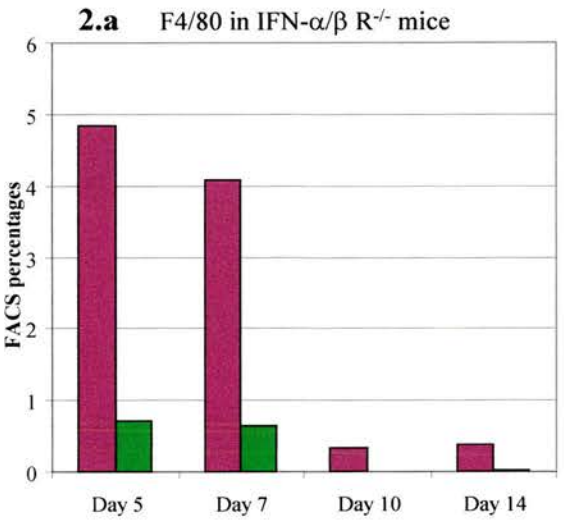


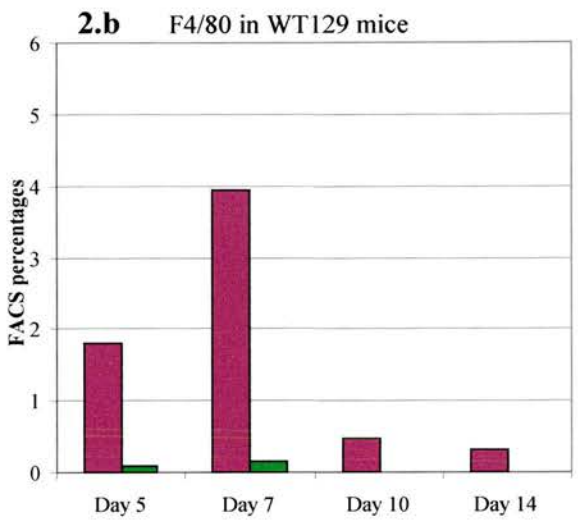


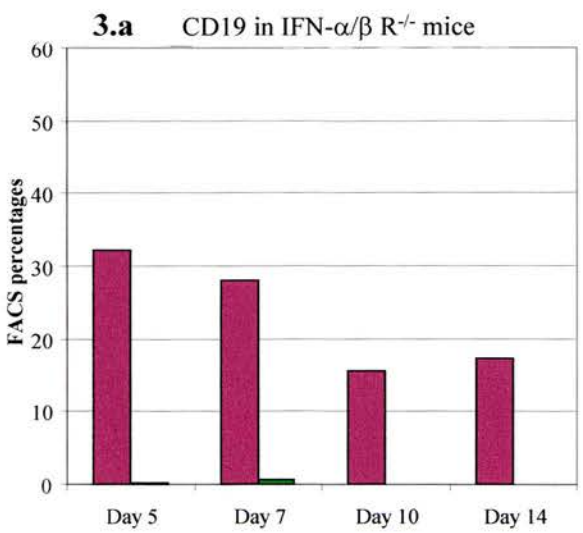


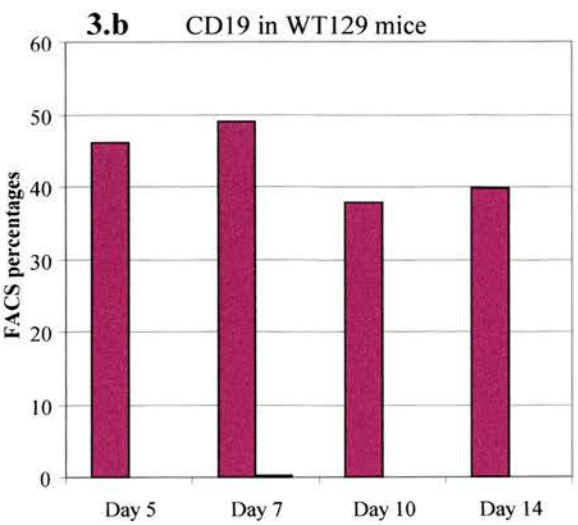


Figure 4.16 (continued on the next page)

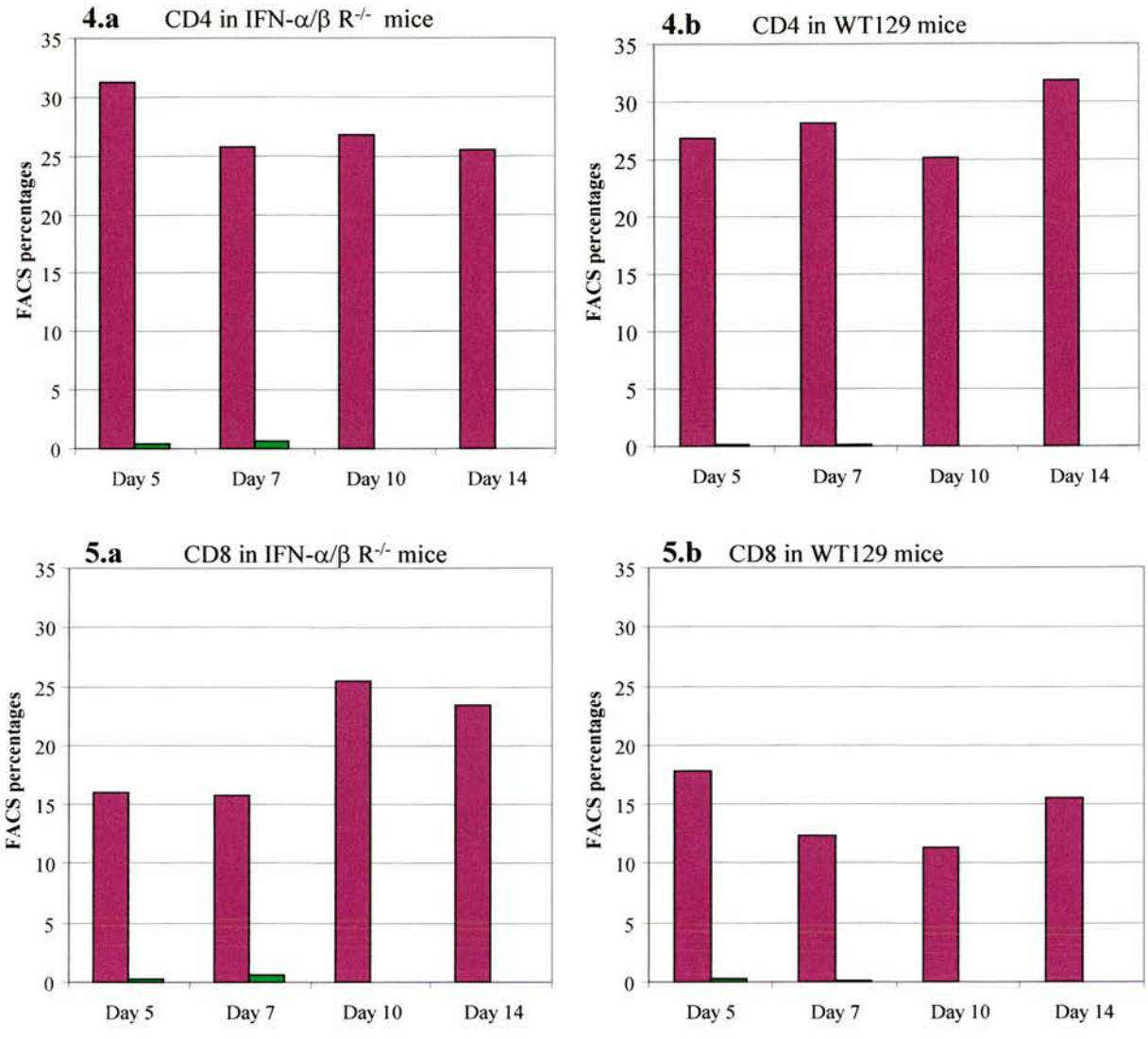


Figure 4.16 The FACS percentages of different cell types and the percentage expressing GFP, in the mediastinal lymph node of IFN-α/β R-/- and WT129 mice infected with LHΔgfp

Figure 4.16 The FACS percentages of different cell types and the percentage expressing GFP, in the mediastinal lymph node of IFN-α/β R-/- and WT129 mice infected with LHΔgfp IFN-α/β $R^{-/-}$ and WT129 mice were infected intranasally with 4 x $10^5$ PFU LHΔgfp. MLNs were pooled from six mice in each group on days 5, 7, 10 and 14 post-infection. The MLNs were dissociated to obtain single cell suspensions counted and taken for flow cytometric analysis (FACS). The cells were stained with either hamster anti-mouse CD11c biotin conjugated monoclonal antibody, rat anti-mouse F4/80 monoclonal antibody, rat anti-mouse CD19 monoclonal antibody, rat anti-mouse CD4 monoclonal antibody (YTS 191) or rat anti-mouse CD8 monoclonal antibody (YTS 169). Antibody positive cells were detected by staining with PE-conjugates. The FACS analysis was performed to determine the cells expressing these markers on FL-2 axis and the cells expressing intracellular GFP on FL-1 axis. 50,000 cells were acquired from each sample for analysis. The Figures 1.a, 2.a, 3.a, 4.a and 5.a show analyses of cells obtained from the MLN of IFN-α/β $R^{-/-}$ mice. The figures 1.b, 2.b, 3.b, 4.b and 5.b represent analyses of cells obtained from the MLN of WT129 mice. In the figures the red bars ( ■ ) show percentage of cells obtained through the staining patterns with the surface antibodies and the green bars ( ■ ) show the percentage of the respective cell type also expressing intracellular GFP. The figures 1.a and 1.b show the FACS percentages of cells stained with anti-CD11c antibody; 2.a and 2.b are for cell stained with anti-F4/80 antibody ; 3.a and 3.b are for cells stained with anti-CD19 antibody; 4.a and 4.b are for cells stained with anti-CD4 antibody; and 5.a and 5.b are for cells stained with anti-CD8 antibody.

.

cells, 20% were also found to be expressing GFP on days 5 and 7 post-infection but the percentages decreased to 3-5% on subsequent days analysed.

The graph 4.16 (1.b) represents the analysis of MLN cells from the WT129 mice. In these mice, there were 2-3% CD11c+ cells on days 5 and 7, and around 1-2% on days 10 and 14 post-infection. Among these CD11c+ cells, 9% were also expressing GFP on days 5 and 7 post-infection. The GFP expressing cells were fewer on day 10 but increased to 3% on day 14 post-infection.

The results demonstrate that many more CD11c+ cells express GFP in the first week of infection than in the second week of infection both in the immuno-deficient and the wild type environments.

### 4.5.2 F4/80 staining for macrophages

The graphs 4.16 (2.a and 2.b) show FACS percentages of cells that were stained with rat-anti-mouse F4/80 antibody followed by anti-rat IgG conjugated to PE. The graph 4.16 (2.a) shows the number of F4/80 stained macrophages in the MLN of IFN-$\alpha/\beta$ $R^{-/-}$ mice. On days 5 and 7 post-infection there were 4-5% macrophages in this environment. Of these cells 12-14% were detected with intracellular GFP expression. By days 10 and 14 post infection the percentages of macrophages decreased to less than 1% but there were still 3% to 7% of the cells expressing GFP, respectively.

The graph 4.16 (2.b) shows the number of macrophages in the WT129 mice MLN. On days 5 and 7 post-infection there were 2-4% F4/80+ cells but that fell to less than 1% by days 10 and 14 post-infection. Nevertheless, on days 5, 7 and 14 there were over 3% of these cells that were also expressing GFP.

The results demonstrate that both in the IFN $\alpha/\beta$-$R^{-/-}$ and the WT129 mice F4/80+ cells expressing GFP can be found, showing that these cells are susceptible to LH$\Delta$gfp infection. However in the absence of interferon receptor-mediated signalling there was a 3-fold greater number of F4/80+ cells expressing GFP.

### 4.5.3 CD19 staining for B cells

B cell populations were detected using rat-anti-mouse CD19 antibody staining, followed by anti-rat IgG conjugated to PE. The results are presented in Figure 4.16 (3.a and 3.b). The graph 4.16 (3.a) shows the percentage of B cells in the MLN of IFN-α/β $R^{-/-}$ mice. On days 5 and 7 post-infection around 30% B cells are seen in this tissue but by days 10 and 14 post-infection the percentages decreased to around 15%. Among these cells on day 7, 2.5% cells also expressed GFP, the levels were lower on all other days of infection recorded with percentage of GFP expressing cells between 0.1-0.3%.

The Figure 4.16 (3.b) shows the percentage of CD19+ cells in the MLN of WT129 mice. The percentage of CD19+ cells on days 5 and 7 post-infection was 45-50%. However, on days 10 and 14 post-infection in this environment, unlike in the immuno-deficient system, the CD19+ cell population remained over 35% of total MLN cells. The GFP expressing CD19+ cell percentages were as low as 0.05% on day 10 and only as high as 0.22% on day 7 post-infection.

The results demonstrate that in the IFN-α/β $R^{-/-}$ mice the percentages of B cells decreased in the first 2 weeks post-infection as compared to the B cell percentages in the MLN of WT129 mice. This difference may be one of the reasons for the reduction in lymphadenopathy observed in the IFN-α/β $R^{-/-}$ mice (see section 4.4.2). In both the host systems the percentage of GFP expressing CD19+ B cells was much lower than that observed with CD11c+ and F4/80+ cells.

### 4.5.4 Staining for CD4+ T cells

CD4+ T cells were identified using rat-anti-mouse CD4 antibody (YTS191) followed by anti-rat IgG conjugated to PE. The results are presented in the Figure 4.16 (4.a and 4.b). The Figure 4.16 (4.a) shows the percentages of CD4+ cells in the MLN of IFN-α/β $R^{-/-}$ mice. On days 5, 7, 10 and 14 post-infection the levels of CD4+ cell were between 25-35%. The GFP expressing cells were 1.3% and 2.5% on days 5 and

7, respectively. However, these percentages fell to 0.04% and 0.08% by days 10 and 14 post-infection.

The Figure 4.16 (4.b) shows the percentages of CD4+ cells in the MLN of WT129 mice. The percentages on days 5, 7, 10 and 14 post-infection were between 25-35%. The GFP expressing cells among them were either absent or below levels of detection on day 10 and around 0.04% and 0.09% on the subsequent days.

The results demonstrate that the percentages of CD4+ T cell in both the host systems were similar, although the percentages of GFP expressing cells in the IFN-$\alpha/\beta$ $R^{-/-}$ were higher on days 5 and 7 post-infection than in WT129 mice. This difference in the percentages of GFP expressing cells was similar to that observed with the other cell types examined previously.

### 4.5.5 Staining for CD8+ T cells

CD8+ T cells were detected using rat-anti-mouse CD8 antibody (YTS169) followed by anti-rat IgG conjugated to PE. The results are presented in Figure 4.16 (5.a and 5.b). The Figure 4.16 (5.a) shows the percentage of CD8+ cells in the MLN of IFN-$\alpha/\beta$ $R^{-/-}$ mice. On days 5 and 7 post-infection there were 15% CD8+ T cells and among these 1.7% and 3.7% of cells also expressed GFP, respectively. The percentage of CD8+ T cells on days 10 and day 14 post-infection rose to around 25% but the percentages of GFP expressing cells fell to 0.04% and 0.2%, respectively.

The Figure 4.16 (5.b) shows the CD8+ T cell percentages in the MLN of WT129 mice. The percentages of CD8+ cells on days 5, 7, 10 and 14 post-infection fluctuated between 10-20%. On day 5, 1.33% of the total percentage of 17% of CD8+ cells were detected with GFP expression. The levels fell to 0.96% on day 7 and 0.19% on day 14 post-infection.

The results demonstrate that there were 25% CD8+ T cells on days 10 and 14 compared to 15% on days 5 and 7 post-infection in the MLN of IFN-$\alpha/\beta$ $R^{-/-}$ mice. In

WT129 mice the CD8+ T cells were around 15% throughout the course of infection. This might indicate the recruitment of more CD8+ T cells to control MHV-68 infection in the MLN in the absence of an effective anti-viral IFN-α/β response.

The Figure 4.17 is another representation of the data from the above experiment in which the total cell numbers expressing GFP from each cell type was calculated by multiplying FACS percentages by the total number of cells in each lymph node. The data is plotted for each cell type on the days post-infection that were investigated. The graphs compare the approximate number of cells from each cell type expressing GFP on different days post-infection. It also compares LHΔgfp infection in IFN-α/β $R^{-/-}$ and WT129 mice.

The cell types compared are those that express the surface markers CD11c, F4/80, CD19, CD4 or CD8. The FACS percentages of cells expressing GFP in the MLN of IFN-α/β $R^{-/-}$ and WT129 mice on days 5 and 7 post-infection showed that the wild type mice had fewer GFP expressing cells compared to the immuno-deficient system. By day 10 and day 14 post-infection the levels of GFP expressing cells had decreased in both mouse strains.

## 4.6 The FACS percentages of cells expressing GFP in the spleens of IFN-α/β $R^{-/-}$ mice and WT129 mice

The Figure 4.18 shows the FACS percentages of different subsets of cells expressing different markers (CD11c, F4/80, CD19, CD4 and CD8) and the percentage of those expressing GFP in the spleens. The FACS percentages for three spleens were analysed in the IFN-α/β $R^{-/-}$ and the WT129 mice. The data is presented with error bars representing the standard error of the mean.

The graph 4.18 (1.a) shows the FACS percentages of CD11c+ cells, which were 4-5% of the total cell population in the spleens of IFN-α/β $R^{-/-}$ mice, and these percentages remained elevated on days 5, 7, 10 and 14 post-infection. The GFP expressing cells were as high as 27% of the CD11c+ cells in the IFN-α/β $R^{-/-}$ mice

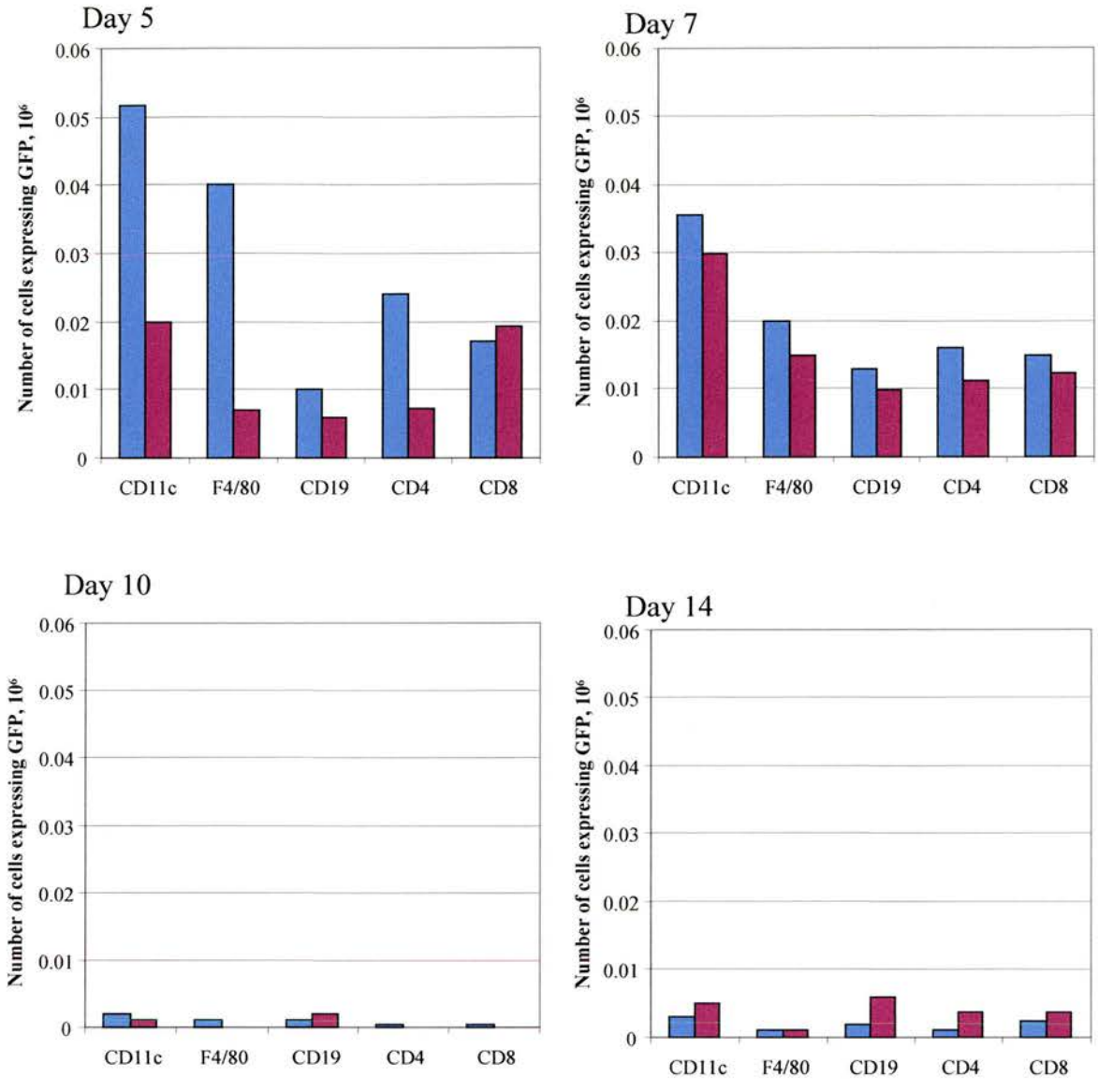


Figure 4.17 The numbers of cells expressing GFP in the mediastinal lymph node of IFN-α/β R-/- and WT129 mice infected with LHΔgfp

Figure 4.17 The total numbers of cells expressing GFP in the mediastinal lymph node of IFN-α/β R-/- and WT129 mice infected with LHΔgfp IFN-α/β $R^{-/-}$ and WT129 mice were infected intranasally with 4 x $10^5$ PFU LHΔgfp. MLNs were removed from six mice in each group on days 5, 7, 10 and 14 post-infection. The MLNs were dissociated to obtain single cell suspensions, counted and taken for flow cytometric analysis (FACS). The cells were stained with either hamster anti-mouse CD11c biotin conjugated monoclonal antibody, rat anti-mouse F4/80 monoclonal antibody, rat anti-mouse CD19 monoclonal antibody, rat anti-mouse CD4 (YTS191) monoclonal antibody or rat anti-mouse CD8(YTS169) monoclonal antibody.The figure represents the total number of cells in each cell type calculated by multiplying the FACS percentages to the number of cells in the MLN of IFN-α/β $R^{-/-}$ ( ■ ) and WT129 mice ( ■ ).

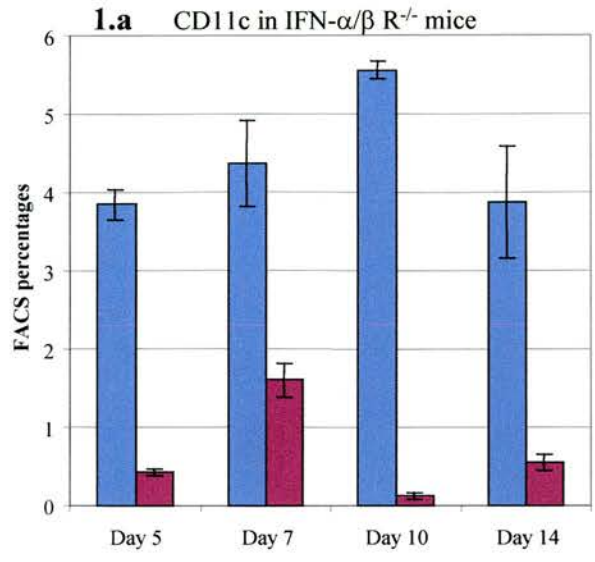


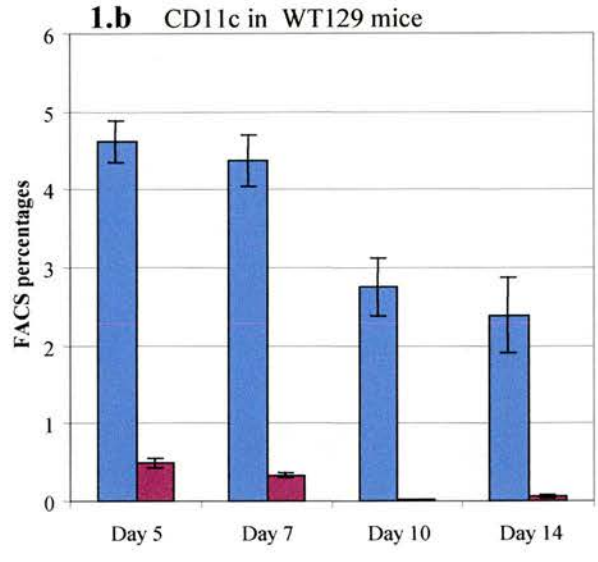


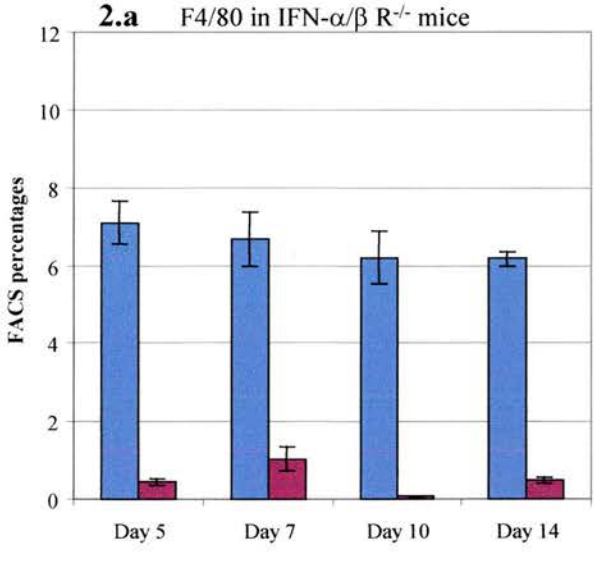


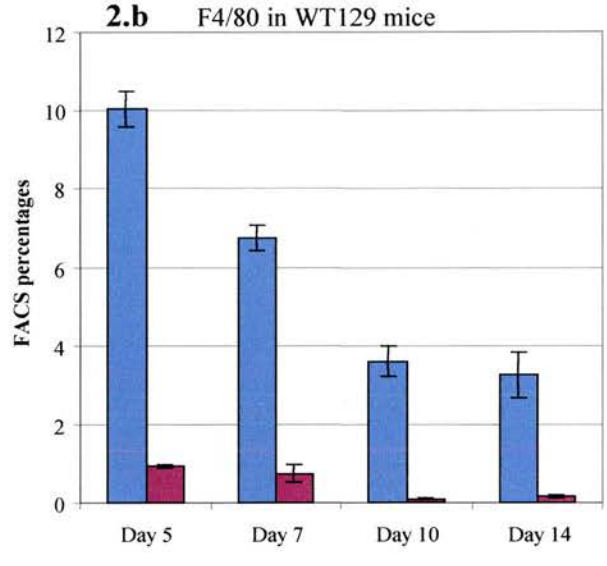


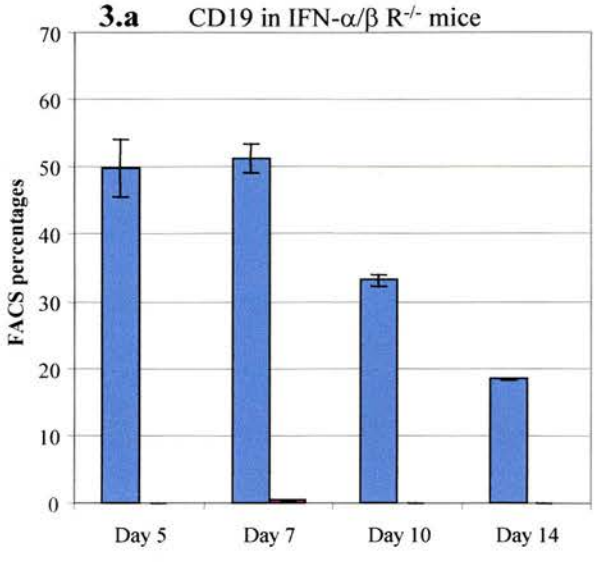


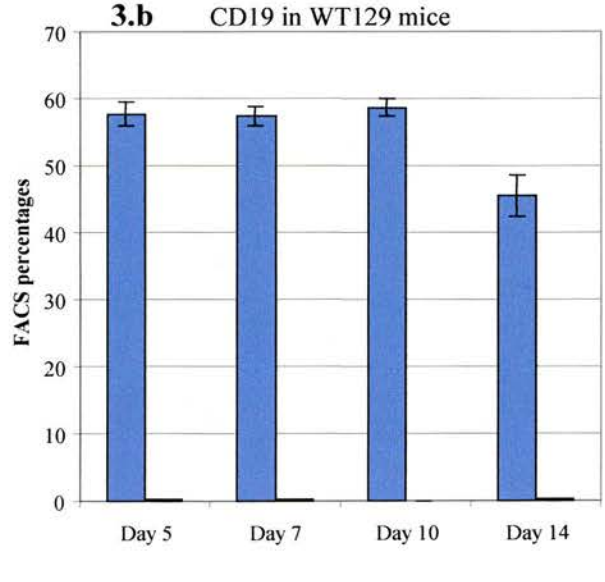


Figure 4.18 (continued on the next page)

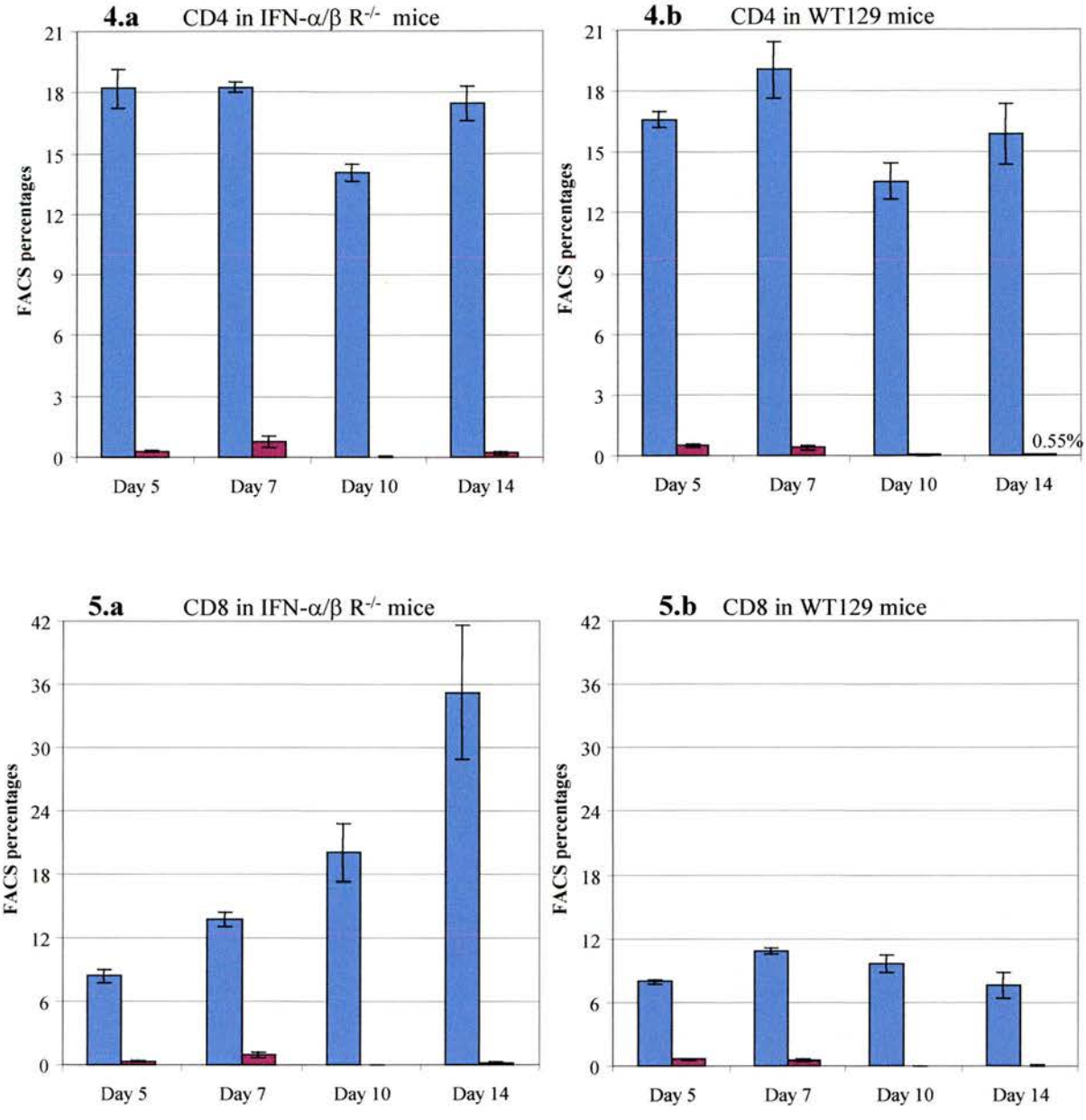


Figure 4.18 The FACS percentages of different cell types and the percentage expressing GFP in the spleens of IFN-α/β R-/- and WT129 mice infected with LHΔgfp

Figure 4.18 The FACS percentages of different cell types and the percentage expressing GFP in the spleen of IFN-α/β R-/- and WT129 mice infected with LHΔgfp IFN-α/β $R^{-/-}$ and WT129 mice were infected intranasally with 4 x $10^5$ PFU LHΔgfp. Spleens were removed from three mice in each group on days 5, 7, 10 and 14 post-infection. The spleens were dissociated to obtain single cell suspensions counted and taken for flow cytometric analysis (FACS). The cells were stained with either hamster anti-mouse CD11c biotin conjugated monoclonal antibody, rat anti-mouse F4/80 monoclonal antibody, rat anti-mouse CD19 monoclonal antibody, rat anti-mouse CD4 monoclonal antibody (YTS 191) or rat anti-mouse CD8 monoclonal antibody (YTS 169). Antibody positive cells were detected by staining with PE-conjugates. The FACS analysis was performed to determine the cells expressing these markers on FL-2 axis the cells expressing intracellular GFP on FL-1 axis. 50,000 cells were acquired from each sample for analysis. The Figures 1.a, 2.a, 3.a, 4.a and 5.a show analyses of splenocytes obtained from the spleens of IFN-α/β $R^{-/-}$ mice. The figures 1.b, 2.b, 3.b, 4.b and 5.b represent analyses of splenocytes obtained from the spleens of WT129 mice. In the figures the purple bars ( ▫ ) show percentage of cells obtained through the staining patterns with the surface antibodies and the red bars ( ▪ ) show the percentage of the respective cell type also expressing intracellular GFP. The figures 1.a and 1.b show the FACS percentages of cells stained with anti-CD11c antibody; 2.a and 2.b are for cell stained with anti-F4/80 antibody ; 3.a and 3.b are for cells stained with anti-CD19 antibody; 4.a and 4.b are for cells stained with anti-CD4 antibody; and 5.a and 5.b are for cells stained with anti-CD8 antibody. The error bars represent standard errors of the mean of three spleens in each case.

.

on day 7, while they were around 10-13% on days 5 and 14 with the lowest level of 2% seen on day 10 post-infection. The graph 4.18 (1.b) shows the percentages in the spleens of WT129 mice in which the CD11c+ cells ranged between 3-5% on the days examined. The spleens of WT129 mice had 7-10% GFP expressing CD11c+ cells on days 5 and 7, and approximately 2% on day 14 post-infection.

The graph 4.18 (1.a) shows that 6-7% F4/80+ cells were infected in the spleens of IFN-α/β $R^{-/-}$ mice on all four days post-infection. The GFP expressing cells among these cells ranged from 6% on day 5 to 14% on day 7. This declined to 1% on day 10 but rose to 8% on day 14 post-infection. The graph 4.18 (1.b) shows F4/80+ cells in the spleens of WT129 mice, which fell from 10% on day 5 to 4% on day 14 post-infection. The expression of GFP expressing cells was 8-10% on days 5 and 7, and 3% and 5% on days 10 and 14 post-infection, respectively.

The frequency of GFP expression in CD11c+ and F4/80+ cells was higher than the other populations such as CD19+, CD4+ or CD8+ cells. The patterns of GFP expression in the spleen resemble those seen in the MLN. The disadvantage is that the GFP expression does not indicate whether these cells were undergoing lytic or latent infection.

An interesting observation in the spleens was that the percentages of B cells (CD19+ staining) in the WT129 mice stays constant while in the IFN-α/β $R^{-/-}$ mice only 20% of total cells on day 14 were B cells compared to 50% on day 5 post-infection. On the other hand in the IFN-α/β $R^{-/-}$ system the CD8+ cells (mainly T cells) rose from 10% on day 5 to 30-40% on day 14 post-infection while in the WT129 mice the levels remained almost constant. The percentages of different cell types have not been examined in the IFN-α/β $R^{-/-}$ system infected with wild type MHV-68 and it would be interesting to see whether similar changes take place during infection.

# CHAPTER FIVE

# DISCUSSION

MHV-68 disease pathogenesis has so far focused on the lungs as the primary site following intranasal infection with the virus undergoing lytic replication in alveolar epithelial cells. This is followed by latent infection of B cells that are found localised mainly in the spleen. Subsequent studies have also shown the presence of latent virus in alveolar epithelial cells (Stewart *et al.*, 1998), F4/80+ macrophages in the peritoneum (Weck *et al.*, 1999b), CD11b+ macrophages and CD11c+ dendritic cells in the spleen (Flano *et al.*, 2000). However, the presence of B cells in the host environment was shown to be essential for the maintenance of latency in the spleen (Usherwood *et al.*, 1996b) as well as in the transfer of virus from the lungs to the spleen (Stewart *et al.*, 1998). The work described in this thesis focuses on the intermediary site of infection, the mediastinal lymph node (MLN) and has investigated the importance of B cells and other cells in trafficking virus as well as in the maintenance of latency at this site.

These results describe the role of B cells during MHV-68 disease pathogenesis in the MLN by comparing normal mice to B cell deficient (μMT) mice. The lymphadenopathy in C57BL/6 mice was attributed mainly to the accumulation of B cells at this site and this observation was substantiated by the absence of lymphadenopathy in μMT mice. The expansion of B cells in the MLN of C57BL/6 mice was partly dependent on CD4+ T cell signalling. The MLN of μMT mice also provided an opportunity to investigate whether cells other than B cells were latently infected with MHV-68. The use of a green fluorescent protein (GFP) expressing recombinant virus, LHΔgfp, as a tool for studying tropism helped isolate and characterise cell types susceptible to virus infection in the MLN. Cells from the MLN of μMT mice infected with LHΔgfp were enriched for the CD11c marker, specific for dendritic cells, and found to express GFP. LHΔgfp infection of IFN-α/β $R^{-/-}$ mice demonstrated that even in the presence of B cells, dendritic cells expressing

CD11c and macrophages expressing F4/80 surface markers were infected in the MLN.

## 5.1 MLN is a critical site in MHV-68 pathogenesis where the B cells play an important role

### 5.1.1 Requirement for B cells in lymphadenopathy

In C57BL/6 mice infected with 4 x $10^5$ PFU MHV-68 intranasally, the MLN had enlarged by 10-fold during the first ten days post-infection. This observation is similar to the results published by Sarawar *et al* (1996) where a 5-10 fold increase in cellularity was detected in the MLN of C57BL/6J mice infected with 4 x $10^3$ PFU MHV-68. Analysis of the cell subsets in the enlarged lymph nodes of C57BL/6 mice revealed a 10-15 fold increase in B cell numbers and a 4-5 fold increase in the CD4+ and CD8+ T cell numbers. The importance of B cells in establishing lymphadenopathy is highlighted in B cell deficient (μMT) mice. The μMT mice showed a lack of lymphadenopathy with a reduction of all subsets of cells compared to C57BL/6 mice. The increase in cellularity in the MLN has also been observed in the case of other respiratory viruses such as Influenza A virus (Allan *et al*, 1990). However, this dramatic accumulation of B cells in the MLN early in MHV-68 infection is probably an important strategy used by this virus to disseminate within the host. Cells stained for activation markers like CD69 and CD25 showed that there was an increase in CD69 a marker found on B and T cells but there was also an increase in CD25 a marker found on T cells on days 7 and 10 post-infection. However, double staining for IgMμ + CD69 showed minimal level of staining indicating that the increase in CD69 marker was mainly due to T cells expression rather than from activated/proliferation B cells.

EBV is known to infect B cells directly at the mucosal surface. Virus-encoded transcripts such as viral IL-10 can induce proliferation of B cells. Studies on B cells obtained from EBV infected patients have shown that the virus alone can provide these cells with transformation and proliferation signals (Rowe *et al.*, 1991, Kempkes

*et al.*, 1995). In the case of patients suffering from acute EBV infection (infectious mononucleosis), a rapid polyclonal expansion of the B cell pool is seen prior to the development of an effective cellular response (Rickinson and Keiff, 1996). There is evidence *in vitro* that MHV-68 can cause proliferation, albeit not on the scale of EBV (Dutia *et al.*, 1999b, Stevenson and Doherty, 1999). Viral proteins similar to LMP-1 that provide direct B cell proliferation signals have not been found in MHV-68 infection to date. Consequently, the increase in the number of B cells over the first 10 days of infection could be in part attributed to a virus driven polyclonal expansion or a CD4+ T cell-dependent expansion.

### 5.1.2 B cell expansion is only partly dependent on CD4+ T cell signalling

To investigate whether one of the factors in the expansion of B cells is due to CD4+ T cell signalling, these cells were depleted *in vivo* prior to infection with MHV-68. Following depletion of CD4+ T cells, lymphadenopathy developed at a slower rate and the magnitude of the response was greatly reduced compared to that seen in normal mice, with only a 5-fold increase in B cell numbers. CD8+ T cell numbers in the MLN of depleted mice increased, but this could be a mechanism to compensate for the absence of CD4+ T cells in this tissue following their depletion. A similar observation was made in the MLN of CD4+ T cell depleted mice infected with Influenza A virus where an increase in CD8+ T cell numbers were detected during the course of infection (Allan *et al.*, 1990). The manifestation of lymphadenopathy in the CD4+ T cell depleted mice and the increase in B cell numbers observed on day 10 coincide and it can be said that even in the absence of CD4+ T cells, B cells remain the major subset responsible for the enlarged lymph node. The reasons for this could be due to (i) virus-induced B cell proliferation, (ii) CD4+ T cell independent proliferation or (iii) recruitment of B cells signalled by secreted host proteins.

There is evidence that *in vitro* B cells infected with MHV-68 can proliferate in the absence of CD4+ T cells as seen by the expression of the CD69 activation marker and the secretion of IgM antibodies. Although *in vivo* similar changes were not observed, it was demonstrated that CD4+ T cell signalling was required for class

switching and clonal selection of IgG secreting B cells in the long run (Stevenson and Doherty, 1999). The experiments described in this thesis have shown that *in vivo* there might be a small window where B cells are capable of accumulating in the MLN in the absence of direct CD4+ T cell stimulus.

The CD4+ T cell depletion experiments with BALB/c mice showed an absence of splenomegaly and a reduction in the levels of latently infected cells (Usherwood *et al.*, 1996a). The experiments described here show a similar reduction in the number of latently infected cells in C57BL/6 mice depleted of CD4+ T cells on day 16 post-infection in the spleen. In addition, it was shown that the number of latently infected cells was greatly reduced in the MLN of CD4+ T cell depleted mice compared to control mice. Therefore, it can be said that the CD4+ T cells play an important role in the effective establishment of latency in the MLN similar to that seen in the spleen.

### 5.1.3 B cells are required for long-term latency and viral dissemination from the MLN

It was previously shown that μMT mice infected with MHV-68 failed to develop splenomegaly and a latent infection in the spleen (Usherwood, *et al.*, 1996b). Experiments in chapter 3 demonstrated that on days 5 and 7 post-infection latently infected cells were present in the MLN of μMT mice. These infected cells became undetectable by day 10 post-infection as determined by the infective centre assay. In contrast, in the MLN of C57BL/6 mice the levels of latently infected cells were 6-fold higher on day 10 compared to day 7 post-infection. Attempts to identify cells carrying productive virus in the MLN of μMT mice through immunostaining and transmission electron microscopy proved to be unsuccessful. However when RT-PCR that affords greater sensitivity was used viral gene transcripts for ORF50 the immediate early gene was detected on all days investigated including day 10 post-infection in the MLNs of μMT mice. The detection of viral gene expression for M3 both an early and latency associated gene transcript indicated that the virus could be present in a latent state with some cells having a basal level of productive infection. It may be concluded that B cells are essential for the presence of detectable levels of latency in the MLN.

The role of B cells in the transfer of virus to other tissues was highlighted in the work of Stewart *et al* (1998). They showed that the transfer of uninfected B cells to μMT mice (which have virus persisting in lung, but no evidence of latent infection in the spleen) resulted in virus DNA being detected in the spleen. The experiments described in the previous chapters substantiate some of these observations through experiments where latently infected cells although detectable in the MLN of μMT mice in the first week post-infection, could not be detected in the cervical lymph node (CLN). While in the C57BL/6 mice latently infected cells were detected in the CLN during the progression of infection, proving that in the absence of B cells the systemic transfer of virus is limited.

The MLN is a critical tissue in MHV-68 infection and may be compared with tonsils used in the study of EBV infection. The human tonsils from EBV infected asymptomatic patients and IM patients have provided very useful insight in to the *in vivo* infection of B cells and different latency stages adopted by the virus. A recent study by Thorley-Lawson's group describes different gene expression patterns that are dependent on the differentiation stage of the infected B cells (Babcock *et al.*, 2000b). A different study on the tonsillar tissue from IM patients, using PCR on single cells isolated by laser microdissection showed that EBV infected B cells arising from a single clone can exhibit different morphology as well as different EBV gene expression patterns (Kurth *et al.*, 2000). It is speculated that these are some of the ways by which the virus evades immune surveillance. These techniques could be used in future work to unravel B cell latency patterns during MHV-68 infection, at a single cell level in the MLN.

### 5.1.4 Latently infected B cells are required for the presence of an active MHV-68 specific CTL response in the MLN

There were clear differences between the CTL response to MHV-68 infection in C57BL/6 and μMT mice. CTLs were directed against peptides p56 and p79, which have been shown to be highly immunodominant epitopes obtained from lytic

transcripts ORF6 and ORF61 respectively (Stevenson *et al.*, 1998). Using the IFN-γ CTL assay as a means of quantitating the percentage of peptide specific CD8+ T cells, a 1% response on day 10 and a 0.2-0.5% response on day 15 post-infection was observed for p56 and p79 in the MLN of C57BL/6J mice (Stevenson *et al.*, 1999a). A similar response was observed in the MLNs of C57BL/6 mice as shown in Figure 3.13, however in the MLNs of μMT mice the response was only around 0.2% peptide specific T cells on days 10 and 17 post-infection.

Both in C57BL/6 as well as in μMT mice a slightly higher response was seen on day 6 post-infection, which could be interpreted to be due to the ongoing lytic infection in the lung. The reduction in CTL response in μMT mice compared to C57BL/6 mice seems to indicate that in the absence of infected B cells at this site the response fades away at a faster rate. In other words infected B cells might be required for the maintenance of CTL response in the MLN.

## 5.2 Cells other than B cells are infected in the MLN

### 5.2.1 Dendritic cells and macrophages, target cells for MHV-68 infection in the MLN

The mouse MLN is an extremely small tissue with less than 2 million cells and in the work described in chapters 3 and 4, MLN from 4 to 6 mice were pooled together in order to carry out different assays. Latently infected cells were detected in the MLN of μMT mice infected with MHV-68 on days 5 and 7 post-infection. However, relatively small numbers were detected which made phenotyping these cells a difficult exercise. To overcome this a GFP 'marked' virus-LHΔgfp was used. This greatly improved detection of infected cells and GFP expressing CD11c+ dendritic cells were detected in the MLN. This observation suggested that the latently infected cells in the MLN of μMT mice infected with MHV-68 could have a CD11c phenotype. The results with IFN-α/β $R^{-/-}$ and WT129 mice confirmed that CD11c+ dendritic cells and F4/80+ macrophages are infected during the very onset of infection in the MLN.

It is possible that some of the GFP expressing cells had phagocytosed GFP expressing infected cells or apoptosing cells in the lymph node. However, in this case the GFP is likely to have a punctate appearance in the cell, indicating localisation within vacuoles. Comparisons can be made with a recombinant Venezuelan equine encephalitis (VEE) virus expressing GFP and the characterisation of infected cells in a mouse model *in vivo* (MacDonald and Johnston, 2000). They identified that cells with a diffuse GFP expression were the virus-infected cells, which were later identified as dendritic cells and cells with punctate GFP staining pattern which were considered to be the result of phagocytosis. Based on this evidence it is likely that cells with the diffuse GFP expression are infected with LHΔgfp.

Dendritic cells were enriched from the MLN of μMT mice using hamster anti-mouse CD11c antibodies (clone N418) bound to magnetic beads. The FACS analysis of isolated cells showed 55% of these cells to be definitely positive for CD11c and of those 3% were also found to be expressing intracellular GFP. Surface staining for macrophage specific F4/80 marker indicated that some of the GFP expressing cells were macrophages. It is possible that F4/80+ macrophages are infected in the lymph node or become infected in the lungs and move into the lymph node at the on-set of MHV-68 infection. However, there is evidence that freshly isolated dendritic cells from the spleen expressing CD11c marker can express low levels of macrophage markers such as F4/80 and Mac-1 (Leenen *et al.*, 1998). It is known that the expression of macrophage markers at low levels in these dendritic cells is only an indication of these cells differentiating from immature cells to mature dendritic cells. These cells, when isolated and cultured *in vitro*, lost the macrophage markers and expressed mature dendritic cell markers (Leenen *et al.*, 1998). Therefore, from the results presented here regarding the presence of F4/80+ cells expressing GFP among the cells enriched for CD11c, it is difficult to say whether they were macrophages or immature dendritic cells.

The MLN of IFN-α/β $R^{-/-}$ mice enriched for CD11c+ cells also showed 50% purity and of those around 10% expressed intracellular GFP. There was a three-fold

increase in the number of CD11c+ cells expressing GFP in IFN-α/β $R^{-/-}$ mice compared to μMT mice. This increased number of cells in IFN-α/β $R^{-/-}$ mice made it possible to set up analysis using flow cytometry for determining the cell subsets expressing GFP. A high frequency of GFP positive cells were observed among the F4/80 and CD11c populations from MLN and spleen of IFN-α/β $R^{-/-}$ mice on days 5 and 7 post-infection. In contrast, relatively few B cells were GFP positive despite the absence of an anti-viral IFN-α/β response. The WT129 mice had fewer GFP positive cells, but F4/80+ and CD11c+ fraction contained the majority of GFP expressing cells in the first week post-infection.

At the time these experiments were being carried out a paper published by Flano *et al* (2000) showed that dendritic cells and macrophages in the spleen were carriers of latent MHV-68. They were able to FACsort for CD11c+ dendritic cells and CD11b+ macrophages from the spleens of MHV-68 infected C57BL/6 mice. When they compared the number of dendritic cells, macrophages and B cells, they found dendritic cells to have the highest number of latently infected cells. Seven-fold more dendritic cells were latently infected compared to B cells on day 14 post-infection. Although this data looked only at one time point post-infection in the spleen, it does substantiate some of the observations made in chapter 4 regarding the susceptibility of dendritic cells to MHV-68 and the increased frequency of GFP expressing CD11c+ cells in the MLN and spleen of IFN-α/β $R^{-/-}$ and WT129 mice.

### 5.2.2 Dendritic cells in trafficking virus

Studies on rat lung tissues have shown the presence of an extensive network of dendritic cells in the airways and interstitium of the lung. Following infection with Sendai virus, dendritic cell numbers increase in the lung (McWilliam *et al.*, 1997). A recent study *in vivo* by intratracheal instillation of fluorescein isothiocyanate (FITC)-conjugated macromolecules in mice has shown migration of dendritic cells from the airway mucosa to the thoracic lymph node (TLNs). They show that specific subsets of CD11c+ and MHC class II+ dendritic cells called airway-derived lymph node

dendritic cells (AW-LNDCs) upon antigen exposure migrate from the lungs to the T cell rich regions in the TLNs (Vermaelen *et al.*, 2001).

Based on the evidence above it is hypothesised that the CD11c+ and F4/80+ cells expressing GFP seen in the MLN as early as day 5 are cells that were trafficked from the lungs into the lymph node following MHV-68 infection. In future work it will be interesting to determine whether these subsets of cells were positive for virus in the lung.

### 5.2.3 Dendritic cells and macrophages as reservoirs of virus

Studies have shown Langerhans cells in the vaginal mucosa to be infected with SIV in monkeys and also with HIV in mouse models (Miller and Hu, 1999, Masurier *et al.*, 1998). Immature dendritic cells have also been shown to harbour replicating M-tropic HIV and these cells were able to transmit virus to T cells. Recently a dendritic cell specific C-type lectin, DC-SIGN was identified with specific affinity for HIV gp120. HIV virions can bind to this molecule on the surface of dendritic cells and subsequently infect cells that express CD4 and chemokine receptors (Geijtenbeek *et al.*, 2000).

In the case of MHV-68 infection the CD11c+ and F4/80+ cells could carry latent virus or they may be undergoing transient replication. It is possible that during MHV-68 infection the CD11c+ and F4/80+ cells could also act as reservoirs of virus from which B cells in the MLN could become infected. However in the absence of B cells these cells may not be able to maintain long-term latency.

## 5.3 Pathogenesis and use of recombinant LHΔgfp

### 5.3.1 Effects on disease pathogenesis of LHΔgfp as a result of the deleted genes

During the construction of this virus the insertion of the GFP gene had led to the deletion of five tRNAs and the M1 gene coding regions from the wild type MHV-68 genome (Roy, Stewart and Dutia personal communication). Published data on a recombinant MHV-68 virus with deletion of the first four tRNAs and the M1 gene

(Simas *et al.*, 1998) showed that the absence of these genes did not alter the growth patterns *in vitro* nor alter the growth properties and disease pathogenesis *in vivo*. This was confirmed using MHV-68 M1 knockout virus (Clambey *et al.*, 2000). The absence of the M1 gene did not show any significant difference in disease pathogenesis or in the establishment of latency. However this group did observe that the M1 knockout virus had a higher rate of reactivation compared to wild type virus.

LHΔgfp and wild type MHV-68 showed a similar tissue distribution and the LHΔgfp virus was successful in establishing latency in infected animals. The main difference was that the peak levels of latently infected cells in the MLN and spleen using wild type MHV-68 seen during the first two weeks post-infection were not observed in LHΔgfp infected tissues. This means that the five tRNAs and M1 genes could be important in amplifying the numbers of latently infected cells within these tissues. An alternative explanation comes from the work of Clambey *et al* (2000) on the role of the LacZ expression in an M1 knockout virus. They observed decreased levels of latently infected cells in the spleen on day 9 infection of mice infected intraperitoneally, indicating that this region of the genome could have an unknown regulatory function. However it must be considered from these results that the peak levels of latently infected cells is not essential for the establishment of long-term latency in these tissues, indicating that the virus may have alternate pathways not evident from the disease kinetics in successfully establishing latency in the host.

### 5.3.2 LHΔgfp, a useful marker virus

As described in section (5.2), the relatively fewer numbers of latently infected cells in the MLN of MHV-68 infected μMT mice made phenotyping difficult using immunostaining assays or RNA *in-situ* hybridisation techniques. The *in vivo* expression of GFP in virus infected LHΔgfp became a useful tool and helped identify virus infected cells by their GFP expression. There is no evidence from the results of *in vivo* characterisation studies described in the preceding chapters or from previously published data to believe that LHΔgfp would behave any different from the wild type virus in the ability to infect susceptible cell types *in vivo*.

Enriched CD11c cells when viewed under the fluorescence microscope were identified as infected from the diffused pattern of GFP expression. It was also possible to stain the cells with surface antibodies to confirm the cell type. Similarly, stained cells were also used in flow cytometry to determine the percentages of CD11c cells in the MLN of μMT and IFN-α/β $R^{-/-}$ mice that were also expressing GFP. This method was used to determine the percentages of different cell subsets expressing GFP over the time course of infection. Tissue cryosections from the MLN and spleen of LHΔgfp infected mice helped determine the regions where GFP expressing cells localised. However, advanced microdissection techniques may have to be used in future to isolate cells from different regions and determine the specific cell type and differentiation states.

The slight drawback with this marker virus is that the state of infection of these cells cannot be determined from the GFP expression either to be lytic or latent infection. This could be overcome with the generation of antibodies specific to MHV-68 latent proteins e.g. M2, which can be used in conjunction with the above mentioned techniques to differentiate the GFP expression within lytic and latently infected cells.

## 5.4 Pathogenesis of LHΔgfp in IFN-α/β $R^{-/-}$ and WT129 mice

### 5.4.1 Disease pathogenesis in the lung, MLN and spleen

Type 1 interferon has been shown to play a very important regulatory role during virus infections by controlling replication of virus within infected cells and also by inhibiting virus infection in neighbouring cells (Biron, 1998). IFN-α/β $R^{-/-}$ infected with LHΔgfp exhibited a 100 fold higher level of infective virus in the lungs compared to WT129 mice on day 10 post-infection. The higher level of infective virus seen with LHΔgfp is similar to the published data on lung infection in IFN-α/β $R^{-/-}$ mice infected with wild type MHV-68 (Dutia *et al.*, 1999a). The data on MHV-68 infection of IFN-α/β $R^{-/-}$ mice and the IRF $1^{-/-}$ mice deficient of IFN-α/β downstream signalling emphasise the importance of this signalling pathway in regulating MHV-68 infection (Dutia *et al.*, 1999a).

The MLN and spleen tissues from LHΔgfp infected IFN-α/β $R^{-/-}$ mice showed a sudden peak of latently infected cells on day 7 post-infection compared to WT129 mice. The cryosections obtained on day 8 from the spleen show patches of GFP expressing cells were distributed throughout this tissue. The numbers of latently infected cells fall to normal by days 10 and 14 post-infection. This might indicate that at this point other arms of the immune system have taken over the control and elimination of virus from these tissues.

The characterisation studies with LHΔgfp in C57BL/6 mice showed that the virus fails to present peak levels of latent virus two weeks post-infection as observed during wild type MHV-68 infection. However LHΔgfp infection of IFN α/β $R^{-/-}$ mice exhibited disease pathogenesis in the MLN and spleen similar to wild type MHV-68 infection where an increased number of latent virus was seen around day 7 post-infection. This variation in disease kinetics of LHΔgfp infected IFN α/β $R^{-/-}$ mice could be due to an immunomodulatory role played by either the missing vtRNAs or the GFP gene under the CMV promoter. These observations could only be confirmed using targeted rescuant viruses.

The FACS percentages of CD8+ T cells represented in figures 4.16 and 4.18 in the MLN and spleen respectively, might be showing the involvement of these cells in the control of virus. The data clearly shows that on days 10 and 14 compared to days 5 and 7 post-infection; both in the MLN and spleen of IFN-α/β $R^{-/-}$ mice there were increased percentages of CD8+ T cells. This was not the case with WT129 mice, where the CD8+ T cell percentages did not change drastically over the course of infection. However, further experiments are needed to find out whether the increased percentage of CD8+ T cells corresponds to increased levels of MHV-68 specific CTL activity.

### 5.4.2 Reduced lymphadenopathy in IFN-α/β $R^{-/-}$ mice

The IFN-α/β $R^{-/-}$ mice infected with LHΔgfp showed a reduction in lymphadenopathy. When the cell subsets were analysed, a dramatic reduction in the

number of B cells was observed. This effect could not have been due to the deleted genes in LHΔgfp as the WT129 mice showed accumulation of B cells and lymphadenopathy similar to C57BL/6 mice infected with wild type MHV-68 virus. Therefore, the reduction in lymphadenopathy in IFN-α/β $R^{-/-}$ mice could be attributed directly to the absence of IFN-α/β as it has been demonstrated to be a potent cytokine that induces proliferation, recruitment or retention of cells that in turn can lead to lymphadenopathy (Gresser *et al.*, 1981). It is however fascinating that in the MLN of IFN-α/β $R^{-/-}$ mice B cells, in particular, fail to accumulate following LHΔgfp infection. All the factors controlling lymphadenopathy during MHV-68 infection are not fully understood and clearly there are large numbers of contributing factors that need further investigation.

## 5.5 Future work

In both the MLN and spleen of LHΔgfp infected IFN-α/β $R^{-/-}$ and WT129 mice CD4+ and CD8+ cells were found to also express GFP. There has not been any published data on T cells being infected, although there could be low levels of infectivity. A possible explanation for the observation could be that CD4 expression was from myeloid dendritic cells and macrophages while the CD8 expression is by the lymphoid subset of dendritic cells (Pulendran *et al*, 2001, Jenkins *et al.*, 2001). The work on different subtypes of dendritic cells, their lineage and localisation in different compartments of the lymph node are under current research focus in other laboratories. It would be interesting to find out whether some subtypes of dendritic cells are more susceptible to MHV-68 infection which might in turn help discern whether they closely interact with B cells/T cells and transfer virus amongst each other.

*In vitro* work with virus infected dendritic cells has demonstrated that this can lead to either an efficient antigen-presentation and/or immunosuppression due to impairment or depletion of dendritic cells. For example, *in vitro* HSV infected mature dendritic cells were found to have drastically reduced capacity to stimulate T cells (Kruse *et al.*, 2000). They also showed degradation of a maturation marker CD86, although

this study did not address the consequence. In the case of LCMV a mutant clone of the Armstrong strain was found specifically to infect dendritic cells instead of macrophages. It has been shown to bring about immunosuppression in mice infected with this virus by causing degradation of infected dendritic cells (Borrow *et al.*, 1995). The infection of professional antigen-presenting cells such as CD11c+ dendritic cells and F4/80+ macrophages early in the course of MHV-68 infection could mean a careful regulation of cellular events and/or regulation of immune response.

## 5.6 Summary

To summarise, the work described in this thesis has helped identify cellular events that take place in the MLN following MHV-68 infection. It has shown that cell types such as CD11c+ and F4/80+ cells are infected by MHV-68 at this site very early during infection. The work described the *in vivo* characterisation of the GFP expressing recombinant virus, LHΔgfp and has addressed some of the applications of this virus in detecting infected cells. It has also investigated the pathogenesis and cellular tropism of LHΔgfp in IFN-α/β $R^{-/-}$ and WT129 mice.

Cellular events are a key to our understanding of virus infections and their regulation by the host immune response. In the case of MHV-68, work at the single cell level is required to answer some of the cellular events more precisely. It is hoped that the work described in this thesis has shed some light to our current understanding of *in vivo* virus/host interactions during MHV-68 infection.

# BIBLIOGRAPHY

Ahn, K., Gruhler, A., Galocha, B., Jones, T. R., Wiertz, E. J., Ploegh, H. L., Peterson, P. A., Yang, Y. & Fruh, K. (1997). The ER-luminal domain of the HCMV glycoprotein US6 inhibits peptide translocation by TAP. *Immunity* **6**, 613-21.

Ahn, K., Angulo, A., Ghazal, P., Peterson, P. A., Yang, Y. & Fruh, K. (1996). Human cytomegalovirus inhibits antigen presentation by a sequential multistep process. *Proceedings of the National Academy of Sciences USA* **93**, 10990-5.

Ahuja, S. K. & Murphy, P. M. (1993). Molecular piracy of mammalian interleukin-8 receptor type B by herpesvirus saimiri. *Journal of Biological Chemistry* **268**, 20691-4.

Albert, M. L., Sauter, B. & Bhardwaj, N. (1998). Dendritic cells acquire antigen from apoptotic cells and induce class I- restricted CTLs. *Nature* **392**, 86-9.

Allan, W., Tabi, Z., Cleary, A. & Doherty, P. C. (1990). Cellular events in the lymph node and lung of mice with influenza. Consequences of depleting CD4+ T cells. *Journal of Immunology* **144**, 3980-6.

Anagnostopoulos, I., Hummel, M., Kreschel, C. & Stein, H. (1995). Morphology, immunophenotype, and distribution of latently and/or productively Epstein-Barr virus-infected cells in acute infectious mononucleosis: implications for the interindividual infection route of Epstein-Barr virus. *Blood* **85**, 744-50.

Aoki, Y., Yarchoan, R., Wyvill, K., Okamoto, S., Little, R. F. & Tosato, G. (2001). Detection of viral interleukin-6 in Kaposi sarcoma-associated herpesvirus-linked disorders. *Blood* **97**, 2173-6.

Babcock, G. J. & Thorley-Lawson, D. A. (2000a). Tonsillar memory B cells, latently infected with Epstein-Barr virus, express the restricted pattern of latent genes

previously found only in Epstein-Barr virus-associated tumors. *Proceedings of the National Academy of Sciences USA* **97**, 12250-5.

Babcock, J. G., Hochberg, D. & Thorley-Lawson, A. D. (2000b). The expression pattern of Epstein-Barr virus latent genes *in vivo* is dependent upon the differentiation stage of the infected B cell. *Immunity* **13**, 497-506.

Babcock, G. J., Decker, L. L., Volk, M. & Thorley-Lawson, D. A. (1998). EBV persistence in memory B cells *in vivo*. *Immunity* **9**, 395-404.

Bachmann, M. F. & Kopf, M. (1999). The role of B cells in acute and chronic infections. *Current Opinion in Immunology* **11**, 332-9.

Bachmann, M. F. & Zinkernagel, R. M. (1997). Neutralizing antiviral B cell responses. *Annual Reviews of Immunology* **15**, 235-70.

Baer, R., Bankier, A. T., Biggin, M. D., Deininger, P. L., Farrell, P. J., Gibson, T. J., Hatfull, G., Hudson, G. S., Satchwell, S. C., Seguin, C. & et al. (1984). DNA sequence and expression of the B95-8 Epstein-Barr virus genome. *Nature* **310**, 207-11.

Bais, C., Santomasso, B., Coso, O., Arvanitakis, L., Raaka, E. G., Gutkind, J. S., Asch, A. S., Cesarman, E., Gershengorn, M. C., Mesri, E. A. & Gerhengorn, M. C. (1998). G-protein-coupled receptor of Kaposi's sarcoma-associated herpesvirus is a viral oncogene and angiogenesis activator. *Nature* **391**, 86-9.

Banchereau, J. & Steinman, R. M. (1998). Dendritic cells and the control of immunity. *Nature* **392**, 245-52.

Bejarano, M. T. & Masucci, M. G. (1998). Interleukin-10 abrogates the inhibition of Epstein-Barr virus-induced B- cell transformation by memory T-cell responses. *Blood* **92**, 4256-62.

Bellows, D. S., Chau, B. N., Lee, P., Lazebnik, Y., Burns, W. H. & Hardwick, J. M. (2000). Antiapoptotic herpesvirus Bcl-2 homologs escape caspase-mediated conversion to proapoptotic proteins. *Journal of Virology* **74**, 5024-31.

Benschop, R. J. & Cambier, J. C. (1999). B cell development: signal transduction by antigen receptors and their surrogates. *Current Opinion in Immunology* **11**, 143-51.

Bhatt, P. N., Percy, D. H., Craft, J. L. & Jonas, A. M. (1971). Isolation and characterization of a herpeslike (Hsiung-Kaplow) virus from guinea pigs. *Journal of Infectious Diseases* **123**, 178-89.

Biggin, M., Bodescot, M., Perricaudet, M. & Farrell, P. (1987). Epstein-Barr virus gene expression in P3HR1-superinfected Raji cells. *Journal of Virology* **61**, 3120-32.

Biron, C. A. (1999). Initial and innate responses to viral infections--pattern setting in immunity or disease. *Current Opinion in Microbiology* **2**, 374-81.

Biron, C. A. (1998). Role of early cytokines, including alpha and beta interferons (IFN- alpha/beta), in innate and adaptive immune responses to viral infections. *Seminars in Immunology* **10**, 383-90.

Blake, N., Lee, S., Redchenko, I., Thomas, W., Steven, N., Leese, A., Steigerwald-Mullen, P., Kurilla, M. G., Frappier, L. & Rickinson, A. (1997). Human CD8+ T cell responses to EBV EBNA1: HLA class I presentation of the (Gly-Ala)-containing protein requires exogenous processing. *Immunity* **7**, 791-802.

Blakely, G. A., Lourie, B., Morton, W. G., Evans, H. H. & Kaufmann, A. F. (1973). A varicella-like disease in macaque monkeys. *Journal of Infectious Diseases* **127**, 617-25.

Blasig, C., Zietz, C., Haar, B., Neipel, F., Esser, S., Brockmeyer, N. H., Tschachler, E., Colombini, S., Ensoli, B. & Sturzl, M. (1997). Monocytes in Kaposi's sarcoma

lesions are productively infected by human herpesvirus 8. *Journal of Virology* **71**, 7963-8.

Blaskovic, D., Stancekova, M., Svobodova, J. & Mistrikova, J. (1980). Isolation of five strains of herpesviruses from two species of free living small rodents [letter]. *Acta Virologica* **24**, 468.

Bogdan, C. (2000). The function of type I interferons in antimicrobial immunity. *Current Opinion in Immunology* **12**, 419-24.

Borrow, P., Evans, C. F. & Oldstone, M. B. (1995). Virus-induced immunosuppression: immune system-mediated destruction of virus-infected dendritic cells results in generalized immune suppression. *Journal of Virology* **69**, 1059-70.

Bosch, M. L., Harper, E., Schmidt, A., Strand, K. B., Thormahlen, S., Thouless, M. E. & Wang, Y. (1999). Activation *in vivo* of retroperitoneal fibromatosis-associated herpesvirus, a simian homologue of human herpesvirus-8. *Journal of General Virology* **80**, 467-75.

Boshoff, C. & Chang, Y. (2001). Kaposi's sarcoma-associated herpesvirus: a new DNA tumor virus. *Annual Reviews of Medicine* **52**, 453-70.

Boshoff, C. (1998). Kaposi's sarcoma-associated herpesvirus: the 2nd human gammaherpesvirus. *Epstein-Barr Virus Report* **5**, 3-9.

Boshoff, C., Endo, Y., Collins, P. D., Takeuchi, Y., Reeves, J. D., Schweickart, V. L., Siani, M. A., Sasaki, T., Williams, T. J., Gray, P. W., Moore, P. S., Chang, Y. & Weiss, R. A. (1997). Angiogenic and HIV-inhibitory functions of KSHV-encoded chemokines. *Science* **278**, 290-4.

Bowden, R. J., Simas, J. P., Davis, A. J. & Efstathiou, S. (1997). Murine gammaherpesvirus 68 encodes tRNA-like sequences which are expressed during latency. *Journal of General Virology* **78**, 1675-87.

Bridgen, A. & Reid, H. W. (1991). Derivation of a DNA clone corresponding to the viral agent of sheep- associated malignant catarrhal fever. *Research in Veterinary Sciences* **50**, 38-44.

Bridgen, A., Herring, A. J., Inglis, N. F. & Reid, H. W. (1989). Preliminary characterization of the alcelaphine herpesvirus 1 genome. *Journal of General Virology* **70**, 1141-50.

Brousset, P., Cesarman, E., Meggetto, F., Lamant, L. & Delsol, G. (2001). Colocalization of the viral interleukin-6 with latent nuclear antigen-1 of human herpesvirus-8 in endothelial spindle cells of Kaposi's sarcoma and lymphoid cells of multicentric Castleman's disease. *Human Pathology* **32**, 95-100.

Brutkiewicz, R. R. & Welsh, R. M. (1995). Major histocompatibility complex class I antigens and the control of viral infections by natural killer cells. *Journal of Virology* **69**, 3967-71.

Bublot, M., Van Bressem, M. F., Thiry, E., Dubuisson, J. & Pastoret, P. P. (1990). Bovine herpesvirus 4 genome: cloning, mapping and strain variation analysis. *Journal of General Virology* **71**, 133-42.

Burysek, L. & Pitha, P. M. (2001). Latently expressed human herpesvirus 8-encoded interferon regulatory factor 2 inhibits double-stranded RNA-activated protein kinase. *Journal of Virology* **75**, 2345-52.

Callan, M. F., Tan, L., Annels, N., Ogg, G. S., Wilson, J. D., O'Callaghan, C. A., Steven, N., McMichael, A. J. & Rickinson, A. B. (1998). Direct visualization of

antigen-specific CD8+ T cells during the primary immune response to Epstein-Barr virus *in vivo*. *Journal of Experimental Medicine* **187**, 1395-402.

Callan, M. F., Steven, N., Krausa, P., Wilson, J. D., Moss, P. A., Gillespie, G. M., Bell, J. I., Rickinson, A. B. & McMichael, A. J. (1996). Large clonal expansions of CD8+ T cells in acute infectious mononucleosis. *Nature Medicine* **2**, 906-11.

Campbell, J. J. & Butcher, E. C. (2000). Chemokines in tissue-specific and microenvironment-specific lymphocyte homing. *Current Opinion in Immunology* **12**, 336-41.

Campbell, J. J., Hedrick, J., Zlotnik, A., Siani, M. A., Thompson, D. A. & Butcher, E. C. (1998). Chemokines and the arrest of lymphocytes rolling under flow conditions. *Science* **279**, 381-4.

Cardin, R. D., Brooks, J. W., Sarawar, S. R. & Doherty, P. C. (1996). Progressive loss of CD8+ T cell-mediated control of a gamma-herpesvirus in the absence of CD4+ T cells. *Journal of Experimental Medicine* **184**, 863-71.

Carr, J. A., Rogerson, J., Mulqueen, M. J., Roberts, N. A. & Booth, R. F. (1997). Interleukin-12 exhibits potent antiviral activity in experimental herpesvirus infections. *Journal of Virology* **71**, 7799-803.

Cesarman, E., Nador, R. G., Bai, F., Bohenzky, R. A., Russo, J. J., Moore, P. S., Chang, Y. & Knowles, D. M. (1996). Kaposi's sarcoma-associated herpesvirus contains G protein-coupled receptor and cyclin D homologs which are expressed in Kaposi's sarcoma and malignant lymphoma. *Journal of Virology* **70**, 8218-23.

Cesarman, E., Chang, Y., Moore, P. S., Said, J. W. & Knowles, D. M. (1995). Kaposi's sarcoma-associated herpesvirus-like DNA sequences in AIDS- related body-cavity-based lymphomas. *New England Journal of Medicine* **332**, 1186-91.

Chang, Y., Moore, P. S., Talbot, S. J., Boshoff, C. H., Zarkowska, T., Godden, K., Paterson, H., Weiss, R. A. & Mittnacht, S. (1996). Cyclin encoded by KS herpesvirus. *Nature* **382**, 410.

Chang, Y., Cesarman, E., Pessin, M. S., Lee, F., Culpepper, J., Knowles, D. M. & Moore, P. S. (1994). Identification of herpesvirus-like DNA sequences in AIDS-associated Kaposi's sarcoma. *Science* **266**, 1865-9.

Chastel, C., Beaucournu, J. P., Chastel, O., Legrand, M. C. & Le Goff, F. (1994). A herpesvirus from an European shrew (Crocidura russula). *Acta Virologica* **38**, 309.

Cheng, E. H., Nicholas, J., Bellows, D. S., Hayward, G. S., Guo, H. G., Reitz, M. S. & Hardwick, J. M. (1997). A Bcl-2 homolog encoded by Kaposi sarcoma-associated virus, human herpesvirus 8, inhibits apoptosis but does not heterodimerize with Bax or Bak. *Proceedings of the National Academy of Sciences USA* **94**, 690-4.

Chmielewicz, B., Goltz, M. & Ehlers, B. (2001). Detection and multigenic characterization of a novel gammaherpesvirus in goats. *Virus Research* **75**, 87-94.

Christensen, J. P., Cardin, R. D., Branum, K. C. & Doherty, P. C. (1999). CD4(+) T cell-mediated control of a gamma-herpesvirus in B cell- deficient mice is mediated by IFN-gamma. *Proceedings of the National Academy of Sciences USA* **96**, 5135-40.

Christensen, J. P. & Doherty, P. C. (1999). Quantitative analysis of the acute and long-term CD4(+) T-cell response to a persistent gammaherpesvirus. *Journal of Virology* **73**, 4279-83.

Clambey, E. T., Virgin, H. W. t. & Speck, S. H. (2000). Disruption of the murine gammaherpesvirus 68 M1 open reading frame leads to enhanced reactivation from latency. *Journal of Virology* **74**, 1973-84.

Clark, E. A. & Lane, P. J. (1991). Regulation of human B-cell activation and adhesion. *Annual Reviews of Immunology* **9**, 97-127.

Cobbold, S. P., Jayasuriya, A., Nash, A., Prospero, T. D. & Waldmann, H. (1984). Therapy with monoclonal antibodies by elimination of T-cell subsets *in vivo*. *Nature* **312**, 548-51.

Coffman, R. L. & Weissman, I. L. (1981). B220: a B cell-specific member of th T200 glycoprotein family. *Nature* **289**, 681-3.

Cohen, J. I., Wang, F., Mannick, J. & Kieff, E. (1989). Epstein-Barr virus nuclear protein 2 is a key determinant of lymphocyte transformation. *Proceedings of the National Academy of Sciences USA* **86**, 9558-62.

Coscoy, L. & Ganem, D. (2000). Kaposi's sarcoma-associated herpesvirus encodes two proteins that block cell surface display of MHC class I chains by enhancing their endocytosis. *Proceedings of the National Academy of Sciences USA* **97**, 8051-6.

Crouch, E., Hartshorn, K. & Ofek, I. (2000). Collectins and pulmonary innate immunity. *Immunological Reviews* **173**, 52-65.

Deinhardt, F., Falk, L. A. & Wolfe, L. G. (1973). Simian herpesviruses. *Cancer Research* **33**, 1424-6.

Desrosiers, R. C., Sasseville, V. G., Czajak, S. C., Zhang, X., Mansfield, K. G., Kaur, A., Johnson, R. P., Lackner, A. A. & Jung, J. U. (1997). A herpesvirus of rhesus monkeys related to the human Kaposi's sarcoma- associated herpesvirus. *Journal of Virology* **71**, 9764-9.

Dittmer, D., Lagunoff, M., Renne, R., Staskus, K., Haase, A. & Ganem, D. (1998). A cluster of latently expressed genes in Kaposi's sarcoma-associated herpesvirus. *Journal of Virology* **72**, 8309-15.

Djerbi, M., Screpanti, V., Catrina, A. I., Bogen, B., Biberfeld, P. & Grandien, A. (1999). The inhibitor of death receptor signaling, FLICE-inhibitory protein defines a new class of tumor progression factors. *Journal of Experimental Medicine* **190**, 1025-32.

Doherty, P. C., Christensen, J. P., Belz, G. T., Stevenson, P. G. & Sangster, M. Y. (2001). Dissecting the host response to a gamma-herpesvirus. *Philos Trans R Soc Lond B Biol Sci* **356**, 581-93.

Doherty, P. C., Hamilton-Easton, A. M., Topham, D. J., Riberdy, J., Brooks, J. W. & Cardin, R. D. (1997). Consequences of viral infections for lymphocyte compartmentalization and homeostasis. *Seminars in Immunology* **9**, 365-73.

Dubin, G., Socolof, E., Frank, I. & Friedman, H. M. (1991). Herpes simplex virus type 1 Fc receptor protects infected cells from antibody-dependent cellular cytotoxicity. *Journal of Virology* **65**, 7046-50.

Dutia, B. M., Allen, D. J., Dyson, H. & Nash, A. A. (1999a). Type I interferons and IRF-1 play a critical role in the control of a gammaherpesvirus infection. *Virology* **261**, 173-9.

Dutia, B. M., Stewart, J. P., Clayton, R. A., Dyson, H. & Nash, A. A. (1999b). Kinetic and phenotypic changes in murine lymphocytes infected with murine gammaherpesvirus-68 *in vitro*. *Journal of General Virology* **80**, 2729-36.

Dutia, B. M., Clarke, C. J., Allen, D. J. & Nash, A. A. (1997). Pathological changes in the spleens of gamma interferon receptor- deficient mice infected with murine gammaherpesvirus: a role for CD8 T cells. *Journal of Virology* **71**, 4278-83.

Ebrahimi, B., Dutia, B. M., Brownstein, D. G. & Nash, A. A. (2001). Murine gammaherpesvirus-68 infection causes multi-organ fibrosis and alters leukocyte

trafficking in interferon-γ receptor knockout mice. *American Journal of Pathology* **158**, 2117-2125.

Efstathiou, S., Ho, Y. M., Hall, S., Styles, C. J., Scott, S. D. & Gompels, U. A. (1990a). Murine herpesvirus 68 is genetically related to the gammaherpesviruses Epstein-Barr virus and herpesvirus saimiri. *Journal of General Virology* **71**, 1365-72.

Efstathiou, S., Ho, Y. M. & Minson, A. C. (1990b). Cloning and molecular characterization of the murine herpesvirus 68 genome. *Journal of General Virology* **71**, 1355-64.

Eggleton, P. & Reid, K. B. (1999). Lung surfactant proteins involved in innate immunity. *Current Opinion in Immunology* **11**, 28-33.

Ehlers, B., Ulrich, S. & Goltz, M. (1999). Detection of two novel porcine herpesviruses with high similarity to gammaherpesviruses. *Journal of General Virology* **80**, 971-8.

Ehrlich, R. (1997). Modulation of antigen processing and presentation by persistent virus infections and in tumors. *Human Immunology* **54**, 104-16.

Ehtisham, S., Sunil-Chandra, N. P. & Nash, A. A. (1993). Pathogenesis of murine gammaherpesvirus infection in mice deficient in CD4 and CD8 T cells. *Journal of Virology* **67**, 5247-52.

Ellis, M., Chew, Y. P., Fallis, L., Freddersdorf, S., Boshoff, C., Weiss, R. A., Lu, X. & Mittnacht, S. (1999). Degradation of p27(Kip) cdk inhibitor triggered by Kaposi's sarcoma virus cyclin-cdk6 complex. *The Embo Journal* **18**, 644-53.

Epstein, M. A. & Crawford, D. H. (1998). Gammaherpesviruses: Epstein-Barr virus. In Topley and Wilson's Microbiology and microbial infections, 9 edn, pp 352-366. Edited by L. Collier, A. Bakows & M. Sussman. London: Arnold.

Farrell, H. E., Vally, H., Lynch, D. M., Fleming, P., Shellam, G. R., Scalzo, A. A. & Davis-Poynter, N. J. (1997). Inhibition of natural killer cells by a cytomegalovirus MHC class I homologue *in vivo*. *Nature* **386**, 510-4.

Faulkner, G. C., Krajewski, A. S. & Crawford, D. H. (2000). The ins and outs of EBV infection. *Trends in Microbiology* **8**, 185-9.

Faulkner, G. C., Burrows, S. R., Khanna, R., Moss, D. J., Bird, A. G. & Crawford, D. H. (1999). X-Linked agammaglobulinemia patients are not infected with Epstein-Barr virus: implications for the biology of the virus. *Journal of Virology* **73**, 1555-64.

Fernandez, E. J., Wilken, J., Thompson, D. A., Peiper, S. C. & Lolis, E. (2000). Comparison of the structure of vMIP-II with eotaxin-1, RANTES, and MCP- 3 suggests a unique mechanism for CCR3 activation. *Biochemistry* **39**, 12837-44.

Flano, E., Husain, S. M., Sample, J. T., Woodland, D. L. & Blackman, M. A. (2000). Latent murine gamma-herpesvirus infection is established in activated B cells, dendritic cells, and macrophages. *Journal of Immunology* **165**, 1074-81.

Fortunato, E. A., McElroy, A. K., Sanchez, I. & Spector, D. H. (2000). Exploitation of cellular signaling and regulatory pathways by human cytomegalovirus. *Trends in Microbiology* **8**, 111-9.

Freitas, A. A. & Rocha, B. (1999). Peripheral T cell survival. *Current Opinion in Immunology* **11**, 152-6.

Fruh, K., Ahn, K., Djaballah, H., Sempe, P., van Endert, P. M., Tampe, R., Peterson, P. A. & Yang, Y. (1995). A viral inhibitor of peptide transporters for antigen presentation. *Nature* **375**, 415-8.

Fujioka, N., Akazawa, R., Ohashi, K., Fujii, M., Ikeda, M. & Kurimoto, M. (1999). Interleukin-18 protects mice against acute herpes simplex virus type 1 infection. *Journal of Virology* **73**, 2401-9.

Geijtenbeek, T. B., Kwon, D. S., Torensma, R., van Vliet, S. J., van Duijnhoven, G. C., Middel, J., Cornelissen, I. L., Nottet, H. S., KewalRamani, V. N., Littman, D. R., Figdor, C. G. & van Kooyk, Y. (2000). DC-SIGN, a dendritic cell-specific HIV-1-binding protein that enhances *trans*-infection of T cells. *Cell* **100**, 587-97.

Gidlund, M., Orn, A., Wigzell, H., Senik, A. & Gresser, I. (1978). Enhanced NK cell activity in mice injected with interferon and interferon inducers. *Nature* **273**, 759-61.

Gilbert, M. J., Riddell, S. R., Plachter, B. & Greenberg, P. D. (1996). Cytomegalovirus selectively blocks antigen processing and presentation of its immediate-early gene product. *Nature* **383**, 720-2.

Godden-Kent, D., Talbot, S. J., Boshoff, C., Chang, Y., Moore, P., Weiss, R. A. & Mittnacht, S. (1997). The cyclin encoded by Kaposi's sarcoma-associated herpesvirus stimulates cdk6 to phosphorylate the retinoblastoma protein and histone H1. *Journal of Virology* **71**, 4193-8.

Greensill, J., Sheldon, J. A., Renwick, N. M., Beer, B. E., Norley, S., Goudsmit, J. & Schulz, T. F. (2000). Two distinct gamma-2 herpesviruses in African green monkeys: a second gamma-2 herpesvirus lineage among old world primates? *Journal of Virology* **74**, 1572-7.

Gresser, I., Guy-Grand, D., Maury, C. & Maunoury, M. T. (1981). Interferon induces peripheral lymphadenopathy in mice. *Journal of Immunology* **127**, 1569-75.

Hamilton-Easton, A. & Eichelberger, M. (1995). Virus-specific antigen presentation by different subsets of cells from lung and mediastinal lymph node tissues of influenza virus-infected mice. *Journal of Virology* **69**, 6359-66.

Hammerschmidt, W. & Sugden, B. (1989). Genetic analysis of immortalizing functions of Epstein-Barr virus in human B lymphocytes. *Nature* **340**, 393-7.

Harder, T. C., Harder, M., Vos, H., Kulonen, K., Kennedy-Stoskopf, S., Liess, B., Appel, M. J. & Osterhaus, A. D. (1996). Characterization of phocid herpesvirus-1 and -2 as putative alpha- and gammaherpesviruses of North American and European pinnipeds. *Journal of General Virology* **77**, 27-35.

Hardwick, J. M., Lieberman, P. M. & Hayward, S. D. (1988). A new Epstein-Barr virus transactivator, R, induces expression of a cytoplasmic early antigen. *Journal of Virology* **62**, 2274-84.

Hardy, R. R. & Hayakawa, K. (2001). B cell development pathways. *Annual Reviews of Immunology* **19**, 595-621.

Harris, N., Buller, R. M. & Karupiah, G. (1995). Gamma interferon-induced, nitric oxide-mediated inhibition of vaccinia virus replication. *Journal of Virology* **69**, 910-5.

Heise, M. T. & Virgin, H. W. t. (1995). The T-cell-independent role of gamma interferon and tumor necrosis factor alpha in macrophage activation during murine cytomegalovirus and herpes simplex virus infections. *Journal of Virology* **69**, 904-9.

Heller, M., Gerber, P. & Kieff, E. (1982). DNA of herpesvirus pan, a third member of the Epstein-Barr virus- Herpesvirus papio group. *Journal of Virology* **41**, 931-9.

Heller, M. & Kieff, E. (1981). Colinearity between the DNAs of Epstein-Barr virus and herpesvirus papio. *Journal of Virology* **37**, 821-6.

Henderson, S., Huen, D., Rowe, M., Dawson, C., Johnson, G. & Rickinson, A. (1993). Epstein-Barr virus-coded BHRF1 protein, a viral homologue of Bcl-2,

protects human B cells from programmed cell death. *Proceedings of the National Academy of Sciences USA* **90**, 8479-83.

Henle, W., Henle, G., Andersson, J., Ernberg, I., Klein, G., Horwitz, C. A., Marklund, G., Rymo, L., Wellinder, C. & Straus, S. E. (1987). Antibody responses to Epstein-Barr virus-determined nuclear antigen (EBNA)-1 and EBNA-2 in acute and chronic Epstein-Barr virus infection. *Proceedings of the National Academy of Sciences USA* **84**, 570-4.

Hill, A., Jugovic, P., York, I., Russ, G., Bennink, J., Yewdell, J., Ploegh, H. & Johnson, D. (1995). Herpes simplex virus turns off the TAP to evade host immunity. *Nature* **375**, 411-5.

Hinze, H. C. (1971). Induction of lymphoid hyperplasia and lymphoma-like disease in rabbits by Herpesvirus sylvilagus. *International Journal of Cancer* **8**, 514-22.

Honess, R. W. & Roizman, B. (1974). Regulation of herpesvirus macromolecular synthesis. I. Cascade regulation of the synthesis of three groups of viral proteins. *Journal of Virology* **14**, 8-19.

Hsu, D. H., de Waal Malefyt, R., Fiorentino, D. F., Dang, M. N., Vieira, P., de Vries, J., Spits, H., Mosmann, T. R. & Moore, K. W. (1990). Expression of interleukin-10 activity by Epstein-Barr virus protein BCRF1. *Science* **250**, 830-2.

Husain, S. M., Usherwood, E. J., Dyson, H., Coleclough, C., Coppola, M. A., Woodland, D. L., Blackman, M. A., Stewart, J. P. & Sample, J. T. (1999). Murine gammaherpesvirus M2 gene is latency-associated and its protein a target for CD8(+) T lymphocytes. *Proceedings of the National Academy of Sciences USA* **96**, 7508-13.

Ishido, S., Choi, J. K., Lee, B. S., Wang, C., DeMaria, M., Johnson, R. P., Cohen, G. B. & Jung, J. U. (2000). Inhibition of natural killer cell-mediated cytotoxicity by Kaposi's sarcoma-associated herpesvirus K5 protein. *Immunity* **13**, 365-74.

Jenkins, M. K., Khoruts, A., Ingulli, E., Mueller, D. L., McSorley, S. J., Reinhardt, R. L., Itano, A. & Pape, K. A. (2001). *In vivo* activation of antigen-specific CD4 T cells. *Annual Reviews of Immunology* **19**, 23-45.

Karre, K. & Welsh, R. M. (1997). Viral decoy vetoes killer cell. *Nature* **386**, 446-7.

Kaye, K. M., Izumi, K. M. & Kieff, E. (1993). Epstein-Barr virus latent membrane protein 1 is essential for B- lymphocyte growth transformation. *Proceedings of the National Academy of Sciences USA* **90**, 9150-4.

Kieff, E. (1996). Epstein-barr virus and its replication. In Fileds Virology, 3 edn, pp. 2343-2396. Edited by B. N. Fields, D. M. Knipe & P. M. Howley. Philadelphia. Lippincott-Raven Publishers.

Kempkes, B., Spitkovsky, D., Jansen-Durr, P., Ellwart, J. W., Kremmer, E., Delecluse, H. J., Rottenberger, C., Bornkamm, G. W. & Hammerschmidt, W. (1995). B-cell proliferation and induction of early G1-regulating proteins by Epstein-Barr virus mutants conditional for EBNA2. *The Embo Journal* **14**, 88-96.

Khanna, R., Burrows, S. R., Moss, D. J. & Silins, S. L. (1996). Peptide transporter (TAP-1 and TAP-2)-independent endogenous processing of Epstein-Barr virus (EBV) latent membrane protein 2A: implications for cytotoxic T-lymphocyte control of EBV-associated malignancies. *Journal of Virology* **70**, 5357-62.

Khanna, R., Burrows, S. R., Kurilla, M. G., Jacob, C. A., Misko, I. S., Sculley, T. B., Kieff, E. & Moss, D. J. (1992). Localization of Epstein-Barr virus cytotoxic T cell epitopes using recombinant vaccinia: implications for vaccine development. *Journal of Experimental Medicine* **176**, 169-76.

Kitamura, D., Roes, J., Kuhn, R. & Rajewsky, K. (1991). A B cell-deficient mouse by targeted disruption of the membrane exon of the immunoglobulin mu chain gene. *Nature* **350**, 423-6.

Kledal, T. N., Rosenkilde, M. M., Coulin, F., Simmons, G., Johnsen, A. H., Alouani, S., Power, C. A., Luttichau, H. R., Gerstoft, J., Clapham, P. R., Clark-Lewis, I., Wells, T. N. & Schwartz, T. W. (1997). A broad-spectrum chemokine antagonist encoded by Kaposi's sarcoma- associated herpesvirus. *Science* **277**, 1656-9.

Kleijnen, M. F., Huppa, J. B., Lucin, P., Mukherjee, S., Farrell, H., Campbell, A. E., Koszinowski, U. H., Hill, A. B. & Ploegh, H. L. (1997). A mouse cytomegalovirus glycoprotein, gp34, forms a complex with folded class I MHC molecules in the ER which is not retained but is transported to the cell surface. *The Embo Journal* **16**, 685-94.

Knight, S. C. & Patterson, S. (1997). Bone marrow-derived dendritic cells, infection with human immunodeficiency virus, and immunopathology. *Annual Reviews of Immunology* **15**, 593-615.

Koppelman, B., Neefjes, J. J., de Vries, J. E. & de Waal Malefyt, R. (1997). Interleukin-10 down-regulates MHC class II alphabeta peptide complexes at the plasma membrane of monocytes by affecting arrival and recycling. *Immunity* **7**, 861-71.

Kotwal, G. J. (2000). Poxviral mimicry of complement and chemokine system components: what's the end game? *Immunology Today* **21**, 242-8.

Kraal, G., Breel, M., Janse, M. & Bruin, G. (1986). Langerhans' cells, veiled cells, and interdigitating cells in the mouse recognized by a monoclonal antibody. *Journal of Experimental Medicine* **163**, 981-97.

Kruse, M., Rosorius, O., Kratzer, F., Stelz, G., Kuhnt, C., Schuler, G., Hauber, J. & Steinkasserer, A. (2000). Mature dendritic cells infected with herpes simplex virus type 1 exhibit inhibited T-cell stimulatory capacity. *Journal of Virology* **74**, 7127-36.

Kulkarni, A. B., Holmes, K. L., Fredrickson, T. N., Hartley, J. W. & Morse, H. C. (1997). Characteristics of a murine gammaherpesvirus infection immunocompromised mice. *In Vivo* **11**, 281-91.

Kurth, J., Spieker, T., Wustrow, J., Strickler, G. J., Hansmann, L. M., Rajewsky, K. & Kuppers, R. (2000). EBV-infected B cells in infectious mononucleosis: viral strategies for spreading in the B cell compartment and establishing latency. *Immunity* **13**, 485-95.

Lacoste, V., Mauclere, P., Dubreuil, G., Lewis, J., Georges-Courbot, M. C. & Gessain, A. (2000). KSHV-like herpesviruses in chimps and gorillas. *Nature* **407**, 151-2.

Lalani, A. S., Barrett, J. W. & McFadden, G. (2000). Modulating chemokines: more lessons from viruses. *Immunology Today* **21**, 100-6.

Lambris, J. D., Reid, K. B. & Volanakis, J. E. (1999). The evolution, structure, biology and pathophysiology of complement. *Immunology Today* **20**, 207-11.

Lane, P. J. & Brocker, T. (1999). Developmental regulation of dendritic cell function. *Current Opinion in Immunology* **11**, 308-13.

Leenen, P. J., Radosevic, K., Voerman, J. S., Salomon, B., van Rooijen, N., Klatzmann, D. & van Ewijk, W. (1998). Heterogeneity of mouse spleen dendritic cells: *in vivo* phagocytic activity, expression of macrophage markers, and subpopulation turnover. *Journal of Immunology* **160**, 2166-73.

Levitskaya, J., Coram, M., Levitsky, V., Imreh, S., Steigerwald-Mullen, P. M., Klein, G., Kurilla, M. G. & Masucci, M. G. (1995). Inhibition of antigen processing by the internal repeat region of the Epstein-Barr virus nuclear antigen-1. *Nature* **375**, 685-8.

Li, H., Keller, J., Knowles, D. P. & Crawford, T. B. (2001a). Recognition of another member of the malignant catarrhal fever virus group: an endemic gammaherpesvirus in domestic goats. *Journal of General Virology* **82**, 227-32.

Li, H., Wang, H. & Nicholas, J. (2001b). Detection of direct binding of human herpesvirus 8-encoded interleukin- 6 (vIL-6) to both gp130 and IL-6 receptor (IL-6R) and identification of amino acid residues of vIL-6 important for IL-6R-dependent and - independent signaling. *Journal of Virology* **75**, 3325-34.

Lindahl, G., Sjobring, U. & Johnsson, E. (2000). Human complement regulators: a major target for pathogenic microorganisms. *Current Opinion in Immunology* **12**, 44-51.

Lubyova, B. & Pitha, P. M. (2000). Characterization of a novel human herpesvirus 8-encoded protein, vIRF- 3, that shows homology to viral and cellular interferon regulatory factors. *Journal of Virology* **74**, 8194-201.

Lupu-Meiri, M., Silver, R. B., Simons, A. H., Gershengorn, M. C. & Oron, Y. (2001). Constitutive signaling by Kaposi's sarcoma-associated herpesvirus G-protein-coupled receptor desensitizes calcium mobilization by other receptors. *Journal of Biological Chemistry* **276**, 7122-8.

MacDonald, G. H. & Johnston, R. E. (2000). Role of dendritic cell targeting in Venezuelan equine encephalitis virus pathogenesis. *Journal of Virology* **74**, 914-22.

Mantovani, A. (1999). The chemokine system: redundancy for robust outputs. *Immunology Today* **20**, 254-7.

Marshall, W. L., Yim, C., Gustafson, E., Graf, T., Sage, D. R., Hanify, K., Williams, L., Fingeroth, J. & Finberg, R. W. (1999). Epstein-Barr virus encodes a novel homolog of the bcl-2 oncogene that inhibits apoptosis and associates with Bax and Bak. *Journal of Virology* **73**, 5181-5.

Masurier, C., Salomon, B., Guettari, N., Pioche, C., Lachapelle, F., Guigon, M. & Klatzmann, D. (1998). Dendritic cells route human immunodeficiency virus to lymph nodes after vaginal or intravenous administration to mice. *Journal of Virology* **72**, 7822-9.

McHeyzer-Williams, M. G. & Ahmed, R. (1999). B cell memory and the long-lived plasma cell. *Current Opinion in Immunology* **11**, 172-9.

McWilliam, A. S., Marsh, A. M. & Holt, P. G. (1997). Inflammatory infiltration of the upper airway epithelium during Sendai virus infection: involvement of epithelial dendritic cells. *Journal of Virology* **71**, 226-36.

Medzhitov, R. & Janeway, C. A., Jr. (1998). Innate immune recognition and control of adaptive immune responses. *Seminars in Immunology* **10**, 351-3.

Meinl, E., Fickenscher, H., Thome, M., Tschopp, J. & Fleckenstein, B. (1998). Anti-apoptotic strategies of lymphotropic viruses. *Immunology Today* **19**, 474-9.

Miller, C. J. & Hu, J. (1999). T cell-tropic simian immunodeficiency virus (SIV) and simian-human immunodeficiency viruses are readily transmitted by vaginal inoculation of rhesus macaques, and Langerhans' cells of the female genital tract are infected with SIV. *Journal of Infectious Diseases* **179 Suppl 3**, S413-7.

Miller, C. L., Burkhardt, A. L., Lee, J. H., Stealey, B., Longnecker, R., Bolen, J. B. & Kieff, E. (1995). Integral membrane protein 2 of Epstein-Barr virus regulates reactivation from latency through dominant negative effects on protein- tyrosine kinases. *Immunity* **2**, 155-66.

Miller, D. M. & Sedmak, D. D. (1999). Viral effects on antigen processing. *Current Opinion in Immunology* **11**, 94-9.

Miyashita, E. M., Yang, B., Babcock, G. J. & Thorley-Lawson, D. A. (1997). Identification of the site of Epstein-Barr virus persistence *in vivo* as a resting B cell. *Journal of Virology* **71**, 4882-91.

Miyashita, E. M., Yang, B., Lam, K. M., Crawford, D. H. & Thorley-Lawson, D. A. (1995). A novel form of Epstein-Barr virus latency in normal B cells *in vivo*. *Cell* **80**, 593-601.

Moore, P. S., Boshoff, C., Weiss, R. A. & Chang, Y. (1996a). Molecular mimicry of human cytokine and cytokine response pathway genes by KSHV. *Science* **274**, 1739-44.

Moore, P. S., Gao, S. J., Dominguez, G., Cesarman, E., Lungu, O., Knowles, D. M., Garber, R., Pellett, P. E., McGeoch, D. J. & Chang, Y. (1996b). Primary characterization of a herpesvirus agent associated with Kaposi's sarcomae. *Journal of Virology* **70**, 549-58.

Moreau, J. L., Nabholz, M., Diamantstein, T., Malek, T., Shevach, E. & Theze, J. (1987). Monoclonal antibodies identify three epitope clusters on the mouse p55 subunit of the interleukin 2 receptor: relationship to the interleukin 2-binding site. *European Journal of Immunology* **17**, 929-35.

Muller, U., Steinhoff, U., Reis, L. F., Hemmi, S., Pavlovic, J., Zinkernagel, R. M. & Aguet, M. (1994). Functional role of type I and type II interferons in antiviral defence. *Science* **264**, 1918-21.

Murali-Krishna, K., Altman, J. D., Suresh, M., Sourdive, D. J., Zajac, A. J., Miller, J. D., Slansky, J. & Ahmed, R. (1998). Counting antigen-specific CD8 T cells: a reevaluation of bystander activation during viral infection. *Immunity* **8**, 177-87.

Murray, R. J., Kurilla, M. G., Brooks, J. M., Thomas, W. A., Rowe, M., Kieff, E. & Rickinson, A. B. (1992). Identification of target antigens for the human cytotoxic T

cell response to Epstein-Barr virus (EBV): implications for the immune control of EBV-positive malignancies. *Journal of Experimental Medicine* **176**, 157-68.

Nash, A. A., Dutia, B. M., Stewart, J. P. & Davison, A. J. (2001). Natural history of murine gamma-herpesvirus infection. *Philos Trans R Soc Lond B Biol Sci* **356**, 569-79.

Nash, A. A. & Usherwood, E. J. (1998). The immune response to viral infections. In Topley and Wilson's Microbiology and Microbial Infections, 9 edn, pp 352-366. Edited by L. Collier, A. Bakows & M. Sussman. London: Arnold.

Nash, A. A. & Cambouropoulos, P. (1993). The immune response to Herpes Simple virus. *Seminars in Virology* **4**, 181-186.

Nemerow, G. R., Mold, C., Schwend, V. K., Tollefson, V. & Cooper, N. R. (1987). Identification of gp350 as the viral glycoprotein mediating attachment of Epstein-Barr virus (EBV) to the EBV/C3d receptor of B cells: sequence homology of gp350 and C3 complement fragment C3d. *Journal of Virology* **61**, 1416-20.

Neubauer, R. H., Rabin, H., Strnad, B. C., Nonoyama, M. & Nelson-Rees, W. A. (1979). Establishment of a lymphoblastoid cell line and isolation of an Epstein- Barr-related virus of gorilla origin. *Journal of Virology* **31**, 845-8.

Nicholas, J., Ruvolo, V., Zong, J., Ciufo, D., Guo, H. G., Reitz, M. S. & Hayward, G. S. (1997a). A single 13-kilobase divergent locus in the Kaposi sarcoma-associated herpesvirus (human herpesvirus 8) genome contains nine open reading frames that are homologous to or related to cellular proteins. *Journal of Virology* **71**, 1963-74.

Nicholas, J., Ruvolo, V. R., Burns, W. H., Sandford, G., Wan, X., Ciufo, D., Hendrickson, S. B., Guo, H. G., Hayward, G. S. & Reitz, M. S. (1997b). Kaposi's sarcoma-associated human herpesvirus-8 encodes homologues of macrophage inflammatory protein-1 and interleukin-6. *Nature Medicine* **3**, 287-92.

Nicholas, J., Cameron, K. R. & Honess, R. W. (1992). Herpesvirus saimiri encodes homologues of G protein-coupled receptors and cyclins. *Nature* **355**, 362-5.

Ochsenbein, A. F., Fehr, T., Lutz, C., Suter, M., Brombacher, F., Hengartner, H. & Zinkernagel, R. M. (1999). Control of early viral and bacterial distribution and disease by natural antibodies. *Science* **286**, 2156-9.

Ojala, P. M., Yamamoto, K., Castanos-Velez, E., Biberfeld, P., Korsmeyer, S. J. & Makela, T. P. (2000). The apoptotic v-cyclin-CDK6 complex phosphorylates and inactivates Bcl- 2. *Nature Cell Biology* **2**, 819-25.

Parry, C. M., Simas, J. P., Smith, V. P., Stewart, C. A., Minson, A. C., Efstathiou, S. & Alcami, A. (2000). A broad spectrum secreted chemokine binding protein encoded by a herpesvirus. *Journal of Experimental Medicine* **191**, 573-8.

Ploegh, H. L. (1998). Viral strategies of immune evasion. *Science* **280**, 248-53.

Price, D. A., Klenerman, P., Booth, B. L., Phillips, R. E. & Sewell, A. K. (1999). Cytotoxic T lymphocytes, chemokines and antiviral immunity. *Immunology Today* **20**, 212-6.

Pulendran, B., Banchereau, J., Maraskovsky, E. & Maliszewski, C. (2001). Modulating the immune response with dendritic cells and their growth factors. *Trends in Immunology* **22**, 41-7.

Rangan, S. R., Martin, L. N., Bozelka, B. E., Wang, N. & Gormus, B. J. (1986). Epstein-Barr virus-related herpesvirus from a rhesus monkey (Macaca mulatta) with malignant lymphoma. *International Journal of Cancer* **38**, 425-32.

Rasheed, S., Rongey, R. W., Bruszweski, J., Nelson-Rees, W. A., Rabin, H., Neubauer, R. H., Esra, G. & Gardner, M. B. (1977). Establishment of a cell line with associated Epstein-Barr-like virus from a leukemic orangutan. *Science* **198**, 407-9.

Ravetch, J. V. & Kinet, J. P. (1991). Fc receptors. *Annual Reviews of Immunology* **9**, 457-92.

Reddehase, M. J. (2000). The immunogenicity of human and murine cytomegaloviruses. *Current Opinion in Immunology* **12**, 738.

Reid, H. W. & Rowe, L. (1973). The attenuation of a herpes virus (malignant catarrhal fever virus) isolated from hartebeest (Alcelaphus buselaphus cokei Gunther). *Research in Veterinary Science* **15**, 144-6.

Renne, R., Zhong, W., Herndier, B., McGrath, M., Abbey, N., Kedes, D. & Ganem, D. (1996). Lytic growth of Kaposi's sarcoma-associated herpesvirus (human herpesvirus 8) in culture. *Nature Medicine* **2**, 342-6.

Reusch, U., Muranyi, W., Lucin, P., Burgert, H. G., Hengel, H. & Koszinowski, U. H. (1999). A cytomegalovirus glycoprotein re-routes MHC class I complexes to lysosomes for degradation. *The Embo Journal* **18**, 1081-91.

Reyburn, H. T., Mandelboim, O., Vales-Gomez, M., Davis, D. M., Pazmany, L. & Strominger, J. L. (1997). The class I MHC homologue of human cytomegalovirus inhibits attack by natural killer cells. *Nature* **386**, 514-7.

Rickinson, A. B & Keiff, E. (1996). Epstein-Barr virus. In Field's Virology, 3 edn, pp. 2397-2446. Edited by B.N.Fields, D.M.Knipe & P.M.Howley. Philadelphia: Lippincott-Raven Publishers.

Rickinson, A. B. & Moss, D. J. (1997). Human cytotoxic T lymphocyte responses to Epstein-Barr virus infection. *Annual Reviews of Immunology* **15**, 405-31.

Roberts, M. L., Luxembourg, A. T. & Cooper, N. R. (1996). Epstein-Barr virus binding to CD21, the virus receptor, activates resting B cells via an intracellular pathway that is linked to B cell infection. *Journal of General Virology* **77**, 3077-85.

Robertson, K. A., Usherwood, E. J. & Nash, A. A. (2001). Regression of a Murine gammaherpesvirus 68-positive B-cell lymphoma mediated by CD4 T lymphocytes. *Journal of Virology* **75**, 3480-3482.

Robertson, K. D. & Ambinder, R. F. (1997). Methylation of the Epstein-Barr virus genome in normal lymphocytes. *Blood* **90**, 4480-4.

Rogoczy, T., Heston, L. & Miller, G. (1998). The Epstein-Barr virus Rta protein activates lytic cycle genes and can disrupt latency in B lymphocytes. *Journal of Virology* **72**, 7978-7984.

Roizmann, B., Desrosiers, R. C., Fleckenstein, B., Lopez, C., Minson, A. C. & Studdert, M. J. (1992). The family Herpesviridae: an update. The Herpesvirus Study Group of the International Committee on Taxonomy of Viruses. *Archives in Virology* **123**, 425-49.

Rose, T. M., Strand, K. B., Schultz, E. R., Schaefer, G., Rankin, G. W., Jr., Thouless, M. E., Tsai, C. C. & Bosch, M. L. (1997). Identification of two homologs of the Kaposi's sarcoma-associated herpesvirus (human herpesvirus 8) in retroperitoneal fibromatosis of different macaque species. *Journal of Virology* **71**, 4138-44.

Rother, R. P., Rollins, S. A., Fodor, W. L., Albrecht, J. C., Setter, E., Fleckenstein, B. & Squinto, S. P. (1994). Inhibition of complement-mediated cytolysis by the terminal complement inhibitor of herpesvirus saimiri. *Journal of Virology* **68**, 730-7.

Rowe, M., Peng-Pilon, M., Huen, D. S., Hardy, R., Croom-Carter, D., Lundgren, E. & Rickinson, A. B. (1994). Upregulation of bcl-2 by the Epstein-Barr virus latent membrane protein LMP1: a B-cell-specific response that is delayed relative to NF-kappa B activation and to induction of cell surface markers. *Journal of Virology* **68**, 5602-12.

Rowe, M., Young, L. S., Crocker, J., Stokes, H., Henderson, S. & Rickinson, A. B. (1991). Epstein-Barr virus (EBV)-associated lymphoproliferative disease in the SCID mouse model: implications for the pathogenesis of EBV-positive lymphomas in man. *Journal of Experimental Medicine* **173**, 147-58.

Rowe, M., Rowe, D. T., Gregory, C. D., Young, L. S., Farrell, P. J., Rupani, H. & Rickinson, A. B. (1987). Differences in B cell growth phenotype reflect novel patterns of Epstein-Barr virus latent gene expression in Burkitt's lymphoma cells. *The Embo Journal* **6**, 2743-51.

Roy, D. J., Ebrahimi, B. C., Dutia, B. M., Nash, A. A. & Stewart, J. P. (2000). Murine gammaherpesvirus M11 gene product inhibits apoptosis and is expressed during virus persistence. *Archives in Virology* **145**, 2411-20.

Russo, J. J., Bohenzky, R. A., Chien, M. C., Chen, J., Yan, M., Maddalena, D., Parry, J. P., Peruzzi, D., Edelman, I. S., Chang, Y. & Moore, P. S. (1996). Nucleotide sequence of the Kaposi sarcoma-associated herpesvirus (HHV8). *Proceedings of the National Academy of Sciences USA* **93**, 14862-7.

Salazar-Mather, T. P., Orange, J. S. & Biron, C. A. (1998). Early murine cytomegalovirus (MCMV) infection induces liver natural killer (NK) cell inflammation and protection through macrophage inflammatory protein 1alpha (MIP-1alpha)-dependent pathways. *Journal of Experimental Medicine* **187**, 1-14.

Salazar-Mather, T. P., Ishikawa, R. & Biron, C. A. (1996). NK cell trafficking and cytokine expression in splenic compartments after IFN induction and viral infection. *Journal of Immunology* **157**, 3054-64.

Sambrook, J., Fritsch, E. F. & Maniatis, T. (1989). Molecular Cloning. A Laboratory Manual. Second Edition. Cold Spring Harbor Laboratory Press.

Sangster, M. Y., Topham, D. J., D'Costa, S., Cardin, R. D., Marion, T. N., Myers, L. K. & Doherty, P. C. (2000). Analysis of the virus-specific and nonspecific B cell response to a persistent B-lymphotropic gammaherpesvirus. *Journal of Immunology* **164**, 1820-8.

Sarawar, S. R., Cardin, R. D., Brooks, J. W., Mehrpooya, M., Hamilton-Easton, A. M., Mo, X. Y. & Doherty, P. C. (1997). Gamma interferon is not essential for recovery from acute infection with murine gammaherpesvirus 68. *Journal of Virology* **71**, 3916-21.

Sarawar, S. R., Cardin, R. D., Brooks, J. W., Mehrpooya, M., Tripp, R. A. & Doherty, P. C. (1996). Cytokine production in the immune response to murine gammaherpesvirus 68. *Journal of Virology* **70**, 3264-8.

Sarid, R., Olsen, S. J. & Moore, P. S. (1999). Kaposi's sarcoma-associated herpesvirus: epidemiology, virology, and molecular biology. *Advances in Virus Research* **52**, 139-232.

Sarid, R., Flore, O., Bohenzky, R. A., Chang, Y. & Moore, P. S. (1998). Transcription mapping of the Kaposi's sarcoma-associated herpesvirus (human herpesvirus 8) genome in a body cavity-based lymphoma cell line (BC-1). *Journal of Virology* **72**, 1005-12.

Schechter, E. M., Summers, J. & Ogston, C. W. (1988). Characterization of a herpesvirus isolated from woodchuck hepatocytes. *Journal of General Virology* **69**, 1591-9.

Schrag, J. D., Prasad, B. V., Rixon, F. J. & Chiu, W. (1989). Three-dimensional structure of the HSV1 nucleocapsid. *Cell* **56**, 651-60.

Sevilla, N., Kunz, S., Holz, A., Lewicki, H., Homann, D., Yamada, H., Campbell, K. P., de La Torre, J. C. & Oldstone, M. B. (2000). Immunosuppression and resultant

viral persistence by specific viral targeting of dendritic cells. *Journal of Experimental Medicine* **192**, 1249-60.

Siegal, F. P., Kadowaki, N., Shodell, M., Fitzgerald-Bocarsly, P. A., Shah, K., Ho, S., Antonenko, S. & Liu, Y. J. (1999). The nature of the principal type 1 interferon-producing cells in human blood. *Science* **284**, 1835-7.

Simas, J. P., Bowden, R. J., Paige, V. & Efstathiou, S. (1998). Four tRNA-like sequences and a serpin homologue encoded by murine gammaherpesvirus 68 are dispensable for lytic replication *in vitro* and latency *in vivo*. *Journal of General Virology* **79**, 149-53.

Simonds, J. A., Robey, W. G., Graham, B. J., Oie, H. & Vande Woude, G. F. (1975). Purification of herpesvirus saimiri and properties of the viral DNA. *Archives in Virology* **49**, 249-59.

Sinclair, A. J., Brimmell, M., Shanahan, F. & Farrell, P. J. (1991). Pathways of activation of the Epstein-Barr virus productive cycle. *Journal of Virology* **65**, 2237-44.

Sixbey, J. W. & Yao, Q. Y. (1992). Immunoglobulin A-induced shift of Epstein-Barr virus tissue tropism. *Science* **255**, 1578-80.

Slifka, M. K. & Whitton, J. L. (2000). Antigen-specific regulation of T cell-mediated cytokine production. *Immunity* **12**, 451-7.

Song, W. C., Sarrias, M. R. & Lambris, J. D. (2000). Complement and innate immunity. *Immunopharmacology* **49**, 187-98.

Spriggs, M. K. (1999). Virus-encoded modulators of cytokines and growth factors. *Cytokine Growth Factor Reviews* **10**, 1-4.

Spriggs, M. K., Armitage, R. J., Comeau, M. R., Strockbine, L., Farrah, T., Macduff, B., Ulrich, D., Alderson, M. R., Mullberg, J. & Cohen, J. I. (1996). The extracellular domain of the Epstein-Barr virus BZLF2 protein binds the HLA-DR beta chain and inhibits antigen presentation. *Journal of Virology* **70**, 5557-63.

Steinman, R. M. (1991). The dendritic cell system and its role in immunogenicity. *Annual Reviews of Immunology* **9**, 271-96.

Steven, N. M., Annels, N. E., Kumar, A., Leese, A. M., Kurilla, M. G. & Rickinson, A. B. (1997). Immediate early and early lytic cycle proteins are frequent targets of the Epstein-Barr virus-induced cytotoxic T cell response. *Journal of Experimental Medicine* **185**, 1605-17.

Steven, N. M., Leese, A. M., Annels, N. E., Lee, S. P. & Rickinson, A. B. (1996). Epitope focusing in the primary cytotoxic T cell response to Epstein- Barr virus and its relationship to T cell memory. *Journal of Experimental Medicine* **184**, 1801-13.

Stevenson, P. G., Efstathiou, S., Doherty, P. C. & Lehner, P. J. (2000). Inhibition of MHC class I-restricted antigen presentation by gamma 2- herpesviruses. *Proceedings of the National Academy of Sciences USA* **97**, 8455-60.

Stevenson, P. G., Belz, G. T., Altman, J. D. & Doherty, P. C. (1999a). Changing patterns of dominance in the CD8+ T cell response during acute and persistent murine gamma-herpesvirus infection. *European Journal of Immunology* **29**, 1059-67.

Stevenson, P. G., Belz, G. T., Castrucci, M. R., Altman, J. D. & Doherty, P. C. (1999b). A gamma-herpesvirus sneaks through a CD8(+) T cell response primed to a lytic-phase epitope. *Proceedings of the National Academy of Sciences USA* **96**, 9281-9286.

Stevenson, P. G., Cardin, R. D., Christensen, J. P. & Doherty, P. C. (1999c). Immunological control of a murine gammaherpesvirus independent of CD8+ T cells. *Journal of General Virology* **80**, 477-83.

Stevenson, P. G. & Doherty, P. C. (1999). Non-antigen-specific B-cell activation following murine gammaherpesvirus infection is CD4 independent *in vitro* but CD4 dependent *in vivo*. *Journal of Virology* **73**, 1075-1079.

Stevenson, P. G., Belz, G. T., Altman, J. D. & Doherty, P. C. (1998). Virus-specific CD8(+) T cell numbers are maintained during gamma- herpesvirus reactivation in CD4-deficient mice. *Proceedings of the National Academy of Sciences of the United States of America* **95**, 15565-15570.

Stevenson, P. G. & Doherty, P. C. (1998). Kinetic analysis of the specific host response to a murine gammaherpesvirus. *Journal of Virology* **72**, 943-9.

Stewart, J. P., Usherwood, E. J., Dutia, B. M., Sunil-Chandra, N. P. & Nash, A. A. (1999). Murine gammaherpesvirus. Persistent Viral infections, pp 467-476. Edited by R. Ahmed & I. Chen. John Wiley & Sons Ltd.

Stewart, J. P., Usherwood, E. J., Ross, A., Dyson, H. & Nash, T. (1998). Lung epithelial cells are a major site of murine gammaherpesvirus persistence. *Journal of Experimental Medicine* **187**, 1941-51.

Strockbine, L. D., Cohen, J. I., Farrah, T., Lyman, S. D., Wagener, F., DuBose, R. F., Armitage, R. J. & Spriggs, M. K. (1998). The Epstein-Barr virus BARF1 gene encodes a novel, soluble colony- stimulating factor-1 receptor. *Journal of Virology* **72**, 4015-21.

Sunil-Chandra, N. P., Arno, J., Fazakerley, J. & Nash, A. A. (1994). Lymphoproliferative disease in mice infected with murine gammaherpesvirus 68. *American Journal of Pathology* **145**, 818-26.

Sunil-Chandra, N. P., Efstathiou, S., Arno, J. & Nash, A. A. (1992a). Virological and pathological features of mice infected with murine gamma-herpesvirus 68. *Journal of General Virology* **73**, 2347-56.

Sunil-Chandra, N. P., Efstathiou, S. & Nash, A. A. (1992b). Murine gammaherpesvirus 68 establishes a latent infection in mouse B lymphocytes *in vivo*. *Journal of General Virology* **73**, 3275-9.

Svedmyr, E. & Jondal, M. (1975). Cytotoxic effector cells specific for B Cell lines transformed by Epstein-Barr virus are present in patients with infectious mononucleosis. *Proceedings of the National Academy of Sciences USA* **72**, 1622-6.

Swanton, C., Mann, D. J., Fleckenstein, B., Neipel, F., Peters, G. & Jones, N. (1997). Herpes viral cyclin/Cdk6 complexes evade inhibition by CDK inhibitor proteins. *Nature* **390**, 184-7.

Takada, K. & Ono, Y. (1989). Synchronous and sequential activation of latently infected Epstein-Barr virus genomes. *Journal of Virology* **63**, 445-9.

Tanner, J. E., Alfieri, C., Chatila, T. A. & Diaz-Mitoma, F. (1996). Induction of interleukin-6 after stimulation of human B-cell CD21 by Epstein-Barr virus glycoproteins gp350 and gp220. *Journal of Virology* **70**, 570-5.

Telford, E. A., Studdert, M. J., Agius, C. T., Watson, M. S., Aird, H. C. & Davison, A. J. (1993). Equine herpesviruses 2 and 5 are gamma-herpesviruses. *Virology* **195**, 492-9.

Thome, M., Schneider, P., Hofmann, K., Fickenscher, H., Meinl, E., Neipel, F., Mattmann, C., Burns, K., Bodmer, J. L., Schroter, M., Scaffidi, C., Krammer, P. H., Peter, M. E. & Tschopp, J. (1997). Viral FLICE-inhibitory proteins (FLIPs) prevent apoptosis induced by death receptors. *Nature* **386**, 517-21.

Thorley-Lawson, D. A. & Geilinger, K. (1980). Monoclonal antibodies against the major glycoprotein (gp350/220) of Epstein-Barr virus neutralize infectivity. *Proceedings of the National Academy of Sciences USA* **77**, 5307-11.

Tomazin, R., Boname, J., Hegde, N. R., Lewinsohn, D. M., Altschuler, Y., Jones, T. R., Cresswell, P., Nelson, J. A., Riddell, S. R. & Johnson, D. C. (1999). Cytomegalovirus US2 destroys two components of the MHC class II pathway, preventing recognition by CD4+ T cells. *Nature Medicine* **5**, 1039-43.

Tomazin, R., Hill, A. B., Jugovic, P., York, I., van Endert, P., Ploegh, H. L., Andrews, D. W. & Johnson, D. C. (1996). Stable binding of the herpes simplex virus ICP47 protein to the peptide binding site of TAP. *The Embo Journal* **15**, 3256-66.

Tortorella, D., Gewurz, B. E., Furman, M. H., Schust, D. J. & Ploegh, H. L. (2000). Viral subversion of the immune system. *Annual Reviews of Immunology* **18**, 861-926.

Tosato, G., Tanner, J., Jones, K. D., Revel, M. & Pike, S. E. (1990). Identification of interleukin-6 as an autocrine growth factor for Epstein-Barr virus-immortalized B cells. *Journal of Virology* **64**, 3033-41.

Tough, D. F., Borrow, P. & Sprent, J. (1996). Induction of bystander T cell proliferation by viruses and type I interferon *in vivo*. *Science* **272**, 1947-50.

Trapani, J. A., Sutton, V. R. & Smyth, M. J. (1999). CTL granules: evolution of vesicles essential for combating virus infections. *Immunology Today* **20**, 351-6.

Tripp, R. A., Hou, S., McMickle, A., Houston, J. & Doherty, P. C. (1995). Recruitment and proliferation of CD8+ T cells in respiratory virus infections. *Journal of Immunology* **154**, 6013-21.

Ulrich, S., Goltz, M. & Ehlers, B. (1999). Characterization of the DNA polymerase loci of the novel porcine lymphotropic herpesviruses 1 and 2 in domestic and feral pigs. *Journal of General Virology* **80**, 3199-205.

Usherwood, E. J., Brooks, J. W., Sarawar, S. R., Cardin, R. D., Young, W. D., Allen, D. J., Doherty, P. C. & Nash, A. A. (1997). Immunological control of murine gammaherpesvirus infection is independent of perforin. *Journal of General Virology* **78**, 2025-30.

Usherwood, E. J., Ross, A. J., Allen, D. J. & Nash, A. A. (1996a). Murine gammaherpesvirus-induced splenomegaly: a critical role for CD4 T cells. *Journal of General Virology* **77**, 627-30.

Usherwood, E. J., Stewart, J. P., Robertson, K., Allen, D. J. & Nash, A. A. (1996b). Absence of splenic latency in murine gammaherpesvirus 68-infected B cell-deficient mice. *Journal of General Virology* **77**, 2819-25.

van Berkel, V., Barrett, J., Tiffany, H. L., Fremont, D. H., Murphy, P. M., McFadden, G., Speck, S. H. & Virgin, H. I. (2000). Identification of a gammaherpesvirus selective chemokine binding protein that inhibits chemokine action. *Journal of Virology* **74**, 6741-7.

van Berkel, V., Preiter, K., Virgin, H. W. t. & Speck, S. H. (1999). Identification and initial characterization of the murine gammaherpesvirus 68 gene M3, encoding an abundantly secreted protein. *Journal of Virology* **73**, 4524-9.

van Dyk, L. F., Hess, J. L., Katz, J. D., Jacoby, M., Speck, S. H. & Virgin, H. I. (1999). The murine gammaherpesvirus 68 v-cyclin gene is an oncogene that promotes cell cycle progression in primary lymphocytes. *Journal of Virology* **73**, 5110-22.

Vermaelen, K. Y., Carro-Muino, I., Lambrecht, B. N. & Pauwels, R. A. (2001). Specific migratory dendritic cells rapidly transport antigen from the airways to the thoracic lymph nodes. *Journal of Experimental Medicine* **193**, 51-60.

Virgin, H. W., Latreille, P., Wamsley, P., Hallsworth, K., Weck, K. E., Dal Canto, A. J. & Speck, S. H. (1997). Complete sequence and genomic analysis of murine gammaherpesvirus 68. *Journal of Virology* **71**, 5894-904.

Wakeling, M. N., Roy, D. J., Nash, A. A. & Stewart, J. P. (2001). Characterization of the murine gammaherpesvirus 68 ORF74 product: a novel oncogenic G protein-coupled receptor. *Journal of General Virology* **82**, 1187-97.

Wallace, L. E., Rickinson, A. B., Rowe, M. & Epstein, M. A. (1982). Epstein-Barr virus-specific cytotoxic T-cell clones restricted through a single HLA antigen. *Nature* **297**, 413-5.

Wang, F., Gregory, C., Sample, C., Rowe, M., Liebowitz, D., Murray, R., Rickinson, A. & Kieff, E. (1990). Epstein-Barr virus latent membrane protein (LMP1) and nuclear proteins 2 and 3C are effectors of phenotypic changes in B lymphocytes: EBNA-2 and LMP1 cooperatively induce CD23. *Journal of Virology* **64**, 2309-18.

Wang, G. H., Garvey, T. L. & Cohen, J. I. (1999). The murine gammaherpesvirus-68 M11 protein inhibits Fas- and TNF- induced apoptosis. *Journal of General Virology* **80**, 2737-40.

Weck, K. E., Kim, S. S., Virgin, H. I. & Speck, S. H. (1999a). B cells regulate murine gammaherpesvirus 68 latency. *Journal of Virology* **73**, 4651-61.

Weck, K. E., Kim, S. S., Virgin, H. I. & Speck, S. H. (1999b). Macrophages are the major reservoir of latent murine gammaherpesvirus 68 in peritoneal cells. *Journal of Virology* **73**, 3273-83.

Weck, K. E., Barkon, M. L., Yoo, L. I., Speck, S. H. & Virgin, H. I. (1996). Mature B cells are required for acute splenic infection, but not for establishment of latency, by murine gammaherpesvirus 68. *Journal of Virology* **70**, 6775-80.

Welsh, R. M., Brubaker, J. O., Vargas-Cortes, M. & O'Donnell, C. L. (1991). Natural killer (NK) cell response to virus infections in mice with severe combined immunodeficiency. The stimulation of NK cells and the NK cell-dependent control of virus infections occur independently of T and B cell function. *Journal of Experimental Medicine* **173**, 1053-63.

Whitmire, J. K. & Ahmed, R. (2000). Costimulation in antiviral immunity: differential requirements for CD4(+) and CD8(+) T cell responses. *Current Opinion in Immunology* **12**, 448-55.

Wiertz, E. J., Jones, T. R., Sun, L., Bogyo, M., Geuze, H. J. & Ploegh, H. L. (1996). The human cytomegalovirus US11 gene product dislocates MHC class I heavy chains from the endoplasmic reticulum to the cytosol. *Cell* **84**, 769-79.

Wutzler, P., Meerbach, A., Farber, I., Wolf, H. & Scheibner, K. (1995). Malignant lymphomas induced by an Epstein-Barr virus-related herpesvirus from Macaca arctoides--a rabbit model. *Archives in Virology* **140**, 1979-95.

Wykes, M., Pombo, A., Jenkins, C. & MacPherson, G. G. (1998). Dendritic cells interact directly with naive B lymphocytes to transfer antigen and initiate class switching in a primary T-dependent response. *Journal of Immunology* **161**, 1313-9.

York, I. A., Roop, C., Andrews, D. W., Riddell, S. R., Graham, F. L. & Johnson, D. C. (1994). A cytosolic herpes simplex virus protein inhibits antigen presentation to CD8+ T lymphocytes. *Cell* **77**, 525-35.

Zacny, V. L., Wilson, J. & Pagano, J. S. (1998). The Epstein-Barr virus immediate-early gene product, BRLF1, interacts with the retinoblastoma protein during the viral lytic cycle. *Journal of Virology* **72**, 8043-51.

Zalani, S., Holley-Guthrie, E. & Kenney, S. (1996). Epstein-Barr viral latency is disrupted by the immediate-early BRLF1 protein through a cell-specific mechanism. *Proceedings of the National Academy of Sciences USA* **93**, 9194-9.

Zeidler, R., Eissner, G., Meissner, P., Uebel, S., Tampe, R., Lazis, S. & Hammerschmidt, W. (1997). Downregulation of TAP1 in B lymphocytes by cellular and Epstein-Barr virus-encoded interleukin-10. *Blood* **90**, 2390-7.

Zhang, Q., Gutsch, D. & Kenney, S. (1994). Functional and physical interaction between p53 and BZLF1: implications for Epstein-Barr virus latency. *Molecular Cell Biology* **14**, 1929-38.

Ziegler, H., Thale, R., Lucin, P., Muranyi, W., Flohr, T., Hengel, H., Farrell, H., Rawlinson, W. & Koszinowski, U. H. (1997). A mouse cytomegalovirus glycoprotein retains MHC class I complexes in the ERGIC/cis-Golgi compartments. *Immunity* **6**, 57-66.

Zimring, J. C., Goodbourn, S. & Offermann, M. K. (1998). Human herpesvirus 8 encodes an interferon regulatory factor (IRF) homolog that represses IRF-1-mediated transcription. *Journal of Virology* **72**, 701-7.

zur Hausen, H., O'Neill, F. J., Freese, U. K. & Hecker, E. (1978). Persisting oncogenic herpesvirus induced by the tumour promotor TPA. *Nature* **272**, 373-5.